DECISION-MAKING FOR OFFSHORE RESOURCE DEVELOPMENT

MARK FUGLEM


CENTRE FOR NFLD. STUDIES
MEMORIAL UNIVERSITY
OF NEWFOUNDLAND

DECISION-MAKING FOR

OFFSHORE RESOURCE DEVELOPMENT

by

© Mark Fuglem, B.Sc.

A Thesis Submitted to the School of Graduate Studies

in Partial Fulfilment of the Requirements for the Degree of

Doctor of Philosophy in Engineering

Faculty of Engineering and Applied Science

Memorial University of Newfoundland

1997

St. John's Newfoundland Canada

Table of Contents

List of Figures

List of Tables

Nomenclature

General remarks

In the text, symbols are shown in italics. As a general rule, symbols for random quantities shown in capital letters and symbols for specific or constant values are shown in small letters.

Units

All money is in Canadian dollars unless indicated otherwise. Millions of dollars are denoted as M$ or M$US for US currency.

DWT	dead weight tonnes

Abbreviations

pdf	probability density function
cdf	cumulative distribution function
edf	exceedance distribution function

Acronyms

AES	Atmospheric and Environmental Services (Canada)
API	American Petroleum Institute
ASPPR	Arctic Shipping Pollution Prevention Regulations
CAC	Canadian Arctic Class (icebreakers)
CODIE	Canadian Offshore Design for Ice Environments

CSA	Canadian Standards Association
FPSO	Floating Production, Storage, and Offloading System
GBS	Gravity Based Structure
IIP	International Ice Patrol
IMO	International Maritime Organization
MARPOL	International Convention for the Prevention of Pollution from Ships
NOAA	National Oceanic and Atmospheric Administration
NOIA	Newfoundland Ocean Industries Association
NPV	Net Present Value
NRC	National Research Council (US)
OPA 90	Oil Pollution Act (1990), US
OPEC	Organization of the Petroleum Exporting Countries
PIP	Petroleum Incentive Package
RAO	Response Amplitude Operator
SLAR	Side-Looking Airborne Radar
SORM	Second Order Reliability Method
SWOPS	Single Well Oil Production System

Symbols

Economics

C_t	cashflow in period t
NPV	net present value

CRF	capital recovery factor

Decision Theory

$\alpha_i, i=1..n$	i'th of n possible alternatives
$\theta_{ij}, j=1..n_i$	j'th of n_i possible outcomes associated with alternative i
$\mu_{ij}, j=1..n_i$	the utility associated with j'th of n_i possible outcomes associated with alternative i
$P_1 \prec P_2$	the distribution of outcomes P_2 is preferred to the distribution of outcomes P_1
$P_1 \approx P_2$	the distribution of outcomes P_1 is equally preferred to the distribution of outcomes P_2
$\overline{\mu}(d_i)$	expected utility associated with decision i
μ_C	utility associated with a certain equivalent event

Probability

$Pr(A)$	probability of event A
$p_N(r)$	probability that the discrete random quantity N takes value r (probability mass function)
$f_X(x)$	probability that the random quantity X takes value x (probability density function)
$F_X(x)$	probability that the random quantity X is less than or equal to the value x (cumulative distribution function)

$1-F_X(x)$ probability that the random quantity X is greater than the value x (exceedance distribution function)

$f_{X|\Lambda}(x|\lambda)$ probability density function for random quantity X conditional on specific value λ for random quantity Λ

$f_{X|\Theta}(x|\theta)$ probability of x given parametric distribution f with parameter Θ

$f_{\Theta}(\theta)$ for Θ prior distribution for parameter Θ

$\mathcal{L}_{X|\Theta}(x|\theta)$ likelihood of x given distribution with parameter Θ

$f_{\Theta|X}(\theta|x)$ posterior probability distribution for parametric Θ given observation x

Reliability-based design

L_D design iceberg impact load

p_p peak pressure associated with nominal contact area a during an ice-structure interaction

p average ice crushing pressure associated with nominal contact area

a nominal contact area

V_N component of impact velocity normal to face of structure

Fmax maximum force during impact

$Fmax^0$ maximum force during impact given no rotation of iceberg

ϵ^0 eccentricity of impact

r_i radius of gyration of iceberg

Icebergs

L	iceberg waterline length (m)
A_A	projected above water area (m^2) of the iceberg perpendicular to the wind direction
A_B	projected below water area (m^2) of the iceberg perpendicular to its direction of movement relative to the current (when considered uniform)
D_I	characteristic dimension of the iceberg (m) for wave drift forces
ρ	average areal density of icebergs (icebergs per m^2)

Environmental

H_S	significant wave height
T_P	peak period
L_P	wave length associated with peak period
$S_w(f)$	spectral wave energy at frequency f
H_z	average height of background swell (m)
v_{tz}	wind speed averaged over the time interval t at a height of z meters above sea level (where t must be one of the times for which α and β are provided)
v_{ref}	wind speed averaged over 1 hour at 10 m above sea level
α	gust factor for t, referenced to V_{ref}
β	height exponent for t
U_A	wind velocity (m/s)
H	regular wave height (m)

$\eta_E(\tilde{I}, \tilde{E})$ number of encounters of icebergs with characters $\tilde{I}$ in environmental conditions defined by $\tilde{E}$

η_F annual expected flux of icebergs across a line segment

Iceberg Management

r range of iceberg from production site

P_M probability of successfully detecting the iceberg and avoiding collision

$P_{M|D}(r)$ probability of avoiding collision given detection at range r

$P_D(r)$ probability of first detecting the iceberg at range r

$P_T(r)$ probability of successfully towing the iceberg

$P_A(r)$ probability of successfully disconnecting the production vessel and moving off site.

Hydrodynamics and wave-induced motions

$f_N(u)$ probability density function for instantaneous iceberg velocity u

σ^2 variance of the iceberg heave or surge velocity in open water

m_0 zeroth moment of the iceberg open water velocity spectrum

V_S is the significant velocity component of interest.

$f_R(u, \sigma)$ probability density function for instantaneous forward iceberg velocity u (Rayleigh distribution) given Gaussian motion and zero net drift

$f_{SR}(u, \sigma, k)$ probability density function for instantaneous forward iceberg velocity u (Special Rayleigh distribution) given Gaussian motion and net drift of k m/s

u_{SR} mean of Special Rayleigh distribution

$s(\sigma)$ normalizing constant when updating Gaussian distribution with forward velocity to get Rayleigh distribution

Scour events

$\eta_{te}(w_s)$ number of scour events over a subsea structure of with w_s

$\eta_{tl}(s)$ number of scour events over a subsea pipeline segment of length l

Implementation

ΔI bin size for iceberg water line length

ΔE bin size for H_S

1 INTRODUCTION

This thesis describes a methodology for optimizing the choice and design of oil production systems in offshore regions where there is a significant iceberg hazard. The work focuses in particular on the future of oil fields on the Grand Banks off Canada's east coast. The problem of designing for possible iceberg impacts has many of the features associated with offshore development such as significant uncertainty regarding environmental parameters, and implementation of complex systems requiring a range of expertise. A number of significant oil and gas fields have been discovered on the Grand Banks and further discoveries are expected. At present, the large Hibernia and Terra Nova fields are being for developed.

When considering the development of a particular offshore resource, one needs to make a number of decisions including whether or not the project is viable, which production systems should be used, what the best operating strategies are, what environmental loads can be expected, and whether further data acquisition or research and development are required. It is necessary in each case to identify the problem and the associated criteria for success, to determine alternative courses of action and their possible outcomes, to assess the probability of occurrence of each outcome, and finally choose the best alternatives. The amount of effort which should be expended in evaluating each case depends on the potential increase in benefits.

Choosing a production system is usually an iterative process. In the preliminary stages, the advantages and disadvantages of different types of systems are identified and requirements for further environmental data, research and development, and specific studies

are identified. Approximate analyses sufficient to understand the main aspects of the problem and to narrow down the number of alternatives is required. In the later design stages, detailed optimization, model testing, and analysis may be performed for several of the more promising options.

The main criteria when evaluating and comparing production systems are safety and economics. First, it must be shown that the systems proposed pose acceptably small risks to personnel and the environment. In accessing risks of structural failure, wave, iceberg impact, and ship collision loads need to be considered. Sources of other risk include fire, explosions, blowouts, and capsize. The total risk due to all sources is often difficult to estimate because of factors such as misconception in design, poor communication, computational error, poor fabrication, poor maintenance, and human error during operation. These types of risks are generally reduced through proper training and checking procedures; they can also be reduced through simpler design and through designs with redundant load paths.

In the case of structural loads, design criteria specified in codes are imposed to ensure that the structure is safe. These criteria may be derived based on experience or calibrated using probabilistic methods. The presence of icebergs on the Grand Banks has resulted in special design requirements. Fixed systems, such as the Hibernia gravity based production platform, must be able to withstand impacts by large icebergs. For such large icebergs, wave-induced velocities are small and drift velocities range up to about 1 m/s in extreme cases. Design for such large icebergs results in more massive and therefore expensive platforms than those used in the North Sea, which are made slender at the waterline to

minimize wave loads. If floating systems are to be used, they must be designed to avoid impacts by larger icebergs. This is done by towing the icebergs or by moving the vessel off site. Some ice strengthening will be required as small icebergs are difficult to detect in moderate and high sea states. Wave-induced motions are important in such cases and impact velocities could be as high as four to five m/s for very small icebergs. Shuttle tankers should be able to detect larger icebergs and manoeuvre to avoid them, but may require strengthening for smaller icebergs which are difficult to detect. Impact speeds may range up to 10 m/s depending on the vessel speed. In the case of subsea equipment such as well heads, manifolds, and flowlines, scouring of the seabed by large icebergs is a concern. Possible solutions include burial of equipment deep enough to avoid damage, placement of equipment in subsea glory holes deep enough to avoid contact, or acceptance of occasional damage with repairs and replacement where the systems can be made fail safe to avoid environmental pollution.

To evaluate the economic viability of a development it is necessary to estimate the magnitudes and timing of cash flows. A common measure for evaluating and comparing systems is the net present value which indicates the present value when all future cash flows are discounted to the present at a given threshold rate of return. Generally one wants to reduce initial capital costs and reduce the time required before revenues are achieved. Revenues are determined by the price of oil and the rate of production. Capital and operating costs are dictated by the capacity required and the particular design. There is usually a tradeoff between initial capital costs and later costs for repair and maintenance. Capital costs associated with icebergs including ice strengthening of structures and vessels and burial of

subsea equipment. Increased operating costs result from ice management and repair of damaged equipment. The expected amount of production downtime associated with a given system is also very important. Downtime will result when moving off location to avoid icebergs and when repairing equipment. The downtime will be affected by the amount of time waiting for an appropriate weather window to reconnect or enact repairs.

In this thesis, a methodology for optimizing design is presented. First, available probabilistic methods applicable to situations where there is limited data and uncertainty regarding processes are reviewed. In particular, the Bayesian framework is considered. The possibility of extending the range of Bayesian applications to employ more complex likelihood functions is explored. Emphasis is given to problems relevant to offshore development. Second, criteria and models for comparing the economics of different systems are presented. These include models to estimate the capital and operating costs of the production systems, and to estimate lost revenues due to downtime. Third, methods for determining the number of incidences involving icebergs are developed. For determining design impact loads, reliability-based design methods are implemented. Factors that are considered include the iceberg population, the environment, iceberg detection, iceberg management, avoidance strategies, and the ice-structure interaction processes. To illustrate the methodology, preliminary analyses are conducted for a number of example field scenarios and systems.

2 BACKGROUND

2.1 Overview

In this chapter, an overview is given of the problem of designing production systems for offshore regions where icebergs are present, the types of production systems being proposed, available methods for analysing iceberg loads, risks, and downtime, and areas where improvements are required. In Section 2.2, the importance of the petroleum resources off Newfoundland is discussed, and a brief overview is given of discovered and potential fields. In Section 2.3, an overview is given of the environmental conditions on the Grand Banks, with emphasis on those parameters needed in analyses. An overview is given of the available data, including methods of collection, parameters recorded, and limitations. In Section 2.4, the requirements for developing a field and the types of production systems that have been proposed will be discussed. In Section 2.5, the importance of iceberg impact risks in the overall design is discussed and a review is given of published methods for determining design iceberg impact loads, risk, and downtime. In Section 2.6, the general factors determining the economic viability of a field are discussed. In Section 2.7, the requirements for good decision making are discussed and aspects of formal decision theory, including the use of decision trees, probability theory, and utility theory are briefly outlined.

2.2 Petroleum resources

Total energy demand in Canada is expected to rise from 9,600 Peta Joules in 1990 to 13,800 Peta Joules in 2010, with oil and gas comprising approximately 60% of this (Croasdale and McDougall, 1994). Conventional reserves are being depleted in Canada and

if they cannot be replaced domestically, they must be replaced through imports. Possible sources for increasing the domestic supply of oil include improved recovery methods, the development of tar sands and heavy oil deposits, and the development of frontier oil and gas. Total estimated recoverable reserves in the Canadian frontier regions are about 3.4 billion barrels of oil and 44 trillion cubic feet of gas. Of this, approximately 1.6 billion barrels of oil, 4 trillion cubic feet of gas, and 240 million barrels of natural gas liquids, have been found on the Grand Banks. Exploration costs have been relatively low, averaging less than $2 US per barrel, and licences have been granted for further exploration work in the immediate vicinity of existing discoveries. It was not indicated how these costs reflected the government Petroleum Incentive Package (PIP) grants available at that time. Future potential discoveries on the Grand Banks are estimated at 3 billion barrels of oil and 5 trillion cubic feet of gas.

For the objectives of this study, it is necessary to determine the likely field characteristics of future developments so that example field scenarios can be set up for analyses. The main parameters required are the amount of reserves, the reservoir depths (for drilling costs), the extent and continuity of the reservoirs (affecting the number and types of wells), the likely flow rates, and any requirements for water and gas injection, special treatments for hydrates, wax, CO_2, and H_2S, or abnormal temperatures or pressures.

A description of oil and gas fields already discovered on the Grand Banks and off Labrador may be found in Chipman (1992). The locations of the different finds on the Grand Banks and off Labrador are shown in Figure 2.1 and the magnitudes of the finds are shown in Table 1. All of the significant oil discoveries to date are on the Grand Banks. Of these

the majority of oil is found in four fields (Hibernia, Terra Nova, Hebron, and Whiterose). The remaining discovered fields all have proven reserves of less than 25 million barrels. All of the oil fields are found in the Jeanne d'Arc basin, except South Tempest. Five gas fields with greater than 20 billion cubic metres have been found. These are Whiterose and Hibernia on the Grand Banks and North Bjarni, Bjarni and Gudrid off Labrador. In addition, significant natural gas liquids associated with gas are found in Hibernia, Whiterose, and Ben Nevis on the Grand Banks, and North Bjarni and Bjarni off Labrador. The Hebron field comprises four reservoirs. These are Ben Nevis (129 million barrels), Hibernia (46 million barrels), Fortune Bay (14 million barrels), and Jeanne d'Arc (6 million barrels). The Ben Nevis oil is relatively heavy so artificial lift will be required.

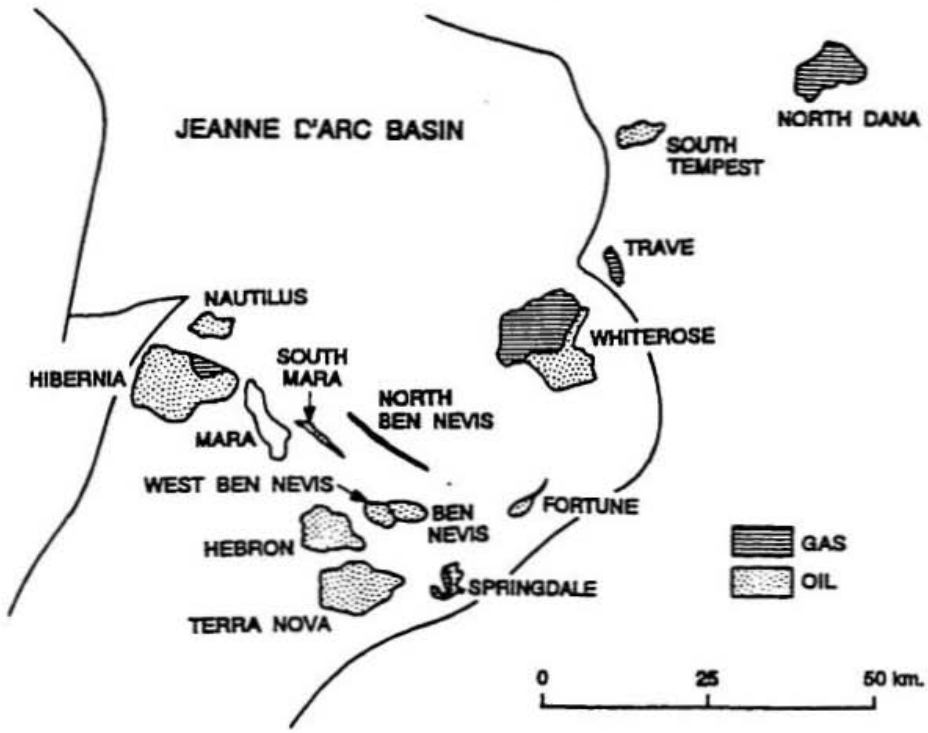

Figure 2.1 Locations of discovered oil and gas fields (Chipman, 1992)

Table 1 Sizes of discovered fields (Chipman, 1992)

Fields on the Grand Banks	Oil (millions)		Gas (billions)		NGL's (millions)	
	m^3	bbl	m^3	cu. ft.	m^3	bbl
Hibernia	106.0	666	28.7	1017	17.7	111
Terra Nova	64.6	406	7.6	269	2.2	14
Hebron	31.0	195	-	-	-	-
Whiterose	28.4	178	42.7	1509	9.2	58
West Ben Nevis	4.0	25	-	-	-	-
Mara	3.6	23	-	-	-	-
Ben Nevis	3.0	19	6.5	229	4.7	30
North Ben Nevis	2.9	18	3.3	115	0.7	4
Springdale	2.2	14	6.7	236	-	-
Nautilus	2.1	13	-	-	-	-
South Tempest	1.3	8	-	-	-	-
Fortune	0.9	6	-	-	-	-
South Mara	0.6	4	4.1	144	1.2	8
North Dana	-	-	13.3	470	1.8	11
Trave	-	-	0.8	30	0.2	1
Subtotals	250.6	1575	113.7	4019	37.7	237

Fields off Labrador	Oil (millions)		Gas (billions)		NGL's (millions)	
	m^3	bbl	m^3	cu. ft.	m^3	bbl
North Bjarni	-	-	63.3	2235	13.1	82
Gudrid	-	-	26.0	920	1.0	6
Hopedale	-	-	24.3	859	5.0	31
Snorri	-	-	3.0	105	0.4	2
Subtotals	-	-	119.6	4224	19.9	123

Most of the oil in the Whiterose field is found in the Ben Nevis reservoir (158 million barrels) which consists of a number of different pools. One particular pool has 122 million barrels in a small area with good production potential.

Clearly, the development of the reserves off Newfoundland and Labrador will play a significant role in ensuring Canada's energy self sufficiency in the near future. While the total reserves are very significant, the environment in which they are located is very severe and for most of the smaller fields, the cost of development is prohibitive at present. To allocate present research and development efforts efficiently to reduce these costs, it is important to identify the most important factors and to determine those systems and strategies which have the best promise of leading to reduced costs and risks.

2.3 Environment factors

One of the main deterrents to the development of smaller fields on the Grand Banks is the combination of relatively high sea states in the region and the seasonal occurrence of icebergs. A number of other environmental factors on the Grand Banks which require special attention include cold air and water temperatures and icing in the winter, and the presence of sea ice and extreme fog conditions in the spring.

Icebergs originate from glaciers in Greenland and arctic Canada. The main transport mechanism bringing icebergs south is the Labrador current. The current flows north along the west coast of Greenland, then south along the east coasts of Baffin Island and Labrador. Where the current reaches Newfoundland, it swings to the east and then splits around the Grand Banks (Figure 2.2). One branch follows the east coast of Newfoundland while the

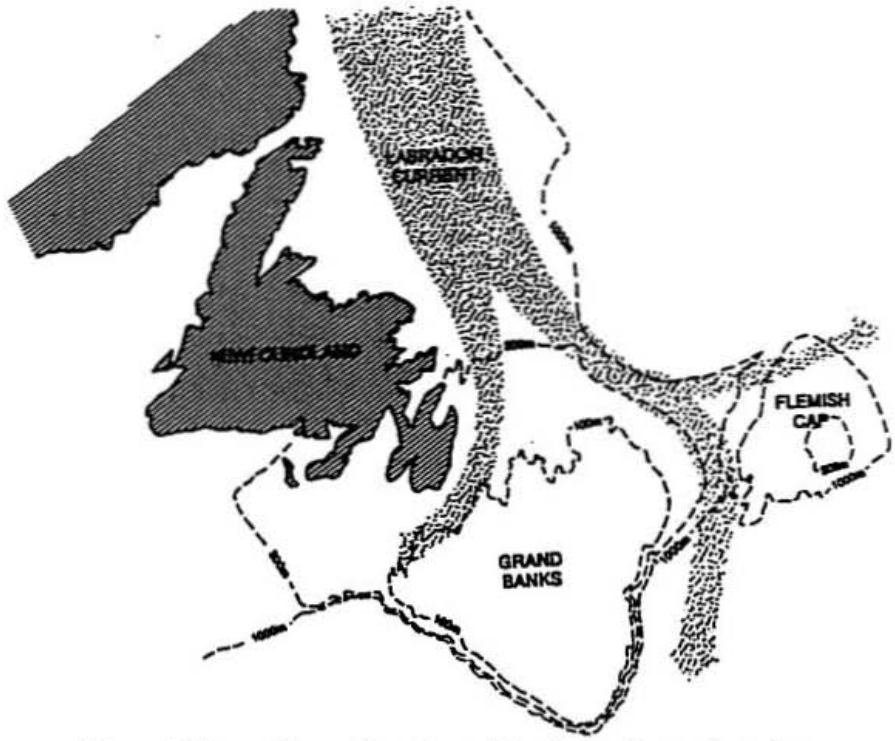

Figure 2.2 General motion of icebergs through region

other moves east along the northern edge of the banks to the Flemish pass and south. The two branches meet the warm northerly flowing Gulf Stream current near the southern edge of the Grand Banks. It takes approximately two seasons for an iceberg to reach the Grand Banks, the exact time depends on when and where the iceberg is calved, the variations in the strength of the Labrador current, the winter sea ice conditions, and the local winds which may trap the iceberg inshore or move it off the main current. At the Grand Banks, persistent wind patterns can cause the icebergs to be blown well to east or west of the banks for a significant portion of a season. When the winds are onshore, large numbers of icebergs can be held along the shores of Newfoundland.

The rate of deterioration of icebergs determines how far south they travel. Icebergs deteriorate mainly through melting, erosion, calving, and splitting. The rate of melting

increases proportionately to the temperature gradient in the water at the surface of the iceberg. This in turn is a function of the ambient water temperature, wave action, and the motion of the iceberg relative to the surrounding current. The most significant erosion occurs around the waterline of the iceberg due to wave action and can result in undercutting and eventually calving of ice pieces from the resulting overhangs. The presence of sea ice reduces the influence on the erosion of icebergs by damping waves and reducing water temperature. The number of icebergs reaching the Grand Banks is significantly higher in years when sea ice off Labrador extends out over the main part of the Labrador current (Marko, 1993). Most icebergs arrive on the Grand Banks in the spring and early summer; though they have occurred in small numbers at other times of the year. Icebergs generally do not travel far south of the Grand Banks, as the relatively warm Gulf stream causes quick erosion and melting.

The collection of data on the population of icebergs is both difficult and expensive. The annual variation in the number of icebergs is such that a significant number of years are required to get a good estimate of the distribution of areal density of icebergs at a given site. The problem is made more difficult because smaller icebergs can be difficult to detect except in very moderate environmental conditions. To describe the iceberg shape and size parameters and their correlations accurately, three dimensional contours are required. Above water profiles can be determined from stereoscopic photographs, however the measurements of underwater shapes using sophisticated sonar systems suspended from a ship are quite expensive. More often, icebergs are classified according to size classes (growler, bergy bit,

small, medium, large, very large) or by estimates of their simplest visible above-water dimensions (waterline length, waterline width, and height).

Relatively good historical data is available on the number and locations of icebergs on the Grand Banks from the International Ice Patrol (IIP), the oil industry, and research institutes. The IIP was set up in 1912, after the sinking of the Titanic, with the mandate to notify mariners of the presence of iceberg in the normal shipping lanes. To do this, the IIP composes maps of the positions of sited icebergs based on ship reports and dedicated overflights. The IIP now uses an iceberg trajectory model to predict where to search for sighted icebergs on subsequent trips; to reduce the number of double counts due to resightings, and to be able to account for any icebergs in subsequent maps that can not be found due to either bad weather or insufficient time. The IIP has also performed numerous scientific studies over the years to improve their prediction capabilities. The reports produced by the IIP provide a unique and valuable source of information on the numbers and movements of icebergs over the past 90 years.

There are a number of limitations in applying the IIP data for risk analyses which should be noted. Flight paths were chosen to follow the southern extent of the iceberg incursion and to relocate icebergs which had been previously sighted, therefore the coverage at any given location may be biased. It is often difficult to determine if areas on the maps which show no icebergs result because there is no coverage, the conditions are poor for detection, or there are no icebergs. Furthermore the data collection procedures have changed over time as technology and demands for information changed. For example, dedicated overflights were introduced after the second world war, the use of the iceberg trajectory

forecasting model was introduced in 1979, and the use of SLAR (Side-Looking Airborne Radar) was introduced in 1982. Clear documentation of the procedures used each year is no longer available, making it difficult to estimate the effects of these changes. For example, the weather conditions along the routes and the reasons for choosing particular routes are not always provided. Neither are the methods used for determining whether or not a given iceberg was a recount when using the forecast model. While the IIP maps provide good information on the positions of the icebergs, only a simple size classification was used; this specifies only the classes iceberg and growler. It is known that the number of small icebergs is somewhat underestimated and that the number of growlers is significantly underestimated.

Data on the numbers and types of icebergs at different drilling sites on the Grand Banks have been collected by oil companies over the last 15 years. Available data includes iceberg trajectory positions determined by radar, records of iceberg positions from overflights, and measurements of the physical dimensions of icebergs from support ships. A reasonably large data base of waterline length, height, width, and shape class observed from support vessels has been collected. As well, a smaller high quality data-base of detailed measurements of above and below water profiles is available. When considering estimating the average areal densities of icebergs from this data, it should be noted that the rigs are only located at a given site long enough to drill the well. Also, the oil companies have the same problems with determining resightings of icebergs and detecting small icebergs as the IIP.

The wind is the major driving force during storm conditions. It acts directly on the icebergs and indirectly through the generation of surface waves and current. The wind also plays a major role in limiting the radar detection capability through the generation of small

capillary waves which cause backscatter (sea clutter); this can mask out the signal returned from the iceberg. Distributions giving the wind velocity as functions of direction and month may be found in the AES Wind and Wave Atlas (MacLaren Plansearch Ltd., 1991). On the Grand Banks, winds are most common from the southwest and are strongest in January.

The sea state is often modelled as a combination of local wind generated waves and low frequency swell. The intensity of the locally generated waves is a function of the strength, duration, and fetch of the wind. On the Grand Banks, the wind is usually associated with cyclonic weather patterns. At a given location, the wind usually slowly turns in direction. This affects the generation of waves (and surface current) by limiting the effective fetch. The resulting sea states can be quite complex, containing wave energy at a number of frequencies and directions. Distributions for parameters such as the significant wave height H_S can be found in the AES Wind and Wave Climate Atlas for the East Coast (MacLaren Plansearch, 1991). This data is based on wave-rider and NOAA wave-buoy data for the northern Grand Banks during the period 1970 to 1989. Where a sea spectrum is required, the Jonswap spectrum recommended by LeBlond et. al. (1982) can be used.

The ocean currents are the resultant of a number of forcing functions which include the stresses associated with large-scale wind patterns (resulting in geostrophic currents), tidal forces, differences in water densities at different locations, and local winds. These forces can result in complex current patterns. An approximate estimate of the locally generated current can be found using Ekman's model (see Pond and Pickard, 1983, pg. 109).

Other parameters which influence detection include lighting, visibility, fog, and precipitation. The lighting and visibility determine the visual detection capabilities; the

visibility ceiling affects when flying is permitted; and fog and precipitation affect radar detection.

2.4 Systems, strategies, and criteria for evaluation

The number, types, spacing, and timing of wells and the production rates achieved will be determined largely based on reservoir engineering requirements. The amount of oil that can be produced is roughly proportional to the size of the reservoir, but also depends on the continuity of the reservoir, the shapes and orientations of the individual pay zones, the permeability of the rock, the characteristics of the fluid, and the amount of natural drive available. The produced fluids may come from different reservoirs situated at different vertical and horizontal offsets and these reservoirs may be broken into numerous individual pools through faulting and other processes. The number, sizes, shapes and relative locations of these individual pools affects the number and type of development wells required, where they are located, and how deep they must be drilled. Horizontal drilling techniques are used to control the path which the drill pipe takes through the reservoir and thus increase contact with the pay zone. Extended reach drilling techniques are used to reach pools at large horizontal displacements from the drill site. Drilling reaches typically reach 9 km (i.e. 2 km down and 7 km horizontal), though reaches of about 4 km are more common and there may be difficulty in drilling longer sections (Lever, 1995). The drill reach that can be achieved is largely determined by the size of the drill rig. The rigs are rated for particular well depths and have limitations in terms of pump capacity and hook capacity (the ability to bring the

drill pipe out of the well). There is not a significant difference in the distances achievable from floating and fixed production systems.

The amount of natural drive in a reservoir has a significant effect on the fraction of oil which can be economically produced. Sources of natural drive include gravity, natural gas caps, natural gas in solution, and water drive through aquifers. The viscosity of the oil and the amount of gas in solution determine how easily the fluids flow. Also, as the reservoir is developed, the relative proportions of oil, gas, and water can change, affecting the flow properties. Where natural drive is insufficient, recovery can be enhanced using gas or water injection. This requires additional wells, tubing, and flowlines, as well as additional equipment on the platform for compressing gas and cleaning water. Where water injection is used, large amounts of produced water may need to be separated out and cleaned.

The nature of the produced fluids also can affect the design. Large amounts of gas can cause multiflow problems if the oil and gas separate out. Sand and corrosion due to sulphur can cause high rates of deterioration to the well and subsea equipment, requiring frequent work overs. Where wax and hydrates are present, these can plug equipment if not handled correctly. Problems such as corrosion, wax, and hydrates can be reduced through chemical injection, though these require additional flowlines and controls. Special subsea equipment may be required to handle high fluid pressures and temperatures. In addition, pressures and temperatures may need to be maintained to reduce wax and hydrate build up.

The basic processing requirements on the platform include removal of sand and water, separation of oil and gas, and preparation of oil and gas for storage or transportation. Different separators may be required if the products from the different wells have separate

lines or flows from individual wells need to be periodically tested. The optimal type of separator in each case will depend on the volume of flow and on the composition, pressure, and temperature of the produced fluids. Before the produced oil can be stored or transported, it may need to be stabilized so that it does not separate out into components. Excess water in the produced gases need to be removed before the gas is either transported, used as a fuel, or reinjected. Where the gas is reinjected, compressors will be required. Equipment is also required to clean produced water before it is disposed of or reinjected. If water injection is increased as natural drive is depleted, significant amounts of water may need to be handled late in the life of the field development.

Either a gravity based platform, a ship or semi-submersible floating system, or a subsea tie-in can be used to develop a field on the Grand Banks. The main advantage of using a fixed platform is that many, if not all of the wells can be drilled and completed at the surface of the platform. Where floating platforms are used, all of the wells are completed subsea, resulting in significantly higher capital completion and work over costs. Another advantage of using a fixed platform is that downtime due to waves and icebergs is significantly reduced. The main disadvantage of using gravity based platforms are significantly higher capital costs. Whereas in the North Sea gravity based structures are slender to reduce the amount of concrete required and to reduce wave loads, structures on the Grand Banks must be much larger to be able to withstand iceberg impacts loads. An additional disadvantage is the inability to move the structure during or after the field development.

Floating production systems consist of the subsea development, a riser base manifold and riser with flow lines and control lines between the seabed and the vessel, and the vessel itself which houses the processing equipment and possibly storage. Both ship or semi-submersible systems have been used. The semi-submersible has somewhat better motion characteristics but less deck weight and storage capacity. Where ship production systems are considered, turret-moored systems will likely to be used to reduce environmental loads and allow quick disconnect. The main design parameters for a floating production system are the water depth, the production rate, the number of flow lines and control lines required, the environmental conditions, and the storage requirements. The water depth determines the cost of the mooring and riser systems. The production rate and the requirements for water and gas injection determine the capacity of equipment required and thus the deck space and weight requirements. The number of flow-lines and umbilicals required affect the design of the riser system required. This will also significantly affect the design and cost of turret-mooring systems. The environment determines how strong the vessel and mooring system must be and influences down-time. The required storage capacity is determined based on the production rate and the expected down-time of the shuttle tanker system. Some storage capacity may also be desirable for wet production (before the water is separated out) in case the processing equipment breaks down. A dedicated storage tanker may be used to reduce downtime when shuttle tankers are not available or cannot moor.

If a well is not completed at the surface, it must be completed at the seabed and a subsea flowlines used to transport the produced fluids to the production site. The subsea system will also include control lines to adjust the pressure at the well head, and injection

lines to bring chemicals, water, and gas to the well bore and reservoir. The well head itself consists of a production tree with which flows to and from the well bore can be controlled and access can be gained for work overs. Wells may be drilled separately or in close proximity from a template. Where templates are not used, subsea wells are generally spaced at least 25 m apart to protect the well heads from falling drilling and work over equipment. Originally, many wells would be drilled from a single subsea template, this has been largely replaced by the use of wells which are completed individually. Individual well completions are less complex than integrated templates, and are more flexible as drilling can take place before installing the manifold, or even designing it. Because of the risk of iceberg scour on the Grand Banks, well heads will be encased in a concrete glory hole just below the seabed. Flowlines may either be buried in trenches or left on the surface, depending on the expected number of incidences and whether or not they can be made failsafe. At present, produced fluids from subsea wells are transported as a multiphase fluid to the host platform. The maximum distance over which multi-phase fluid can be transported is about 15 km, the ability to achieve this distance depends on the particular circumstances, such as the extent of natural drive available. If the distances over which produced fluids can be transported subsea can be increased, then the number of production sites required can be reduced, and additional marginal wells may become profitable. A number of areas of research are being followed to increase subsea transport distance, these include better pumping systems for multiphase fluids; better methods to suppress separation of multiphase fluids and problems related to wax, hydrates, and corrosion; and the development of equipment for subsea separation so that liquid and gas can be transported in separate lines. When considering

development of smaller oil fields, it is of note that if subsea transport distances could be increased to 25 km, many of the smaller fields would be within the range of both Hibernia and Terra Nova. Hibernia could potentially receive tie-ins 10 years after production starts, this may be longer if the reserve base is increased.

The ability to avoid icebergs successfully when choosing a floating production system, and the amount of downtime that will be incurred, are influenced by the iceberg detection, management, and avoidance system. The operators will most likely use iceberg detection and management systems similar to that used for drilling operations. The procedures taken when an iceberg is detected will depend on the range from the platform at which the iceberg is initially detected, its approach speed, the weather conditions, and the operations underway on the platform. The actions likely will be specified in terms of alert zones similar to those that have been used for drilling operations. For drilling operations, three alert zones are defined based on the required time to cease operations and disconnect the vessel mooring system, and the estimated time in which the iceberg could reach the platform. If an iceberg is detected in the outer zone 3, it is monitored. If it appeared to be approaching the platform an attempt to deflect it away by towing will be made. Once the iceberg reaches zone 2, or if it is detected in zone 2, the operators attempt to deflect the iceberg by towing, shut down operations, and disconnect the mooring system. Once the iceberg reaches the inner zone 1 or if it is detected in zone 1, the operators move off site as quickly as possible.

The success of these operations ultimately depends on the effectiveness of the detection system, the towing systems, and the mooring release systems. Aircraft provide

good advance detection capabilities for the general region, but are restricted when environmental conditions are poor. Support vessels can operate in most environmental conditions, however the detection range for their radar systems is generally less than those on production vessels or aircraft. Support vessels extend the overall detection range by conducting search patterns beyond the radar detection range of the production vessel, and they can concentrate their efforts on areas from which icebergs are expected to approach. Though the redundancy provided by the different systems should result in improved overall detection, all the systems are limited when it comes to detecting smaller icebergs in storm conditions.

To model the detection of icebergs using radar, it is necessary to consider the characteristics of the particular radar system, the proportion of received electromagnetic radiation the iceberg returns, the strength of competing signals such as sea clutter, and the proportion of signal lost due to absorption by fog and rain. Detection depends on whether the returned source signal can be distinguished from the competing signals and noise generated within the radar system. Little work has been done to determine the risk of an iceberg reaching the platform. Part of the reason may be that there are large uncertainties regarding the magnitude of sea clutter in high sea states and the effects of sea spray and over wash on the returns from the iceberg. One of the objectives of this research is to do sensitivity analysis to determine how much variations in the radar system capabilities affect the overall risk.

The success of towing operations depends on the environmental conditions, the size and shape of the iceberg, and how soon it is detected. Generally, towing capability decreases with the severity of the sea state. Towing is not efficient when significant wave heights

exceed 4 m. The ability of the operators to disconnect the mooring system is critical in avoiding approach icebergs which cannot be towed. A rough estimate of the reliability would range from 0 if less than 21 minutes are available to 0.98 if more than 12 hours are available (Berry, 1992)

2.5 Risk and reliability-based design

It is important to distinguish between the total risk to personnel and the environment on the one hand, and the target levels of safety used in structural design. Risk to personnel is often defined in terms of the annual probabilities of injury and fatality for an individual. Published levels of risk, based on statistics, can be found for different activities and occupations. In the case of an offshore system, the total risk may include causes such as fire, ship collision, capsize, and wave loads in addition to ice loads. Other factors determining total risk include human errors in conceptualization, calculation, and fabrication, and improper installation and maintenance. The total level of safety is generally very difficult to predict, though it may be possible to qualitatively differentiate between systems. Structural design requirements, on the other hand, are often based on "target" safety levels specified in codes. In limit state design, a number of safety levels may be specified corresponding to the consequences of failure. For example, it may be specified that the probability of a major structural (ultimate) failure possibly resulting in loss of life must be less than 10^{-5} per year and the probability of minor structural (serviceability) failure requiring repair is less than 10^{-2} per year. Total failure rates are approximately an order of magnitude higher than failure rates resulting from extreme loads.

Probabilistic methods are applied to design problems because of the need to give explicit consideration to the uncertainties involved. Madsen et al. (1986), give a brief description of the development of structural reliability, and point out some of the strengths and limitations of using probabilistic methods for design. The main purpose of probabilistic design methods is to provide a rational framework for those parts of the design process that can be controlled.

Structures are generally designed to meet specified standards as set out in national codes. These codes are developed to insure adequate levels of safety to personnel and to the environment, and are developed in consensus by industry, government, and other interested parties. The code for the design of offshore structures in Canada (CSA-S471, 1992) is specified by the Canadian Standards Association (CSA); this is a non-profit independent organization. The design criteria are specified as a number of load combinations and corresponding load factors which the structure must be able to withstand. The rationale used for obtaining these criteria is documented in Jordaan and Maes (1991); the values were determined using a calibration procedure such that the minimal safety level to personnel and the environment is similar to that accepted in other industries. In the case of iceberg loads, which are rare events on the Grand Banks, it is recommended that the design loads be chosen based on a probability of exceedance between 10^{-3} and 10^{-4}.

To determine design loads, analytical models are developed to predict the load corresponding to any set of input parameters. The models must determine appropriate probability distributions, both for these input parameters and for the number of collision

events. Then a probabilistic method can be used to determine the resulting distribution of loads and from this, the design value.

A good review of the use of the different probabilistic methods, such as Monte Carlo simulation, important sampling, and first and second order reliability methods, that can be used to determine the resulting load distributions or design values is given in Melchers (1987). The choice of a design load, given an estimated distribution of loads and the estimated number of collisions, is an extreme value problem. Jordaan and Maes (1984) consider different solution techniques for rare and frequent loading events.

The methods of subjective probability have been applied to the design process by Jordaan and Maes (1984). They assume that the load distribution can be described in terms of a distribution $F_{X|\Lambda}(x|\lambda)$ which is a function of a set of parameters defined by the array λ. If λ is described by the distribution $F_{\Lambda}(\lambda)$, then by applying de Finetti's theorem, the joint probability distribution, F_X for any sequence of loads, $X_1, \ldots, X_n$ which are exchangeable, i.e. the order of the loads has no effect on their probability of occurrence, can be expressed as

$$F_X(x_1, \ldots, x_n) = \int_{-\infty}^{+\infty} F_{X|\Lambda}(x_1|\lambda) \ldots F_{X|\Lambda}(x_n|\lambda)\, dF_{\Lambda}(\lambda) \tag{1}$$

and the distribution for the maximum of the n loads can be expressed as

$$F_Z(z) = \int_{-\infty}^{+\infty} F_{X|\Lambda}(z|\lambda)^n dF_{\Lambda}(\lambda) \tag{2}$$

To find the distribution on the maximum of n future loads if m loads have already been observed, given an initial prior distribution, Bayes' theorem can be used.

Maes (1985) considers the application of subjective probability and exchangeability to design problems in more detail. He briefly touches on the roles of formal decision analysis and design codes as applied to design problems, and gives an excellent review of the different types of extremal problems and the methods which have been used to solve them. Maes then shows how the ideas of subjective probability and exchangeability can be used to develop improved extremal models to handle problems such as short data records, random numbers of events, and uncertainties in data and load scenarios. One particularly useful result is the extension of equation (2) to cases where the load varies as a function of the state of nature α which is itself assumed to be exchangeable. Applications considered include loads due to earthquakes, waves, and ice features.

To determine distributions for iceberg collision loads, models are required to determine the number and types of icebergs encountered in different environmental conditions, the efficiency of the management system, the influence of hydrodynamic effects on the collision locations and velocities, and the collision loads.

One of the earliest studies to determine iceberg risks to offshore platforms on the Grand Banks was carried out by Blenkarn and Knapp (1969). They estimated the number of icebergs passing through a 1/2 degree rectangle based on International Ice Patrol sightings from 1948 to 1956. Their model for the annual impact probability for an iceberg with a platform was based on the assumption that the icebergs traveled in a straight line through the rectangle. Reddy et al. (1980) and Reddy and Cheema (1987) show how to use Monte Carlo simulation to determine confidence limits on the impact probabilities estimated using Blenkarn and Knapps method and show how to use Empirical Bayesian techniques to reduce

the uncertainty as more data on the sizes and directions of motion of the icebergs becomes available.

There are several weaknesses with the basic Blenkarn and Knapp model. First, actual trajectories of icebergs through a degree square can be much longer than straight line approximation. Second, flux depends on both the number and velocities of icebergs passing through a region and can be difficult to measure. In the model described, iceberg trajectories are simulated using a Markov technique in which the statistical variations in iceberg velocities and directions are captured. The number of icebergs in the model is determined by calibrating the model against the number of icebergs observed passing near drill sites.

During the extensive oil exploration in the Arctic during the early 1980's, geometric solutions were developed by the oil industry for determining the probabilities of impacts by ice floes into fixed platforms; these have been published in a number of sources such as Jordaan (1983), Dunwoody (1983), and Sanderson (1988). These methods can be applied to the problem of impacts with icebergs. Because they are simpler and less prone to measurement errors than methods requiring estimates of iceberg flux, they are used here.

Geometrical solutions for determining the expected numbers of encounters with ice features given their sizes and velocities have been presented by Maes and Jordaan (1984) and Sanderson (1988). To determine the number of encounters in different conditions, it is necessary to obtain appropriate data on icebergs and environment and to account for their seasonal variations as discussed earlier. When considering impacts with floating production systems and shuttle tankers, which rely on detecting and avoiding icebergs, it is important to account for the effect of the environment on the probabilities of encounter as well as on

detection. In severe conditions, icebergs may travel several times faster than in ordinary conditions, thus increasing the probability of impact with systems at fixed location. This factor has not been adequately dealt with in published studies.

Models are available to predict the radar probabilities of detection for different sized icebergs and environmental conditions (Ryan and Johnson, 1992). Further verification of the detection probabilities in high sea states are required. The results are in terms of"radar" which relate to the probability of a signal from the iceberg being observed during a single radar scan, rather than the probabilities of detection as required within probabilistic analyses. A number of analyses of iceberg towing records are available (Hotzel and Miller, 1985 and Bishop, 1989) which give an indication of the conditions and number of icebergs for which towing is possible. When applying these results to risk analyses, attention should be given to the definition used for towing success. Ferregut et al. (1987) outline a probabilistic method for determining collision probabilities for ships hitting ice features such as multi-year ice floes. The probability of collision in each case is determined from the probability of detecting the ice feature as a function of range and the probability that the vessel can manoeuvre quickly enough to avoid it.

Aspects of the hydrodynamic interaction problem have been addressed by McTaggart (1989), Isaacson (1988), and Wishahy (1988). These sources describe the basic principles involved and provide analytic solutions for idealized situations. Lever et al. (1988) present a method for determining the distribution of surge velocities of icebergs in random seas. Wishahy, in Cammaert et al. (1993), has extended this analysis to consider the motions of an iceberg in the vicinity of a vessel.

Almost all analytic models used to date to determine global iceberg loads model the ice crushing strength either as a constant or as a function of the nominal contact area. The latter relationships are typically determined by best fits to data based on interactions involving the crushing of both glacial and sea ice in different load scenarios (see for example Sanderson, 1988 and Jordaan and Zou, 1993). Basic research is being done on the failure mechanics of glacial ice (see for example Jordaan et al., 1993), but accurate predictions of global loads from first principles are not yet possible.

The overall collision dynamics in iceberg structure interactions have been considered in a number of studies (Duthinh and Marsden, 1986, Nevel, 1986, and Bruneau, in Cammaert et al., 1993). A better understanding of ice failure mechanics is required to be able to model the effects of friction during eccentric collisions and the variations in loads because of differences in the shape of the icebergs at the point of contact.

The number of published papers dealing with comprehensive probabilistic studies on design iceberg collision loads is fairly small. Two examples, which take significantly different approaches, are briefly outlined here.

Lindberg and Anderson (1987) conducted a preliminary study to determine the return periods associated with various levels of damage due to iceberg collisions for a number of different steel semi-submersible designs. It was proposed that different levels of risk should be allowed for different degrees of damage to the structure. For example: small deformations should be allowed with minimum return periods of 1 to 50 years depending on the member affected; collisions resulting in leakage or bracing failure should be allowed with minimum return periods of 1000 years; and collisions resulting in heavy damage of more than 1.5 m

indentation should be allowed with minimum return periods of 10,000 years. Collision return periods were given for 4 sizes of icebergs. These ranged from 5 years for a 500 tonne iceberg to 25 years for a 15,000 tonne iceberg. The collision velocities were determined from the drift velocities of the icebergs (assumed at 1 m/s) plus the wave-induced relative velocities of the two bodies, assuming sea states of 6, 7, and 10 m significant wave height. The problem of determining whether the iceberg could collide more than once was modelled by assuming that at most 1 collision occurs with each column and two collisions with each pontoon deck can occur. The number in each case was determined based on the initial eccentricity of the collision, which was chosen randomly. The collision loads were determined using a 3 hinge analysis for the plates and stiffeners and a finite element analysis for the stringers and heavier members. The maximum collision area and force were determined based on the initial kinetic energy of the iceberg and a constant ice crushing pressure. Ice strengths ranging from 4 to 10 MPa were assumed and all of the initial collision energy was assumed to be absorbed in the crushing of the ice. The study provided curves showing the force versus penetration for impacts on column bulkheads and between bulkheads. The analysis showed that for the design conditions specified, it should be possible to construct an appropriate vessel. The icebergs are small; this will affect the conclusions significantly.

One of the most comprehensive probabilistic analysis for determining design iceberg collision loads for a fixed structure is the second order reliability method (SORM) implemented by Isaacson and McTaggart (1989) and McTaggart (1989). Though the specific examples presented were not meant to be used for design purposes (for example, an arbitrary collision frequency of 20 events per year was used) the methodology is sound and the cases

run instructive. In the probabilistic model, truncated cylindrically shaped icebergs colliding with a cylindrical structure were considered. The icebergs were assumed to approach the platform with values for the iceberg initial mass, aspect ratio, drift velocity, eccentricity of approach, significant wave height, reference ice crushing pressure, and the ice friction coefficient randomly chosen from given distributions. A major portion of McTaggart's thesis deals with hydrodynamic interaction effects. For the probabilistic analysis he used a simplified model to reduce run times. The collision velocity was determined as the sum of the final drift velocity, when linear diffraction effects were accounted for, and the open water wave-induced velocity of the iceberg. The wave-induced velocity was determined as the value of the calculated response amplitude operator (R.A.O.) for the iceberg at the peak wave period of the random sea, times the significant wave height. The force due to the crushing of ice at each instant was determined as the product of the contact area of the crushed zone normal to the platform times the crushing strength of the ice determined as a function of contact area. A tangential frictional force proportional to the normal crushing force was applied in the model whenever the tangential velocity of the iceberg relative to the structure was greater than zero. The input parameters were modelled using uniform and lognormal distributions based on means and standard deviations from measured data. The iceberg size and velocity distributions were updated to account for the probability of colliding with the platform. A second order reliability method (SORM) was used to integrate the probabilities to get collision loads and kinetic energies. The design force associated with a probability of exceedance of 10% over the life of the structure was determined to be 0.43 GN. The most probable values of the input parameters associated with the design load were as follows: an

iceberg mass of 1.73 million tonnes, an aspect ratio of 0.41, a drift velocity of 0.50 m/s, a significant wave height of 2.21 m, an eccentricity of 0.41, a reference ice pressure of 14.6 MPa, a coefficient of friction of 0.072, and a duration of 3.8 seconds. The SORM analysis showed that for the given application, the iceberg mass and drift velocity were the most critical parameters and the effect of the wave- induced velocity was relatively small. In another run, made for a population of smaller icebergs, it was found that the wave-induced motions were more important than the initial drift velocity.

Ships and floating production systems operating in regions with icebergs must be able to withstand collisions by small icebergs which can not be detected and at the same time, be able to avoid collisions with large icebergs for which the amount of ice strengthening required would be too high. In considering these systems, it is especially important to consider the correlations between the different factors affecting the loads during storm conditions; these will include increased probabilities of collision because of higher drift velocities of the icebergs, increased difficulties in detecting and managing icebergs, and higher collision velocities. One of the main objectives of the thesis is to consider the loads on these types of systems in more detail.

2.6 Economics

Whether or not a field is developed, and the system used to develop it is primarily determined by the oil companies involved. As they have limited resources they need to need to rank development projects. The economic criteria used to evaluate alternatives should

take into account the rate of return on investment, the amount of investment, and the amount of risk involved.

The first step in measuring the investment worth of a project is to estimate its cash flows as a function of time. This requires an estimate of revenues, capital and operating expenses, overhead, taxes and royalties, inflation, depreciation, and insurance and replacement costs. These quantities are in general uncertain and so each option may be associated with a distribution of possible cash flows.

The oil company must be able to compare preferences for different cash flows and distributions of cash flows. The best projects are generally those which provide high returns on investment in the shortest possible time. The calculated net present value of a project at a specified minimal acceptable discount rate is a common measure of economic worth. The discount rate used may be a function of the cost of capital and the rates of return associated with alternative opportunities. The net present value of the project is then the sum of all cash flows discounted to the present year, i.e.

$$NPV = \sum_{t=0}^{n} \frac{C_t}{(1+i)^t} \tag{3}$$

where t is the period, C_t is the cash flow in period t, i is the discount rate, and n is the number of years. The net present value gives an indication of the value of a project over and above the minimal accepted rate of return. Other measures may be used in addition to net present value such as internal rate of return and payback period.

Development strategies and costs can vary tremendously depending on the field location, the characteristics of the reservoir and produced fluids, the particular water depth

and environmental conditions, the amount of infrastructure in place, the market forces at the time (labour, material, supply, demand), and the state of technology. These factors should be considered when using historic data. National and international regulations will also affect the types of systems used, such as the use of double-hulled tankers to reduce the risk of oil spills. Because of the complexity and uniqueness of each oil development, and because detailed costs are rarely published, developing accurate preliminary costs is difficult. Where there is no previous experience in a region, as in the case of floating production and subsea systems on the Grand Banks, accurate estimation is even more difficult. While there is some information on costs from the drilling period in the early 1980's, it is proprietary (Barnes, 1996). The uncertainty in cost estimates for the Terra Nova development in the recent project development plan are given as 30% (Petro-Canada, 1996).

The first step in evaluating an oil field development is to determine the likely production rates and resulting revenues. Oil companies tend to be somewhat conservative in their initial assessments of ultimate recoverable reserves. Often new fields can be tied in when the initial reserves decline and processing capacity becomes available. Tie-ins can be considered in the initial development plan or can be considered on their own merit later. Oil companies usually install extra processing capacity to allow for upside (more reserves than originally forecast). The price of oil over the development of the field must be estimated; in recent years, the price has been relatively stable. The main concern regarding near term oil prices is the possibility of politically related changes. In the longer term, prices may rise significantly if world demand outstrips supply. In estimating revenues, it is also necessary to estimate the amount of production downtime which will occur due to weather,

maintenance, mechanical problems, and icebergs. Rough estimates can be made based on performances in the North Sea. In the case of downtime due to icebergs, estimates must be based on model results and on recorded downtime during drilling operations.

The revenues from a project will depend on the amount of oil produced and the price of oil. The nominal amount of oil produced is predicted as a production curve. Typically there is a stable period at a maximum production rate (determined by the equipment capacity) for a period on the order of 6 years, followed by an exponential decline in production as the reserves are depleted. The rates are determined largely by the reservoir engineers to optimize revenues. The actual production rates may be somewhat lower than the nominal rates due to downtime. Downtime can result if shuttle tankers are not available to off-load crude or if production must be stopped due to mechanical failures, maintenance requirements, high sea states, iceberg encroachment, or damaged subsea equipment.

The price of oil is very significant in determining which fields are economic. Much of the concentrated effort on discovering frontier oil and gas in the seventies and early eighties was a result of the high prices of oil at the time and the projected forecasts of prices. At the time, conventional sources of oil and gas in the U.S. and Canada were in decline and with the OPEC oil embargo, prices rose dramatically. In 1977, the U.S. Central Intelligence Agency published two reports projecting that the world demand for oil would exceed supply by the mid eighties (Lynch, 1996). As a result, analysts projected oil prices based on the assumption of long term oil shortages, even after the fall of oil prices after in 1986. In fact, given inflation there has been a decrease in oil prices in real terms of 3.3% per year since 1986. Since that time, estimates of world oil supplies have been increased and third world

production of oil and gas has increased. According to current estimates, no long term shortages of global oil supplies are expected for at least the next half century. Oil prices are difficult to predict, but current estimates tend to assume relatively stable prices.

When costing a proposed system, the oil company must estimate both the capital and operating costs. Other factors include management and engineering costs, land support, insurance, and taxes and royalties. The capital costs include building or acquiring items, transportation, installation, commissioning, and certification. Installation costs can be quite high, for example to install a large subsea template, a special vessel might be required. As well as the lease time while on site, it might take several days to bring the vessel from the North Sea or elsewhere.

Operating costs include personnel, fuel and other consumables , supplies, inspection, maintenance, replacement, and repair costs. Costs for operating personnel include labour rates, transportation, and food, etc. These consumables are generally delivered by supply boat. There is some tradeoff between capital and operating costs; operating costs can often be reduced by installing more reliable (and in general expensive) equipment. For example, on the Grand Banks, where access to subsea wells is quite expensive, there is considerable incentive to install reliable equipment.

There is in fact very little published literature with costs for offshore production systems and even less giving parametric cost equations. This may be a result of the competitive nature of the industry and the rapid changes in technology and market forces. It is therefore necessary to develop these parametric equations. The form of the equations can be determined either based on theoretical grounds such as the amount of steel and labour

required, or on regressions equations for published cost data. Where published cost data is used, it is important to account for the historical and geographic variations in material costs, labour costs and efficiencies, and both manufacturing technology and the technology of the systems being produced. There may be additional variation depending on particular circumstances such as reduced costs where a shipyard need work or abnormally high costs due to unforeseen consequences.

When looking at historical costs, it is important to consider the conditions at the time and location of the development. Until recently, because the fields being developed in the North Sea were large and because the price of oil was higher, less concern was given to costs than at present. With the lower oil price at present and the necessity to start developing smaller fields, economy is of great importance. The location of the development is important because labour costs vary significantly.

The magnitudes of change in a selection of prices, wages, and borrowing rates are shown in Figure 2.3. The price of oil in the US is seen to have remained between $13 US and $20 US for over 10 years now. The trend in price of fuel oil (not shown) follows that of crude oil quite closely. The Canadian prime rate is seen to have gone up as fuel prices increased through the early 1980's. There may not be such a significant correlation in general. The price of oil production equipment and casing also increased in the early 1980's. The price of casing, which is strongly correlated with the price of steel, has dropped somewhat, while the price of oil and gas production equipment, which is more labour intensive, has continued to rise. There is a limited amount of data on shipbuilding and repair

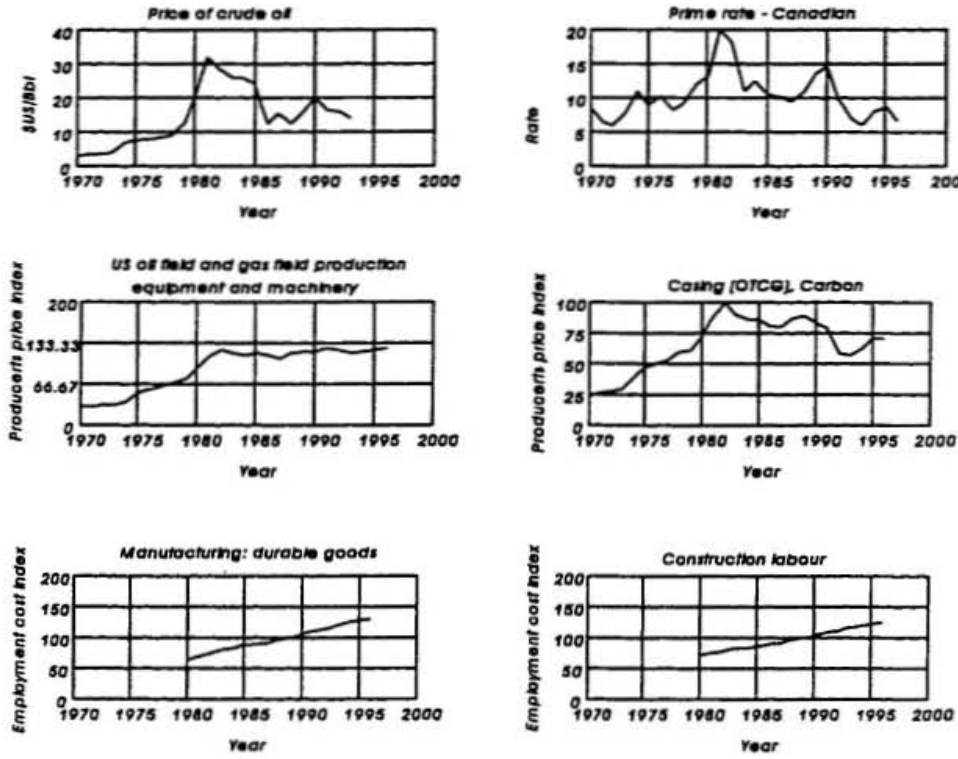

Figure 2.3 Economic indicators

Sources:

Historical Canadian prime rate:
Public survice provided by David Bryson
http://vanbc.wimsey.com/~dbryson
http://www.geocities.com/WallStreet/Floor/4829/disclaim.htm

US price of crude oil:
New Mexico Petroleum Recovery Research Center, New Mexico Tech
http://baervan.nmt.edu/soft/usgas.html

Oil production equipment, casing, construction labour, and manufacturing labour:
US Bureau of Statistics (http://stats.bls.gov)

(not shown), these costs have in general risen with labour costs. The US shipbuilding industry has not remained competitive and may not be representative of the world market. The employment costs indices shown for construction and manufacturing indicate a fairly steady increase in labour costs.

Some selected historical exchange rates are shown in (Figure 2.4). It is seen that over the past 10 years, the variation in exchange rates with Britain and the US has remained relatively stable while the Japanese yen has risen substantially.

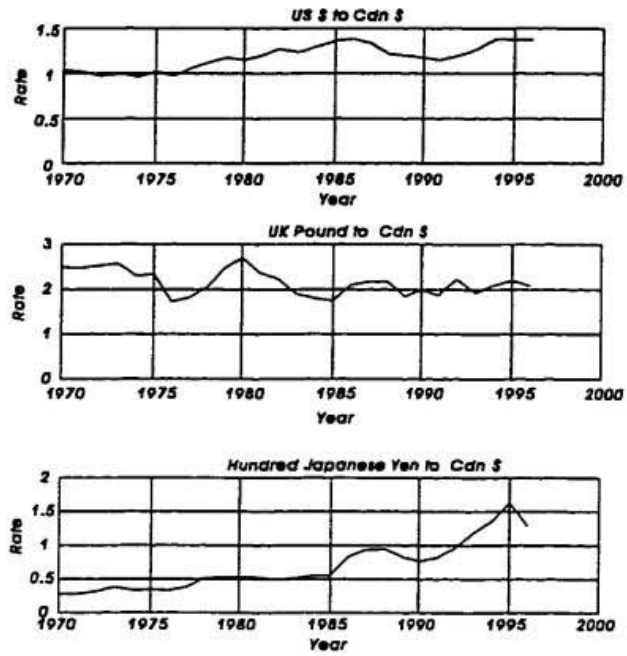

Figure 2.4 Historical exchange rates

Source:

Historical exchange rates from
FRED - Federal Reserve Economic Data, Federal Reserve Bank of St. Louis
http://www.stls.frb.org/fred/abotfred.html

The prices of shuttle tankers and production vessels, which take a large capital investment, time, and availability of an adequate ship yard, are very subject to supply and demand. After the drop in oil prices in the eighties, there was a relatively low demand for new developments and prices consequently were low. Shipyards were also quite competitive for new built ships. More recently, with regulations requiring double-hulled tankers, there have been fewer tankers available for conversion to floating production vessels. Also, the demand for drilling and production vessels has been increasing. An illustration of how much prices can change is given below (Anonymous, 1995). Drill-rig rates dropped around 1983 as demand dropped compared to supply . They have remained low until 1995, when rig day rates increased dramatically in a short time period, in some cases doubling. Deep water and harsh environment rigs commanded around $80,000-90,000 US per day in June, 1995. This has resulted in part because of recent exploration successes in harsh environments and deep water. The rates are not expected to change dramatically as it costs up to $250 million US to build deep water and harsh environment rigs; the author states that it would require rates in the order of $200,000 per day before contractors would start building high specification rigs.

There are a number of additional economic factors more specific to the Grand Banks. Because of the lack of infrastructure, there is less competition at present, fewer construction facilities, and more of a learning curve required than in the North Sea. In addition, because specialized work vessels may need to be brought in from the Gulf of Mexico and the North Sea, mobilization and repair costs may be relatively high.

Other costs incurred with a development will include preliminary engineering, general overhead costs, land based support, and import duties. These will be included at a later date as percentages of capital and operating costs.

A generic royalty regime applicable to all future offshore petroleum development except the Hibernia and Terra Nova fields has been established by the Government of Newfoundland and Labrador (Canada Newswire, 1996 June). The regime is comprised of two components: a basic royalty and a two tier net royalty. The payment of a basic royalty commences upon the start of production increasing in steps as a function of cumulative production level as follows. An earlier increase in the basic royalty rate to 5 and 7.5% will be implemented if cumulative gross revenues exceed project costs prior to the production level indicated above. As the cumulative gross revenue from a field exceeds the cumulative project costs the two tier net royalty is activated. Under Tier 1 when cumulative gross revenue equals cumulative project costs (including a return on project costs of 5% plus the long term government bond rate) a royalty of 20% of net revenue is payable by the field developer. Any basic royalty paid is

Table 2 Generic royalty regime

Basic Royalty (% of Gross Revenue)	Cumulative Production Level (Million Barrels)
1.0	0 - 50 (or 20% of initial reserves)
2.5	50 - 100
5.0	100 - 200
7.5	200 onward

credited against this Tier 1 royalty. When the cumulative gross revenue equals the project costs (including a return on project costs of 15% plus the long term government bond rate) Tier 2 is activated. This requires payment of an additional royalty of 10% of net revenue. In this case any Tier 1 royalty paid is included as an allowed project cost in calculating the Tier 2 royalty payable.

The amount of basic royalty payable is determined solely by the production rate. In system optimization and selection it can be considered a common cost largely unaffected by any higher capital or operating costs characteristic of offshore petroleum production in the ice environment of Canada's East coast. The activation of the two tier net royalty component is dependent on the timing of capital and operating expenditures versus revenue flow. This may be a factor in the NPV analysis of potential production systems with different capital versus operating costs over time. At present taxes and royalties are not modelled.

The detail to which one must estimate capital and operating costs depends on the stage of analysis. In preliminary design, parametric cost equations are often used. These relate costs of the components to the design variables, for example the cost of a floating production vessel may be modelled as a function of vessel displacement, which in turn is a function of the required production capacity. In the final optimization of systems, it may be necessary to obtain costs of individual components available either from manufacturers or through resale.

2.7 Consideration of human life and the environment

While loss of life and environmental damage are not included in the overall analysis, their effects on decision-making are discussed briefly in this section. The evaluation of offshore systems requires consideration of the probability and consequences of accidents in addition to economic evaluations based on straight revenues and costs. Types of risks include excessive environmental loading due to icebergs and waves, ship collision, fire, capsize, blowout, design failure, and improper maintenance. These accidents can result in damage to equipment and environment and loss of life. Damage to equipment is mainly the concern of the companies involved and can be evaluated in monetary terms. In the case of loss of life and environmental damage, more than just the companies involved are affected. In this section, the monetary and intangible costs of fatalities, injuries, and environmental damage to the companies involved and to society and individuals is discussed. Then the effect of these factors on the choice of designs and the viability of developments is briefly considered.

Workplace safety has in general been improving over the recent past (U.S. trends, for example, are shown in Figure 2.5) with higher concern for safety issues and the development of better practices. Increased liabilities for accidents have undoubtably contributed to this.

The offshore oil industry has historical had a relatively high rate of incidents but its record has improved in recent years. For example, following the Piper Alpha incident off Britain and the subsequent inquiry (Lord Cullen's inquiry), a number of changes in offshore safety legislation were implemented, and more effort was expended to include the offshore workforce in decisions (UKOOA, 1997). Almost 5 billion UK pounds have been invested on improved safety since the Lord Cullen's inquiry. Information on the recent rate of injuries

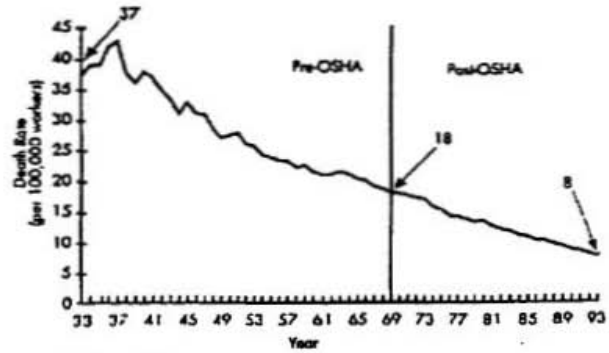

Figure 2.5 Change in fatality rate in US workplace.

Source: CATO Handbook for Congress - 105th Congress,
Section 36 - Occupational Safety and Health Administration
Internet location: http://www.cato.org/pubs/handbook/hb105-36.html

and deaths in the offshore oil industry can be found in an Internet publication by the UK Offshore Operators Association (UKOOA, 1997). The data are based on reports by the United Kingdom's Department of Energy and Health and Safety Executive. Figure 2.6 shows the number of minor injuries and the number of serious injuries and fatalities in the offshore oil industry of the United Kingdom for each year from 1988/1989 through 1994/1995. Figure 2.7 compares the number of injuries and fatalities in the offshore oil industry to other industries. Both figures indicate injuries of all types including fatalities and are given as number per 100,000 employees.

A number of points regarding these figures should be made. First, the time period shown is quite short and the trend in safety is exaggerated. Second, the number of fatalities is usually quite low compared to the number of severe accidents. For example, a UK Government Press Release (1997a) indicates that in the period 1994/95, there was one fatality and 41 serious injuries. In the following period of 1995/96, there were five fatalities, and 42 serious injuries. Based on an estimated worker population of 29,003, for the second

period, this gives fatality and serious injury rates of 17.2 and 144.8 per 100,000 respectively. Third, the injury and fatality rates can change significantly depending on the occurrence of major incidents. For example, the above data are for periods following the 1988 Piper Alpha disaster. The number of fatalities should higher be in 1990 and 1992 when the Brent Spar and Cormorant Alpha helicopter crashes occurred (UK Government Press Release, 1997b).

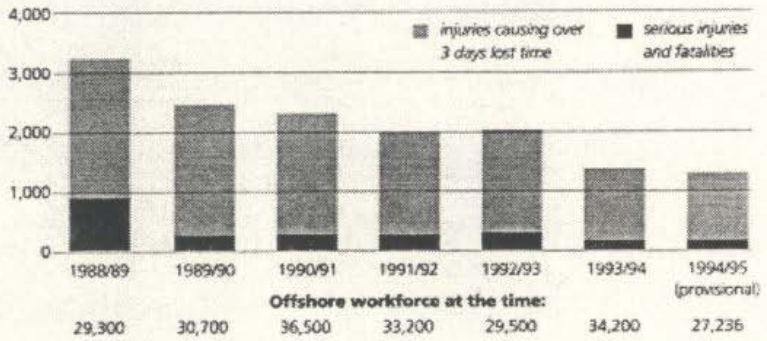

Figure 2.6 Number of injuries and fatalities in UK offshore industry by year.

Source: UK Offshore Operators Association
Internet location: http://www.ukooa.co.uk/safety/offshore.html

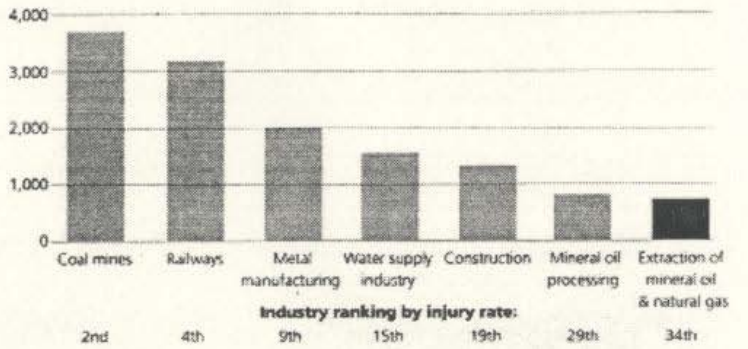

Figure 2.7 Comparison of number of injuries and fatalities in selected UK industries

Source: UK Offshore Operators Association
Internet location: http://www.ukooa.co.uk/safety/offshore.html

These figures show the importance of the total risk to individuals due to smaller accidents. At the same time, a single major accident could affect on the order of 100 people.

Injuries and the loss of human life affect foremost the individuals involved and their families. When considering safety standards, permits for projects, and compensation, it is necessary to consider the worker's point of view in addition to others. It can be argued that, because money becomes worthless to a worker on death, no amount of money can compensate for certain death (the disutility on death in terms of money is negative infinity). With this reasoning and using standard decision-making techniques, it would be irrational for anyone to accept any possible increase in risk, no matter what the possible gains are. In real life, people are subject to a background degree of risk (which depends on age and circumstances) and often choose to increase this exposed risk for reasons such as recreational fun and work which is more interesting and profitable. In most of these cases, the increase in risk is acceptable as long as the total level of risk remains small.

An alternative conceptual framework, which could explain the acceptance for increases in risk, would be to assign a utility of zero to death and assign a positive utility for each moment of life with magnitude depending on life experiences. The utility would depend on the beliefs and circumstances of the individual considered. Suppose that one could assign a utility function representing quality of life for a particular instance of life experiences as shown for curve 1 below (in reality there would be an infinity of possible instances of life experiences with likelihoods which could not be estimated or enumerated). One has an option to exchange Curve 1 with random node having one outcome (Curve 2) with the same life span and an improved quality of life, and the other outcome (Curve 3) with

a short life span. The total utility for each instant of life experiences would be the integral of quality times time.

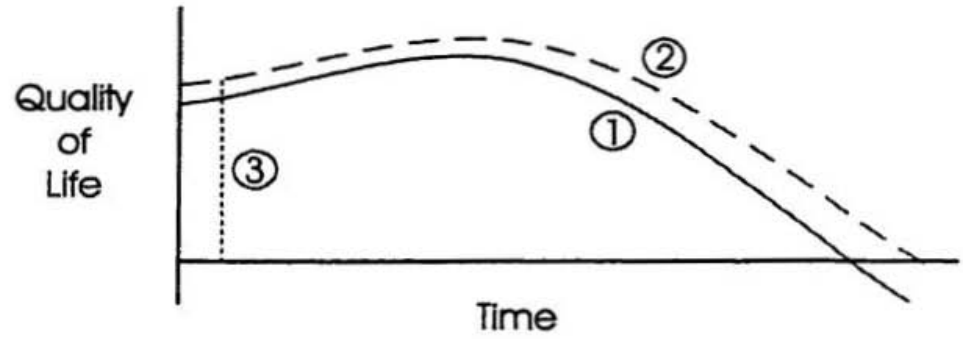

Figure 2.8 Alternative conceptual framework for the value of life

Within this type of framework, one might rationally choose to increase risk.

It is sometimes argued that a worker voluntarily accepts a certain amount of risk in the workplace and in return receives a better salary than would be available otherwise. This may be true if an adequate range of job options are simultaneously available, but it is often the case that the worker is compelled by circumstances to accept a higher than normal degree of risk. In addition, a worker usually does not have the required information to properly assess risks. For these reasons, it is important that first, that the worker be protected through safety regulations; second, adequate compensation packages be in place in case of injury or death; and third, punitive measures be taken out against companies in cases of negligence. It is also important to clearly publish historical and perceived levels of risk.

There are a number of reasons for a company to implement adequate safety measures. Employers are responsibility to workers and families and should attempt to reduce risks. Good safety practices help to keep morale up amongst employees and maintain the company's corporate image. In the case of a major accident, even if insurance covers part

of the accident, rates can go up. In the case of the Piper Alpha, the accident resulted in stiffer regulations, requiring a larger investment in safety. A production system might be shut down until safety regulations are met. In addition, the company suffers the loss of qualified personnel, and possible difficulty in hiring new personnel. Compensation and penalty costs can become quite large if gross negligence is shown; furthermore these type of costs are very unpredictable. Given the costs and benefits of increasing safety, there is a trade-off to industry. This trade-off can be altered somewhat by government through legislation and legal assessments.

A major accident which occurred in the oil industry off the east coast of Canada was the capsize of the Ocean Ranger in 1982 in which 84 men were killed (Schlager, 1994, Maclean's, 1984, Woodworth, 1984). One month after the disaster, families brought a 1.7 billion dollar lawsuit against the rig's owner Ocean Drilling and Exploration Co. As of January 1984, of the claims for the 67 Canadian workers killed, 13 settlements remained unresolved. For single men, the average settlement with their parents was $40,000. For men with families, the average settlement was $444,000 tax free. The article noted that the settlements were considered generous by Canadian standards at time, but that similar types of claims in the US were usually more generous and had produced settlements up to $64 million.

The main type of environmental damage that could occur is spillage of oil. The public has become increasingly intolerant of oil pollution as the awareness of the effects of pollution has increased and both total volume of oil transported and the sizes of individual vessels have increased. Damage to the environment can result directly in loss of income for

fishers if stocks are damaged. For shuttle tankers at the transhipment terminal there is also the possibility that damage to shorelines will affect the livelihoods of people there. There are also more intangible factors including death of animals, the loss of habitat, and pressure on endangered species.

From the view point of companies, environmental issues are becoming increasingly important. Buckley (1991) gives the following possible costs for poor environmental management.

- *statutory penalties for breaching regulations;*
- *forfeiture of assets;*
- *cleanup, repair and rehabilitation costs;*
- *compensation claims, citizens' lawsuits and class actions;*
- *closure by regulatory agencies or court injunctions;*
- *upgrading, retrofitting or replacing equipment to more stringent standards;*
- *delays in approvals for future projects;*
- *lost market share from poor public image of product boycotts;*
- *falls in share prices;*
- *higher cost of finances;*
- *reduced credit from suppliers; and*
- *higher insurance premiums.*

The magnitude of possible costs can be seen in the Exxon Valdez case which occurred in 1989. This accident was severe both because of the amount of oil and the proximity to shorelines. The accident involved the spillage of 258,000 barrels; this was 20% of the oil on board at the time (Robert and White, 1995). The spill contaminated 1000 miles of shoreline (EVOSRP, 1994). The Oil Pollution Act of 1990 (OPA 90) enacted in the US was in part a response to the Exxon Valdez to prevent future incidents (Robert and White, 1995). The main effect of the act is to increase the liability for oil leakage in US waters. Liability is increased to 1200 $US/gross ton or $10 million for vessels larger than 3000 gross

tons. More importantly, the operators could be exposed to unlimited liability under a number of conditions including gross negligence. In addition, the operators must show evidence of financial responsibility. The act also imposes the phase out of single hulled tankers.

The direct costs to Exxon have been very high. Costs unrelated to pollution consisted of vessel damage of 25 million US dollars and cargo loss of 3.4 million US dollars. These were very small compared to losses related to pollution. As of August 1991, Exxon had spent 2.1 billion US dollars in clean up costs. To the State of Alaska and the U.S. Government, Exxon must pay a civil damages claim of ten annual payments totaling 900 million US dollars for restoration and replacement of natural resources, plus a criminal plea agreement of 250 million US dollars. Of the later claim, 125 million US dollars was later remitted because of Exxon's cooperation in the cleanup, payment of claims, and subsequent environmental actions. In addition to the above, Exxon must pay 5 billion US dollars in punitive damages which is to be payed to 14,000 commercial fishers, natives, business owners, landowners and native corporations. Exxon is still appealing this latter settlement (Clarke, 1997). The amount of the above costs that Exxon will recover from insurance companies is still uncertain and is being contested in the courts (Drago, 1996).

Hopkins (1992), based on NRC (1991), gives a range for clean up costs of 12,000 to 68,000 US dollars per ton and an approximate claims cost of 30,00 US dollars per ton. Claims in the Exxon Valdez case may reach 90,000 US dollars per ton. In applying these numbers to Grand Banks, consideration should be given to the distance from shore and the different legal system in Canada.

Given the difficulties in assessing the total risk (in terms of probabilities and consequences) to personnel and the environment, the main question is how should one account for this risk in comparing and assessing proposed production systems. The target probabilities of failure used for choosing design iceberg impact loads are very low (10^{-5}). Using a base case cost associated with an accident of billion dollars, the expected cost is then $10,000. The total probability of an accident may be 10 to 100 times larger than this, in which case the expected cost ranges from 100,000 to one million dollars. Society must choose appropriate penalties to compensate injured parties and at the same time, ensure that companies put a reasonable amount of effort into meeting appropriate safety standards. To incorporate the influences of safety when comparing two systems, for example an FPSO and a GBS, the designers should consider the past accident records for the two systems, how much experience is available, and how well the influence of new problems and approaches on accident rates can be assessed. On the Grand Banks, the main new feature is the presence of icebergs. For floating systems, the key issues are the ability to detect icebergs and, if necessary, move the system off site. There is presently a degree of uncertainty regarding the capability of the different detection systems, disconnect systems, and the failure strength of the ice. The sensitivity of the design loads to these parameters are addressed in Chapter 7. For GBS based systems, uncertainty regarding detection is less important, but the uncertainty regarding ice loads is increased because of the larger contact areas involved. In both cases, a major design issue is the safety factor to use for ice strengthening given these uncertainties.

2.8 Decision and probability theory

The objectives of decision-making are to recognize and choose between alternative courses of action. Where decisions influence more than one person, it is also important to develop a framework in which ideas can be communicated and rationally appraised and modified (Smith, 1988). Good decision-making entails the following steps:

- development of clear objectives,
- recognition of alternatives,
- identification of the possible outcomes associated with each choice,
- evaluation of their probabilities of occurrence, and
- evaluation of ones preferences over the distribution of outcomes associated with each choice.

Recognition of alternatives requires knowledge of the problem at hand and creativity in generating ideas. Typical decisions include choosing whether or not to undertake a proposed project, choosing between alternatives, and deciding if further analysis, data, or research and development is required. The decision makers may be required to generate ideas for new systems and find ways to define uncertainty better and reduce it .

It is important that an appropriate level of effort and detail be chosen that relates to the time and resources available and to the extent to which outcomes can be influenced. This can range from quick intuitive analysis for minor decisions to the use of a complete formal analysis for important decisions potentially with large consequences. Even where formal decision methods are required, it is still essential to break the problem down into a manageable set of alternatives and random outcomes that incorporate the essential elements

of the problem. In many applications, including design, the decision process is iterative. In preliminary design, one considers a broad range of possible alternatives, using approximation analysis to determine if any are viable, which is the best, and if more information is needed. As the number of alternatives is reduced, optimization of each alternative may be required before the final comparison.

Formal decision theory provides a rational method for numerically evaluating and ranking preferences between complex choices. It is applicable when the decision makers can meet a number of general restrictions regarding the assignment of probabilities and preferences. The problem is broken up into a tree incorporating the possible sequences of decisions and chance events. For illustration, consider the tree in Figure 2.9. At the initial point of decision, the decision maker has identified a finite number of options α_i, $i=1..n$. A

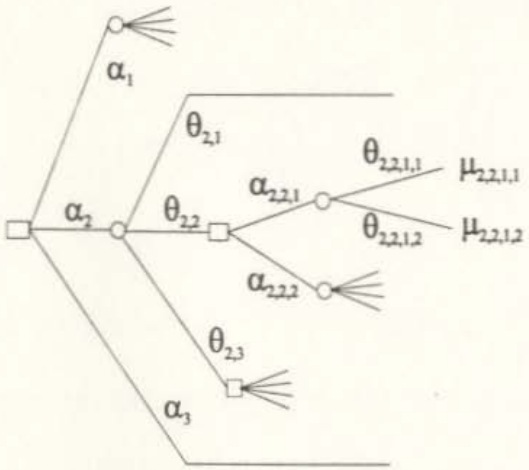

Figure 2.9 Example decision tree

continuous range of options might equally apply, for instance when choosing a continuous quantity such as vessel displacement. For each alternative, the decision maker identifies the subsequent chance outcomes θ_{ij}, $j=1..n_i$ which can occur. Some of these chance events may

then be followed by further decisions, etc. For each path, the decision maker assigns values for the relevant attributes such as profit and risk, or else an appropriate utility value μ associated based on the attribute values (to be discussed).

Once the structure of the decision tree has been laid out, it is necessary to assign probabilities to the different outcomes for each alternative. The decision maker should use all information at hand in assessing probabilities. The operational definition of probability advocated by de Finetti (1972) was developed to reflect the decision maker's best personal judgement. It can be measured in several ways including asking oneself how they would behave given a fair bet. Methods for choosing initial distributions and updating them to include new or additional information may found in de Finetti (1972), Raiffa and Schlaifer (1961), and Maes (1985). Hong and Nessim, (1994) give examples of the use of Bayesian regression analysis. The influence of uncertainty on safety and economics and the assessment of probabilities will be addressed further in Section 3.2. In addition, different probabilistic methods and the use of sensitivity analysis where probability distributions cannot reasonably be assigned are described.

The final step in the decision-making process is to evaluate and rank one's preferences for the different choices given the assessed probabilities for the outcomes. Consider first the choice between two systems A and B whose outcomes are represented in terms of a single attribute X representing profit with assigned probability density functions shown in Figure 2.10. Option A has a higher expected profit, but also a higher probability that the profits could be low, i.e. a higher level of financial risk. To compare options with different distributions of outputs, the decision maker must develop a scheme for evaluating

their preferences given risk. Utility theory provides a solution in cases where the decision maker can specify preferences so that they meet the four rules defined below (Smith, 1988).

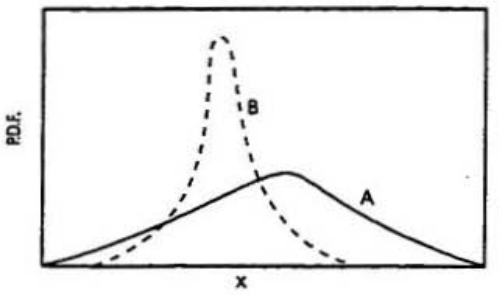

Figure 2.10 PDF's for attribute X corresponding to options A and B

First, write $P_1 \prec P_2$ if the distribution of outcomes P_2 is preferred to the distribution of outcomes P_1 and write $P_1 \approx P_2$ if the distribution of outcomes P_1 is equally preferred to the distribution of outcomes P_2.

Rule 1

if decision rules d_1 and d_2 give rise to identical distributions of rewards P_1 and P_2, then d_1 and d_2 should be equally preferred i.e. $P_1 \approx P_2$.

Rule 2

i) *(comparability)*, for all P_1, P_2, either $P_1 \prec P_2$, $P_1 \approx P_2$, or $P_1 \succ P_2$

ii) *(transitivity)*, for any distributions P_1, P_2, P_3

$P_1 \prec P_2$ and $P_2 \prec P_3 \Rightarrow P_1 \prec P_3$,

$P_1 \prec P_2$ and $P_2 \approx P_3 \Rightarrow P_1 \prec P_3$,

$P_1 \approx P_2$ and $P_2 \prec P_3 \Rightarrow P_1 \prec P_3$,

$P_1 \approx P_2$ and $P_2 \approx P_3 \Rightarrow P_1 \approx P_3$,

Rule 3 *(consistent ordering of lotteries)*

for all distributions P_1, P_2, P and all probabilities $0 < \alpha < 1$,

$P_1 \prec P_2$ if and only if $\alpha P_1 + (1-\alpha) P \prec \alpha P_2 + (1-\alpha) P$

Rule 4 *(comparability of rewards)*

for all distributions P_1, P_2, P such that $P_1 \prec P \prec P_2$, there exists values $0 < \alpha, \beta < 1$ such that

i) $P \prec \alpha P_2 + (1-\alpha) P_1$

ii) $P \succ \beta P_2 + (1-\beta) P_1$

Given that these four rules apply, then the decision maker can define a utility function $u(\mathbf{x})$ mapping vectors of attributes $\mathbf{x}$ to the real line R such that the distribution P_i of outcomes resulting from any decision d_i is equally preferred to any certain event c with utility

$$u_c = \bar{u}(d_i) = \int_{\Omega} u(\boldsymbol{x}) f(\boldsymbol{x}|d_i)\, d\boldsymbol{x} \qquad (4)$$

where $f(x|d_i)$ is the probability density function for $\boldsymbol{x}$ given d_i. Thus, all distributions of preferences can be mapped to a single point on the real line such that they can be compared, i.e. the best decision is the one with maximum expected utility. To evaluate ones utility function, a number of methods are available which involve comparing preferences for specific outcomes against preferences for mixtures of two reference outcomes with preset utility (for example the best and worst outcomes, if they exist, set with utilities 0 and 1 respectively).

The above method must be expanded to the case where chance outcomes are followed by further decisions. To accomplish this, one starts with the terminal nodes at the right of

the decision tree and works back to the start. This is known as folding back the tree. Where there is a chance node, it is replaced with the expected utility over all of the associated paths. Where there is a decision node, it is replaced with the highest utility amongst all of the associated paths.

The disutilities of loss of life and environmental damage are sometimes included in formal decision-making. This requires determining the probabilities and magnitudes of different events (i.e. number of lives, volume of oil spilled, etc.). It is necessary, in the final stages, to map one's preferences for different parameters (money, loss of life, and environmental damage) on to a single scale so that they can be ordered and the best solution chosen. It is generally easier to determine utilities for a given parameter in isolation. In the case of money, one determines a utility function which accounts for one's aversion or preference for risk. In the case of losses of lives, one might have a disutility for large events (i.e. the loss of 100 people in one event as opposed 100 small events), though the main reason for this may be to avoid publicity. In the case of pollution, one large spill may put more stress on the environment than several small ones.

An example methodology for making decisions based on damage, injuries, and number of lives lost, in opposition to costs, may be found in the doctoral thesis by Nessim (1983). The application considered is the amount of effort to expend in control during structural design and fabrication. The problem addressed is whether reliability analysis can be extended to account for the difference between target reliability and total risk when failure due to errors is included. The probability of finding errors increases with effort (though at a decreasing rate) and therefore cost. With less errors, the probability of failure and the

resulting number of injuries and deaths, and requirements for maintenance and repair are reduced. Nessim develops a multidimensional utility function "expressed in terms of unidimensional functions and tradeoff constants under certain assumptions of utility and preferential independence" in Section 4.4 of the thesis. In Section 4.4.2.b), Nessim considers a number of disutility functions for the number of lives lost. For the study, he chooses a risk neutral utility function (in terms of number of lives lost per accident) largely because choosing a risk averse or prone utility function would result in a greater total number of deaths. In the example application, Nessim uses subjectively chosen constants for the tradeoff between cost and the number of lives.

In society, there exist effective tradeoff coefficients between cost on the one hand, and safety and the environment on the other. These tradeoff coefficients change over time and region depending on the economics and the degree of respect for life and environment. Society influences the decisions individual companies make by fostering better awareness of issues and by imposing regulations and fines.

An important question relates to the viability of answers given by probability theory when a system is complex and it is difficult to adequately quantify one's knowledge regarding uncertain parameters and processes in terms of probability distributions. In such cases, it is important that the designer identify such sources of uncertainty and use sensitivity analysis to determine how important they are. It may also be appropriate to run sensitivity analyses within an overall probabilistic framework to determine the effect that different assumptions have on the output distributions and related statistics. The base case analysis should be based on the best available information as safety factors incorporated at each

model step will multiply to give an overly conservative design. The result will be a number of answers, each of which should be considered as conditional on the particular input assumptions. At the end, the designer should consider all of these results, along with the likelihood of the assumptions used, in order to choose a design with a reasonable degree of conservativism, given the current state of information. If a responsible decision cannot be made, then further information may be required.

It should be noted that it is not always possible to meet the conditions for developing a utility function; in particular, the case of transitivity can break down where there is more than one person involved. Furthermore, it can be quite difficult to assess ones own preferences when there are many outcomes and attributes. For the economic analysis considered here, loss of life and environmental damage are not considered and the oil companies are assumed to use risk neutral utility functions (i.e. dollars can be used as the utility function). Because oil companies tend to share large projects in order to reduce risk, any errors resulting because of the assumption of risk neutrality are smaller than might otherwise be the case.

As a conclusion to this section, it is worth briefly considering the choice of a decision framework based on probability and utility theory. One alternative framework which might be considered to probability theory is the fuzzy set approach. The fuzzy set approach has been used quite successfully in control theory in smoothing the response of systems to changes in input parameters. The fuzzy set approach has also been used for encoding vague human language. A brief review of the application of fuzzy set theory to structural safety is given in Nessim (1983), in which a number of approaches based on fuzzy set theory are

discussed. The main conclusion was that analyses based on fuzzy set theory are not precise enough to "be of operational value in decision-making". Nessim also refers to a paper by Lindley (1982) in which Lindley puts forth the generalization that Bayesian probability is the only reasonable measure of uncertainty. Though this has been questioned in general, Nessim supports the results in the case of structural decision-making. With probability theory on the other hand, there exists a well developed decision framework for making rationale decisions. In referring to probability theory, consideration is given to the 'subjective' school of probability in which probability is ultimately a measure of ones beliefs regarding values of uncertain parameters. It is still necessary, especially in engineering applications, to be able to soundly defend these beliefs based on observations, statistics, appropriate logical and physical arguments, and inference. As discussed in the next chapter, there exist methods for measuring ones beliefs. It is also especially important in reliability analysis that there exist well developed probabilistic models for extremal analysis. It should be noted that fuzzy set advocates often criticize probability theory as being objective (i.e. based only on observed data). This ignores the important area of subjective probability which is of special important in decision theory. Furthermore, whereas subjective probability has a rigorous operational definition of probability based on an individual belief as measured in a bet, no rigorous operational definition of fuzzy membership is available.

3 PROBABILISTIC APPROACH

3.1 Overview

In this chapter, the use of the probabilistic approach in reliability-based design and economics is discussed. First, in Section 3.2, different sources of uncertainty and their effect on decision making are discussed. The roles of sensitivity analysis and probability theory are then introduced. In Section 3.3, de Finetti's operative definition of probability and methods for measuring one's probability are described. The issue of defining probability when more than one person is involved is briefly considered. In addition, the requirement for coherence in belief when using different methods for incorporating new information is discussed. In Section 3.4, the concept of "exchangeability" is defined and its role in mathematical inference is discussed. Existing techniques for refining one's probabilities given new data are examined and possible extensions of the general technique are suggested. In Section 3.5, the concept of "partial exchangeability" and possible applications are discussed. In Section 3.6, the use of extremal analysis in determining design loads is discussed. In Section 3.7, methods for integrating probabilities are reviewed and the method used is outlined.

3.2 Introduction

A major aspect of decision making concerns the methods used in dealing with uncertainty. Uncertainty arises in a number of ways. When using quantitative methods to analyse problems, one defines the problem in terms of parameters and models representing the system of interest. Uncertainty results because the models and parameters are only an

approximation of reality. This type of uncertainty can be difficult to quantify and may be quite large if the processes involved are not properly understood. When parameters are measured directly, there may be variance and bias resulting from the methods used. When direct measurements of a parameter are not feasible, it may be possible to determine its value indirectly from other measured parameters through functional relationships. The uncertainty on the output parameter is then a result of both the uncertainty on the input parameters and the uncertainty in the functional relationships.

Inference may be used to assign a probability distribution to a parameter for an entity that cannot be measured directly, when that parameter has been determined for a set of entities or events which are similar. As pointed out by de Finetti (1972) every entity or event is in fact in some way unique, and it is a decision on the part of the modeller regarding which sets to treat as a statistical population. When describing variation in a population using parametric distributions, and the number of samples points on which the parameters for the distribution are based is limited, there is additional uncertainty. The decision maker must then choose a rationale for assigning the parameter values. In the Bayesian approach the parameters are treated as random quantities. Inference is considered further in Sections 3.4 and Section 3.5 .

The decision makers must try to make the best possible decision with the information, resources, and time available. Two important tools used when there is uncertainty are probability theory and sensitivity analysis. Sensitivity analysis entails determining the amount of change in the outputs from a given model when inputs parameters or model assumptions are varied. If the choice of model assumptions affects the decisions

significantly, then the model may need to be enhanced or replaced. If the values of uncertain parameter can affect decisions, then the decision makers may try to acquire better values. Where this is difficult or expensive, the decision makers may be able to use probabilistic methods. Probability theory gives the decision maker quantitative tools to measure their belief regarding the likelihood of different parameter values and to incorporate new information in a coherent manner. These beliefs are described in terms of probabilities or probability distributions. If the decision maker can coherently describe his or her beliefs in terms of probabilities, then rational decisions incorporating these beliefs can be made. When it is not possible to describe one's beliefs regarding decision parameters in terms of probabilities, it is difficult to make rational decisions.

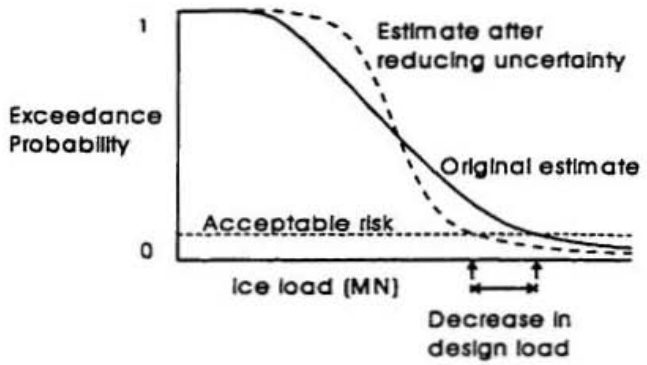

Figure 3.1 Effect of reducing uncertainty on design load

The effect of uncertainty in design problems is illustrated in Figure 3.1. The solid curve shows an exceedance distribution for ice loads on a structure. This distribution must be assigned by the designer given available information at the time. The second curve represents the exceedance curve after obtaining additional information. As the level of

uncertainty is reduced, the design load corresponding to a specified acceptable level of risk is reduced. It should be noted that where the designer chooses to use stochastic models, for example in defining the number of iceberg impacts per year, the stochastic uncertainty associated with annual variations is part of the model. The types of uncertainty which are reduced through additional information are those associated with models, biases, and lack of data. Even when there is considerable uncertainty, it may be possible to choose a design which is conservative enough to ensure safety, and still be economic. The decision maker must also assess whether further work to reduce uncertainty is cost efficient.

In economic problems, one generally is trying to optimize profits. A simple example is presented below to illustrate the problem when there are unknown input parameters. Assume that there is a function defining profit in terms of a continuous parameter x, chosen by the decision maker, and in terms of a discrete random parameter θ which can take on one of three values. The resulting profit from different values of x and θ is shown in Figure 3.2. If the decision maker assigns probabilities p_1, p_2, and p_3 to the corresponding values of θ, the maximum expected profit is determined using the weighted curve

$$f(x) = p_1 f_1(x) + p_2 f_2(x) + p_3 f_3(x) \tag{3.1}$$

Depending on the probabilities assigned, the optimum decision could be the value of x marked with a vertical line and profit marked by an x. As the decision maker gains information regarding the value of θ, the optimization process will be improved. For example, when enough information if available regarding which value of θ is true, the decision maker can choose x so as to maximize the profit curve corresponding to θ, this will be one of the three *'s indicated in Figure 3.2.

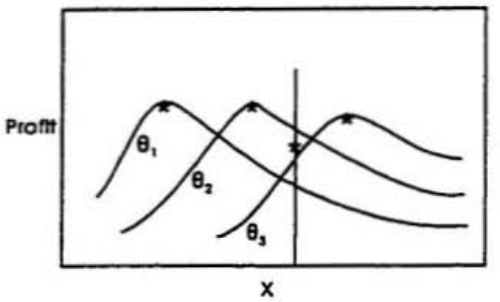

Figure 3.2 Effect of uncertainty on optimization

3.3 Probability and its evaluation

In decision making, once the alternative courses of action are determined, and the possible outcomes identified, it is necessary to evaluate probabilities of occurrence associated with each outcome. de Finetti (1974) gives an operational definition of probability that quantitatively reflects a person's beliefs regarding the outcome of a given event, and can be measured. There are a number of ways to measure a person's belief regarding the likelihood of different outcomes, including rephrasing the problem in terms of a fair bet or in terms of a loss function. The user specifies their probabilities regarding the outcomes so as to minimize expected loss. The rules of probability theory are derived based on the stipulation that one will not choose probabilities in a way that a combination of bets could be posed resulting in a sure loss or that a different set of probabilities would result in a smaller loss no matter what outcome occurs.

de Finetti stressed that probabilities do not exist on their own, but should be evaluated by each individual based on their particular knowledge and information. This is not at odds with engineering design and economics, where many people with different knowledge and

beliefs may be involved. The person suggesting particular actions should be required to make good logical arguments as to why the assigned probabilities are reasonable in order to convince others that the decisions are sound. If this is not possible then in economic decisions it will be difficult to convince investors to put money into a project. In design problems, it will be difficult to convince responsible bodies to approve projects.

As one gains knowledge regarding a problem, one can define parameters more precisely. Knowledge is gained by making measurements, comparing the problem with similar situations, using arguments of logic, using statistical inference, and conducting analytic and physical modelling. When using these methods to describe and change ones probabilities, it important to ensure that they are changed coherently. For example, one may define a joint probability density function $f_X(x)$ for the continuous random parameter X, and may consider the random quantity Y as a function $y = g(x)$ of X. If the modeller feels that g is precise and has no prior opinion regarding the value of Y, then the probability for Y based solely on $f_X(x)$ is

$$f_Y(y) = f_X(x) \left| \frac{dx}{dy} \right| \tag{3.2}$$

After calculating $f_Y(y)$, the modeler should be able to test the new probabilities assigned to Y in terms of appropriate bets or loss functions. If he or she finds that they do not agree with the new probabilities, then there is a contradiction. In this case one would reexamine the probabilities assigned to X, the assumption that g is precise, and the assumption of no prior opinion regarding Y. When modelling complex systems, it is not practical to examine every parameter and step. Many parameters may be treated as fixed, even though there is a small

degree of uncertainty associated with their values. Even more importantly, there may be a significant degree of uncertainty regarding functional models; this is usually difficult to define in probabilistic terms.

Where complex models are involves, a more practical approach is as follows. The input parameters for which there is the greatest uncertainty, and to which the results are most sensitive, should be treated probabilistically. Where there is significant model uncertainty, a broad range of model assumptions should be tested. The resulting distributions on the output parameters should then be treated as conditional on the particular model assumptions. This method helps the decision maker develop a better understanding of the overall system and of the degree to which different assumptions affect the outcome. At this point, the modeller should examine the overall results to determine if they can assign coherent probabilities to the possible values. If not, it may be desirable to revisit the different assumptions and data used.

3.4 Exchangeability and mathematical inference

In this section, the concepts of exchangeability and mathematical inference are introduced and some thoughts on ways in which inference techniques could be improved are outlined.

A straightforward definition of exchangeability, similar to that given in Smith (1988) is as follows.

> Random quantities $\theta_1, \theta_2, ...,\theta_n$ are exchangeable if the permutation of any two indices in the components of θ, leaves the distribution of $\theta_1, \theta_2, ...,\theta_n$ unchanged

Exchangeability is less constraining than the requirement that events be independent and identically distributed (IID). The importance of the concept of exchangeability results because often one does not have enough sample information to adequately describe the limiting distribution of a population. Where a parametric distribution can be applied, it is more appropriate to describe the parameters for the distribution as random than as fixed but unknown. This has been demonstrated in Jordaan and Maes (1984) (see discussion in Chapter 2) where it is shown that the assumption of fixed but unknown parameter values results in design loads which are too small. When the number of samples is limited, one changes one's probabilities regarding the likely outcomes of further samples. In this sense, the different events are not independent.

Often one has a good rationale for choosing a particular form of parametric distribution, but does not have enough data to determine its parameters precisely. Bayes' theorem, can be used to combine assessments of prior probabilities based on indirect information with the likelihood associated with observations. Consider the parametric distribution $f_{x|\theta}(x|\theta)$ of x with parameter Θ where the decision maker has assigned a prior distribution $f_{\Theta}'(\theta)$ to Θ. In this case, Bayes theorem gives the posterior distribution for Θ as

$$f_{\Theta|X}''(\theta|x) = \frac{\mathcal{L}_{\Theta|X}(\theta|x) \times f_{\Theta}'(\theta)}{K} \tag{3.3}$$

where $\mathfrak{L}_{\theta x}(\theta|x)$ is a likelihood function (proportional to $f_{x|\theta}(x|\theta)$) and K normalizes the distribution to one, i.e.

$$K = \int_{-\infty}^{+\infty} f_{X|\Theta}(x|\theta) \times f_{\Theta}{}'(\theta)\, d\theta \tag{3.4}$$

As one acquires enough data, the uncertainty on θ reduces to zero. Once this limiting case is reached the further events are essentially treated as IID. Examples of methods for choosing distributions and combining them may found in sources such as de Finetti (1972), Raiffa and Schlaifer (1961), and Maes (1985).

An example of the use of inductive methods for combining subjective and measured data is as follows. The problem is to estimate the expected number of events m in a time interval of duration Δt, given a Poisson process

$$p_N(r) = Pr(N=r) = \frac{e^{-m} m^r}{r!} \tag{3.5}$$

with constant mean, k observations $r_1, r_2, \ldots r_k$, and prior subjective information as to the mean value. Based on the observed data, the likelihood function for the mean, m, is

$$L(M=m) = \prod_{i=1}^{k} \frac{e^{-m} m^{r_i}}{r_i!} \tag{3.6}$$

There are some cases where the distributions f' and f'' have the same form f for a given likelihood function L, in which case f is known as the conjugate prior to L. When one has such a pair of distributions, it is possible to choose a conjugate prior which encompasses ones initial uncertainty regarding a quantity, then to update this distribution based on consecutive observations without its form changing. In the case of the Poisson distribution, the Gamma distribution is a conjugate prior. The Gamma distribution is also a very good

distribution to use to describe ones uncertainty because it can take a range of different shapes.

To illustrate, random samples from a Poisson process with a mean of 4.5 were generated and equation 3.3 was used with different initial prior Gamma distributions to determine how quickly the distribution on the mean converged. The resulting distributions with a non-informative prior ($f' = 0.1$), followed by 10 sample observations are shown in Figure 3.3. The effect of using an informed prior, namely a Gamma distribution with a mean of 4.2 and an upper 95% limit of 6, is shown in Figure 3.4 . The resulting uncertainty on the mean value is less, especially initially. It should be possible to work out the value of additional sampling in a real application based on the influence of additional data on the outcome and on the resulting increase in expected utility.

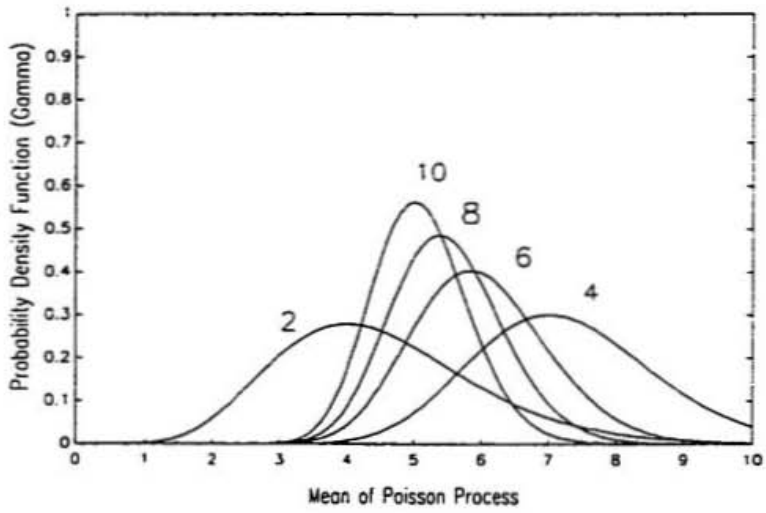

Figure 3.3 Uncertainty on estimate of the mean of a Poisson process given a non-informative prior and different numbers of samples

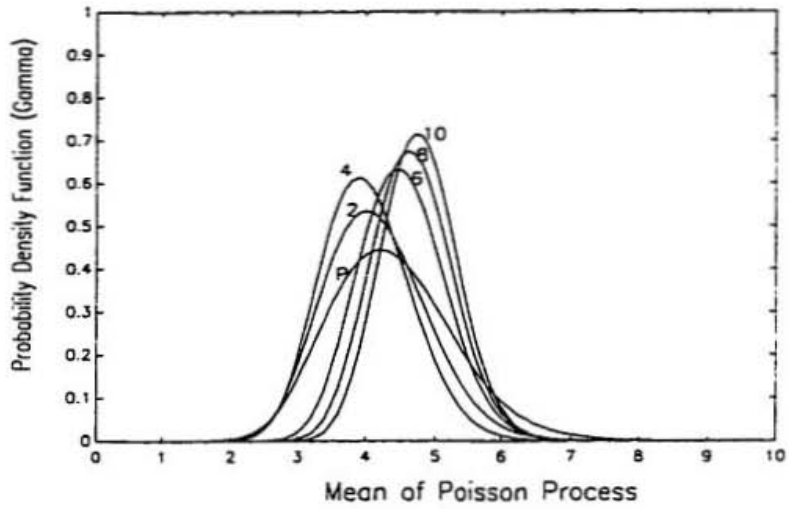

Figure 3.4 Uncertainty on estimate of the mean of a Poisson process given an informative prior and different numbers of samples (P indicates prior distribution)

Bayesian techniques are generally applied for cases where the likelihood distribution is precisely known and where the parameters being determined have well defined values. In many applications of interest, for example the estimation of areal densities of icebergs, there may be measurement uncertainty, measurement techniques that change over time, or variation in the quantity being measured.

3.5 Partial exchangeability

This technique, which was developed by de Finetti (1972), has not been widely recognized and applied. With partial exchangeability, one characterizes mathematically one's belief regarding the similarity of two populations. The method provides an mechanism for refining one's belief regarding this similarity as new data is acquired.

An example application is the evaluating of initial environmental design criteria when starting to work in an area where directly measured data is available. When the designer has data for neighbouring regions, they may choose to initially use it, possibly interpolating or modifying it. At this point the designer must determine the similarity between the conditions in the two regions. The problem is illustrated in Figure 3.5 where the designer is considering the expected annual number of iceberg encounters with a shuttle tanker fleet.

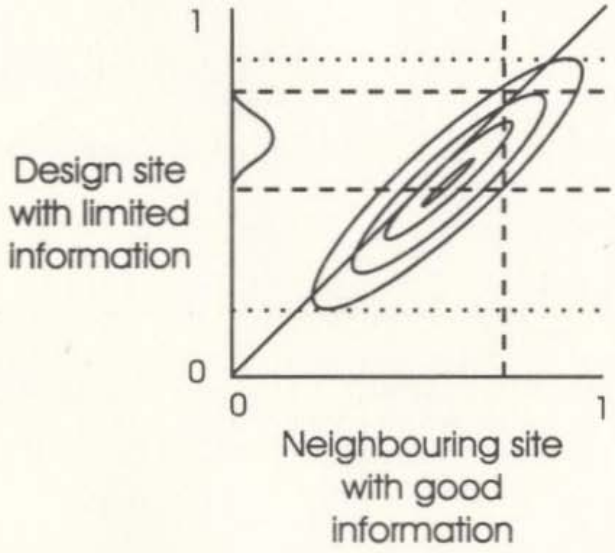

Figure 3.5 Example application of partial exchangeability

The neighbouring site might lie to the north where there are more icebergs in which case they would expect the value at the new site to be lower. The contour lines indicate the initial probability that the designer might assign to different combinations of expected annual number of encounters. This distribution would be based on a study of the relationship between the two sites. Without further information, the marginal distribution for the design site would have a large spread as shown by the dotted lines. When the designers have very

good data at the neighbouring site, they may be justified in assigning a single fixed value for the expected number of encounters. The posterior marginal distribution for the new site would then have a much smaller spread as indicated by the dashed lines. This example demonstrates that a decision maker can include knowledge regarding the similarity of two populations by quantifying his or her beliefs in terms of a prior joint probability distribution. It is then possible to rationally make inferences about one of the populations using data for the other.

3.6 Extremal analysis and design loads

When choosing design iceberg loads one is usually considering a fairly rare event. In the first part of this section a method applied by Jordaan, (1987) for determining extreme loads for rare events is reviewed. In the latter part, the effect of using the expected annual number of icebergs rather than the distribution for the annual number of icebergs is considered.

Assume that there is a set of exchangeable events E_i, i=1, 2, . . . n, with associated random quantities, X_i, taken from the cumulative distribution

$$F_X(x) = Pr(X \leq x) \tag{3.7}$$

then the maximum Z of the X_i has a cumulative distribution

$$F_Z(z) = F_X(z)^n \tag{3.8}$$

where $Pr(N=i)$ is the distribution for the number of events. If the number of events per year is random, then Z has a distribution

$$F_Z(z) = \sum_{i=1}^{\infty} \left[F_X(z)^i \; Pr(N=i) \right] \tag{3.9}$$

It is demonstrated in Chapter 5 that the expected number of collisions in a given year is proportional to the average areal density of icebergs in that year. The actual number of collisions can be shown to have a Poisson distribution

$$p_N(r) = Pr(N=r) = \frac{e^{-\nu} \nu^r}{r!} \tag{3.10}$$

with a mean ν equal to the expected annual number of collisions. The number of these collisions resulting in loads greater than z is a Poisson distribution with an expected value of $\nu(1-F_X(z))$. The probability that the maximum load is less than z is the probability of 0 events, i.e.

$$F_Z(z) = p_N(0) = e^{-\nu[1-F_X(z)]} \tag{3.11}$$

If the events are rare (the number of events ν per year $<< 1$), then

$$F_Z(z) = 1-\nu(1-F_X(z)) \tag{3.12}$$

The corresponding density function for rare events is

$$f_Z(z) = \frac{d F_Z(z)}{dz} = \nu f_X(z) \tag{3.13}$$

plus a dirac delta spike of area $(1-\nu)$ at zero. Note that equation 3.13 is the same as the density function for the collision load $f_X(z)$ given a collision, scaled down by the factor ν.

If the number of icebergs each year is random and the mean of the Poisson process has the distribution $f_\nu(\nu)$, then the maximum annual load will have a distribution with the integral form

$$F_Z(z) = \int_v e^{-v(1-F_X(z))} f_v(v)\, dv \tag{3.14}$$

If the value of v is always small, this can be replaced with

$$F_Z(z) = 1 - \bar{v}(1-F_X(z)) \tag{3.15}$$

where $\bar{v}$ is the expected value of v.

The Gamma distribution is often chosen to fit distributions because of the range of shapes it can take, and could be considered for representing the variation in the annual expected number of collisions. Because there are some years when icebergs do not reach the Grand Banks it would be necessary to represent the distribution as a mixture of years with zero expected collisions and years with the expected number of collisions defined by a Gamma distribution. Where the Gamma distribution alone is used, the extremal distribution becomes

$$\begin{aligned} F_Z(z) &= \int_0^\infty e^{-v(1-F_X(z))} \frac{\theta^\alpha}{\Gamma(\alpha)} v^{\alpha-1} e^{-\theta v}\, dv \\ &= \frac{\theta^\alpha}{\Gamma(\alpha)} \int_0^\infty v^{\alpha-1} e^{-v(\theta+1-F_X(z))}\, dv \\ &= \frac{\theta^\alpha}{\Gamma(\alpha)} \frac{\int_0^\infty [v(\theta+1-F_X(z))]^{\alpha-1} e^{[-v(\theta+1-F_X(z))]}\, d[v(\theta+1-F_X(z))]}{(\theta+1-F_X(z))^{\alpha-1}\,(\theta+1-F_X(z))} \\ &= \frac{\theta^\alpha}{\Gamma(\alpha)} \frac{\Gamma(\alpha-1)}{(\theta+1-F_X(z))^\alpha} \end{aligned} \tag{3.16}$$

If the distributions of sizes and shapes of icebergs and environmental conditions change significantly between years, it may be necessary to also consider annual variations in the collision load distribution, $F_X(x)$. For example, if the annual load distribution varies

according to a single parameter λ, i.e. $F_{X,\Lambda}(x,\lambda)$, then the distribution for the maximum annual load becomes

$$F_Z(z) = \int_{\nu,\lambda} F_{X,\Lambda}(z,\lambda)^{\nu} f(\nu,\lambda)\, d\nu\, d\lambda \tag{3.17}$$

where the joint distribution for $f(\nu, \lambda)$ includes any correlations between ν and λ.

It will now be demonstrated that the distribution for the annual maximum load determined using long term averages for both the expected annual number of collisions and the distribution of loads given a collision will give the same design loads for small enough probabilities of exceedance. The extremal distribution is

$$\begin{aligned} f_Z(z) &= \frac{d}{dz} F_Z(z) \\ &= \iint \nu\, F_{X|\Lambda}(z|\lambda)^{\nu-1} f_{X|\Lambda}(z|\lambda)\, f(\nu,\lambda)\, d\nu\, d\lambda \end{aligned} \tag{3.18}$$

For large enough values of z, the term

$$F_{X|\Lambda}(z|\lambda)^{\nu-1} \tag{3.19}$$

can be approximated as 1, the exact limit of z required will depend on the variations of ν and λ. For example, if F_X is 0.99 and ν is 10, the term is approximately 0.9 whereas if F_X is 0.90 and ν is 0.1, the term is approximately 0.99. In this case, equation 3.18 becomes

$$f_Z(z) = \iint \nu\, f_{X|\Lambda}(z|\lambda)\, f(\nu,\lambda)\, d\nu\, d\lambda \tag{3.20}$$

If long term averages are used, the average number of collisions is calculated as

$$\overline{\nu} = \iint \nu\, f(\nu,\lambda)\, d\nu\, d\lambda \tag{3.21}$$

and the long term average distribution for the load given a collision is calculated as

$$\overline{f_X}(x) = \frac{\iint \nu \, f_{X|\Lambda}(x|\lambda) \, f(\nu,\lambda) \, d\nu \, d\lambda}{\overline{\nu}} \tag{3.22}$$

The extremal distribution is then

$$\frac{d}{dz}F_Z(z) = \frac{d}{dz}\,\overline{F_X}(z)^{\overline{\nu}} = \overline{\nu}\,\overline{F_X}(z)^{\overline{\nu}-1}\,\overline{f_X}(z) \tag{3.23}$$

If the conditions for approximating F as one in equation 3.18 are met then F in equation 3.23 can also be approximated as one. Equation 3.23 then becomes equivalent to 3.13.

A simple example is now used to illustrate the above points. Consider the case where in 50% of the years the mean collision rate is 2, and in 50% of the years, the mean collision rate is 10. The distribution for the maximum annual load based on two collision rates is then

$$F_Z(z) = .5\,e^{-2[1-F_X(z)]} + .5\,e^{-10[1-F_X(z)]} \tag{3.24}$$

The distribution based on an averaged collision rate is

$$F_Z(z) = e^{-6[1-F_X(z)]} \tag{3.25}$$

Given the distribution $F_X(x)$ shown in Figure 3.6, the resulting averaged and combined distributions are shown in Figure 3.7. In this case, the effect of averaging the collision rates is to reduce the number of years with a smaller than or larger than average numbers of collisions. Because the probability that the maximum annual load is small decreases rapidly with the number of collisions, the averaging procedure reduces the probability of small maximum loads. On the other hand, the averaging procedure spreads the large loads over more years, reducing the amount of masking. For example, if there was a year with a high number of collisions, there could be two large loads of which only one is the maximum. The

averaging procedure assumes these are spread out across more years. For the very high collision loads, the probability of two large loads being in the same year is small so it makes little difference whether an averaged mean is used or the yearly distributions are combined. Note that if the expected numbers of collisions per year are always much less than 1, then the averaged and combined distributions for the maximum annual load will be nearly the same.

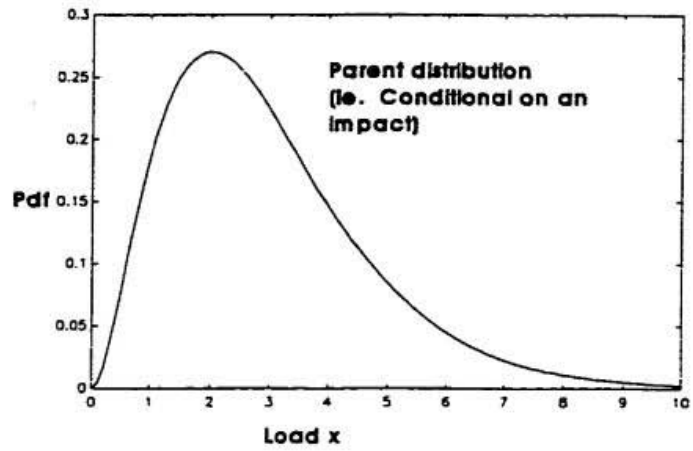

Figure 3.6 Parent load distribution

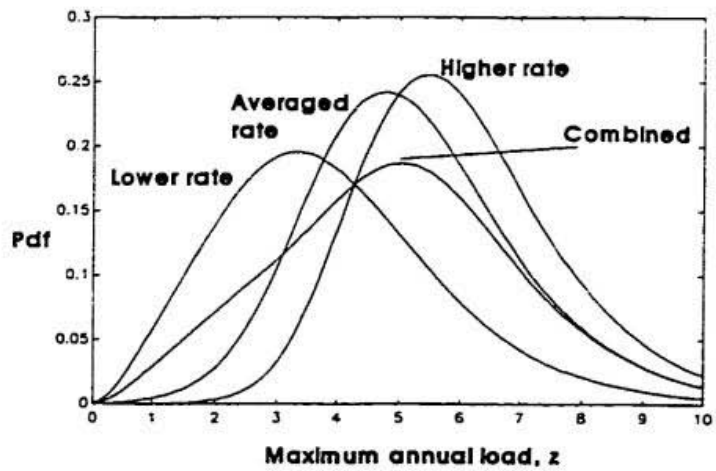

Figure 3.7 Comparison of using average annual number of icebergs versus distribution

3.7 Integration techniques for determining probabilities of failure

The problem of determining probabilities of failure is a case of the general integral,

$$I = \int_V q(\mathbf{x})\, d\mathbf{x} \tag{3.26}$$

of $q(\mathbf{x})$ over the range V. If one replaces $q(\mathbf{x})$ with $g(\mathbf{x})\, f(\mathbf{x})$, where $g(\mathbf{x})$ is a function of random parameters defined by the vector $\mathbf{x}$, and $f(\mathbf{x})$ is the joint probability density function assigned to $\mathbf{x}$, then the integral gives the expected value of g, i.e.

$$E(g) = \int_V g(x) f(x)\, dx \tag{3.27}$$

In reliability analysis, one wants to determine the probability of failure given a limit state function $g(\mathbf{x})$ such that $g(\mathbf{x}) < 0$ implies failure and $f(\mathbf{x})$ is a probability density function for $\mathbf{x}$. The probability of failure is then the expected value of the function g', where $g' = 1$ if $g(x) < 0$ and $g' = 0$ if $g(x) > 0$.

The best integration method to use depends on the dimension d of the domain V, the complexity of V, the characteristics of the function q, and the specific knowledge about q. Generally if d is small, V is simple to define, and q is smooth, then numerical quadrature methods are preferred. If n is large, V is complex, or q is not smooth, Monte Carlo and alternative techniques are often preferred. Two techniques are considered further, simple Monte Carlo and Importance Sampling. Other important techniques that exist for reliability-based design include first and second order reliability methods. Importance sampling has been used here largely because it is easy to implement and is robust.

In simple Monte Carlo, one samples points uniformly over the volume, i.e.

$$I = \int f\, dV = V \langle f \rangle \pm \sqrt{\frac{\langle f^2 \rangle - \langle f \rangle^2}{N}} \tag{3.28}$$

where V is the volume, <f> is the expected value of the function, and N is the number of samples. With Monte Carlo integration, all sampled points are independent and identically distributed so statistical methods can be used. The mean of the sample points is an unbiased estimator of I/V with an error that drops off as $n^{-0.5}$ independent of the complexity of the function or the number of dimensions. Monte Carlo simulation has the advantage that if the shape of V is complex, one can generate points **x** for some simpler space W that encloses V and set q to zero whenever x is not in V. A disadvantage with Monte Carlo simulation is that the error given is statistical whereas for numerical integration schemes, absolute bounds on the error can be determined. An advantage of Monte Carlo is that accuracy can be improved by increasing the number of simulations. With numerical schemes, it may be necessary to restart with a denser set of points.

Techniques for improving the efficiency of the Monte Carlo integration scheme generally require knowledge of the integrand and effectively reduce the variance on the estimated mean. No single uniform approach can be applied. Available techniques include importance sampling, control variates, antithetic variates, and stratified sampling.

An integral can be determined by non-uniform sampling if the integrand at each point **x** is divided by the value of a sampling probability density function p(x), i.e.

$$I = \int q\, dV = \int \frac{q}{p}\, p\, dV = V \left\langle \frac{q}{p} \right\rangle \pm \sqrt{\frac{\left\langle \frac{q^2}{p^2} \right\rangle - \left\langle \frac{q}{p} \right\rangle^2}{N}} \qquad (3.29)$$

The idea in importance sampling is to choose the sampling distribution so as to reduce the variance. Note that if one sets

$$p = \frac{|q|}{\int |q| dV} \tag{3.30}$$

then the variance goes to zero. By adding a large enough constant, q can be made positive; this is equivalent to knowing the value of I already. As the integral I is not known, the best one can do is find a distribution which follows q as closely as possible. When $q(\mathbf{x}) = g'(\mathbf{x})$ $f(\mathbf{x})$, then $q(\mathbf{x})$ is zero wherever $g(\mathbf{x})>0$. The maximum point of q is generally on the line $g(\mathbf{x})=0$ where $f(\mathbf{x})$ is a maximum. A reasonable first approximation to q is to centre the sampling distribution p over this point (Figure 3.8).

In adaptive importance sampling, one keeps track of the sampled values and the variance and adjusts p(x) based on this sampled information. In the analyses for this thesis, the importance sampling distributions were chosen based on judgement and improved iteratively by running the model and observing how well they applied .

An important advantage of importance sampling is that one can set up a sampling distribution for which it is easy to generate the random parameters. In particular, even if the input parameters are dependent, the sampled probability distribution can be set up to be independent.

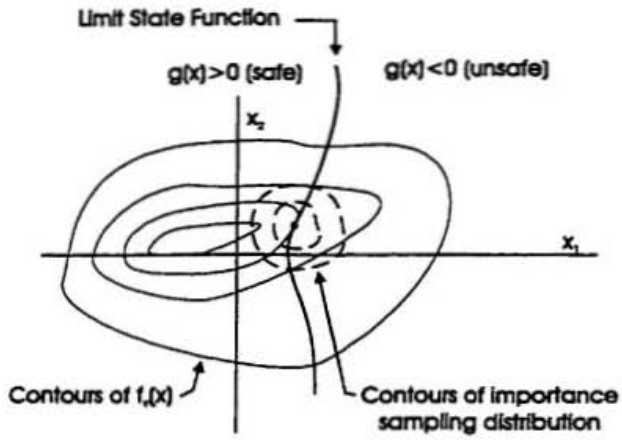

Figure 3.8 Illustration of importance sampling technique

4 BASIC METHODOLOGY

4.1 Overview

In this chapter, the overall methodology for choosing design iceberg impact loads and assessing different systems for regions with icebergs is outlined. In Section 4.1, the overall model framework is presented and the types of systems to be considered are outlined. In Section 4.2, the basic economic model is set up. In Section 4.3, the criteria and models for determining design ice loads using reliability-based methods are outlined.

The general procedure used in designing and evaluating systems is illustrated in Figure 4.1 .

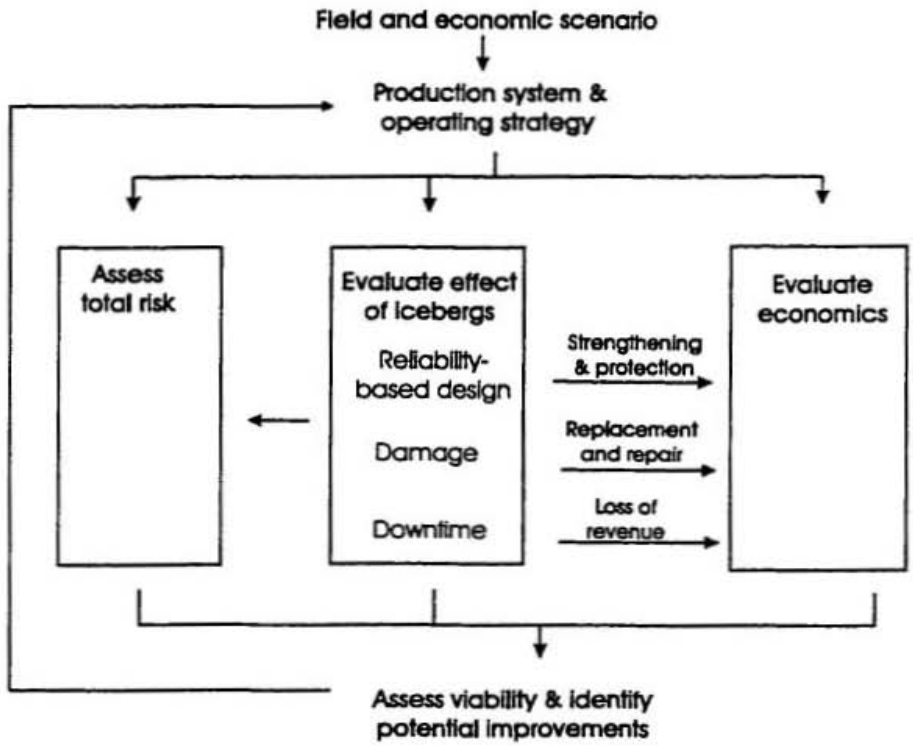

Figure 4.1 Overall methodology for evaluating production systems

The constraints for the problem are determined by the particular field scenario including location, water depth, environmental conditions, amount of oil, production rates, special requirements, and general economic conditions. Given these constraints and the particular system and operating strategy to be considered, the influence of icebergs on structural design, number of damage events, and downtime can be determined. These factors are then input into the economic model where their effect on the overall costs and revenue determined. In addition to evaluating the effect of icebergs on economics, the final decision may involve an assessment of the overall risk to personnel and the environment over and above risks of structural failure. If the system compares favourably with other systems, and the field development looks viable, then refinements and further evaluations of the system may be made.

The emphasis of the analyses is on marginal fields and therefore in the example applications in Chapter 7, fields of relatively small size (50 , 100, and 200 million barrels) will be considered. While design impact loads for gravity based structures will be considered, economic analysis will be presented only for floating systems which might be used for these smaller fields. Production systems that will be considered include floating production storage and off loading (FPSO) systems and single well oil production systems (SWOPS). For the FPSO systems, a shuttle tanker system for transporting the crude is assumed. For both the FPSO and SWOPS systems, the alternative of moving off location during the iceberg season to reduce costs associated with icebergs is considered.

In analysing costs and risks to the subsea systems associated with floating systems, fairly simple subsea configurations are considered. In the model it is assumed that the wells

are drilled individually and that the produced fluids routed from the well heads through relatively short (1 km) subsea flowlines to a manifold (Figure 4.2). The manifolded fluids are then routed to riser bases near the production vessel. Each of these flowlines is assumed to have an associated riser, i.e. there is no manifolding. Small manifolds (in the order of 6 wells per manifold) are assumed; as these can be installed from a conventional semi-submersible used for drilling. The user specifies the number of wells per manifold, the depth of the reservoir, the distance of the well heads from the manifold, and the total area drained per manifold. From this information, the program estimates the distribution of along hole depths required and from this, the average cost per well.

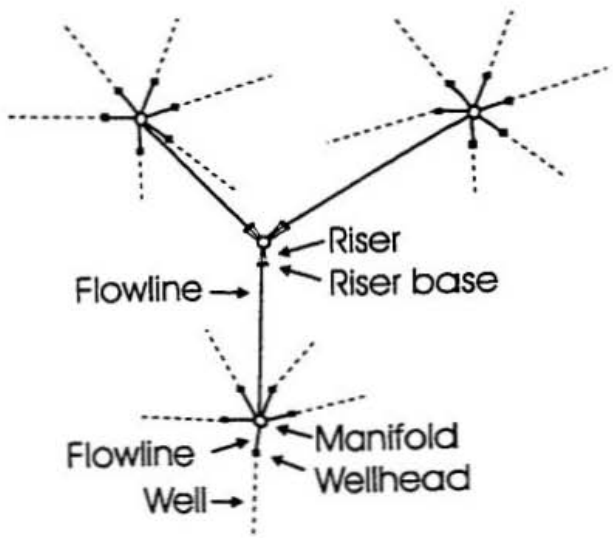

Figure 4.2 Configuration of subsea system

The lengths of flowlines are determined so as to cover the field given the specified width and length of the field. The field is modelled as ellipsoidal in shape and its area can be defined larger than the number of manifolds times the area per manifold; this might occur for

example if the reservoir was not continuous. The program spaces the manifolds equally within this elliptical region and determines the length of the flowlines from each manifold to the riser base accordingly. Notional values are used for the costs of well heads, manifolds, and flowlines; it should be noted that these items can vary significantly both in complexity and cost depending on the flow rates and particular circumstances.

4.2 Evaluation of system economics

4.2.1 Introduction

To determine the economics of a given development, the decision analyst first needs to establish the possible cash flow time lines for capital costs, operating costs, and revenues. Based on these time lines the analyst can then determine appropriate economic criteria such as net present values and assign probability distributions to these. Based on the calculated expected net present values and associated variances, different field developments and production strategies can be compared.

In this section, the factors required to estimate the cost and revenue time lines are presented and notional models are developed to illustrate how a preliminary parametric analysis might be conducted. The basic costs models are treated as deterministic rather than probabilistic as the main emphasis is on iceberg related aspects. In Chapter 7, sensitivity analysis regarding the price of oil and discount rates used are conducted.

In Section 4.2.2, the factors determining the revenue time line are described. These include the nominal production rates over the life of the development, the amount of downtime, and the price of oil. In Section 4.2.3, models are suggested for the base capital

and operating costs. These are meant to represent the costs that result if no icebergs where present. In Section 4.2.4, models for costs related specifically to design for icebergs are suggested.

The components considered and modifications that might be required because of the presence of icebergs are summarized in Table 4.1 .

Table 4.1 Components considered in cost model.

Component	Possible sources of increased costs due to icebergs.
Wells	Better fail safe valves.
Trees	Glory hole, flow line break points
Manifolds	Glory hole, flow line break points.
Flow lines and control lines	Trenching, flow line break points.
Riser base	Glory hole, flow line break points
Riser	Quick disconnect, emergency disconnect systems.
FPSO - Vessel	Ice strengthening, enhanced detection.
FPSO - Process system	
FPSO - Turret-mooring system	Quick disconnect, emergency disconnect systems
FPSO - Off loading system	
Shuttle tankers	Ice strengthening, enhanced detection capability
Support vessels	Ice management and detection capability
Surveillance	Ice surveillance by aircraft

4.2.2 Estimation of revenues

The revenues generated by a given development will be determined by the achieved production rates and by the price of oil at its destination. The price of oil will vary depending on whether it is received at a refinery near markets or at a transhipment terminal, from which it must be reloaded and shipped again. The achieved production rate will depend on the

achievable flow rates from the reservoir over time, the maximum processing capacity, and the amount of downtime.

The "nominal" production rate is defined here as the achievable production rate given zero downtime and is calculated as follows. In the model, the peak production rate per well and the peak processing rate must be specified. As the wells may be drilled over several years, the user must also specify the number of wells drilled per year. Thus over the first few years the production rate will build up to a possible maximum equal to the total processing rate. In the model used, as the reservoir is depleted, the production rate per well declines according to the proportion of reserves left. This accounts in part for the reduced natural drive and in part for increased amounts of water produced with the oil. The total production at any time is then the minimum of the sum of the production from individual wells and the processing capacity.

Downtime can result in a number of ways. Flow from wells can be disrupted requiring workovers or subsea equipment may malfunction requiring subsea work. These types of problems will often reduce the total production rather than stop it. Problems with the turret system or process equipment can result in reduced or stopped production. In extreme sea states, it may be necessary to shut down production. Also there will be limiting conditions for mooring shuttle tankers. The amount of downtime because shuttle tankers cannot moor or are late getting to the production site will depend in part on the amount of storage available at the production site. As a general rule, an FPSO is sized for about 6 days of storage at the peak production rate. When the production vessel leaves site because of an iceberg incursion, or repairs to subsea equipment is required, additional downtime may result

when waiting for an appropriate weather window for the operations required. The overall downtime estimated for the Terra Nova development is 76 days per year (Petro Canada Development Plan, 1996). This estimate should include all of the above factors. The same amount of total downtime will be used in the examples in Chapter 7. The proportion of this downtime related to the presence of icebergs is estimated in Chapter 6.

Downtime results in delays in revenue, and also increases in the project life and therefore in the total operating costs required to produce a given amount of oil. While the downtime can be analysed for a number of ideal revenue profiles using analytic solutions based on Laplace transforms (see Buck, 1989 for example), to be able to analyse quickly any given production curve a simple numerical computer model was developed. The example of a constant nominal production rate of 50,000 bopd over 15 years is used for illustrative purposes. At an oil price of 18$ US per barrel, this would generate total revenues of 6.8 billion dollars with a net present value of $3.4 billion dollars at 12%.

The decrease in the project net present value at 12%, resulting from 10 days of downtime in different years is shown in Figure 4.3a). It is seen that because of the time effect, downtime in the initial years has a larger effect on NPV than downtime in later years. The effect of different amounts of annual downtime has also been considered. The total loss of NPV is shown in Figure 4.3b) and the incremental loss (per additional day of downtime) is shown in Figure 4.3c). It is seen that the relationship in Figure 4.3b) is almost linear, there is a slight increase because as the project life is extended with the increased downtime per year, additional downtime in the final years occurs. The jumps in Figure 4.3c) results because in the model, the downtime in each year is treated as though it occurs at the end of

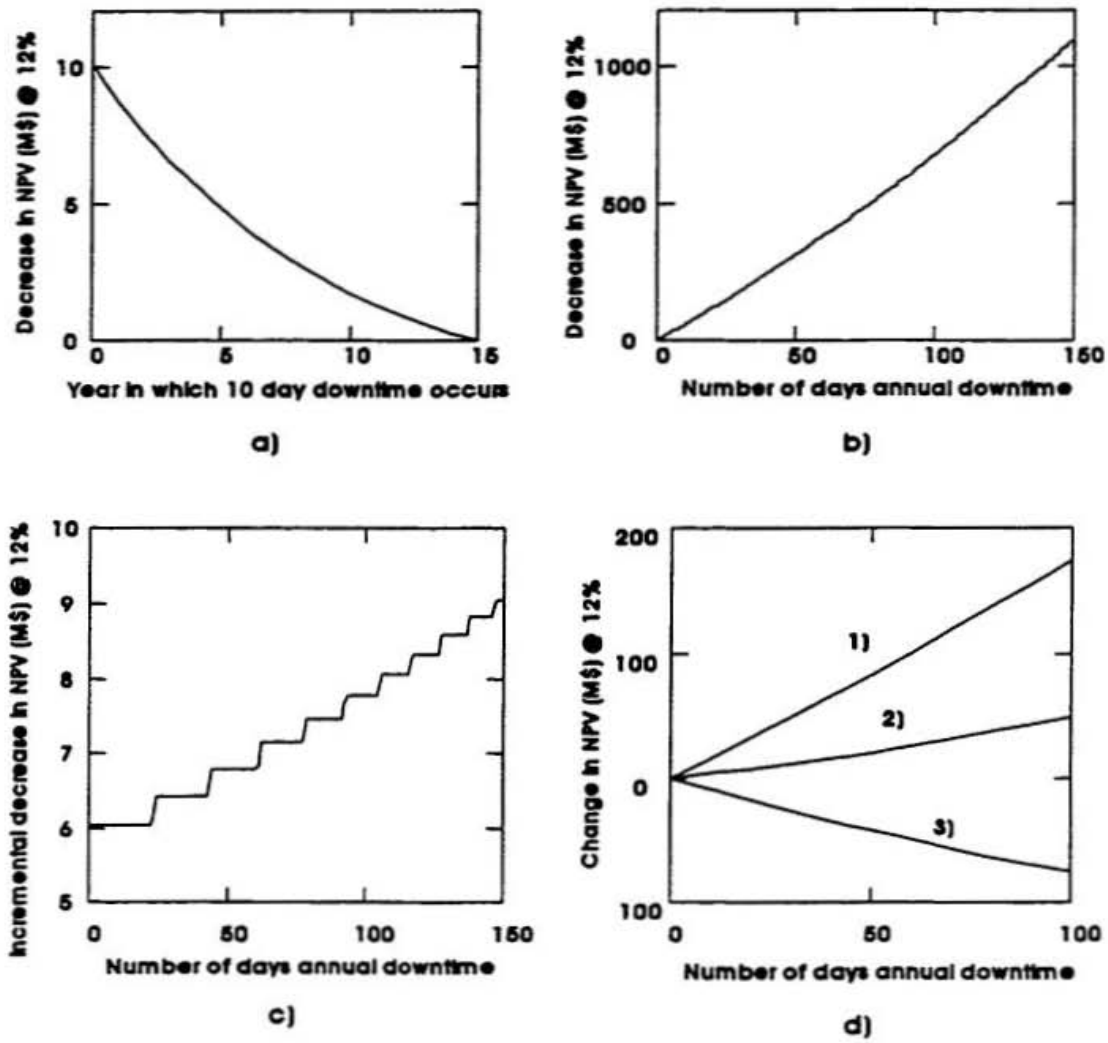

Figure 4.3 Effect of downtime on economics

a) Effect of 10 day downtime on NPV as a function of year occur (*1)

b) Effect of various amounts of annual downtime on NPV (*1)

c) Incremental effect of various amounts of annual downtime on NPV (*1)

d) Effect of various amounts of annual downtime on NPV with (*2)

- i) no operating cost during downtime
- ii) 50% of working operating cost during downtime
- iii) 100% of working operating cost during downtime

(*1) Only the effect of delayed revenues is considered, not changes in operating costs

(*2) Only the effect of changes in operating costs is considered.

the year. It is seen that the loss in NPV is initially about 6 million dollars per additional day of annual downtime over the life of the project. If the downtime is high, for example if the production system were moved off site during the iceberg period, then the loss of NPV could be very significant. The loss in the example for 60 days annual downtime would be $383 million.

Downtime will also have an effect on operating costs. If the downtime is related to iceberg incursions, weather, or repairs, it is likely that the operating costs will be nearly the same as during production; there may be some decrease because chemicals are not injected into the well and the demand on the shuttle tankers is reduced, necessitating less fuel. If the decision is made to shut the system down for an extended period, for example because of the presence of icebergs, it may be possible to reduce operating costs further. The effect of different proportions M of nominal operating costs during downtime is shown in Figure 4.3d). The Y axis is the change in NPV solely due to changes in operating costs over the life of the field. If the operating costs remain the same (M=1) when downtime occurs, the effect is to decrease the NPV (this results because the duration of the project is increased). If the operating costs could be reduced to zero during downtime, then the operating costs are delayed (because it takes longer to get the same amount of oil out of the ground). The loss in NPV because of operating costs is reduced but the net NPV still reduces because of delays in revenues).

In considering moving off location for an average 60 day period each year during the iceberg season, the loss in NPV due to delayed revenues would be $383 million. The change in NPV due to changes in operating costs would range from -50 to +100 million dollars.

Assuming that a savings of $50 million in NPV could be achieved, then the change to the NPV due to both reduced production and changes in operating cost would be a decrease of $333 million. Choosing a strategy based on moving off location during the iceberg season would have to result in a significant savings in initial capital expenditure to compensate for this.

4.2.3 Base capital and operating costs

4.2.3.1 General cost factors

In choosing representative costs for the model inputs, values representative of the Grand Banks are used if available. These may be based on records from previous drilling operations, actual or estimated expenses for the Hibernia development, or estimated expenses for the planned Terra Nova development. When using Grand Banks data, it may be difficult to ascertain what portion of costs are related to icebergs as opposed to other factors such as the particular location and environment and the lack of infrastructure. A second course of action is to use data from similar fields in the North Sea and modify it to apply for the Grand Banks. A third course of action is to try to build up costs from material, labour, vessel hire, and transportation costs. Finally if appropriate cost data can not be found, then judgement is used to come up with reasonable notational values.

It is not always clear whether a given expense is better treated as capital or operating cost. Where only capital cost information is available and the expense is to be treated as an operating cost, the conversion is made using an appropriate capital recovery factor (CRF).

Some costs may pertain to a number of items and are difficult to allocate exactly. A specific example is the cost of mobilizing and transporting a semi-submersible to a site. This cost pertains to all the tasks that are carried out which may include drilling several wells, working over wells, and installing subsea manifolds and trees.

It should be noted that a large part of capital and operating costs results from mobilizing vessels and bringing them to the Grand Banks. The mobilization costs could be broken into the costs to prepare the vessel and the transportation costs for the vessel and personnel. In addition, the day rates required for the vessels used usually often makes up a significant proportion of the associated costs.

4.2.3.2 Drilling, completion, and work over costs.

Where monohulls are used, drilling will be conducted from a separate semi-submersible drilling vessel. If the vessel is leased, then the cost to drill a well is related to the time and effort to prepare the semi and move it to the general location, the time and effort to set up at the site, the total along hole depth, the time to drill and case to this depth, and the amount of drilling mud and casing. Other costs include the cost of the drilling temporary guide base and wellhead (assuming individually drilled wells), the cost of tubing, and the cost of completion. If several wells are drilled sequentially, then the cost of bringing the vessel to the site per well is reduced. The maximum along hole depth that can be reached presently is around 10 km. The distance one can reach horizontally from a drill site is limited by the reservoir, with a ratio of 3 horizontal to 1 vertical being the limit (Henry and Ingles,

1995). As one approaches this limit, one would expect problems and costs to increase significantly.

An idea of how drilling costs vary with depth drilled can be ascertained from annually published data from the Joint Association Survey on Drilling Costs (API). A table of costs published in Offshore (Feb., 1990) is plotted in Figure 4.4 . It is seen that the costs tend to increase in an exponential manner. It is of note that these costs are significantly less than those required for drilling on the Grand Banks. Also, the costs are averaged over many scenarios, eg. different water depth, reservoir depth, etc.

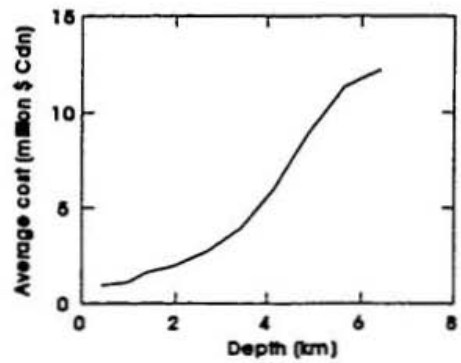

Figure 4.4 Average cost of US offshore wells by depth drilled.

Some drilling cost information which may be more applicable to the Grand Banks is a summary of initial drilling costs for the Hadrian field in the North Sea (Offshore Aug '95 pg 134). In this case, 16 wells were redrilled by the semi-submersible Transocean 8. Eight production wells and two gas injection wells were drilled from a template, plus another six water injection wells were drilled subsea. Based on the information given, the average well depth was calculated to be 4.5 km, the average cost $21 million US, and the average drill

time 57 days. The drilling downtime due to weather was calculated as 2.3% and the rig repair downtime 3.2%. In addition, an average of 42 dives per well was required.

In a study by Croasdale and McDougall (1994) for the Canadian Panel of Energy Research Development, the cost of development wells for a 350 million barrel field is given as $1150 million in Table 19 of that reference. Assuming that 34 wells are required to produce the field, this is an average of $34 million per well. The cost of development wells for the Terra Nova field is given as 23% of the total cost in Table 18 of that reference. It is also stated that the cost of the Terra Nova project is approximately 60% that of the Hibernia project which is given as $5139 million. This gives a cost per well for Terra Nova of $21 million.

In the recent Terra Nova Development Plan (Part 1 - Table 11.1-1), the cost of drilling 9 wells at Terra Nova is given as $357.8 million. The wells included "the K-08 discovery well, two additional exploration wells, and 6 subsequent delineation wells". Assuming that these drilling costs are representative, the cost per well is about $40 million.

A single relationship between cost and along depth is used, this might apply for example for a set of similar wells drilled with different horizontal offsets to the same reservoir depths. The capital costs of the wells are modelled using a single curve giving notional cost versus total depth (along well bore) defined as

$$C(x) = 10.9\, e^{.0002x} \tag{4.1}$$

where x is the along hole depth and C is the cost in millions of dollars. The relationship is shown below in Figure 4.5 .

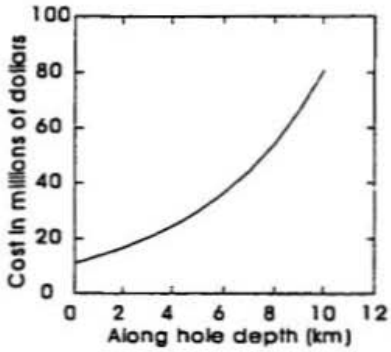

Figure 4.5 Cost of completed wells as a function of depth drilled.

The total capital cost for all wells is determined by suming the calculated cost for each well.

The cost to work over subsea wells makes up a major portion of the total operating expenses of a floating production development. Because of this every attempt is made to reduce the required number of work overs, this often requires increased capital expenses for better subsea equipment. According to Henery and Ingles (1995), in the North Sea, subsea wells are entered every 4-5 years, whereas surface completed wells in Gulf of Mexico are typically entered more than twice per year. Other factors which include the number of work overs include the flow rates, temperature, pressures, mechanical failures, and the amount of sand and corrosives.

4.2.3.3 Subsea equipment costs

As mentioned in the introduction, the overall subsea system is configured of trees, manifolds, intra-field flowlines, and risers. The costs developed should include design costs, costs of hardware, and costs for installation and commissioning. It should be noted that subsea system costs can vary significantly depending on the amount of manifolding, the use of TFL systems, gas lift, chemical injection, electro-hydraulic or direct hydraulic control, etc.

Lever (1994) indicated that costs of subsea systems per well (excluding drilling) for the Grand Banks would be in the order of $15 - 20 million per well. Because the amount of detailed cost data available in the literature is limited, notional values have been used in the cases in the cost model.

The model costs for the subsea system are shown in Table 4.1. These are taken as the costs of baseline systems without protection from icebergs. Protection from icebergs may include pipeline burial by trenching, and protection of the wellheads, manifolds, flowlines, and the riser base using glory holes or caissed glory holes. These are discussed in Section 4.3.8.

Table 4.1 Notional capital costs for subsea system

Component	Cost
Subsea tree cost	$4 million
Manifold - cost per well (6 well)	$2 million
Riser base (per flow line)	$2 million
Intra-field flow lines (per km per 10000 barrel per day)	$1 million
Risers (per km per 10000 barrel per day)	$2 million
Cost of control system for production wells as a percentage of base cost for production well system.	20%
Cost of system for water and gas injection wells as a percentage of system for production wells	50%

4.2.3.4 Shuttle tanker costs

A review of cost data on crude oil tankers is presented before discussing shuttle tankers as more cost information is available. Some of this data will be used in developing a shuttle tanker cost model. First information on double hulled tankers devleoped as part of

an NRC (U.S.) study (NRC, 1991) will be reviewed and and the results of a simple model based on this presented. Next, a breakdown of costs for a double hulled tanker given in Hunt and Butman (1995) will be presented. Finally, published data on the Hibernia shuttle tankers will be presented and a simple model for analysis developed. No attempt is made to optimize the size of the production vessel and shuttle tankers.

Estimates of capital and operating costs for three sizes of single and double hulled tankers are given in NRC (1991), pp 305-307. The capital costs for the two types of vessels are plotted in Figure 4.6 in tonnes and Canadian dollars.

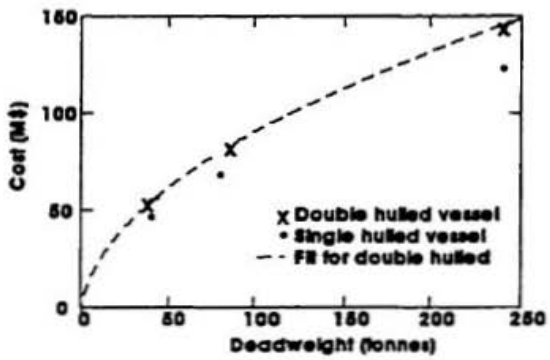

Figure 4.6 Cost of single and double hulled tankers. (NRC, 1991)

The cost of a double hulled tanker is approximately 17% more than that of single hulled tanker, with the difference increasing slightly with vessel displacement. An equation of the form $c = a + b\,d^{e}$, namely

$$c = 0.1833\,d^{0.512} \tag{4.2}$$

was fit through the points for the double hulled vessel where a, b, and e are constants, d is the deadweight (1000 tons), and c is capital cost in US dollars. The fit is approximate and was forced to go through the origin. This equation will be used for costing the shuttle tankers, with factors applied for ice strengthening and other factors described later.

If the tankers are sized based on required cargo deadweight, it is necessary to determine the ratio between cargo and vessel deadweight. Estimates of the proportion cargo deadweight (NRC, 1991) are plotted in Figure 4.7 for single and double hulled vessels.

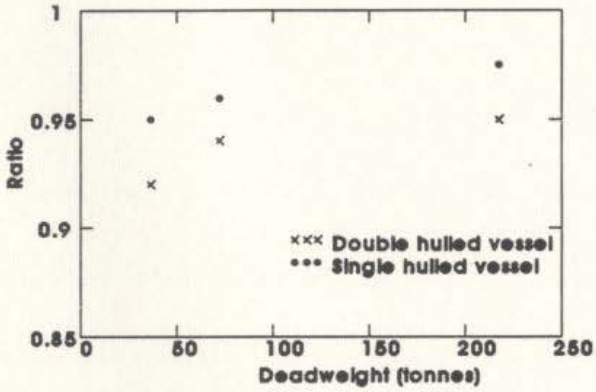

Figure 4.7 Cargo deadweight / vessel deadweight

In the model, the shuttle tanker deadweights will be estimated as 1.064 times the required cargo deadweight.

Some information on operating costs was also supplied in NRC (1991). Annual manning and daily fuel costs, as a function of vessel deadweight, are shown in Figure 4.8

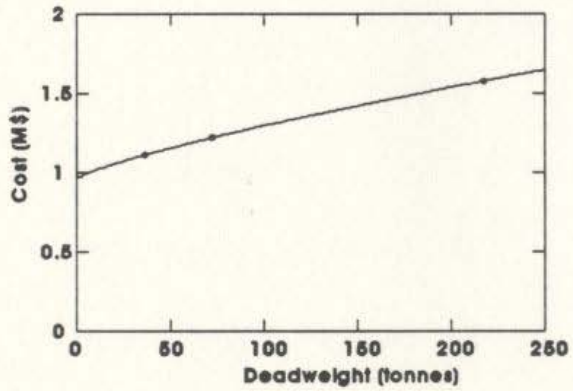

Figure 4.8 Annual manning cost

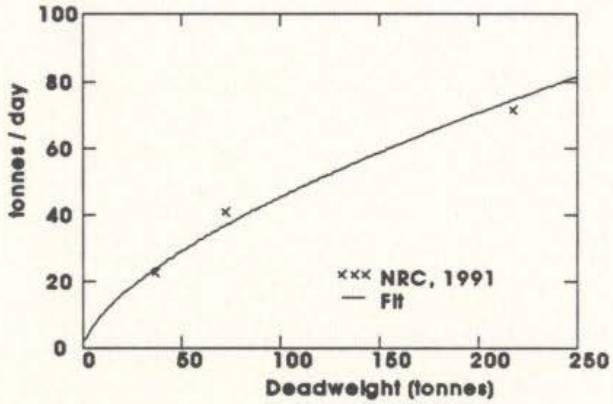

Figure 4.9 Daily fuel consumption

For the annual manning costs, an equation of the form

$$c = 0.699 + .00002831\, d^{0.781} \tag{4.3}$$

was fit to the data where c is the cost in million US$ and d is the deadweight in 1000 tons was fit through these points. Fuel consumption rates in tons per day were given in NRC (1991) and are shown in Figure 4.9 . For fuel consumption, an equation of the form

$$f = 0.2933\, d^{0.640} \tag{4.4}$$

where f is the fuel consumption in tons / day and d is the deadweight in 1000 tons was fit. For this fit, the curve was forced through the origin and the points for the 40,000 and 240,000 ton vessels. The curve was then scaled up slightly to give a better overall fit.

The annual insurance costs from NRC (1991) are 1.2% of the initial capital cost of the vessel. Costs were given for the classes 'administration and other costs', 'stores and lubes', and 'maintenance and repairs'. For these, following equations

$$c = 0178 + 2.022\times10^{-5}\, d^{0.696} \tag{4.5}$$

$$c = 0.202 + 2.406\times10^{-4}\, d^{0.5} \tag{4.6}$$

$$c = 0.381 + 4.752\times10^{-5}\, d^{0.739} \tag{4.7}$$

were determined such that the points fit the data points, where c is the cost in million US$ and d is the deadweight in 1000 tons.

An example scenario was run to show the overall costs assuming these crude tankers could be used unmodified as shuttle tankers. In the example, it is assumed that the shuttle tankers is operating year round and that there is no excess capacity in shuttle tankers, i.e. the shuttle tankers can unload at the nominal unloading rate and do not have to wait for oil to be processed at the nominal production rate plus production downtime. In fact, it appears that there is significant overcapacity to avoid production downtime waiting on shuttle tankers

because of weather and mechanical failures. The shuttle tankers were modelled to travel at 15 knots and must cover a 500 km distance to port. A one hour time penalty is applied each way for the vessel to reduce speed as it approaches port or the production site. An average penalty of 2 hours is applied waiting on other vessels at port, and an average penalty of 2 hours is applied at the production site for waiting on weather. Assuming an off loading rate of 40000 bbl / hour, total trip times would be in the order of 2.5 to 3.5 days depending on the size of the vessel. Annual fuel costs were therefore calculated assuming average trip times of 3 days and assuming that the average fuel cost is 1/5 of the voyage fuel cost when the vessel is not on route. The total annual shuttle tanker cost given the above assumptions and the breakdown of costs is shown in Figure 4.10 . It is seen that the highest annual cost is the capital cost repayment followed by fuel, manning, insurance, and finally maintenance and repairs. Costs for "stores and lubes" and for "administration and other", are significantly lower.

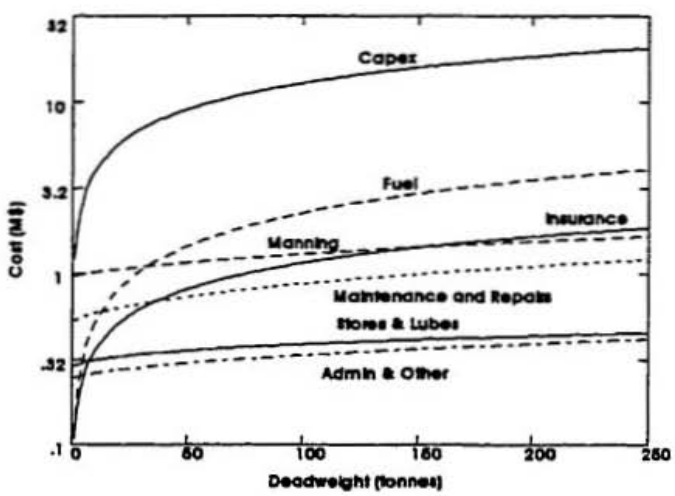

Figure 4.10 Example case - breakdown of costs

In considering additional vessel costs for ice strengthening and other modifications it is useful to have a breakdown of the costs for different parts of a vessel. A cost breakdown of the capital cost of a 119,054 ton deadweight double hulled tanker is given in Hunt and Butman (1995) on page 9-9 of that reference; the breakdown is shown in Table 4.2 .

The total cost of the vessel is not given. The hull cost consists predominantly of the cost for the steel structure. The mechanical costs include the main engine, heavy lift systems, bow thrusters, etc. More detailed breakdowns may be found in Appendix C-1 of that text (note that the portions in Appendix C-1 do not sum to 1). In applying the data from Hunt and Butman, it should be noted that the cost breakdown may not be the same for other sizes of vessel. Also, the accuracy of the breakdown can not be verified.

Table 4.2 Breakdown of costs by proportion for a double-hulled tanker.

Component	Material	Labour
Hull	.2426	.4412
Mechanical	.4047	.2107
Electrical	.1136	.0476
Outfit	.1225	.0689
Engineering	.0041	.0432
Yard	.0544	.1813
Other	.0581	.0071

A limited amount of information has been published regarding the Hibernia shuttle tankers, this information indicates that modifications of the tankers over and above ice strengthening would be carried out. In Canada NewsWire (Sept. 1996) information is given regarding the Hibernia shuttle tanker Motor Tanker Kometik which will be owned by Mobil,

Chevron, and Murphy Oil and will be operated by Canship Ugland Ltd. The vessel will carry 850,000 barrels of oil and will be doubled hulled and ice strengthened. To provide good manoeuvrability, the vessel will have "two propellers each driven by a separate diesel engines, two high performance rudders, and two bow thrusters". The operating costs for the vessel are estimated to be about $8 M per year. The St. John's Evening Telegram (1995, Mar. 25, Provincial News) gives additional information. Two vessels of 120,000 d.w.t. will be built initially for the project; one will be owned by the operators and one will be chartered. The vessels will be Canadian manned and subject to Canadian Coast Guard regulations. With direct shipment of oil to the U.S., three or more tankers would be used. Refineries which might receive the oil are as follows where the approximate distances from Hibernia (in km) are indicated in parenthesis: Come-by-Chance (250), Halifax (650), St. John (850), Montreal (1400), U.S. Gulf Coast (Delaware Bay - 1250), Gulf Coast (2500), England(1750), and St. Croix(1800). The NOIA news (Oct./Nov., 1995) gives the size of the operators vessel as 127,000 d.w.t. The publication "Offshore Canada" gives the tanker sizes as 275 m long and 48 m in beam. Two controllable pitch propellers each with 13,000 HP diesel engines will be used for propulsion.

In modelling the costs of equivalent shuttle tankers with no costs related to icebergs, equation 4.2 will be used with an additional notional cost factor of .35 to account for modifications to meet current regulations and to operate in harsh wave environments.

4.2.3.5 Production vessel, turret, and process equipment - general information

The design of a floating production storage and off loading vessel (FPSO) is dictated largely by storage requirements, processing requirements, environmental conditions, and water depth. The storage requirements is dictated by the overall optimization of the shuttle tanker transportation system and is chosen so that overall transportation costs can be minimized while ensuring that associated production downtime is close to zero. A large amount of on site storage allows more flexibility and cost efficiency in the shuttle tanker system as it may be possible to use a small number of large shuttle tankers. As a rule of thumb, the FPSO is sized for approximately 6 days of storage. The floating production system will be more expensive than an equivalent sized tankers because of requirements for smaller tanks to reduce motions, an off loading system, and additional accommodation. While the FPSO will have thrusters for positioning and avoiding icebergs, it may not require the efficient propulsion system that a shuttle tanker requires.

The process equipment on the vessel is determined largely by the volumes of oil, water, and gas received, requirements for gas and water injection, and the viscosity of the fluid. Generally, except for very small FPSO's, there is adequate area and weight capacity for processing equipment so this is not a design factor. Special processing systems which can allow production in rough seas may be installed.

The environmental conditions and water depth affect the type of turret-mooring system required. For harsh environments such as the Grand Banks, internal turrets are required to limit motions and wave forces. The size of the turret system depends on the number and sizes of risers required for produced fluids, control, and injection of gas, water,

and chemicals. While drilling and work over operations have been performed from large central open turrets, these have not been considered appropriate for harsher environments. There is a trade-off between using large numbers of risers and an expensive turret-mooring system, or using subsea manifolds to reduce the number of risers. With subsea manifolds, operating expenses can go up significantly if repairs are required.

Where the off loading rate to the shuttle tankers is required, a value of 6000 m^3/hr based on the Gryphon field will be used. The average time spent by shuttle tankers at the Gryphon mooring site is 24 hours (Doble et al., 1994)

A good general source of information on the costs of FPSO's is a paper by Henery and Inglis (1995). Costs for FPSO's can range from $50 million US to $700 million depending on environmental conditions, the peak production rate, number of risers, and complexity of the processing. The smaller cost corresponds to a small field with mild environment and simple processing requirements. The higher cost corresponds to a large field, deep water, harsh environment, large number of risers, and complex processing system.

The authors break down the FPSO costs into vessel, process, mooring and fluid transfer, and installation costs. A typical breakdown for the North Sea would be 39, 42, 14, and 4 percent respectively of the total cost. In another example, based on a field in the far east, the process cost made up only 24% of the total cost; in that case water injection was not required and a more economical process system was developed.

Example costs are given for vessels in terms of US$/bbl storage, for process costs in terms of US$/bbl/day, and for turrets. The costs appear to be based on a limited data set. The costs include project management, engineering, certification, and overhead which

typically add 15% to cost of the hardware items. The authors note that of the FPS systems which had completed operations on site by that date, most were on site for less than 6 years, the longest was on site for 11.5 years. These were roughly evenly split between FPSO and semi-submersible systems. It is of note that these duration are considerably shorter than that planned for the Terra Nova field.

Costs for new built vessels range from $100 US/bbl for a ship-like vessel to $275/bbl for a fully custom designed vessel. For an FPSO with a 700,000 bbl storage capacity, the above costs indicate a range from $75 M US to $206 M US. One feature of the custom designed vessel mentioned is a ballast system which allows the operators to keep the FPSO at nearly constant draught. The authors recommend that FPSO's be kept ship like, because the design methods are better established and cheaper, the construction is highly redundant and crack tolerant, and is also easily inspected and repaired. It would appear that the paper refers mainly to single hulled vessels; they mention that the IMO MARPOL 13G regulation for double hulled tankers is resulting in increasing cost conversions and that ship yards cost may increase as "they become busy rebuilding the world fleet". In the case of conversions, the authors indicate that for a long field life, the cost of a conversion and ship-like new build will be about the same. For shorter field lives, the conversion may have an advantage.

The process costs shown range from $500 US / bbl / day for a system of far east construction with no water injection to $2500 - 3000 US / bbl / day for European construction, with water injection. For a 100,000 bopd rate, this gives a large range from $50 - 300 M US. The authors claim that the process units of European construction did not use

the larger space of FPSO's effectively and could be built cheaper using a fit for purpose approach.

The costs of internal FPSO turret mooring and fluid transfer systems range from $40 M for a small turret in shallow water and moderate conditions to $120 M for a large system in deep water and hostile environment. The particular design will depend on the vessel size, environmental conditions, water depth, number of risers, whether or not the system is disconnectable, and whether the direction the vessel takes is controlled or passive.

The authors provide a plot that shows the average FPSO cost would be about $6,500 - 0.01667 x US where x is the peak production rate in bbl/day. The production rate ranged from 0 to 180,000 bopd. The points in the figure show a very large variation with respect to this line. In an example application for a 50,000 bopd system with 700000 bbl storage, the authors use an installation cost is $15 M. They indicate that the cost per subsea well, including drilling, subsea equipment, and risers, can range from $20-50 M US "depending primarily on the time taken to drill the well and the length of the flow lines and risers". They indicate that roughly half of this cost would be for hardware and half for drilling. The data they present shows costs ranges from $10 - 50 M US in the UK and from $25 - 65 M US in Norway.

4.2.3.6 Shuttle tankers - cost model

The capital cost of shuttle tankers, will be taken from Equation 4.2. A notional correction factor of 0.35 will be applied to include any modifications to meet regulations and particular requirements for a shuttle tanker. The vessel will be sized to match the storage

capacity at the FPSO (namely 6 days of storage at peak production). It will be assumed that three shuttle tankers are required. The operating cost per shuttle tanker is determined from the quote cost of $8 million per year for a 127,000 tonne vessel for Hibernia by scaling linearly by deadweight.

4.2.3.7 Cost models for production vessels, turrets, and topsides

The capital costs are modelled separately for the vessel, process system, turret-mooring system, and are chosen to include installation costs. The base cost of the FPSO vessel and the process equipment are determined as a function of the peak production rate. The cost of the FPSO is determined as

$$c = 38000\, p^{0.75} \tag{4.8}$$

and the cost of the topside equipment as

$$c = 60639\, p^{0.512} \tag{4.9}$$

where c is cost in in dollars and p is the peak production rate. The exponents are notional values and the constant coefficients were chosen to match the cost of the FPSO vessel and topsides for Terra Nova as considered in Croasdale and McDougall (1994). The production rate was used rather than deadweight in the case of the FPSO because of difficulty in breaking down published weights and costs between the vessel, turret, and topsides equipment.

The turret-mooring cost is modelled according to equation

$$c = 40 + .0003\, p \tag{4.10}$$

where c is the cost in millions of dollars and P is the production rate in bopd. This equation is based in part on Croasdale and McDougall (1994) and in part on Henery and Inglis (1995). It is assumed that this is the cost for a turret on a vessel designed for conditions similar to the Grand Banks but without the need for a quick release system for icebergs.

4.2.3.8 Additional costs

Additional expenditures may be required for other items such as supply and standby vessels, aircraft, on shore support, engineering, etc. These costs have been modelled using the equation

$$c = 5.16\, R_I^{0.75} \tag{4.11}$$

where R_I is the magnitude of the initial field reserves in millions of barrels. The exponent is notional and the constant coefficient was chosen to match half of the additional costs quoted in Croasdale and McDougall (1994).

4.2.3.9 Operating expenses

The annual operating expenses for all items except the shuttle tankers and ice management are taken as .085 times the total capital cost for all items other than the shuttle tanker. This value was based on the approximate ratio for operational costs to capital costs from the Terra Nova Development Plan (1996).

4.2.4 Costs related to the presence of icebergs

4.2.4.1 Ice surveillance and managment

The ice surveillance system will consist of the use of marine radar from the production vessel and support vessels, aircraft for overflights, offshore and land based personnel, computer systems and communication and co-operation with government and international agencies such as the Canadian Atmospheric and Environmental Services (AES) and the International Ice Patrol (IIP). The total annual cost will therefore be much greater than just the costs of overflights. At present, a notional value of $3 million dollars per year is used for ice surveillance. One may be able to improve the system somewhat with further research and better equipment. For example, analytic methods for scan to scan integration are improving detection capabilities considerably.

The ice management system consists of support vessels which can deflect icebergs by towing, prop washing, or water cannon. This would require upgrading supply vessels and possibly using additional vessels. At present, a notional value of $3 million dollars per year to hire upgraded towing vessels is used.

4.2.4.2 Riser and mooring release systems

The quick release system for the Grand Banks will be different than previous quick release systems in that it is still desired to keep the system on site during high sea states. The advantages of quick release systems in the South China Sea were that typhoons could be avoided and therefor the overall mooring system could be designed more cheaply. The cost of the riser mooring system will depend on how quickly and reliably the system needs to be

disconnected. Though there is a trade-off between cost and reliability, a fixed extra cost of $20 million will be modelled to acquire an upgraded turret system.

4.2.4.3 Ice strengthening and modification of vessels

As part of the study Canadian Offshore Design for Ice Environments (CODIE, 1996) project a study was conducted by N. Roudasoya to estimate costs for vessel ice strengthening.The approach used was roughly as follows. First, basic structural design plans without ice strengthening were developed for three sizes of double hulled bulbous bowed tankers and from these the amount of steel required was estimated. The sizes of vessels were 44,367, 78,228, and 127,000 tonnes deadweight respectively. Then, the changes in design to meet both the Finnish-Swedish 1AS class rules for the Baltic, and the Canadian ASPRR CAC 4 rules for the arctic were determined. From this the resulting changes to the light ship weight was calculated. These sets of rules give an idea of the range of ice strengthening that might be required for Canada's east coast since Baltic conditions are relatively mild whereas in the Canadian Arctic the vessels may occassionally need to ram their way through multi-year ridges. Because the Baltic rules apply only for first year sea ice, ice strengthened is only required in a belt around the waterline.

A parametric costing model was developed by Roudasoya to estiate the increases in costs for ice strenghtening. The costing model is based in part on a method by Carayette (Naval Architect, 1978) and was further modified by Professor Dag Friis (MUN Engineering and Applied Science) and Mr. Raudasoja. In the model, parametric equations were used to determine costs for the categories steel, machinery, outfitting, steel work labour, machinery

installation labour, and outfitting labour. These equations are based largely on the amount of steel required for the vessel. A shipyard overhead of 100% was applied to the sum of these costs, and a shipyard profit of 15% is applied to that.

The results of the study are summarized in Table 4.3 . It is seen that the price of 1AS vessels increased between 1.3 and 1.4 percent and the displacement was reduced by 0.5 to 0.7 percent. For the CAC 4 vessel the price increased between 3.3 and 4.0 percent and the displacement was reduced by 1.5 to 1.9 percent. In costing a vessel which will have ice strenghtening, it should be noted that a slightly larger ice strengthened vessel is required to achieve the same deadweight, thus increasing costs more.

Table 4.3 Results from study on costs associated with ice strengthening of vessels

Vessel	Class/ Source	DWT (tonne)	Change (%)	Price (million $)	Change (%)
Model 1	Open	129990		64.15	
(127000 dwt)	A1S	129200	-.5	65.09	1.4
	CAC 4	127900	-1.5	66.77	4.0
	(NRC)			79	
Polyclipper	Open	83120		51.38	
(78228 dwt)	A1S	82630	-.6	52.05	1.3
	CAC 4	81870	-1.5	53.08	3.3
	(NRC)			62	
Torm Asia	Open	44500		35.37	
(44367 dwt)	A1S	44190	-.7	35.82	1.3
	CAC 4	43660	-1.9	36.59	3.4
	(NRC)			46	

As discussed in the previous sections, the tankers being used for Hibernia will have better manoeuvrability than normal shuttle tankers, further work in understanding the design requirements and costs is required. Therefore for the shuttle tankers, a factor of .05 will be applied to the cost for ice strengthening and an additional factor of .10 will be applied for improving the vessels manouevability.

For the FPSO, a a factor of .05 will be applied to the cost for ice strengthening.

4.2.4.4 Protection vs replacement of subsea equipment

The designer must consider whether or not to protect subsea equipment and flowlines. If considering an option to leave the equipment unprotected then the expected rate and cost of scour damages, including downtime while waiting on weather conditions, needs to be accounted for. In addition, the risk of damage by trawlers may be a factor. The use of weak links to limit damage if flowlines are dragged along by an iceberg keel or trawler may be one option to consider. The risk of environmental damage due to leaked oil or blowouts must also be considered. The use of fail safe valves below iceberg scour depths reduces this risk.

In modelling costs related to iceberg scour events, the costs were modelled using the following notional values: $1 million to repair a flowline, $2.5 million to repair a tree, $2 million to repair a manifold, and $2 million to repair a riser base result. The average amounts of time required to get on site and repair these items will be taken as 30 days for a flowline, 70 days for a subsea tree, 40 days for a manifold, and 20 days for a riser base. The overall downtime if the flow from a single well is shut down will be taken as 0 since it may

be possible to increase the flow from other wells to compenstate. When the flow from a manifold is disrupted, then downtime of that amount of flow over the time to invoke repairs is assumed.

Subsea equipment can be protected by placing it in an open glory hole or in a cased glory hole (Lever, 1994). Individually drilled wells can also be placed in a caisson wellhead; with this system the wellhead and some of the tree valves are inserted into a slim caisson for protection. Flowlines can be protected by using trenching. The cost will depend on the sizes and lengths of lines to be trenched, and the required depths to ensure they are safe. It should be noted that when flowlines are buried, operating costs associated with maintenance and repairs will be increased.

In modelling costs for protecting subsea equipment, the average cost per glory hole will be taken as $500,000 and the cost of trenching will be modelled as be 60% of the installed cost of the flowline.

4.3 Reliability-based design

4.3.1 Design criteria and approach

In this section, the approach used to determine global iceberg impact loads for design is outlined. The objective is to determine the load associated with a specified probability of exceedance. The designers may be requested, for example, to design the structure so that the probability of failure due to an iceberg impact is less than of 10^{-5} per year. Rather than consider the complete distributions of impact loads and structural capacity, they may estimate

the design load L_D based on a probability of exceedance of 10^{-4} and design the structure to $L_D \gamma$ where $\gamma>1$ is a load factor such that the extra order of safety is included in the design.

To determine the design load L_D, it is necessary to consider both the number of iceberg impact events, and the distribution of loads given an impact. Figure 4.11 illustrates

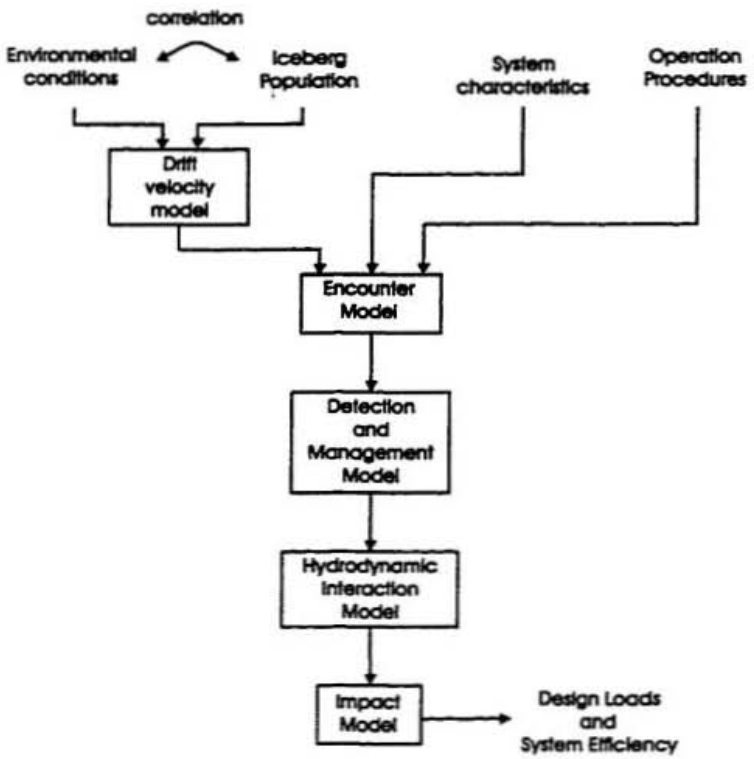

Figure 4.11 Overview of methodology for determining design iceberg impact loads

the steps that are required, details will vary depending on the type of system considered.

In the first step, the expected annual number of encounters with icebergs is determined. An encounter is defined as an event in which an iceberg would hit the structure if no mitigating actions are taken and the iceberg do not deflect due to hydrodynamcis interaction effects such as pressure gradients in front of the structure or diffraction. To be

able to determine the effectiveness of detection and management and to determine the impact loads, it is also necessary to estimate the number of encounters as a function of the iceberg characteristics and the environmental characteristics. The iceberg characteristics will be denoted by the vector $\tilde{I}$, and the characteristics of the environment by the vector $\tilde{E}$. The expected annual number of encounters as a function of the characteristics of the iceberg and environment will be denoted by $\eta_E(\tilde{I}, \tilde{E})$. As the number of encounters may be influenced by the drift velocities of the icebergs in the given environmental conditions it is necessary to determine the drift velocities of the icebergs, $V_D(\tilde{I}, \tilde{E})$. For structures at a fixed location, the probability of impact is proportional to the drift velocity. For moving vessels, the influence of the iceberg velocity reduces as the vessel velocity increases. Methods for determining the number of encounters will be outlined in Chapter 5. In addition, the distribution of impact velocities given an impact in given environmental conditions will be considered.

The effectiveness of operational procedures to reducing the number of impacts with a production system will be considered in Chapter 6. For gravity based platforms, this will include detection and towing of icebergs. For floating production systems, this will include detection, towing, and disconnection of the production and mooring systems. For shuttle tankers and other vessels this includes detection and avoidance manoeuvres. These are not considered.

Once the number of impacts is determined along with the associated distribution of iceberg size and shape, as well as impact velocity and location, the resulting distribution of impact loads is determined. The impact dynamics and ice failure mechanics are not

considered in detail, the models used for illustration purposes are outlined in the section 4.3.2.

4.3.2 Impact load modelling

4.3.2.1 Ice Failure Mechanics

Ice is a complex material which can deform and fail in a number of ways. At the high strain rates that occur in impacts, important mechanisms may include spalling, micro-fracturing, pressure melting, and recrystallization. Recent publications on these ice failure mechanics include Jordaan et al. (1993) and Jordaan et al. (1996). The average pressure at which the ice fails has been found to decrease as the contact area increases. Field observations of the global crushing force show that the change in force over time is quite random and it is important to consider this aspect when determining global design loads. The maximum local pressures increase with contact area. These high loads are likely the result of the confining effect of the surrounding ice; under a hydrostatic load, a larger applied force is required to cause shear failure. Experiments by Frederking et al. (1990) indicate that local pressures exceeding 70 MPa can occur over small contact areas within the high pressure zones. The local loads are an important consideration when considering damage to concrete or to a ships plating. The distribution of local loads will be a function of the number of high pressure areas and the amount of confinement, these is turn will depend on the duration and contact areas of the collisions. Jordaan et al. (1992) have considered different statistical methods to determine these distributions.

There is limited data available at present on the crushing strengths of glacial ice at the contact areas and velocities expected during a full scale iceberg impact. Some ship impacts with icebergs have occurred but it is difficult to determine the ice failure pressures based on the observed damage to the vessel alone. Given the lack of directly applicable data, it is necessary to estimate the loads based on experimental data and on measured data from other types of ice interaction scenarios. Sanderson (1988) analyzed measured data from a number of different full scale first year and multi-year interactions in the arctic and developed the equation

$$p_P = 9.3\, a^{-\frac{1}{2}} \tag{4.12}$$

describing the approximate relationship between peak pressure and contact area. Jordaan et al. (1992), using medium scale experimental data from Pond Inlet and Hobson's choice, have verified that interactions with glacial ice follow the same general relationship. These data include interactions with contact areas up to 1 m^2 and indentation rates up to 0.1 m/s. Jordaan and Zou (Cammaert et al., 1992) analysed data from a number experiments involving icebreakers ramming into multi-year flows (Dome Petroleum, 1982; Glen and Blount, 1984). The events involved higher impact velocities and so may be more representative of the collisions that would occur between an iceberg and a vessel or structure. Using the data from Hobson's choice, Pond Inlet, the Moliqpak, and the Kigoriak, they suggest a relationship of the form

$$p = 3\, a^{-\frac{1}{2}} \tag{4.13}$$

for the average ice crushing pressure during a collision.

If a single pressure area relationship such as Equation 4.13 is used, this ignores variations between impact events and also variatons during events. This is illustrated in Figure 4.12.

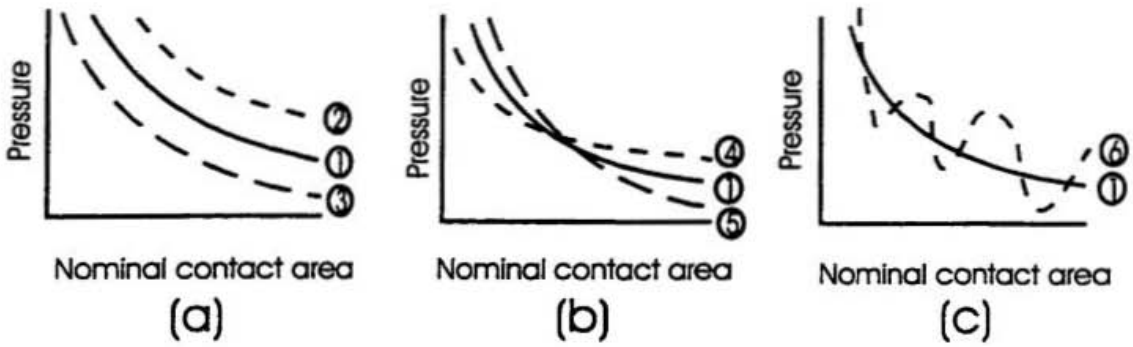

Figure 4.12 Variations in average ice crushing pressure versus nominal contact area

If the pressure during an impact remains higher than average (curve 2 relative to curve 1), then the maximum penetration and the final contact area will both be smaller. Whether or not the predicted peak load is higher will depend on the particular relationship. Alternatively if the pressure is always lower (curve 3), then there will be a smaller final pressure but a higher area. If there is a difference in the exponent of the pressure area curve, such that the initial pressure is low and the final pressure is high (curve 4), then a significantly higher peak load may result. Including the variations in this exponent can influence the estimated design loads considerably. If the load varies about the mean (curve 6), then the final area will be approximately the same as the load determined using the average pressure area relationship. The final force, however, will depend on whether there was a peak or a trough. Clearly, the maximum force could occur before the end of the collision.

One aspect of a recent study by Carter et al. (1996), dealt with the largest loads that icebreakers in the Canadian Artic would be subjected to during ramming. As part of this study, an ice failure model consisting of a pressure area curve

$$P = Ca^{D}$$

with random coefficients C and D was calibrated using data from available ramming trials. The relavent parts of this study are summarized in Appendix A. It was found that reasonable results could be obtained for rams (where crushing was the primary failure mechanism as opposed to flexural failure) by modelling the coefficient C with a lognormal distribution with mean of 3.0 MPa and standard deviation of 1.5 MPa and modelling the coefficient D with a normal distribution with a mean of -0.4 and a standard deviation of 0.2. Two differences between the rams modelled and impacts with icebergs should be noted. First, the rams involved multi year sea ice rather than glacial ice. In multiyear ice the salt is has been largely extruded from the ice, but the grain structure may be more columnar than glacial ice. Also, the temperature and flaw structures of the ice may differ. Second, during ice ramming, smaller vessels beach. After the initial impact the vessel acquires sufficient large vertical component such that the velocity of the ship plating is largely tangential to the ice contact face. In this case the driving is limited to some extent by the weight of the vessel. This factor was incorporated into the model and reasonable calibration was achieved, given the uncertainties in the measurements, for both small and large vessels.

To test the sensitivity of results to the assumptions regarding the ice failure, several models will be used. These include models of constant failure strengths of .5, 1, and 4 MPa, the use of a pressure area curve $P= 3\ A^{-.5}$, the use of this pressure area relationship with a cut

off minimum pressure of .25 MPa, and the use of a pressure area relationship with the same random coefficients developed in Carter et al. (1996).

4.3.2.2 Impact Dynamics

The maximum contact area during a collision requires consideration of the initial velocities of the two bodies, the ice crushing pressure and the local response of the structure, the shapes of the two bodies at the point of contact, and the global responses of the iceberg and vessel/ structure.

In modelling impacts between icebergs and both gravity based structures and FPSO's, the impact has been modelled in terms of a spherically shaped iceberg of equivalent mass hitting a rigid vertical wall. This has allowed the development of reasonably simple interaction models which is used to give an indication of the sensitivity of design loads to such factors as the number of icebergs, the impact velocities, and the ice failure mechanics. In order to assess the effect of these simplifications, some recent publications on impact dynamics and shape are mentioned briefly.

Figure 4.13 illustrates an impact between an iceberg and a GBS. The velocity of the iceberg is indicated as V. Only the component V_N of velocity normal to the structure at the point of contact is considered; the effect of the tangential force due to friction has been shown to be small (Matskevitch, 1996). As the impact proceeds, the iceberg will start to rotate around the point of contact due to the applied moment.

The effect of impact eccentricity on the maximum impact load has been considered recently by Matskevitch (1997). Matskevitch analytically determined the ratio $Fmax/Fmax^0$

as a function of ε_0 / r_i for elliptical cylinders where $Fmax^0$ is the maximum force in a direct impact and Fmax is the maximum force given eccentricty ε_0 and radius of gyration r_i . Matskecitch found that the the ratio would nearly always be greater than .75 and generally would be much closer to 1.

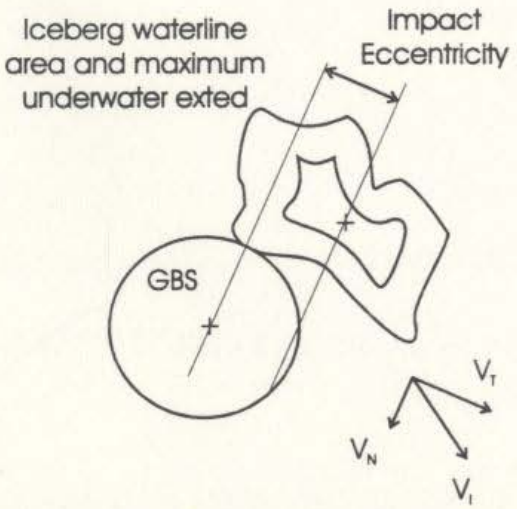

Figure 4.13 Iceberg impact with GBS

The variation in the shape of the iceberg at the point of contact is significant since it affects the maximum contact area achieved before the kinetic energy of the iceberg is absorbed. Little published data on local shapes of icebergs is available and data in this area would be helpful for analyses.

A factor which could have an effect in lowering the estimated collision loads is whether icebergs may break up before the maximum force following the pressure area curve is reached. Often when iceberg are observed rolling over, they appear to break up into pieces due to the changes in buoyancy forces (alternatively they could appear to roll as they break up). This phenomenon may be dependent on the shapes and temperatures of the icebergs.

5 NUMBER OF ENCOUNTERS WITH ICEBERGS

5.1 Introduction

In this Chapter, methodologies are presented for determining both the annual expected flux η_F of icebergs across line segments and the annual expected number of encounters η_E of icebergs with various types of structures. So that the probabilities of detection and management can be determined as well as the impact velocities, the flux and number of encounters are required as a function of iceberg size and environmental conditions. In this case they are denoted as $\eta_F(\tilde{I}, \tilde{E})$ and $\eta_E(\tilde{I}, \tilde{E})$. The methods used are based on geometric arguments and thus avoid the need to simulate iceberg trajectories. In addition, a method for estimating the distribution of wave-induced impact velocities of smaller icebergs is given.

In Section 5.2, the areal density of icebergs on the Grand Banks as a function of location and time is described. In addition, distributions of relevant iceberg parameters required in later analyses and relationships between them are presented. In Section 5.3, distributions for the relevant environmental parameters and relationships between them are considered. When estimating the environmental conditions during iceberg interactions, the seasonal correlation between the number of icebergs and the environmental conditions must be accounted for. Most icebergs reach the Grand Banks in the spring and summer. The worst sea states occur during winter, and heavy fog conditions generally occur in the spring. While there may be a weak correlation between the number and sizes of icebergs and the environmental conditions in different years, this would be of secondary importance and was not considered. It was assumed that the sizes and shapes of the icebergs are independent of

the environment, so $\eta(\tilde{I},\tilde{E}) = \eta f(\tilde{I},\tilde{E}) = \eta f(\tilde{I})\, f(\tilde{E})$. Where year round operations are considered, a single distribution representing the probability of different values of H_s given an iceberg encounter can be used; determined by combining the distribution of H_s for each month, weighted by the expected number of icebergs in the month. In Section 5.4, an analytical method for obtaining a rough estimate of iceberg drift velocity as a function of iceberg size and environmental conditions is presented. The iceberg velocities are required as the probability of impact with fixed structures in given conditions is proportional to the iceberg velocities.

In Section 5.5, a method for estimating iceberg flux is presented. Flux is defined as the number of icebergs crossing a unit line per unit time. Flux estimates are of interest when determining how many icebergs could scour a subsea pipeline and when determining the amount of downtime as a result of icebergs entering production alert zones. In Section 5.6, methods for determining the expected number of encounters with different structures and vessels are presented. An *encounter* is defined as an event in which an iceberg impact will occur if no avoidance or management procedures are used and hydrodynamic interaction effects are ignored. Estimates of the number encounters are required when estimating iceberg impact loads for fixed platforms, floating platforms, ships, and subsea equipment. In Section 5.7 a statistical method is presented for estimating wave-induced impact velocities in random seas. In Section 5.8, a method for making rough estimates of the expected annual number of scour events is presented.

5.2 Areal density and relevant characteristics of icebergs

In this section, a brief overview of the required iceberg information and available data is given, followed by a description of the rationale used for choosing the methods used. Following this, the distribution of iceberg waterline length L used is developed. Relationships giving other parameters in terms of L are then outlined. Finally, an estimate of the areal density of icebergs is given.

The number of incidents with icebergs will be proportional to the number of icebergs in the region. The distribution of icebergs over time is important when considering strategies to avoid the main iceberg season. The shape and size of the icebergs present in a region will influence their motions, the probability of detection and management, and the probability of impact. Characteristics such as mass, rotational inertia, added mass, and the local shape of the iceberg at the point of contact influence the collision dynamics and ultimately the maximum impact loads. Because the shapes of icebergs are complex and unique, it is difficult to incorporate all of their characteristics in terms of a few parameters. Also, it is expensive and very difficult to measure underwater shapes. The approach taken is to define the iceberg shapes in terms of a few measured quantities, deduce other necessary parameters from these using approximate relationships, and use sensitivity analysis to determine if the assumptions and approximations are adequate.

Consider the iceberg illustrated in Figure 1. It is difficult for an observer to define precisely the shape of such an iceberg. Easily measured parameters include the maximum height, h, the maximum waterline length, L, and the maximum waterline width, W, measured at 90 degrees with respect to L. Sometimes rough estimates of the above water volume are

estimated from these three parameters, accounting for the general shape. In other cases, more accurate above water volumes are determined from stereo photography. Below water measurements, taken using sonar, are rare and can be subject to significant error.

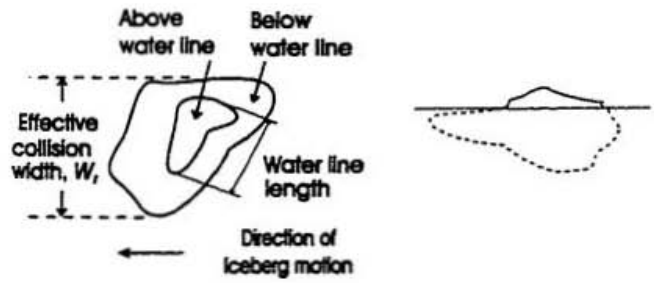

Figure 5.1 Seasonal distributions of number of icebergs and significant wave height.

It was decided to characterize the size of icebergs in terms of a single variable, the waterline length L. This variable is relatively easy to measure and is commonly quoted in the literature. While the mass of an iceberg may be a better overall indicator of size, it was felt that available length measurements were more accurate. A distribution was developed giving the probability of different sizes of icebergs in terms of L, then other iceberg dimensions were determined as needed from L using empirical or theoretical relationships.

Care must be taken when estimating an appropriate waterline length distribution, as recorded iceberg lengths may be based on a biased population and may be subject to significant error. For example, in recent reports the IIP has provided breakdowns of the number of icebergs by size classes and also give the ranges of waterline lengths within each size class. Problems with the data are that small icebergs are difficult to detect in many conditions, the size ranges are fairly coarse, and there may be significant error in the

observed size and the relationship between size and waterline length. A better source of data is the collection of measured waterline lengths measured by oil companies during exploration. This data is based on observations in which measurements were made from vessels which were in close proximity to the icebergs.

A distribution of waterline lengths was developed using an approach suggested by Crocker (1997). Crocker suggests based on observed distributions of larger icebergs, that an exponential distribution with a mean of 60 m is reasonable. Based on observations, he suggests that there is a calving mechanism which generates a greater number of small icebergs than this distribution shows. Crocker suggests that for the calved population, an exponential distribution with a mean of 8 m is appropriate. To determine the overall combined distribution, Crocker suggests that the number of icebergs of waterline length greater than 20 m should approximately equal the number of icebergs between 5 and 20 m. This is based on studies using overflights with good resolution photography. The waterline distribution used here was determined as the sum of the distributions of larger and calved icebergs weighted to meet this stipulation. The resulting distribution (shown in Figure 5.2) is

$$f_L(l) = .43\left[\frac{1}{60}e^{-\frac{l}{60}}\right] + .57\left[\frac{1}{8}e^{-\frac{l}{8}}\right] \qquad (5.1)$$

The associated mean iceberg length is 40 m.

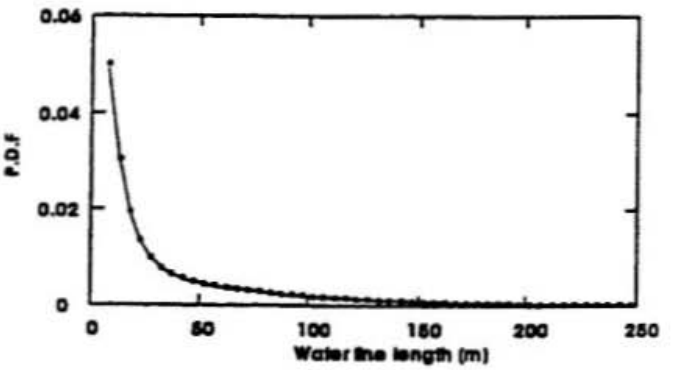

Figure 5.2 Iceberg water line length distribution

From Figure 5.1 , it can be seen that the probability of an iceberg impact is proportional to the effective encounter width, defined by the maximum extent of the iceberg perpendicular to its direction of motion. The maximum encounter width is greater than the waterline length because of the underwater extension of the iceberg. The actual encounter width depends on the orientation of the iceberg, which is a function of the current, wind, and waves, and will be less than or equal to the maximum encounter width. An estimate of the maximum encounter width could be obtained from complete iceberg profiles by assuming a random orientation with respect to direction. For the analyses here, the effective encounter width is approximated as 1.05 L based on an analysis of a limited number of icebergs (Crocker, 1994).

When using the wind and current drag forces to determine the iceberg drift velocities, the above and below water projected areas normal to the wind and the current, A_A and A_B, are required. These were determined from the water line length using relationships determined based on a set of 9 detailed iceberg measurements by Smith and Donaldson (1987). Though the sample was small, it spanned a considerable range of iceberg sizes and was based on

reliable measurements. Using best fits, the equations $A_A = .077\ L^{2.0841}$ and $A_B = .4451\ L^{2.0646}$ were determined. These results indicate that projected areas are nearly proportional to L^2. It was therefore decided to use equations of the form $A_A = a\ L^2$ and $A_B = b\ L^2$. Dividing the measured projected areas by L^2 gives a ratio of $a = 0.115 \pm .014$ for the above water portion and $b = .612 \pm .119$ for the below water portion. For determining the wave drift force, the characteristic dimension of the iceberg was required, for this the water line length was used.

The iceberg mass m is estimated from waterline length L using the relationship

$$m = 0.3L^3 \tag{5.2}$$

suggested by G. Crocker as a reasonable fit based on an analysis of several data sources (Cammaert et al., 1992).

In the encounter models, the number of icebergs is described in terms of areal density, i.e., the number of icebergs per unit area at a given time. This quantity is both simpler and easier to measure than flux quantities which depend on iceberg velocities as well as the distribution of directions in which they travel. The areal densities of icebergs are determined from the IIP's monthly and bi-monthly maps of iceberg counts collected between 1960 and 1994. These maps represent the IIP's best estimate of the positions of icebergs off the east coast at a given time. Though the IIP's main mandate is to delineate the southern most extent of icebergs at any time into shipping lanes, analysis of the data has shown that the counts are reasonably accurate over the Grand Banks. From these maps, an estimate of the areal density of icebergs by degree square and by year and month can be determined.

The expected areal density for a selected range of degree squares is shown in Figure 5.3 below. The numbers shown represent the expected (average) number of icebergs in the

each degree square at any instance, averaged over all months. During the iceberg season, the counts would be higher, whereas during the off season the counts would be near zero. The expected areal densities as shown are appropriate for systems which will be on site all year. The counts represent those ice pieces classified by the IIP as "icebergs" as opposed to "growlers". In terms of waterline length, the cut-off between growlers and icebergs is 16 m. It should be noted that there are alternative definitions for iceberg sizes classes.

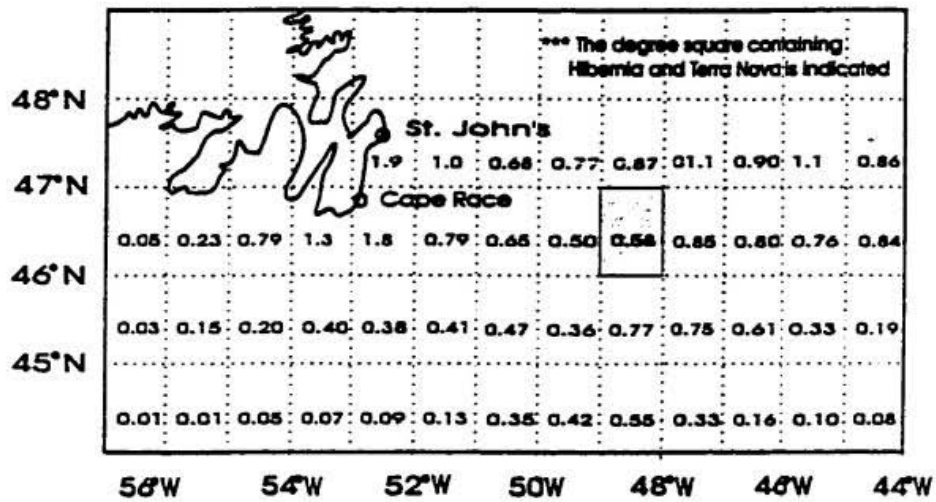

Figure 5.3 Average number of icebergs in a degree square based on IIP counts excluding growlers.

The number of averaged monthly counts for the degree square containing Terra Nova and Hibernia for each year and month over the 35 year period is shown in Figure 5.4.

Because small icebergs are not always detected, a correction was developed to the above IIP iceberg counts as follows. The IIP divides the counts of icebergs into icebergs (small, medium, and large icebergs which have waterline lengths greater than 16 m), and growlers (which have waterline length less than 16 m). As we felt that the number of growlers was significantly underestimated, we did not include these in the counts. To correct

the areal densities, it is necessary to add in the estimated proportion of undetected icebergs greater than 16 m plus the proportion of icebergs between 5 and 16 m. The estimated proportion of undetected icebergs greater than 16 m was determined in part based on a study of IIP airborne SLAR detection (Rossiter et al., 1985). The estimated fraction of icebergs detected is

$$p_D(l) = .98 - 1.2e^{-0.1l} \tag{5.3}$$

This relationship is plotted in Figure 5.5.

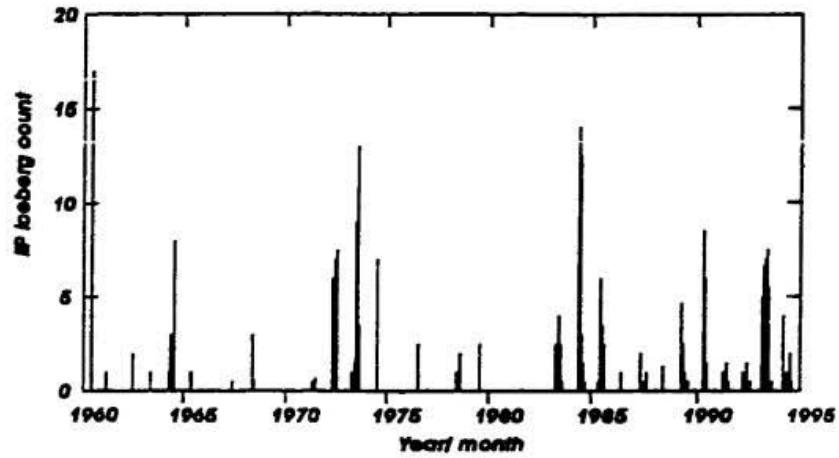

Figure 5.4 IIP iceberg counts - averages for year/month

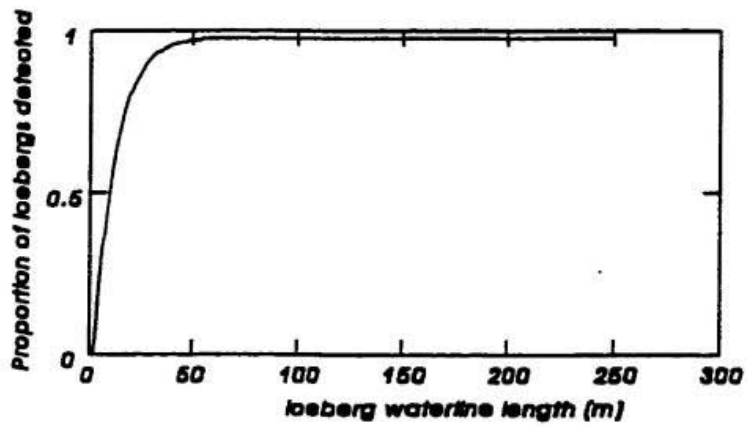

Figure 5.5 Proportion of icebergs detected by waterline length (IIP Airborne SLAR detection)

If one applies this relationship to the distribution of icebergs greater than 16 m, the resulting areal density would be underestimated by a factor of 1/1.04. We believe that this estimate is somewhat optimistic. Roughly 60% of the icebergs on IIP maps are detected using airborne SLAR. Radar systems from ships are not as good at detecting smaller icebergs (as discussed in Chapter 6) and so the 40% of icebergs detected from sources other than IIP SLAR are likely to consist of larger icebergs on average. For this reason, and because we suspect that the IIP SLAR tests may have involved better than average conditions for detecting small icebergs, a correction factor of 1.1 is used for the population of icebergs greater than 16 m. From equation 5.1 the proportion of icebergs which are growlers is determined as 42%.

The distribution of areal density of icebergs by month is required for determining the distribution of environmental conditions present when encountering an iceberg. This distribution was determined for the Hibernia/Terra Nova degree square using the data presented in Figure 5.4; the resulting distribution is shown below in Table 5.1.

Table 5.1 Proportion of icebergs by month

Jan	Feb	Mar	Apr	May	Jun	Jul	Aug	Sep	Oct	Nov	Dec
0	.056	.105	.256	.345	.203	.033	.002	0	0	0	0

5.3 Environmental characteristics

5.3.1 Sea state

The distribution for significant wave height H_s was derived from Atmosphere and Environmental Services (AES) Canada data. The data is based on wave-rider and NOAA wave-buoy data for the northern Grand Banks during the period 1970 to 1989. A distribution

representing the probability of the sea state given the presence of an iceberg was determined by averaging the monthly sea state distributions, weighted by the number of icebergs per month as shown in Figures 5.6 and 5.7. It should be noted that the highest sea states occur in January and February when there are fewer icebergs. During the main iceberg season the sea states are less severe.

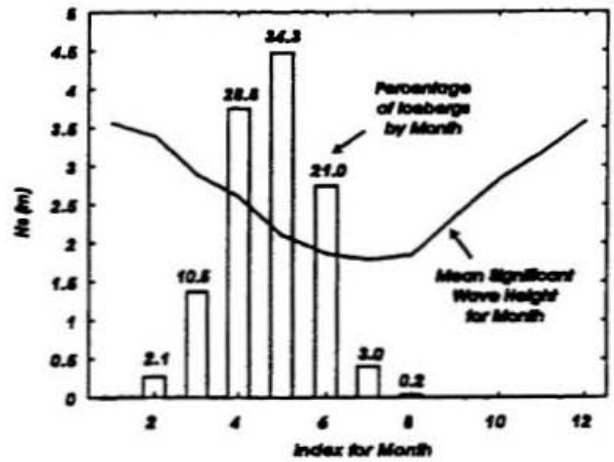

Figure 5.6 Seasonal distributions of number of icebergs and significant wave height.

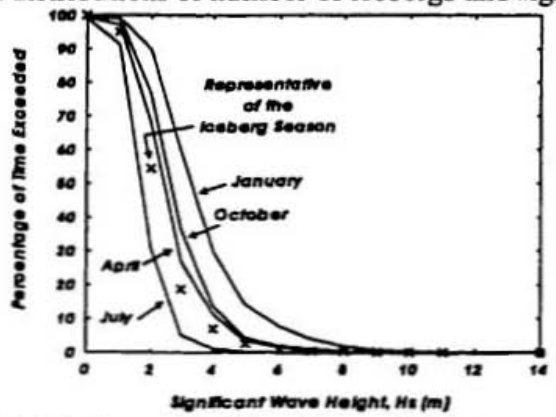

Figure 5.7 Distribution of significant wave height representative of the iceberg season.

For the iceberg drift model, the significant wave height H_S and the peak period T_P and associated wave length L_p are required to determine wave drift forces. The most likely peak

period T_P and associated wave length L_p, for each sea state were determined using the empirical relationships

$$T_p = 4.42\, H_s^{\frac{1}{2}} \tag{5.4}$$

and

$$L_p = 30.6\, H_s \tag{5.5}$$

derived by LeBlond et al. (1982) using Grand Banks data.

Where a sea spectrum was required for estimating iceberg and vessel random wave-induced motions, the Jonswap spectrum recommended by LeBlond et. al. (1982) was used. They recommended the following form as most closely resembling the sea state on the Grand Banks in storms:

$$S_w(f) = \frac{A}{f^5}\, e^{-\left[\frac{5}{4}\left(\frac{f_0}{f}\right)^4\right]}\, \gamma^a \tag{5.6}$$

where:

f	is frequency,
$S_w(f)$	is the spectral density at frequency f,
f_0	is the peak frequency (at which S_w is maximum),
$\gamma = 2.2$,	is the ratio of the maximum spectral density to that of the Pierson Moskowitz spectrum,
$a = e^{\frac{-(f-f_0)^2}{2\sigma^2 f_0^2}}$	
$\sigma = s_a = 0.07$	is the width of the left side of the spectral peak (for $f < f_0$),
$\sigma = s_b = 0.09$	is the width of the right side of the spectral peak (for $f > f_0$),
	and

$$A = \frac{5\, H_s^2\, f_0^4}{16\, \gamma^{1/3}}$$ holds for $1 < \gamma < 4$ where H_S is the significant wave height .

5.3.2 *Wind*

The wind associated with a given significant wave height H_S, was calculated using the following equation (Seaconsult, 1988, eqn. 3.2.1.1)

$$\overline{H_S}^2 = (aW^n)^2 + H_2^2 \qquad (5.6)$$

where:

$\overline{H_S}$ is the mean significant wave height for the given wind speed,

W is the wind speed (knots) at a height of 80 m,

H_2 = 2.1 m is the average background swell height (m),

a = 6.73 x 10^{-3}, and

n = 1.69 are coefficients determined empirically.

For values of H_S less than 2.1, a wind speed of 0 was used. In Figure 5.8 , the distribution of observed wind speeds from AES is compared to the distribution of wind speeds generated using equation 5.6 with the distribution of H_S (Figure 5.7) as an input.

When using the above wind estimates either to determine the wind drag force on an iceberg or to determine the wind generated surface current, it may be necessary to apply a correction factor to account for different reference elevations above sea level. Where required, the equation

$$v_{tz} = \alpha\, v_{ref} \left(\frac{z}{10} \right)^{\beta} \qquad (5.9)$$

(Det norske Veritas, 1977) was used, where:

v_{tz} is the wind speed averaged over the time interval t at a height of z meters above sea level (where t must be one of the times for which α and β are provided),

v_{ref} is the wind speed averaged over 1 hour at 10 m above sea level,

α is the gust factor for t, referenced to v_{ref}, and

β is the height exponent for t.

For example, a wind measured as V_w at 80 m height is reduced to 0.72 V_w at 10 m height. A comparison of the simulated and observed wind velocity distributions are shown in Figure 5.8.

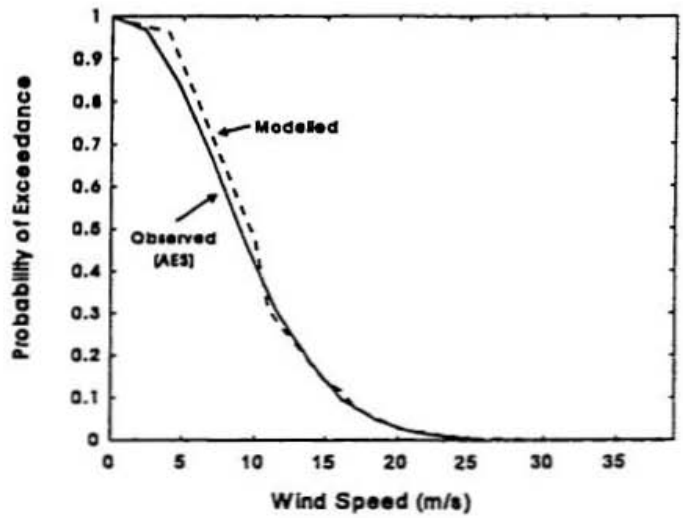

Figure 5.8 Comparison of simulated and observed distributions of wind velocity.

5.3.3 Current

An estimate of the most representative current associated with a given value of H_s was required for determining the drift velocities of icebergs. Only the component of the current generated by local winds was considered; this component will dominate in storm conditions. An approximate estimate of the locally generated current was obtained as

follows, using Ekman's model. First, the magnitude of the surface current was determined from the wind speed at a height of 10 m above the water surface using the relation

$$\frac{V_0}{W} = \frac{0.0127}{\sqrt{\sin|\phi|}} \tag{5.10}$$

where V_0 is the surface current speed, W is the wind speed, and ϕ is the latitude (Pond and Pickard, 1983, p. 109). At latitude 45 degrees north, this gives a current speed that is 1.5% of the wind speed. The direction of the surface current and its variation in magnitude and direction with depth are influenced by the Coriolis effect as outlined by Ekman. Because of the Coriolis effect, a forced wind or current will appear to turn to the right in the northern hemisphere. Where the wind contacts the water, there is a large change in density and it can be shown theoretically (with certain assumptions) that the surface current should move at an angle of 45° clockwise to the wind. The momentum imparted to the surface layer is transferred downward due to friction and the Coriolis effect causes the current direction at each depth to be oriented slightly clockwise to the current above it. This results in a spiral pattern. The velocity of the current decreases exponentially with depth. Ekman's equation for the variation in the current magnitude with depth z is

$$V = V_0 \exp\left(\frac{\pi z}{D_E}\right) \tag{5.11}$$

where V_0 is the magnitude of the current at the surface and D_E is the Ekman depth at which the current has 0.04 times the magnitude on the surface. This equation assumes that the water is at least as deep as D_E which is calculated as

$$D_E = \frac{4.3\,W}{\sqrt{\sin|\phi|}} \tag{5.12}$$

The net direction of the Ekman current can be shown to be 90 degrees to the right of the wind. When applying the above equations to determine the drift velocities of an iceberg, the Ekman current was averaged over its depth. This may result in a slight underestimation of effects of the current since most of the iceberg is near the surface. It should be noted that the equations derived by Ekman are only approximate because they do not incorporate factors such as limited water depths or density changes in the water with depth. The resulting distribution of current velocities using the distribution of H_S (Figure 5.7) as an input is shown in Figure 5.9 along with observed distributions.

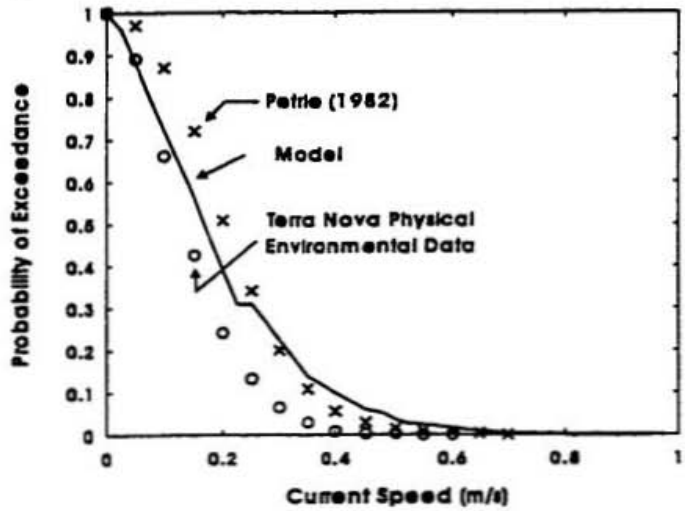

Figure 5.9 Comparison of simulated and observed distributions of current velocity.

5.4 Iceberg drift velocity

The drift velocities of icebergs of waterline length L in environmental conditions associated with H_S were estimated as follows. First, the combined wind and wave force on the iceberg in each case was determined. These forces could be directly determined because they are reasonably independent of the velocity of the iceberg. Then, the velocity of the

iceberg relative to the current was determined such that the water drag force was in equilibrium with the wind drag and wave drift forces.

The wind drag force was calculated using the equation

$$F_A = \frac{1}{2} C_A \rho_A A_A U_A^2 \tag{5.13}$$

where:

F_A is the wind drag force (N),

C_A is the wind drag coefficient for the given iceberg shape,

ρ_A is the density of air (kg/m^3),

A_A is the projected area (m^2) of the iceberg perpendicular to the wind direction, and

U_A is the wind velocity (m/s).

When applying this equation, the parameter A_A was taken as the mean above water projected area ($.115\ L^2$) and the wind drag coefficient was taken as 1.0.

When an object is large enough relative to the wave length, scattering of the waves occurs and a net force results on the object due to the diffraction of wave energy. For a given iceberg shape, this wave drift force may be estimated using the equation

$$F_D = \frac{1}{2} C_D \rho_w g D_I H^2 \tag{5.14}$$

(Isaacson, 1988) where:

F_D is the wave drift force (N),

C_D is the wave drift coefficient for the given iceberg shape,

ρ_W is the density of water (kg/m^3),

g is the acceleration due to gravity (m/s^2),

D_I is a characteristic dimension of the iceberg (m), and

H is the regular wave height (m).

The wave drift coefficient C_D is a function of the ratio D_I/L_W where L_W is the regular wave length; C_D is usually estimated analytically using models based on potential flow theory.

Wave drag coefficients for two different shapes of icebergs are plotted in Figure 5.10. The first curve, which is from Isaacson (1988), gives coefficients for cylindrically shaped icebergs with a draft to diameter ratio of 0.5. These drag coefficients may be indicative of the wave drift forces on tabular icebergs, which have steep sides. Isaacson also presented some results for square cylinders (with sides parallel to the wave crest). These give substantially higher wave drift coefficients (25-75% depending on the value of D_I / L). The second curve was determined by Momem Wishahy (Cammaert et al., 1992) assuming spherically shaped icebergs. These coefficients may be indicative of the wave drift forces for domed icebergs, growlers, and bergy bits which have rounded sides.

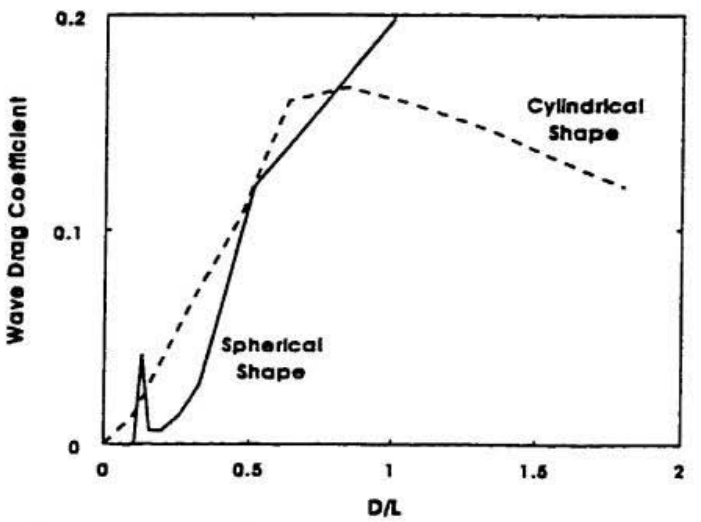

Figure 5.10 Wave drift coefficients for spherically and cylindrically shaped icebergs.

When applying the wave drift model, a spherical iceberg shape was assumed and the characteristic dimension D_I was set to the waterline length. The root mean square wave

height, $H = 0.706\ H_S$, was used to give the appropriate drag force representative of the random sea state. The wave length L was set to the peak wave length $L_p = 30.6\ H_S$. It should be noted that this method is only approximate, especially for light sea states where the swell could make up a relatively large proportion of the wave energy. The swell will have a relatively low frequency and could have a random direction with respect to the wind generated waves. When using the curve of wave drift coefficients, there was no data available for large D/L; in these cases a value of $C_D = 0.2$ was used.

The water drag force was calculated using the equation

$$F_W = \frac{1}{2} C_W \rho_W A_B U_W^2 \tag{5.15}$$

where:

- F_W is the water drag force (N),
- C_W is the water drag coefficient for the given iceberg shape
- ρ_W is the density of water (kg/m^3),
- A_B is the below water projected area (m^2) of the iceberg perpendicular to its direction of movement relative to the water, and
- U_W is the velocity (m/s) of the water relative to the iceberg.

Note that single values for C_W and A_B were used since the current was approximated as the Ekman current over the draft of the iceberg. When applying the water drag equation, the parameter A_B was taken as the mean average underwater area ($0.612\ L^2$) and the water drag coefficient was taken as 1.0. The residual current was set to zero.

In applying the above equations, the wind drag force F_A and wave drift force F_D were assumed to act in the same direction. F_W was set to $F_A + F_D$ and U_W was calculated from

equation (5.15). The drift velocity of the iceberg U_I was then determined as the vector sum of U_w (the velocity of the iceberg relative to the current) and the current velocity U_C (the Ekman current assumed to act at 90 degrees to the wind and waves).

A partial test of the validity of the drift velocity model was carried out by determining the marginal distribution of iceberg drift velocities for all iceberg sizes and environmental conditions and comparing this against an observed distribution. The marginal probability density function for any drift velocity $\hat{v}_I$ is determined as the integral of the probability of all iceberg sizes and environmental conditions resulting in that velocity, i.e.

$$f_{V_I}(\hat{v}_I) = \int \delta(\hat{v}_I, v_I(\bar{I},\bar{E}))\, f(\bar{I})\, f(\bar{E})\, d\bar{I}\, d\bar{E} \qquad (5.17)$$

This probability density function was determined using the distributions of L and H_S and the relationships for other parameters. This distribution used for comparison is from Seaconsult (1988), and is based on iceberg trajectories recorded from drilling platforms. The comparison is shown Figure 5.11. It should be noted that the distribution of observed drift velocities may be biased if the proportion of higher drift velocities in storm conditions is underestimated because of poor detection capabilities.

5.5 Estimation of iceberg flux and applications

In this section, a method is outlined for determining the flux of icebergs across line and curve segments, given the areal densities of icebergs and the distributions of drift velocities. Potential applications include determining the average rate at which icebergs will enter an alert zone and the rate at which large icebergs cross over a pipeline.

Consider the line segment in Figure 5.12 of length Δs, surrounded by randomly placed icebergs, with areal density ρ, and moving at speed v_I with direction defined by and

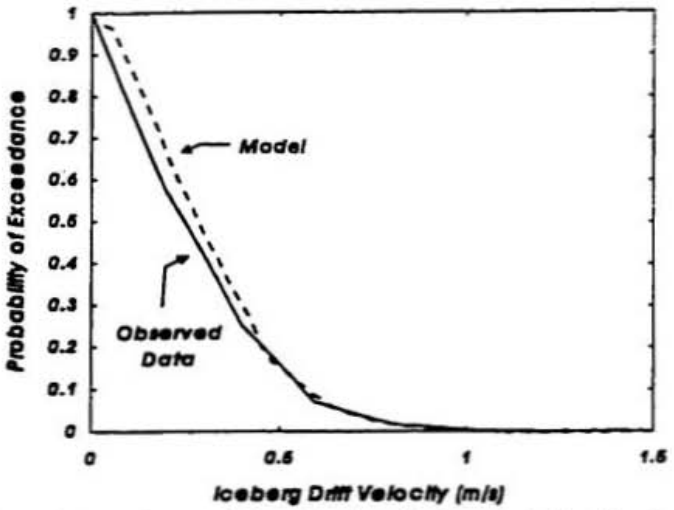

Figure 5.11 Comparison of simulated and observed distributions of iceberg drift velocities.

angle θ relative to the normal to the line segment. The expected number of icebergs crossing the line in time Δt is the areal density of icebergs times the area of the section outlined, i.e.

$$\rho \; v_I \; \Delta s \cos(\theta) \tag{5.18}$$

More generally, if one considers a curve s from point a to point b, and icebergs with random motions defined by the probability density function $f(v_x,v_y)$ then the expected annual number of crossings from a to b is calculated as

$$\int_{-\infty}^{\infty} \int_{-\infty}^{\infty} \left[\int_{a}^{b} |\vec{v} \cdot \vec{n}(s)| \; \rho \; T \; ds \right] f(v_x,v_y) \; dv_x \; dv_y \tag{5.19}$$

where v is the velocity vector, $n(s)$ is the normal vector to the curve at position s, and T is the number of time units per year. Equation (5.19) is the proper relationship to use to relate

iceberg areal density, iceberg velocity, and flux. If the areal density of icebergs and their velocity distribution vary over the region containing s, then v and ρ must be taken as functions of s as well. Note that the orientation of the path relative to the most prominent iceberg direction will affect the result. A example application of equation (5.19) is the estimation of the number of icebergs crossing over a subsea pipeline.

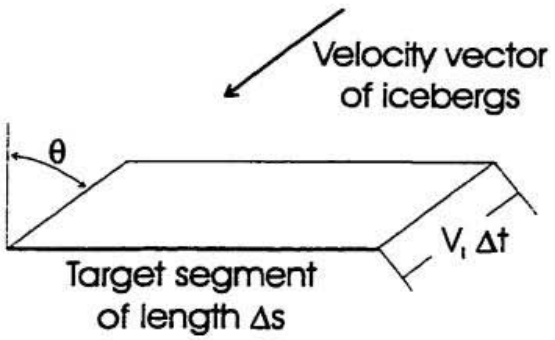

Figure 5.12 Illustration for determining number of icebergs crossing a line segment

In the case where the iceberg direction is random, one has the expected number of icebergs crossing a path of length s in either direction is

$$\eta_E = \int_{-\infty}^{\infty} \int_{-\pi}^{\pi} s\, v_I \cos\theta \, \frac{1}{2\pi} d\theta$$
$$= \frac{2}{\pi} \rho \, \langle v_I \rangle \, T \, s \qquad (5.20)$$

The number of crossings in one direction is half this.

Consider now the expected annual number of icebergs entering an alert zone of radius r. Assume that the areal density and distributions of iceberg velocities is constant over the region concerned. With reference to Figure 5.13 , it is seen that the expected number of icebergs with speed v_I in direction θ which enter the alert zone is

$$\int_{-\pi/2}^{\pi/2} \rho \, v_I \, \Delta t \cos\alpha \, r \, d\alpha \tag{5.21}$$

and integrating gives the number entering per year as

$$2 r \rho \, v_I \, T f(v_I, \theta) \, \Delta\theta \, \Delta v_I \tag{5.22}$$

Since θ is not involved in the main part of the equation, one can integrate over all angles and all velocities giving

$$\eta_E = 2 r \rho \, \langle v_I \rangle \, T \tag{5.23}$$

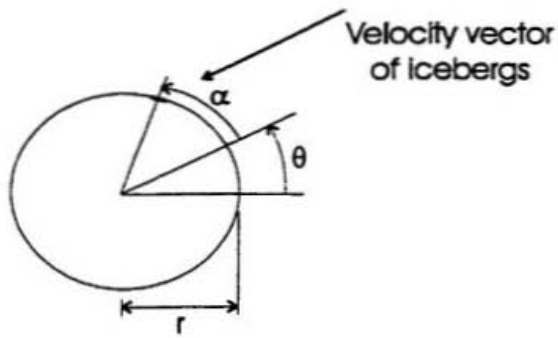

Figure 5.13 Illustration for determining number of icebergs entering an alert zone

In the above examples, it is of note that the distributions of velocities and angles for icebergs crossing a line segment must be updated using Bayes' theorem, since

$$f_{CR}(V,\theta) \propto V \cos\theta \, f(V,\theta) \tag{5.24}$$

Where the velocities are independent of direction, this becomes

$$f_{CR}(V,\theta) \propto V \cos\theta \; 1/(2\pi) \, f(V) \tag{5.25}$$

The probability of incursion therefore increases linearly with velocity and as the cosine of the angle relative to perpendicular. This means that the population of icebergs crossing a line

or entering an alert zone are more likely to be moving quickly and at a normal angle than the population in general.

5.6 Estimation of encounter rates and applications

In considering impacts between an iceberg and a structure, the method is similar, but the size and shape of the iceberg must also be accounted for. To illustrate the method to be used, consider an iceberg, circular in plan and of radius R_I, approaching an object of general shape as shown in Figure 5.14.

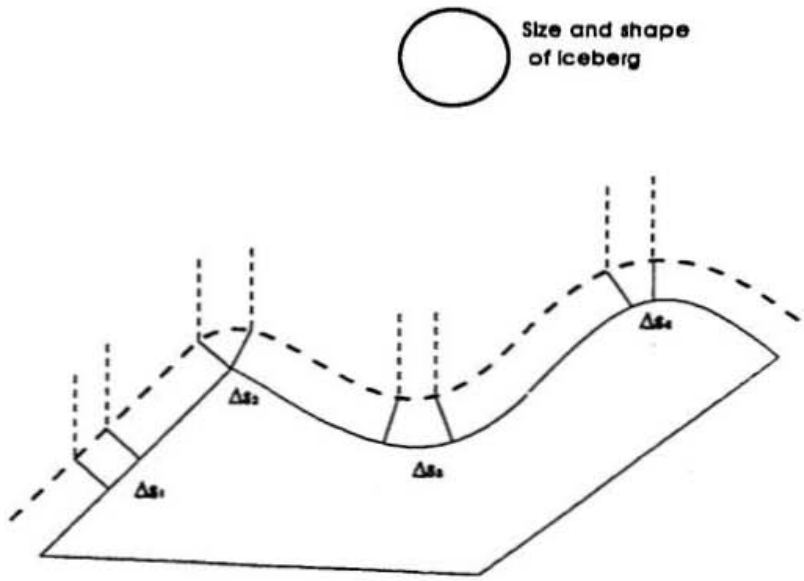

Figure 5.14 Possible impact locations for a structure of arbitrary geometry

Consider the initial position of the iceberg to be random. Contact will occur when the centre of the iceberg reaches any point on the dotted line a distance r from the structure. The same method can then be used as for the flux one way across a line. For example, the probability of an iceberg impacting a section of width Δ_S in a given time Δt (chosen small enough that

the velocity V_I of the iceberg does not vary) is proportional to $V_I \Delta s \Delta t \cos\theta$ where Δs is the target width, projected to include the size and shape of the iceberg, and θ is the relative angle of approach as indicated. The effect of the local curvature on the probability of impact is illustrated in Figure 5.14. Note that the probability of hitting a corner is enhanced significantly, especially for large smoothly shaped icebergs. If the iceberg is small or has a rough exterior, this effect is reduced.

If iceberg velocity is independent of iceberg size, then the expected number of encounters per year for a cylindrical structure can be determined from equation 5.20, using $W_I + W_S$ instead of $2 R_I$, i.e.

$$\eta_E = (\overline{W_I} + W_S)\, \rho\, \overline{V}\, T \tag{5.26}$$

To include the dependence of iceberg size on velocity, one requires the joint distribution $f_{W,V}(w, v)$ of iceberg effective widths and velocities, in which the correct equation is

$$\eta_E = \rho \iint (w_S + w_I) v_I f_{W,V}(w_I, v_I)\, dw_I\, dv_I \tag{5.27}$$

When applying the above equations, it is important to be careful that ρ and the distributions $f(w_I)$ and $f(v_I)$ are based on number of icebergs and their sizes and velocities given instantaneous snap shots of the region. If instead, one counts the number of icebergs entering some region around the vessel or structure, this is a measurement of flux and must be handled differently.

Determining the number of encounters for a ship (either at fixed location or moving) is slightly more complex. Impacts between small icebergs and vessels with vertical sides will be considered here (i.e. collisions on the vessel bilge, etc., are not considered). The icebergs are modelled as spheres, this should not affect the results significantly if representative radii

are chosen. The problem is illustrated in Figure 5.15 . The outline around the vessel shows the positions of the centre of the iceberg at which collisions with the specified size and shape of iceberg will result. Consider now a vessel with width w_S, length l_S, and speed v_S and an

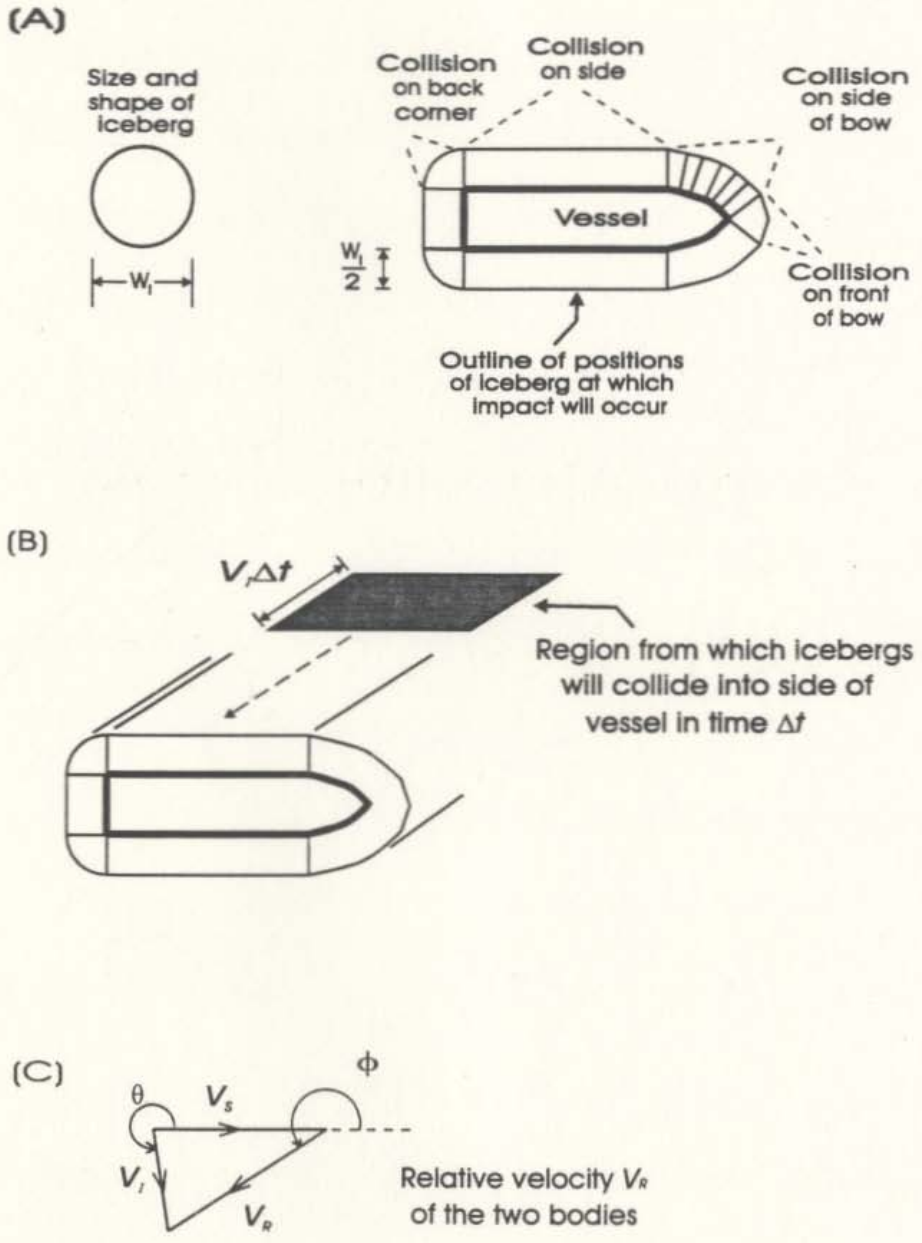

Figure 5.15 Illustration of iceberg contact positions around a ship

iceberg with diameter w_I and speed v_I which is moving at an angle θ relative to the heading of the vessel, as shown in Figure 5.15 b). The velocity and direction of the iceberg relative to an observer on the ship are denoted as v_R and ϕ.

The probability that the iceberg will hit a particular section of the vessel in a small time increment Δt is equal to the probability that the iceberg is within a distance $v_R \Delta t$ in front of that location. Note that the probability of one of the stern corners being hit decreases as the ship speed increases relative to that of the iceberg. In the case of a side collision, the area of the indicated region from which a collision will occur is

$$A(v_I, \phi) = l_S v_R \sin\phi \, \Delta t = l_S v_I \sin\theta \, \Delta t \tag{5.28}$$

where l_S is the length of the side. Assuming that all directions of relative motion of the icebergs are equally probable (as might be expected over many trips), the expected number of collisions on the side of the vessel in a time period T is found to be

$$\eta_E = \rho \int_0^\infty \int_0^\pi \int_0^\infty l_S \, v_I \, \sin\theta \, p(w_I) \, p(v_I) \, p(\theta) \, dw_I \, d\theta \, dv_I \, T \tag{5.29}$$

where $p(\theta)=1/(2\pi)$. The areal density and iceberg velocities should be averaged over the time period T. The distributions of iceberg size and velocity are assumed to be essentially independent, as before. Equation (5.29) integrates to give

$$\eta_E = \frac{1}{\pi} \rho \, l_S \, \overline{v_I} \, T \tag{5.30}$$

Note that the expected number of side collisions depends on the velocities of the icebergs and not on the vessel velocity except as vessel velocity influences T.

To find analogous equations for impacts on the bow, the exact geometry of the bow may need to be considered if the vessel is moving slowly. When the vessel is moving at a

velocity significantly greater than that of the icebergs, then ϕ will be close to -180 degrees and the effective collision width of the bow can be taken as w_S. The area of the region from which bow collisions can occur in a time Δt is then

$$A = (w_S + w_I)\ (v_S + v_I \cos\theta)\ \Delta t \tag{5.31}$$

It is again assumed that all directions of relative motion of the icebergs are equally probable. Integrating over all angles, iceberg sizes, and iceberg velocities, the expected number of bow impacts is found to be

$$\eta_E = \rho\ (w_S + \overline{w_I})\ v_S\ T = \rho\ (w_S + \overline{w_I})\ d_S \tag{5.32}$$

where d_S is the distance travelled. The areal density and ship velocity should be averaged over the time period T. Note that the expected number of collisions depends on the average iceberg size and is independent of the iceberg velocities.

For a turret-moored or dynamically-positioned ship at a fixed position, the analysis is slightly different. The vessel generally is pointed into the prevailing weather conditions. Assuming that this is the general direction from which icebergs come, the expected number of collisions on the bow is approximately

$$\eta_E = \rho\ \left(w_S + \overline{w_I}\right)\ \overline{v_I}\ T \tag{5.33}$$

To determine the number of collisions more accurately, and to determine the number of collisions on the sides, it would be necessary to determine the distribution of directions of iceberg approach with respect to the vessel. This would require information on the headings of turret-moored vessels and on the motions of icebergs in different environmental conditions.

For the case of a moored semi-submersible, held at a fixed orientation, the number of collisions and their locations will depend on the directions from which the icebergs approach. On the Grand Banks, a reasonable approximation is to assume that all angles of approach are equally probable since the net southerly drift of icebergs is much weaker than the tidal and storm induced motions. The problem of determining collision locations is complicated because of the geometry of the structure and possible hydrodynamic interaction effects. For example, to determine the number of collisions on pontoons, it is necessary to consider the random motions of the icebergs in waves.

5.7 Collision velocities, locations, and hydrodynamic effects

5.7.1 Overview

The velocity of the iceberg at the point of impact depends on the wave drift and wave-induced forces acting on it and the hydrodynamic interaction forces between the structure or vessel and the iceberg. In open water, drift speeds up to 1.5 m/s have been observed and for small icebergs in severe wave conditions, wave-induced velocities may reach 5 m/s. A GBS will be fixed, a production vessel may have wave-induced motions, and a shuttle or cargo vessel may move up to 8 m/s. The hydrodynamic effects will depend on the relative sizes of the two bodies and the dominant wave length. Important hydrodynamic effects include pressure distributions and diffraction effects which may cause smaller icebergs to deflect around a structure, added mass effects, and drag effects.

The hydrodynamic interaction problem is difficult to solve and not all aspects of the problem have been dealt with adequately to date. In the examples in this thesis, the

hydrodynamic interaction effects are not modelled (other than the use of simple added mass coefficients), instead the collision velocities are based solely on the random surge motions of the icebergs in open seas. Generally, hydrodynamic interaction effects will act to deflect or decelerate the icebergs so the omission of these effects will have a conservative influence on the estimated loads. To determine the possible effects of this omission, sensitivity analyses are performed with respect to the collision velocity in the example applications.

Methods for estimating the random surge motions of icebergs at collision have been outlined by Lever (1989) and the general method is followed here. A modified Rayleigh distribution was developed in order to include iceberg drift velocities and ship velocities correctly.

5.7.2 Comments on hydrodynamic effects

Even though the hydrodynamic interaction effects are not modelled, some of the different aspects of the problem are considered briefly here. The collision velocities will be determined by the wind, current, and waves present and by the sizes of the iceberg and vessel/structure relative to each other and to the wave lengths. Different aspects of the hydrodynamic interaction problem, including wave diffraction effects and collision added masses, have been addressed by Isaacson and McTaggart (1989) and Wishahy (1988). These analyses are generally conducted for ideal conditions, such as a uniform current or regular uni-directional waves. To date, no comprehensive model has been developed which can be used to predict accurately the number and severity of collisions. One of the important findings of model tests is that the collision probabilities are very sensitive to the initial

conditions. In repeated experiments with waves approaching a structure in a wave field, the icebergs followed different trajectories, so that collision events can not be predicted accurately even in ideal conditions. In actual conditions, the environmental loads will be in different directions and the sea state will consist of components with different wave lengths and directions; this will make predictions even more difficult.

In the ideal case of a uniform current moving past a fixed structure (or fixed vessel) there will be a pressure gradient in front of the structure and a wake behind it (the problem of a vessel moving at a constant velocity through the water is analogous). As an iceberg approaches the structure, this pressure gradient will act to slow the iceberg or divert it to the side. The distance that the iceberg is deflected will depend on its size relative to the structure. If the iceberg is relatively small, it will move with approximately the same speed and direction as the surface current; this is because the pressure gradient will vary nearly linearly over the length of the iceberg (unless the iceberg gets very close to the structure). In most cases the iceberg will be swept to the side of the structure, those that approach nearly dead on will decelerate significantly before collision.

When an iceberg is large enough that the pressure over its length varies non-linearly, then the iceberg will affect the overall flow regime. This is a difficult problem to solve, especially given that there is a free surface so that gravity waves will be generated. If, as a very rough rule, one models the iceberg as having the same velocity that a water particle at its centre point would have had, it can be easily seen that both the probability of collision and the average collision velocity will increase as a function of the icebergs size. Another approximate solution is to ignore the effect of the iceberg on the flow and integrate the

pressure gradient over the iceberg's surface at each instant to determine the net force on the iceberg and its acceleration. Even though the effect of viscosity causes a wake behind the structure, an inviscid flow solution will give an approximate analysis for the pressure gradient in front of it. An alternative solution which could be used to determine whether there will be significant 'cushioning' by the water between the structure and iceberg just before collision would be to approximate the problem using a closed form analytic solutions for the joint motions of two submersed bodies under the assumptions of an ideal fluid; for example, Lamb (1932) considers the motions of two submersed spheres.

The interaction effects due to waves will depend on the sizes of the iceberg and structure (or vessel) relative to each other and relative to the predominant wave length. Where the structure is small compared to the wave length (for example, the column of a semisubmersible in most sea states or a GBS in a high sea state), the structure will have little effect on the overall wave regime. As the wave accelerates and moves past the structure, a pressure gradient effect similar to that for a current will apply for an approaching piece of ice.

In situations in which the wave lengths are smaller relative to the size of the structure or vessel, diffraction effects become important. Wave energy diffracted from the vessel or structure can cause the icebergs to be decelerated or deflected. The combined incoming waves and diffracted waves result in a sea state with a different relationship between the wave height, period, and length than in open sea conditions and a different wave drift force and direction acting on the iceberg. Generally, the surge velocities of the waves are decreased near the structure resulting in smaller wave-induced collision velocities. The heave motions

may be enhanced; this could result in larger vertical collision velocities where pontoons or overhanging decks are present. Wave diffraction effects can be modelled analytically or using model tank tests. Higher order diffraction effects and interaction effects between two bodies can be difficult to model. A possible solution where the iceberg is relatively small is to use a linear diffraction model to account for the waves diffracted from the structure and then model the motion of the iceberg within this modified wave field.

The wave induced velocities of icebergs will depend on their size relative to the wave length and on the wave height. For icebergs that are small compared to the wave length, the velocities will be similar to the velocities of the water particles. As the size of iceberg considered increases relative to the wave length, the wave-induced velocities will in general decrease (there may however be peak values in the heave component at the resonance frequency of the iceberg). In a high sea state, the wave lengths may be long enough that a production vessel will have appreciable motions, in this case the joint motions of the vessel and iceberg will need to be considered.

It should be noted that the hydrostatic forces acting on irregularly shaped icebergs will be highly non-linearly (for example, for spherical shapes where the water plane area changes with heave). Where ice shelves are near the waterline, the non-linearity could be extreme. In such cases the superposition methods used do not strictly apply and the iceberg motions may well be chaotic. Lever et al. (1988b) used physical modelling to estimate the motions of cubical, cylindrical, trapezoidal, spherical icebergs and found that different shaped icebergs had different motion characteristics in heave and surge. While further work to determine the magnitude of these differences may be warrented, first a sensitivity analysis

based on available data should be conducted to determine if the differences will affect the design impact loads significantly. Some concern may be given regarding the chaotic response of icebergs. It should be recognized that the sea is a random forcing function that may overwhelm any chaotic effects. Even if chaotic effects occur, it needs to be demonstrated whether or not the statistical distribution of motions is significantly different than when linear superposition is used. Lever et al. (1989) used physical modelling to determine the locations and velocities of cubically shaped icebergs impacting a semi-submersible. The authors found reasonably good correlation between the observed distribution of impact surge velocities and that estimated based on significant open water surge velocities using superposition.

5.7.3 Random wave induced collision velocities

When determining the collision velocities, the random nature of the sea state and the resulting motions of the iceberg must be accounted for. An approach developed by Lever et al. (1989) can be used to model random wave-induced motions. Because the sea surface elevation in a random sea follows a Gaussian distribution, then as long as the motions of the icebergs vary nearly linearly with wave height it can be shown that the surge and heave component velocities in open water will have Gaussian distributions

$$f_N(u) = \frac{1}{\sigma \sqrt{2\pi}} e^{-\left(\frac{u^2}{2\sigma^2}\right)} \tag{3.41}$$

where:

$f_N(u)$ is the probability that the iceberg has velocity u at a given instant, and

σ^2 is the variance of the iceberg heave or surge velocity in open water.

The variance can be determined using the relation

$$\sigma^2 = M_0 = \left[\frac{V_s}{2}\right]^2 \tag{5.35}$$

where:

m_0 is the zeroth moment of the iceberg open water velocity spectrum, and

V_S is the significant velocity component of interest.

Using the results and analyses of model tests of the motions of spherical icebergs in random seas (Lever et. al., 1988b), and assuming Jonswap type spectra characteristic of the Grand Banks, Lever was able to determine non-dimensionalized curves for the significant surge and heave motions of the icebergs. The non-dimensional coefficients are 1) for the x-axis: the ratio of the wave length associated with the peak period to the waterline length of the iceberg and 2) for the y-axis: the ratio of the significant velocity to π times the significant wave height divided by the peak period. From these curves, significant motions for any iceberg size and significant wave height can be found.

Given the significant iceberg motions, random instantaneous collision velocities can be determined as follows (Lever et al., 1988a). For the case when an iceberg hits a vertical wall or cylinder, and the motion of the iceberg is sufficiently random, then the probability of a collision at any instant is proportional to the iceberg's forward surge velocity, i.e. the resulting distribution is proportional to

$$u \frac{1}{\sigma\sqrt{2\pi}} e^{-\frac{u^2}{2\sigma^2}} \tag{5.36}$$

Integrating from zero to infinity gives the normalization constant

$$s(\sigma) = \frac{\sigma}{\sqrt{2\pi}} \tag{5.37}$$

The resulting Rayleigh distribution has the form

$$f_R(u,\sigma) = \frac{u}{\sigma^2} e^{-\frac{u^2}{2\sigma^2}} \tag{5.38}$$

and the cumulative Rayleigh distribution is

$$F_R(u,\sigma) = 1 - e^{-\frac{u^2}{2\sigma^2}} \tag{5.39}$$

The above method is applicable for the open water case. Lever et al. (1989), analytically determined the distribution of collision velocities for icebergs in random seas with a steel semi-submersible using the above method and showed that the results correlated reasonably well with small scale model data in a wave basin. Because the semi-submersible had small members, causing minimal hydrodynamic interaction effects, they used the open water significant surge velocities of the iceberg. For a gravity- based structure or ship, this is not the case and the effect of the vessel or structure on the wave field should be determined. Wishahy (Cammaert, 1992) used the second generation radiation / diffraction program WAMIT (Wave Analysis MIT) to determine the significant motions of icebergs in the vicinity of a ship. He determined that the surge motions for a small iceberg near the vessel were decreased by 15 to 25%.

In order to properly model the random wave-induced motions for collision velocities, a new method has been developed. To include the constant wave drift or vessel velocities, the following modification must be made to the Rayleigh distribution (Lever has suggested using convolution integrals to do the same thing). Consider the case where the iceberg has a constant forward drift velocity k in this same direction (this can also include a constant

component of the ship velocity) and the random wave-induced velocity of the iceberg is Gaussian, i.e. the instantaneous velocity U follows the Gaussian distribution

$$f_U(u) = f_N(u-k,0,\sigma) \tag{5.40}$$

The distribution for the impact velocity, assuming that the probability of impact is proportional to the forward velocity will be called the 'Special Rayleigh ' distribution here. A solution for its cumulative distribution, $F_{SR}(u, \sigma, k)$ is derived below. This solution requires only that an algorithm for the cumulative normal distribution be available. To determine the mean of the distribution, an algorithm for the *erf* function is also required.

The cumulative Special Rayleigh distribution is given as

$$F_{SR}(u,\sigma,k) = \frac{\int_0^u x f_N(x-k,0,\sigma)\,dx}{\int_0^\infty x f_N(x-k,0,\sigma)\,dx} \tag{5.41}$$

The numerator may be rewritten as

$$\int_0^u (x-k) f_N(x-k,0,\sigma)\,dx + \int_0^u k f_N(x-k,0,\sigma)\,dx \tag{5.42}$$

The first term of the numerator may be rewritten as

$$\begin{aligned} &\int_{-k}^{u-k} t f_N(t,0,\sigma)\,dt \\ &= \int_0^{u-k} t f_N(t,0,\sigma)\,dt - \int_0^k t f_N(t,0,\sigma)\,dt \\ &= s(\sigma)\,[F_R(u-k,\sigma) - F_R(k,\sigma)] \end{aligned} \tag{5.43}$$

The second term in the numerator may be rewritten as

$$\begin{aligned} &k\left[\int_{-\infty}^{u-k} f_N(x,0,\sigma)\,dx - \int_{-\infty}^{-k} f_N(x,0,\sigma)\,dx\right] \\ &= k\left[F_N(u-k,0,\sigma) - F_N(-k,0,\sigma)\right] \end{aligned} \tag{5.44}$$

The numerator can thus be rewritten as

$$s(\sigma)\,[F_R(u-k,\sigma)-F_R(k,\sigma)]+k\left[F_N(u-k,0,\sigma)-F_N(-k,0,\sigma)\right] \tag{5.45}$$

Substituting infinity for k in the numerator, the denominator is seen to be

$$N_{RS}=s(\sigma)\,[1-F_R(k,\sigma)]+k\left[1-F_N(-k,0,\sigma)\right] \tag{5.46}$$

The Special Rayleigh distribution is thus

$$F_{SR}=\frac{s(\sigma)\,[F_R(u-k,\sigma)-F_R(k,\sigma)]+k\left[F_N(u-k,0,\sigma)-F_N(-k,0,\sigma)\right]}{N_{SR}} \tag{5.47}$$

The mean of this distribution may be found in a similar fashion and is given by the equation

$$\mu_{SR}=\frac{s(\sigma)\sqrt{\frac{\pi}{2}}\left[erf\left(\frac{k}{\sqrt{2}\sigma}\right)+1\right]+k\left[\frac{\sigma}{\sqrt{2\pi}}\exp\left(\frac{-k^2}{2\sigma^2}\right)+\frac{k}{2}\left(erf\left(\frac{k}{\sqrt{2}\sigma}\right)+1\right)\right]}{N_{SR}} \tag{5.48}$$

The method developed above applies for the case of forward surge. For the case of heave motions of icebergs, Lever has conducted additional work applicable in the case of collisions with pontoons on a semi-submersible. The collision velocity will then depend on the depth of the pontoon relative to the draft of the iceberg, and the problem of updating the surge and heave motions to account for the increased distance swept out becomes more difficult. It should be noted that these methods do not account for the effect of the sea bottom on waves in higher sea states. The effect of a limited depth is to increase the wave surge motions and decrease the heave motions, this could result in more severe collisions. Another point of note is whether repeated impacts by an iceberg in a wave field will be important. If so, this could impact upon the analysis since the largest collision load should be considered. For this analysis the assumption of one collision per interaction was used; the

possible effect of repeat impact can be seen by examining the sensitivity of results to the number of impacts.

5.8 Number of scour events

The rate of iceberg scouring varies over the North East Grand Banks depending on the water depth, bathymetric slope, and currents. The number of scour events at a given location can be estimated based on either observed scour rates or can be inferred from the number, sizes and shapes of icebergs, observed velocity distributions, and the distribution of environmental driving forces. There are significant uncertainties at present with both methods as will be briefly discussed.

The most straightforward method to determine scour risks is to use repetitive mapping to determine scour rates and the properties of the scours. There are two main problems with this approach. First, the rate of scouring is so low and the population of icebergs each year so varied that it takes a long time period to obtain a statistically representative sample. Attempts have been made to estimate scour rates from historical scours, but uncertainties due to various rates of infill of scours make this difficult. Second, it is difficult to detect shallower scours. Estimates of the number of scours per year per 100 km^2 in the Terra Nova / Hibernia region range from 0.04 to 0.35 depending on the method used (Lewis et al., 1987). In the Terra Nova Development plan (1996), the average scour width near Terra Nova is given as 25 m and the average scour length is given as 566 m. There is uncertainty regarding the proportion of shallow scours missed and regarding the measurement of scour lengths.

Crocker (1996) suggested the following approach (based on the above number, widths, and lengths of scours) as one alternative to determine the rate of scour events; this method is implemented in Chapter 7. If one assumes that these numbers are representative of the general region, and uses a value of 0.1 for number of scours per year per 100 km^2 the resulting scour rates may be determined as follows. The expected number of scouring icebergs per year passing over a subsea structure of width w_s may then be taken as (based on equation 5.23)

$$\eta_{se}(w_s) = \frac{0.1 \cdot (w_s + 25) \cdot 566}{100 \cdot 10^6} \tag{5.49}$$

The expected number of scouring iceberg per year crossing over a segment of subsea pipeline of length s may then be taken as (based on equation 5.19)

$$\eta_{sl}(s) = \frac{0.1 \cdot 2 \cdot 566 \cdot s}{\pi \cdot 100 \cdot 10^6} \tag{5.50}$$

If the structure extends above the seabed, then interactions with floating icebergs must be considered. Where the structure or line is buried, it is necessary to consider how deep icebergs scour and their effect on the soil at deeper depths. For equipment placed in caissons, it is necessary to determine the distribution of iceberg scour loads. If the equipment is placed below the sea bed in a glory hole, then it is necessary to determine how deep icebergs scour and how far into the glory hole they can move once the soil resistance is reduced and wave heave and pitch induced motions result.

Trying to infer the rate of scouring from the population of icebergs, observed trajectories, and distribution of environmental conditions would be relatively difficult. It would be necessary to consider the shape distribution of icebergs and the distribution of

driving forces to determine how often environmental driving forces would be sufficient to push an iceberg to a given water depth. The required driving force will depend on the soil type, the keel shape of the iceberg, and the hydrostatic restoring forces of the iceberg in heave and pitch (i.e. how easily it will lift and pitch). In considering the driving forces, the persistence and direction of the forces will be important (i.e. how often are icebergs driven onto the banks from deeper water). Finally, when icebergs do scour, their velocities will be different from those of freely floating icebergs in the same conditions.

An simpler approach has been suggested by Jordaan (1997). Observations of iceberg trajectories in the Terra-Nova region indicate that on average about 20% of the icebergs are grounded at any time (Jordaan, 1997). Based on the areal density of icebergs and the distribution of iceberg sizes, one can then estimated the average areal density of grounded icebergs. Jordaan estimated scour rates based on a rough estimate of the ratio of time that icebergs are scouring to grounded and based on average scour velocities from Crocker (1997). The resulting scour rate estimates are larger than those determined using the method above, even when a rate of 0.35 rather than 0.10 scour events per 100 km^2 is used.

6 OPERATIONAL ASPECTS

6.1 Introduction

In this chapter, the use of detection, management, and avoidance techniques to reduce risks related to icebergs is considered. In Section 6.2, the methods used for different systems are introduced along with possible overall approaches. In Section 6.3, the modelling of radar detection is addressed. A relatively simple model is proposed for the overall detection capability. In addition, a more detailed model for detection from supply and standby vessels is suggested which could be used in trying to optimize the overall detection system. In Section 6.4, a review is given of available data on towing success rates is given. A simple model which is used for sensitivity analyses in Chapter 7 is outlined. Finally, in Section 6.5 a simple model for determining the sensitivity of design loads to the mooring disconnect system is outlined.

6.2 Overview

The operational procedures that are used to reduce iceberg impact risks depend on the type of system considered. Figure 6.1 shows the steps involved in determining if an impact can be avoided in the case of a floating production system. The iceberg must be detected and then either towed or the production vessel successfully moved off site.
In the case of a GBS, impact is avoided if the iceberg is both detected and successfully towed. In the case of a shuttle tanker, rather than towing the iceberg, the course of the vessel must be altered by manoeuvring.

The first problem is to determine the probability of successfully detecting icebergs.

For floating and fixed production systems, methods of detecting icebergs include visual and radar surveillance from the production vessel or platform, from the support vessels, and from aircraft as illustrated in Figures 6.2 and 6.3.

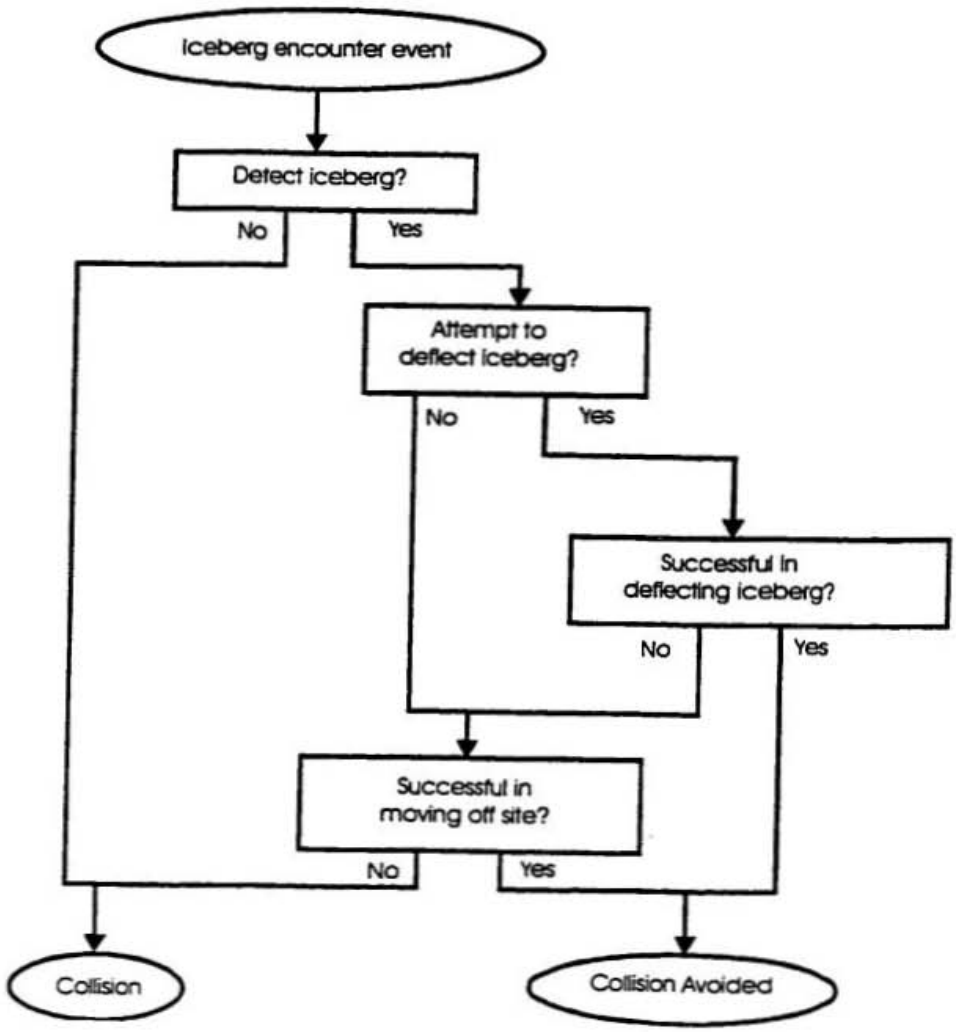

Figure 6.1 Event tree for iceberg detection, management, avoidance.

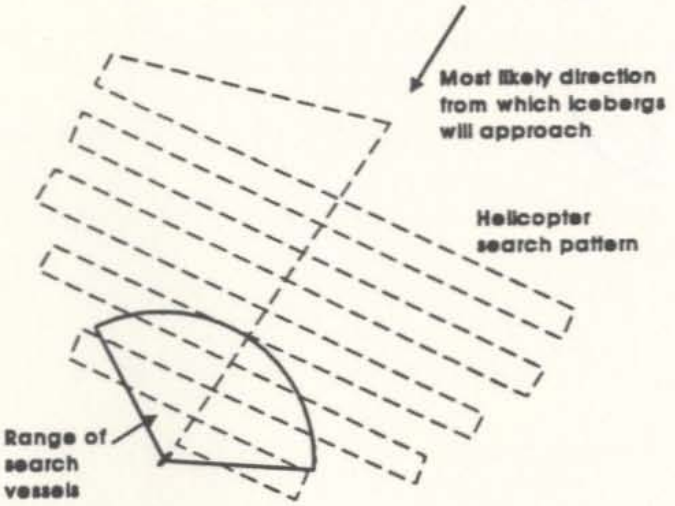

Figure 6.2 Model for search path by aircraft.

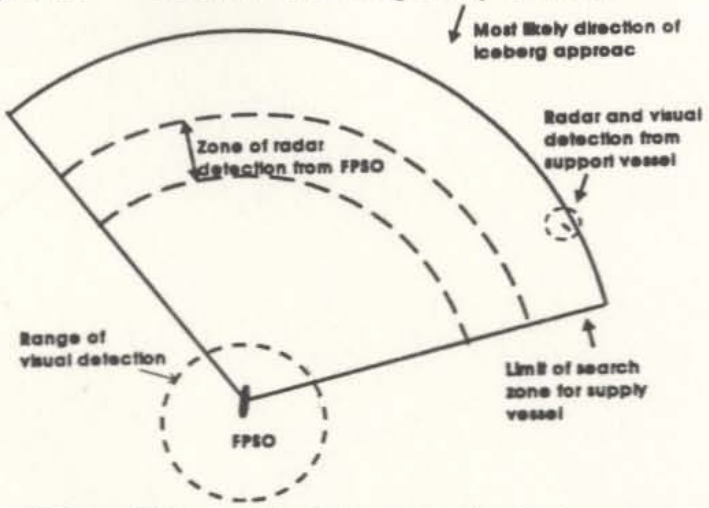

Figure 6.3 Other methods for detecting icebergs

By providing these different systems, redundancy in the detection capability is given. In addition, both the probability of detection and the range at which icebergs are detected is improved. Aircraft can cover a lot of ground quickly and are high up (giving extended radar coverage), and therefore can provide good advance detection capabilities for the general region. On the other hand, aircraft are subject to restrictions regarding the environmental conditions during which they can fly. Unlike aircraft, support vessels can operate in most environmental conditions. The detection range for radar systems mounted on support vessels is generally less than that for systems mounted on production vessels or aircraft since the

antenna is not as high above the water surface. Support vessels extend the overall detection range by conducting search patterns beyond the radar detection range of the production vessel. Also, if there have been previous sightings by aircraft or ships, the support vessels can concentrate their efforts to areas from which icebergs are expected to approach. A support vessel sweeping back and forth will only be able to detect those icebergs which come within its detection range; if it takes a long time between sweeps an iceberg may pass by before it returns to a given position. Figure 6.4 illustrates the general characteristics of the different detection methods. Actual curves will vary significantly depending on the iceberg and environmental conditions; for example, in conditions which prohibit flying, the probability of detection from aircraft will be zero.

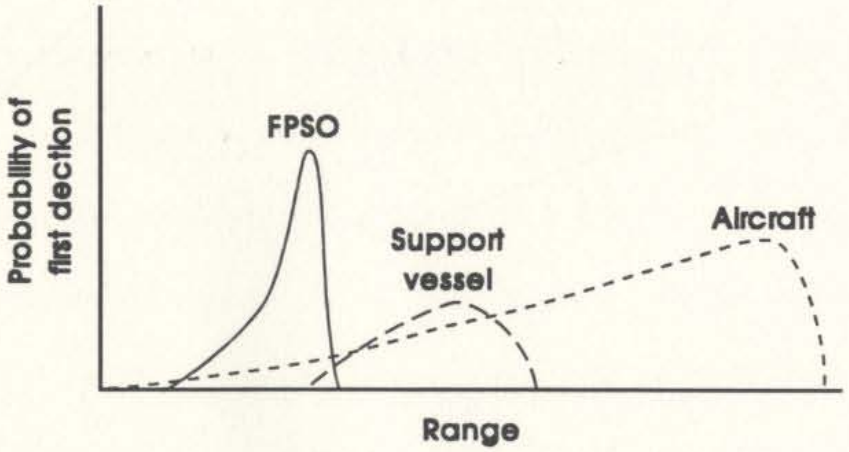

Figure 6.4 Illustration of detection capabilities from different sources

Though the different detection systems provide redundancy and should result in an improved overall detection, they are all limited when it comes to detecting smaller icebergs in storm conditions. The probability and range of visual detection decreases for smaller

icebergs and also decreases with the amount of white capping, which reduces contrast. The visual detection range is strongly correlated to visibility, which measures how far away one can see an object given the effects of atmospheric conditions such as fog and precipitation. Also, the efficiency of the eye decreases significantly in reduced light conditions. At the same time, the probability and range of detection using radar decreases for smaller icebergs and also decreases with the amount of sea clutter return. Sea clutter results mainly from wind generated surface capillary waves and is strongly correlated with wind velocity. Radar detection capability is somewhat diminished by heavy fog and precipitation, though not nearly to the same extent as visual detection. The result of these similarities in the detection limitations for the different systems is that the sizes of icebergs reaching the production site undetected will increase significantly with the severity of the wind and wave conditions and to a lesser degree with fog and precipitation. The exact relationships depend on the types and setups of radar systems used and on the availability of aircraft and support vessels. Human factors such as attentiveness and the amount of time dedicated will also affect detection.

A gravity based structure will have a similar overall detection capability to that on a floating system, it may be possible to improve detection from the platform itself because of its greater height. In the case of shuttle tankers, detection of icebergs consists of visual and radar observation from the vessel itself.

For determining the expected risk in the case of floating and fixed production systems, it is first necessary to clearly describe the iceberg management procedures that will be used. In the case of floating systems, these may be described in terms of alert zones (as illustrated in Figure 6.5. If an iceberg is detected in zone 3, it will be monitored and if it

appears to be heading to zone 2, an attempt made to deflect the iceberg away by towing. If a detected iceberg reaches zone 2, or a previously undetected iceberg is first detected there, the operators will attempt to deflect the iceberg by towing and will shut down production and prepare to move the vessel. If the iceberg reaches zone 1 or is detected in zone 1, the operators will move off site as quickly as possible. The zone sizes will be chosen based on the time required to both suspend whatever operations are being conducted and disconnect the mooring system. The sizes of the zones could be specified in terms of radii, but are more likely to be specified in terms of the required time (sometimes referred to as the "T-Time") to shut down operations. In this case the range in distance depends on the speed and direction of the particular iceberg being considered and on the environment forecasts.

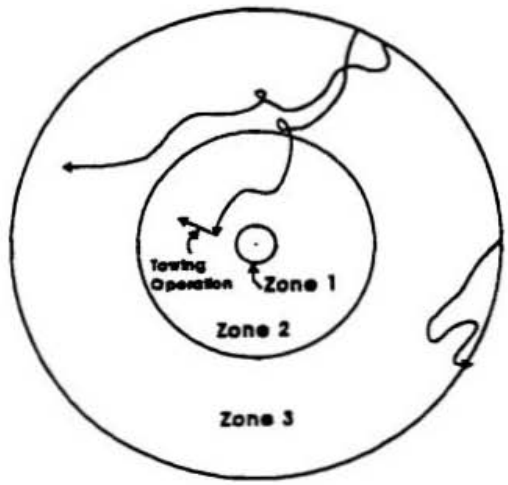

Figure 6.5 Iceberg alert zones

For a shuttle tanker, once an iceberg is detected, the operator must decide whether or not to manoeuvre the vessel to avoid impact. Avoidance of impact will be a function of detection distance, ship speed, ship characteristics, environmental conditions, operator skill,

and iceberg size. If there is not enough time to clearly avoid the iceberg, the operator may decide to hold course so as to take the impact on the bow rather than on the sides.

In the case of a floating platform, the amount of production downtime that the operators incur when shutting down because of approaching icebergs will also depend on the iceberg management plan. To estimate this downtime, one must determine how often icebergs enter alert zone 2 and what the duration of downtime is afterwards. If the iceberg is detected in time that proper procedures can be used to stop production and disconnect the mooring system (approximately 8 hours), production can generally be resumed in 3 to 4 days (Lever, 1995). In emergencies, for example if the iceberg is first detected within zone 1 or 2, an emergency disconnect can be made in about 1 hour, but the time to restore production may be as high as six to seven months.

To determine the probability of an iceberg reaching a floating production vessel, the following approach could be used. If for a given iceberg and environment, the different detection methods are independent, then the probability $P_D(r)$ of first detection at range r is

$$P_D(r) = 1 - \prod_{i=1}^{n} \left[1 - P_{D_i}(r)\right] \tag{6.1}$$

where the factors $_{PBI}(r)$ are the probabilities of first detection for each of the $i = 1, 2, \ldots n$ methods available. The overall probability P_M of successfully detecting the iceberg and avoiding collision can then be calculated as

$$P_M = \int_0^{\infty} P_D(r)\ P_{M|D}(r)\ dr \tag{6.2}$$

where

$$P_{M|D}(r) = 1 - \left(1 - P_T(r)\right)\left(1 - P_A(r)\right) \tag{6.3}$$

is the probability of avoiding impact by either towing an iceberg or moving off site given detection at range r, $P_T(r)$ is the probability of successfully towing the iceberg, and $P_A(r)$ is the probability of successfully disconnecting the production vessel and moving off site. Here the probabilities $P_T(r)$ and $P_A(r)$ are assumed to be independent. The probabilities $P_{M|D}(r)$, $P_T(r)$, and $P_A(r)$ are required as a function of r for the particular sets of iceberg parameters and environmental conditions of interest. It should be noted that the iceberg will not generally approach the platform in a straight line and the environmental conditions may be varying. On the other hand, icebergs paths are straighter in harsh conditions (when the detection is poor) so the approximation that the iceberg approaches the production site in a straight line may be reasonable (and slightly conservative).

For the case of a gravity based structure, the term for moving the vessel off site would be removed. For the case of a shuttle tanker, the probability of impact P_A would be determined as

$$P_A = \int_0^\infty P_D(r)\ P_{A|D}(r)\ dr \tag{6.4}$$

where $P_D(r)$ is the probability that the iceberg is first detected at distance r, and $P_{A|D}(r)$ is the probability of avoiding the iceberg by manoeuvring. The particular values of P_D and $P_{A|D}$ are required as a function of r and the particular sets of iceberg parameters and environmental conditions of interest. The method could be enhanced to give the probability of impact on different parts of the vessel and the impact velocity, though the present capability to model manoeuvring in sufficient detail limits the accuracy which can be achieved.

For a complete solution, the above integrals would be required for each combination of iceberg size and environmental conditions considered. For the analyses in Chapter 7, a

simpler approach (see Section 6.3.2) will be used in which the overall detection probability is estimated without consideration of the detection range.

6.3 Detection of Icebergs

6.3.1 Radar Detection

To model the detection of icebergs using radar, it is necessary to consider the characteristics of the particular radar system, the proportion of received electromagnetic radiation the iceberg returns, the strength of competing signals such as sea clutter, and the proportion of signal lost due to absorption by fog and rain. Detection depends on whether the returned source signal can be distinguished from the competing signals and noise generated within the radar system.

The type and set up of the radar system has a large effect on detection. Important parameters include wave frequency, types of antennas for transmitting and receiving, power and noise characteristics, and the signal processing system. The wave frequency determines how much of the propagated wave energy will be lost if water droplets and other particles are present in the air and affects the amounts of energy returned from both the iceberg and waves. Marine and search radars are typically chosen in the X-Band or S-Band regimes. X-Band radar generally provides a longer detection range than S-Band when good atmospheric conditions are present but is not as reliable in fog or rain. The type of antenna system used controls the search pattern and the target resolution. For search and marine radar systems, a rotating antenna which can scan 360 degrees is used. Systems such as synthetic aperture radar (SAR) and side looking airborne radar (SLAR), which are fixed to aircraft, rely on the

motion of the aircraft to increase the effective size of the transmitter. SAR and SLAR require a great deal of data processing and are not generally used for real time systems. The resolution of rotating systems depends on the radar pulse length and beam width. The height of the antenna has a large effect on the optimal detection range, mainly through its affect on the amount of sea clutter which is returned. Generally, the range of minimum sea clutter return, which is a function of incidence angle, increases with the height of the antenna. Increased power output from the system can help to overcome energy losses due to fog and rain and also extend the range of detection since the power returned from the iceberg decreases with the range squared. The internal noise produced by a radar system can mask out weak signals.

The choice of signal processing system is very important. If a Plan Position Indicator (PPI) conventional radar display is used, then detection is dependent on the experience of the operator in choosing an appropriate gain setting and in recognizing targets. The gain setting determines the amount of returned power required to give a signal in one of the resolution grids on the display. It is generally set to reduce the number of false signals from sea clutter and noise while still showing desired targets. If the gain is set too high the desired target will be hidden amongst all the false targets in adjacent radar cells. If the gain is set too low, then the iceberg will not give a signal. When the gain is correctly set and the target return is large enough relative to the sea clutter, then on consecutive radar sweeps the observer will see a persistent signal at the location of the iceberg while occasional signals from sea clutter will come and go. For PPI systems, the attentiveness of the operator is important, if they are preoccupied they could miss sighting an iceberg while it is within the optimal detection

range. Some new computer signal processing systems are available which do automatic statistical analysis of the returns from different cells to determine if there is a target.

The return from an iceberg is generally specified in terms of its radar cross-section. This parameter is a measure of the proportion of the energy received in a given area that will be reflected back from the iceberg; it is usually specified in decibels. The radar cross section is determined by the electrical properties of the ice and by the size and shape of the iceberg. It increases roughly in proportion with the projected above water area of the iceberg and depends to a lesser degree on how far above the sea surface the iceberg extends and on the angles the ice presents relative to the direction of the radar signal. The drift and wave induced motions of the iceberg may cause the radar cross-section to vary with time affecting the duration of detection.

The main factor limiting detection is the amount of 'sea clutter' returned from small wind induced capillary waves on the ocean surface. The sea clutter radar cross-section is strongly correlated with the wind speed and is also affected by the wind direction, generally being strongest when looking upwind. Sea clutter also changes dramatically with the incidence angle of the radar, which in turn is dependent on the height of the antenna and the range. At larger ranges the curvature of the earth must be accounted for. The optimal detection range with respect to sea clutter can be increased by increasing the height of the antenna. An important difference between the source and sea clutter signals is that the area of ocean surface covered, and therefore the sea clutter, is the same as the resolution cell, which increases as the R^2, whereas the iceberg radar cross-section remains constant. As a

consequence of this, the power returned from the iceberg is proportional R^{-2} whereas the clutter signal decreases as R^{-1}, thereby limiting the range of detection.

An analysis of the detection capability at a floating production facility carried out for Petro Canada (Cammaert et al., 1992) is of direct relevance to this study. Standard radars (see Table 6.1 and Table 6.2 for parameters) were modelled for the production vessel, support vessels, and aircraft; the detection capability for each was estimated by Sigma Engineering using their in-house model (Johnson and Ryan, 1991). For the production vessel a 50 kW X-band (10 GHz) radar and a 30 kW S-band (3 GHz) radar, both mounted at a height of 75 metres, were modelled. For the support vessels, an S band radar mounted at a height of 15 metres was modelled. For the aircraft, an APS-504(V)5 radar (8.9 - 9.4 GHz) used at an altitude of 152 metres was modelled. Other radar parameters were chosen as believed appropriate for actual operations. The radar cross-sections in the Sigma Engineering model were determined based on observations for 39 icebergs which ranged in size from growlers to large icebergs. The sea clutter cross-sections were based on field data which included wind speeds ranging from 2 to 43 knots and significant wave heights ranging from 0.3 to 8 metres.

The general characteristics of radar detection systems and the sensitivity of detection to different parameters are illustrated in Figures 6.6- 6.9. Clear atmospheric conditions were assumed unless otherwise indicated. Detection curves for a 50 m iceberg in 5 m seas, based on an S-Band platform mounted system, is shown in Figure 6.6. The probability indicated represents the proportion of time that a signal from the iceberg will appear on the radar screen, given that the gain is chosen so that the time between false alarms caused by noise

or sea clutter is 6 hours. A probability of about 0.5 corresponds roughly to the detection limit for a human observer. This value could change depending on the experience of the operator. Also, as mentioned, improved methods in which the signals are statistically analysed by computer are now available. A number of features of this curve
are fairly typical. In this case there is an optimal detection range at about 27 kilometres, then the detection is good again near the vessel. This pattern is largely due to the variations in sea clutter with incidence angle. In clear atmospheric conditions, the probability of detection near the vessel and at the optimum detection range further out are approximately the same. An approaching iceberg will be within the optimal detectable range for a duration which depends on the depth of the zone and on the velocity of the iceberg. Where a PPI display is used, the actual probability of detection will be influenced by the frequency with which the display is checked.

Figure 6.6 also shows how the probability of detection changes with iceberg size. For given radar system, sea state, and atmospheric conditions there is usually a limiting size below which it becomes very hard to detect icebergs at any range. Icebergs larger than this limit are detectable within the optimal detection range. As the size of the iceberg increases, there is an increase in the probability of detection, a slight increase in the initial range at which the iceberg can first be detected. There is also an increase in the range over which the iceberg can be detected. Figures 6.7 and 6.8 show the effect of rain and fog on radar detection. These factors both act to decrease the probability of detection at greater ranges. The probability of detecting icebergs at the optimal detection ranges and the range over which they can be detected both decrease. In some cases, smaller icebergs may not be seen

Table 6.1 Marine Radar Specifications

	X band	S band
Frequency(GHz)	9.5	3.0
Transmitter Power(kW)	50	30
Receiver Noise Figure(dB)	5	5
Receiver Bandwidth(MHZ)	4	4
Pulse Length(ns)	250	250
Range Resolution(m)	37.5	37.5
Pulse Repetition Freq.(Hz)	1600	1600
Antenna Gain(dB)	32	27
Horizontal Beamwidth(deg	0.8	2.0
Antenna Speed(rpm)	30	30
Antenna Height(m)	75	75. and 15[1]
Signal Processing		
Pulse to Pulse Integration	Yes - standard	
Scan to Scan Integration	No	
Typical clutter controls such as STC[2]		

1. Antenna height is 75 m for platform mounted radar and 15 m for support vessel radar.
2. STC (Sensitivity Time Control) is used by the operator to remove background clutter that is range dependent.

Table 6.2 APS-504(V)5 Radar Specifications.

	X band
Frequency(GHz)	8.9 - 9.4
Transmitter Peak Power(kW)	8
Receiver Noise Figure(dB)	5
Receiver Bandwidth(MHZ)	50
Pulse Length(ns)	
Uncompressed	10000
Compressed	30
Range Resolution(m)	4.5
Pulse Repetition Freq.(Hz)	1350
Antenna Gain(dB)	32
Horizontal Beamwidth(deg)	2.3
Antenna Speed(rpm)	30
Antenna Height(m)	152
Signal Processing	
Pulse to Pulse Integration	Yes
Scan to Scan Integration	Yes
Clutter controls	Cell Averaging CFAR STC[1]

1. STC (Sensitivity Time Control) is used by the operator to remove background clutter that is range dependent.

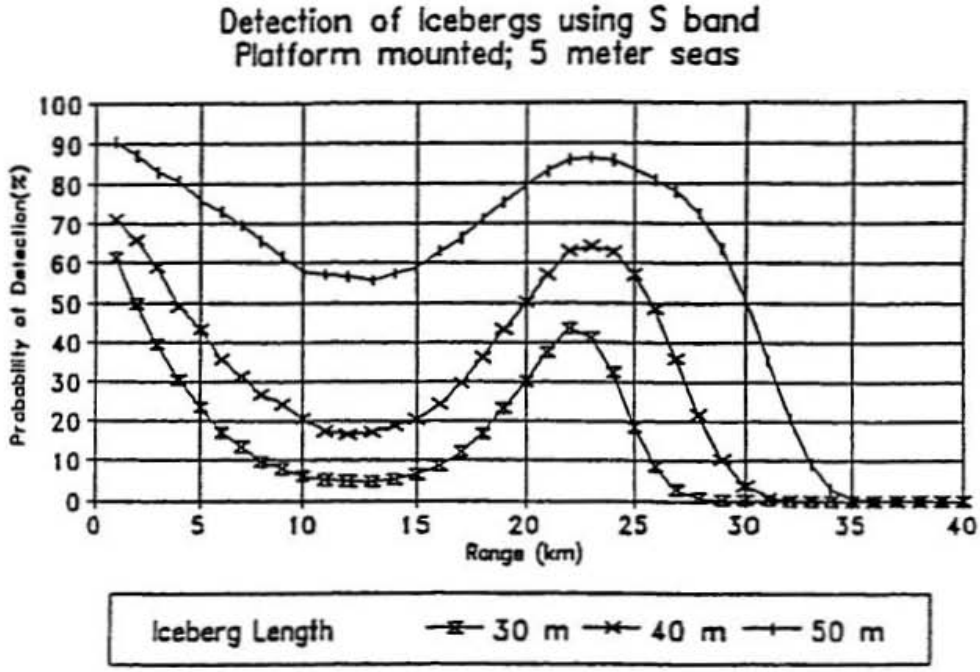

Figure 6.6 Effect of iceberg size on platform mounted S band radar performance (Cammaert et al., 1992)

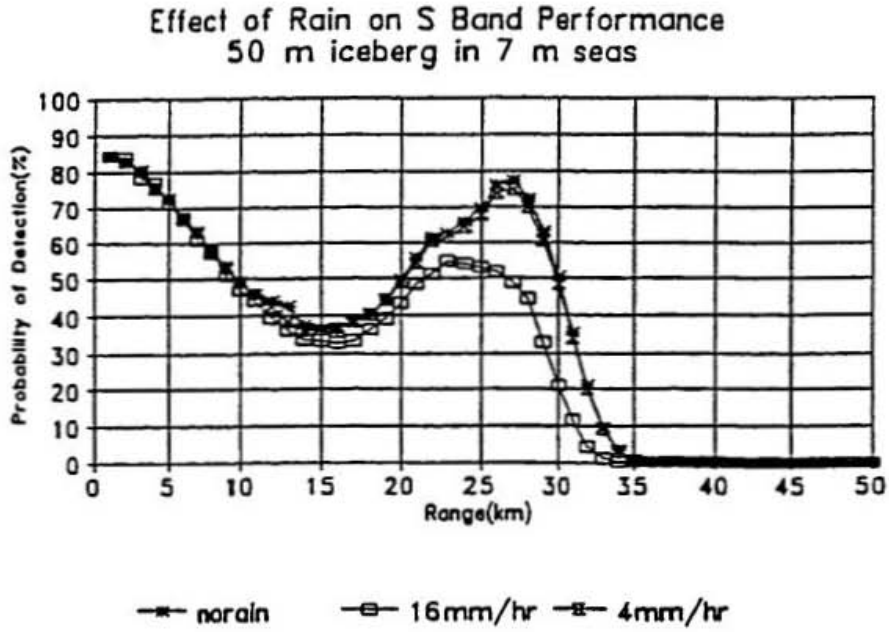

Figure 6.7 Effect of rain on platform mounted S band radar performance (Cammaert et al., 1992)

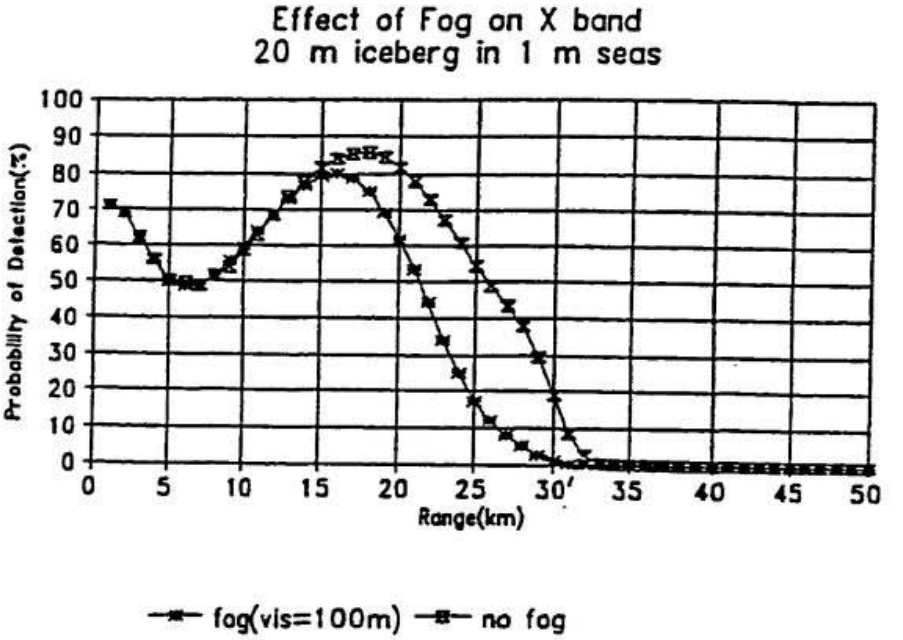

Figure 6.8 Effect of fog on platform mounted X band radar performance (Cammaert et al., 1992)

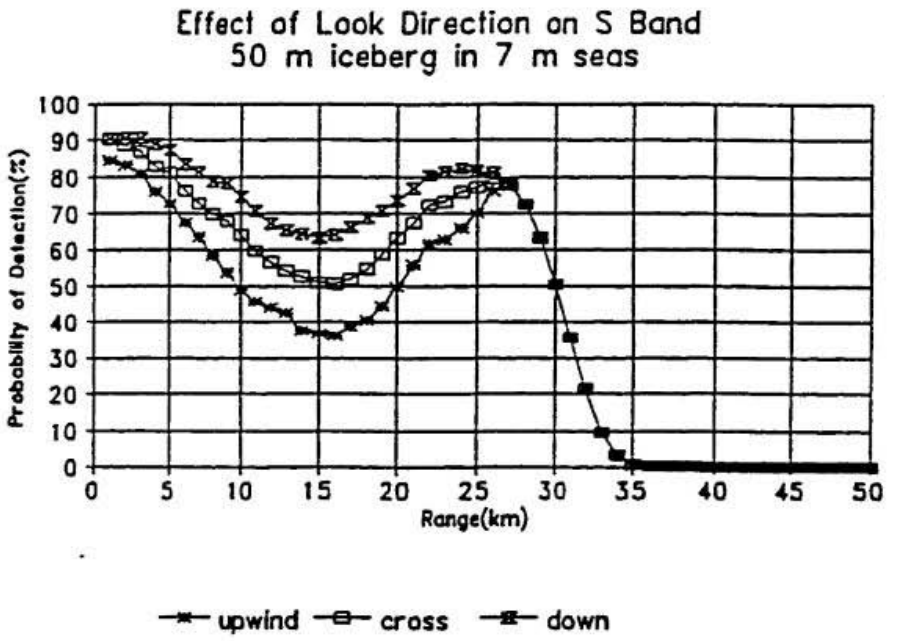

Figure 6.9 Effect of look direction with respect to wind on S band radar performance (Cammaert et al., 1992)

until they reach the relatively unaffected detection area near the vessel. The effect of the look direction is shown in Figure 6.9; the upwind direction is significantly worse than the cross wind direction.

In the Petro Canada study, detection ranges where estimated for a selection of iceberg sizes and environmental conditions characterized by significant wave height. The detection ranges were chosen assuming detection when the radar probability first exceeds 0.5. The runs all assumed clear environmental conditions. The sizes of icebergs that can be detected appear to vary approximately linearly with significant wave height, with slopes given in Table 6.3 and Figure 6.10 . Approximate values for the initial detection range are also given in Table 6.3 , in fact they vary slightly with environmental conditions and iceberg size. Note that flying conditions permitting, aircraft provide the best detection both in terms of the sizes of icebergs detectable and the range at which they can be detected. The size of iceberg detectable from the support vessel is slightly better than for the production vessel but the range is reduced.

Table 6.3 Approximate Detection Ranges of Icebergs and Limiting Detectable Iceberg Sizes as a Function of Sea State

Radar System	Approximate Ratio of Limiting Detectable Iceberg Length (m) to Significant Wave Height (m)	Approximate First Detection Range (km)
Production Vessel X band	6	36
Production Vessel S band	6	28
Supply Vessel S band	5	
Aircraft	3	56

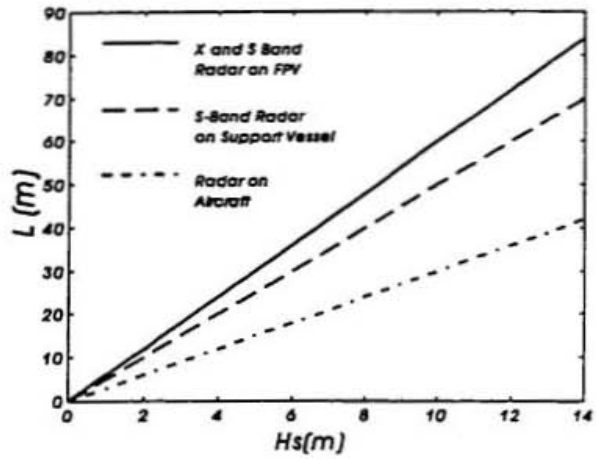

Figure 6.10 Approximate detection limits in terms of iceberg water line length as a function of significant wave height.

The above relationships must be considered as preliminary, as further refinement and verification of the model are required for some iceberg size/ environmental conditions, and more simulations are required. An estimate of the variations in radar cross sections for icebergs of a given size would be useful. Similarly, the range of sea clutter for given H_S would be useful. It should be noted that there is relatively little sea clutter data for storm conditions. It should be noted that the relationships in Figure 6.10 do not account for possible fog or precipitation. In the presence of precipitation or fog, one would expect the ratio of the limiting detectable iceberg length to significant wave height to increase slightly. Because detection near the vessels would not decrease as much, in some cases there would still be detection but at a much diminished range. Because the use of S-Band radar is much less sensitive to fog and precipitation, an estimate of relative effect of fog and precipitation can be obtained by running the different detection systems with S-Band radar only. The linear relationships used in effect results in a detection model which is deterministic. The

actual method for determining detection could be modelled in more detail. A statistical model could be developed which accounts for the randomness of the iceberg signal and sea clutter as well as the frequency and duration of observations. Uncertainty due to differences in experience of the operators and in the particular setup up of the radar system would be more difficult.

6.3.2 Overall detection model with uncertainty

The model as set up for the Petro-Canada study essentially gives a yes/no answer to the question of whether or not a given sized iceberg can be detected in given conditions. To compensate for this, a number of sensitivity analysis were run to see the effect of changes in the model assumptions on the design loads. For this study, it was decided to set up a simpler detection model, but to include uncertainty regarding the sizes of icebergs which could be detected in given conditions. First, the range at which icebergs are detected is not accounted for. Generally the radar systems are optimized for detection at ranges of about 25 to 40 km. This should give a reasonable amount of time to attempt towing operations and if necessary disconnect. Second, it is assumed that the mean detectable iceberg size for a given sea state follows the linear relation 6 H_S. Finally, it is assumed that the probability of detecting an iceberg of waterline length L in a sea state with significant wave height H_S has a probability density function equal to the cumulative normal distribution with mean 6 H_S and standard deviation 6 σ, where σ has be chosen with a notional value of 0.3. Thus the probability of detecting a very small iceberg is 0, the probability of detecting an iceberg of length L=6 H_S is 0.5, and the probability of detecting a very large iceberg is 1.

6.3.3 *Detailed models which could be used for optimization*

If a decision maker is required to optimize the positions of the standby and support vessels for detecting and towing icebergs, it is necessary to consider the detection ranges for given sizes of icebergs and environmental conditions, and the vessel speeds. A geometric model which could be used is suggested here, the optimization problem has not been attempted.

To model detection from support vessels or aircraft, the search patterns carried out must be modelled. To illustrate how one could model detection where a search pattern is used, a simple back and forth search pattern from a support vessel is considered. It is assumed that the iceberg moves in a straight line at constant velocity v_i towards the production vessel and the support vessel sweeps back and forth at right angles to the direction of the iceberg at a distance r_s from the production vessel. The velocity of the vessel is denoted as v_s and the width of the sweep pattern is denoted as W. The above conditions could apply in the case of storm conditions with the support vessel positioned upwind from the production site. It is also assumed that there is a 100% probability of detection if the iceberg comes within the detection range of the vessel.

The analysis is made easier by considering the search pattern from the reference frame of the iceberg as shown in Figure 6. 11. The detection sweep width D_1, is two times the detection range. During one sweep back and forth, the vessel will appear to a person moving with the iceberg to move forward a distance:

$$D = \frac{V_i\,(2\,W)}{V_s} \tag{6.5}$$

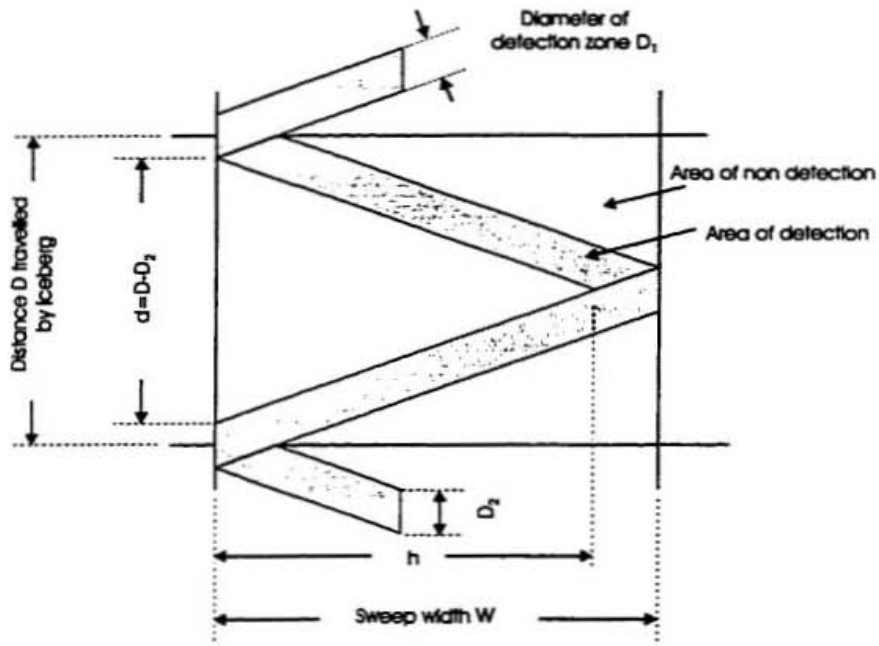

Figure 6.11 Method for calculating probability of detection from a support vessel

The probability of the iceberg not being detected is equal to proportion of area not covered:

$$P_0 = \frac{h\,d}{W\,D} \tag{6.6}$$

where:

$$d = D - D_2$$

$$D_2 = \sqrt{1 + (v_i/v_s)^2}\; D_r \tag{6.7}$$

$$h = \frac{W\,d}{D}$$

This is simplified to

$$P_0 = \frac{d^2}{D^2} \tag{6.8}$$

Models such as this can be used to evaluate the effectiveness of alternative search patterns (the use of alternative radar systems and settings could be used as well) for detecting icebergs approaching at different velocities). Different sweep widths might be chosen for different ranges upwind from the production platform, or if the position of an approaching iceberg is approximately known. It is required by law to have a standby vessel remaining close to the production site in case of emergencies; the radar system and search pattern on this vessel could be set to optimize detection within the optimal range of the radar system on the production vessel.

6.4 Iceberg Towing

Once an iceberg is detected and the decision to deflect it away from the floating production vessel is made, the probability of success will depend on the amount of time available and the characteristics of the icebergs and environment. Several hours may be required for a support vessel to reach the iceberg and set up, so adequate warning time is required. With the detection model used, it is assumed that the iceberg is first detected at sufficient range to allow several towing attempts. If detection at closer ranges was added, for example by including visual detection from the production site, it would be necessary to explicitly consider the effect of available time.

Even when there is adequate time to set up, towing may be difficult and in some cases impossible. If the iceberg is dome shaped it may be difficult to get the tow line to hold without slipping off. If the iceberg is unstable, it may roll when a force is applied to it. With larger icebergs, a greater force is required to accelerate and move them because of their large

mass and drag resistance. Therefore both the distance that an iceberg can be moved in a given time and the associated margin of safety may be limited. The environmental conditions will also affect the operators ability to deflect an iceberg successfully. In storm conditions management can be difficult for a number of reasons. First, the iceberg will move faster, reducing the available reaction time. Second, the icebergs will generally have larger wave induced motions, making it harder to keep a tow line on. Third, the vessel and towing equipment will be more difficult to operate.

If the iceberg cannot be successfully deflected, then an attempt will be made to move the production vessel out of its path. The operators will first try to shut down the well in an orderly fashion; the amount of time required for this will depend on the production operations being conducted at the time. As a last resort, emergency shut down procedures will usually be available. If a mooring system is used to keep the vessel on location, the reliability of the mooring disconnect system will be critical. In a worst case scenario, it might not be possible to disconnect the mooring system even if a large iceberg, initially detected some distance away, approaches. Where a dynamic positioning system is used, this problem can be avoided.

One of the more comprehensive reports available on towing success rates is the Mobil report "Assessment of Iceberg Management for the Grand Banks Area: Analysis of Detection and Deflection Techniques" (Bishop, 1989). A towing operation is defined to be successful if 1) the iceberg was obviously deflected from its course and the rig did not have to disconnect, 2) tension was applied to the iceberg for a whole hour, or 3) the tow eliminated or reduced downtime caused by well securing operations. Bishop analysed 354 towing

operations and categorized the number of successes in terms of a number of parameters including iceberg size and sea state effects. The towing data was taken from the Environmental Well-site History Reports on file at the Canada-Newfoundland Offshore Petroleum Library. Overall, it was found that 86% of icebergs were successfully towed, 64.9% easily towed and 21.1% towed with some difficulty.

The breakdown of probability of towing success by size of iceberg is shown in Table 6.4. The data shows no distinguishable difference in success with iceberg size. One might have expected that larger icebergs would be harder to tow because of the increased drag and inertial forces. A possible explanation is that the smaller icebergs are less stable and tend to be more rounded making it more difficult to tow them. Another explanation is that the definition of a successful tow is such that the mass of the iceberg is not important, i.e. it did not matter how far the iceberg could be towed as long as it could be moved noticeably.

Bishop also conducted an analysis to determine the success at towing as a function of sea state. It is interesting that little change was shown in the success of towing with the environmental conditions. An analysis of success in towing icebergs as a function of iceberg shape indicated that spherically shaped icebergs were slightly more difficult to tow than other shapes. A similar analysis with respect to wind speed showed that if anything, towing success increased very slightly with wind speed. Given the unexpectedness of the above results, a more in depth analysis of towing success would be useful. This would require a more rigorous definition of the definition of the success of towing, consideration of factors such as the criteria for attempting tows, and a comparison with towing success rates predicted based on estimated inertial and drag forces.

Table 6.4 Towing Success Rate by Size Class

Size Class	Number of Records	Percentage Towing Success
Bergy Bits	12	83.3
Small Icebergs	166	88.8
Medium Icebergs	111	84.7
Large Icebergs	56	82.1

For the model in the Petro-Canada study, Berry (1993) suggested that the probability of successfully towing icebergs be modelled as a function of time available and the sea state. He also suggested that the probability of successfully towing an iceberg when H_s is greater than 4 m be taken as 0.

The model for towing developed for used in Chapter 7 was set up to give a probability of successful towing an iceberg equal to 0 when H_s is greater than 5 m and was set up to give a probability of success which reduces with size. The form of the equation used is

$$p_{ST} = \left[1 - \left(\frac{Hs}{5}\right)^4\right]\left[1 - \left(\frac{L}{250}\right)^5\right] \tag{6.9}$$

The equation is somewhat arbitrary but the distribution of towing successes, as shown in Chapter 7, seems to be a reasonable first guess for purposes of sensitivity analyses. Comments on the need for a more precise model are given there.

6.5 Reliability of Disconnect Procedures

The probability that the operators can avoid a collision by moving off site will depend on the reliabilities of the release mechanisms for the riser and the mooring system (if moored) as a function of the time available. Problems in shutting in the production well may also reduce the amount of time left to disconnect. In critical situations, the time required to accelerate the vessel might also be important. To determine the sensitivity of the design loads to the disconnect reliability, in Chapter 7 analyses are conducted for two reliability values, 100% and 98%.

7 APPLICATIONS

7.1 Overview

In this chapter, example global design load calculations and economic analyses are presented. In Section 7.2, design load calculations are given for a gravity based platform and for the bow of an FPSO. The results of sensitivity analyses regarding the number of icebergs, the success of the iceberg detection management system, the impact velocities, and the global ice failure mechanics model are also presented. In Section 7.3, an example calculation of downtime due to iceberg incursions into alert zones is presented. In Section 7.4, economic analyses are presented for the case of FPSO type systems used to produce a number of field sizes. Consideration is given to the following three cases. First, the economics are determined for the situation where no icebergs are present. Second, the economics are determined assuming icebergs are present and a strategy of protecting subsea equipment is used. Third, the economics are determined assuming icebergs are present and a strategy of replacing damaged subsea equipment whenever an incident occurs is implemented.

7.2 Estimation of global design loads

7.2.1 Overview

In this section, the necessary inputs to determine global design forces are set up, then design values are estimated for a GBS and an FPSO. For calculations requiring integration over the parameters L, H_S, and V, the parameters are divided into intervals of 5 m, 1 m, and 0.2 m/s respectively and discrete integration using midpoints values of the intervals is used.

In Section 7.2.2, the environmental conditions in the Hibernia/ Terra Nova region are quantified in terms of the joint probability that, given an iceberg is present, the iceberg has waterline length L and the sea state has an associated significant wave height H_S. A matrix of iceberg drift velocities at the discrete values of L and H_S is also developed, using the method in Chapter 5.

In Section 7.2.3, the probabilities of successfully detecting and towing an iceberg are estimated as a function of H_S and L.

In Section 7.2.4, design loads for a 100 m diameter cylindrical GBS are determined using the models developed in Chapter 5 for impact velocity and Chapter 4 for global impact loads. Sensitivity analyses are conducted to determine the effect of different assumptions for the ice failure criteria.

In Section 7.2.5, designs loads are estimated and sensitivity analysis are carried out for iceberg impacts on the bow of a FPSO vessel. Because the FPSO relies on moving off site when towing operations are not successful, consideration is also given to the probability of being able to successfully disconnect the vessel.

7.2.2 General conditions

The joint probability density function $f(L, H_S)$ given the presence of an iceberg, is shown in Figure 7.1. The numbers shown represent the negative logarithm (base 10) of f. For example, the value 3 represents a probably of 10^{-3}. The distribution is determined from the probability density functions for L and H_S described in Chapter 5.

Iceberg drift velocities were determined as a function of L and H_S and are shown in Figure 7.2

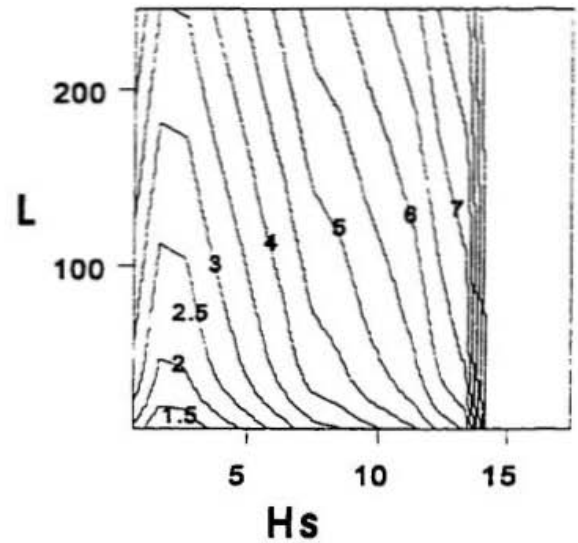

Figure 7.1 $-\log_{10} f(H_S, L)$ given an iceberg is present

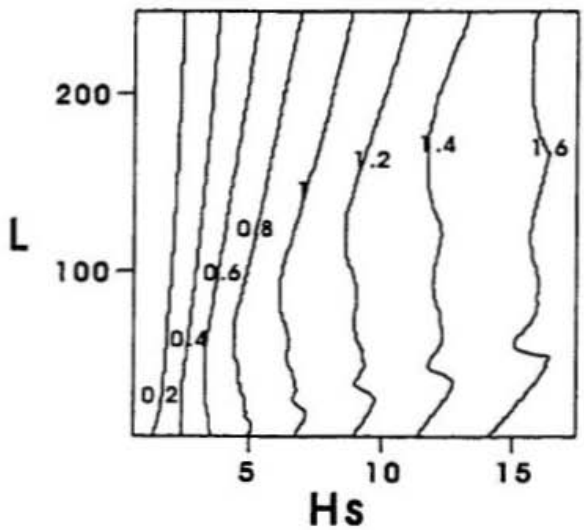

Figure 7.2 Iceberg drift velocity V_D (m/s) as a function of H_S and L

7.2.3 Detection and management

The detection and towing model described in Chapter 6 is applied for both the cylindrical GBS and the FPSO. The probability of successfully detecting an iceberg is shown in Figure 7.3 a). The probability varies from one for icebergs which are large compared to H_S to zero for icebergs which are small relative to H_S. The probability of successfully towing a detected iceberg is shown in Figure 7.3 b). The probability is high for small to medium sized icebergs in low sea states. The probability decreases for large icebergs. The probability goes to zero for all iceberg sizes in sea states greater than 5 m. The combined probability of detecting and towing an iceberg is shown in 7.4..

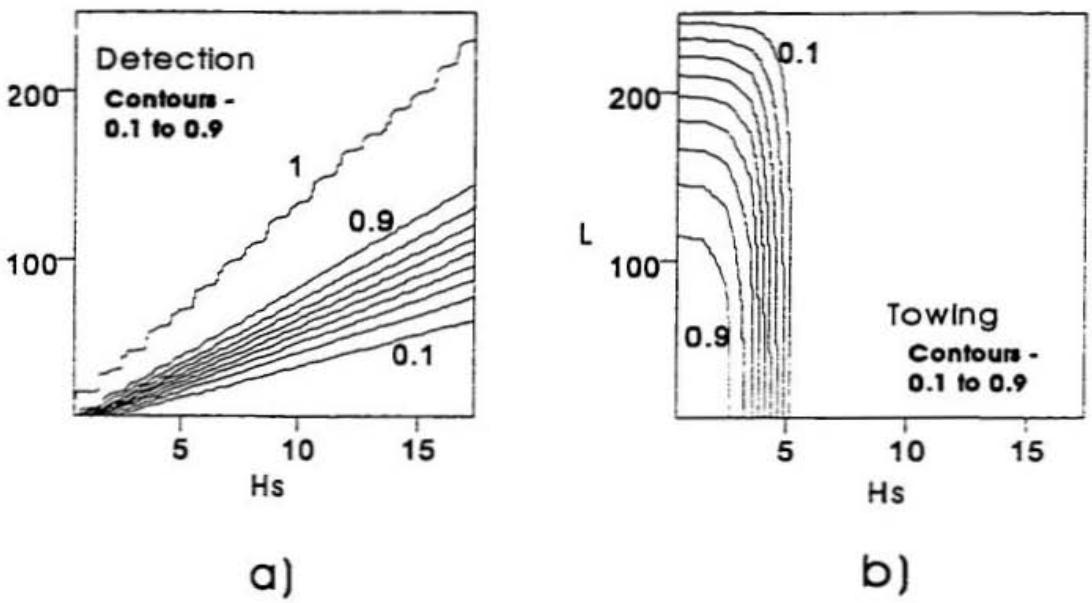

Figure 7.3 Probability a) of detecting an iceberg and b) towing it given detection.

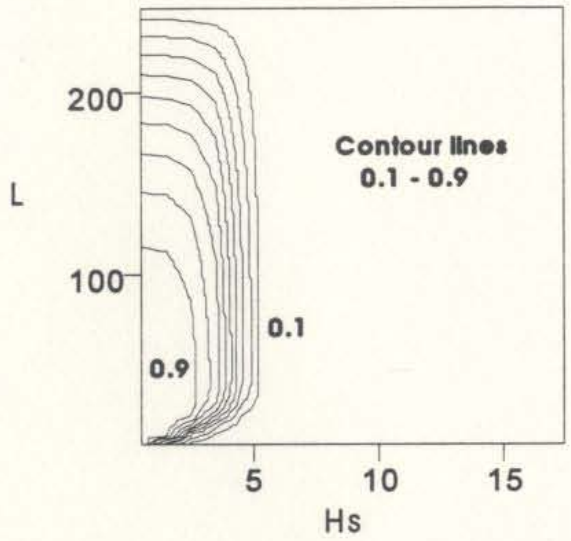

Figure 7.4 Probability of successfully detecting and towing and iceberg

7.2.4 Design loads for a 100 m diameter cylindrical GBS

To determine the design loads for a 100 m diameter cylindrical GBS, first the number of encounters are determined using the method developed in Chapter 5. The expected number of encounters per year, $\eta_E(\tilde{I}, \tilde{E})$, is shown in Figure 7.5 a). The expected number of encounters are determined for each 1 m H_S and 5 m L intervals and the numbers shown represent the negative logarithm (base 10) of η_E. For example, if the number associated with a particular combination of L and H_S is 4, this indicates that the expected number of encounters per year by icebergs with waterline length in the interval L - 2.5 m to L + 2.5 m, in sea states with significant height in the interval H_S - 0.5 m to H_S + 0.5 m is 10^{-4}.

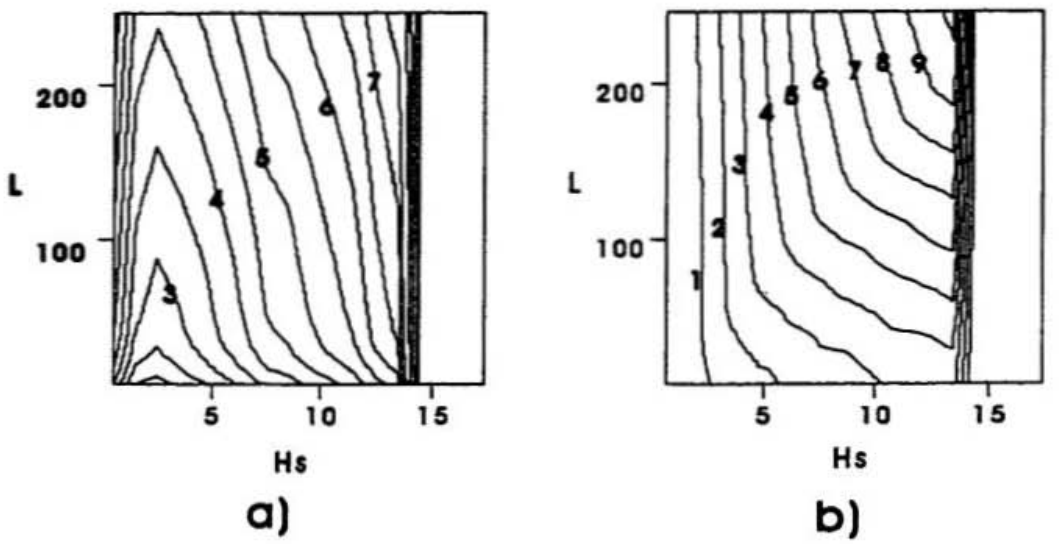

Figure 7.5 a) $-\log_{10}\eta_E$ for 1 m H_S by 5 m L interval
b) increase in probability of L and H_S conditional on impact

Figure 7.5 b) shows the ratio of the probability of H_S and L given an impact to the probability of H_S and L given an iceberg in the vicinity. The variation arises because the probability of an encounter increases with the size and speed of the iceberg. The speed of the iceberg increases with H_S.

For the GBS, it is assumed that if the iceberg is not detected and avoided through towing, an impact results. The resulting expected annual number of impacts $\eta_I(\tilde{I},\tilde{E})$ is shown in Figure 7.6. The number of encounters is determined directly from Figures 7.5a) and 7.4. The figure gives the negative logarithm (base 10) of η_I for 1 m H_S by 5 m L intervals.

The significant surge velocities of the icebergs (in open water) are shown as a function of H_S and L in Figure 7.7 a). The distributions of impact velocities were determined

based on the drift velocities and the open water random motions using the modified Rayleigh distribution developed in Chapter 5. The average impact velocities determined from these distributions are shown as a function of H_S and L in 7.7 b).

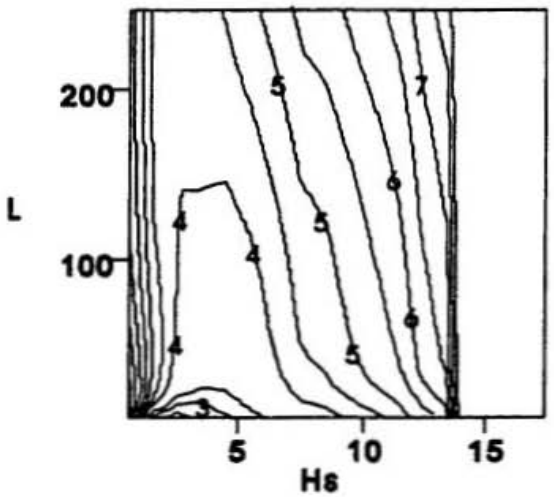

Figure 7.6 $-\log_{10}\eta_t$ for 1 m H_S by 5 m L intervals

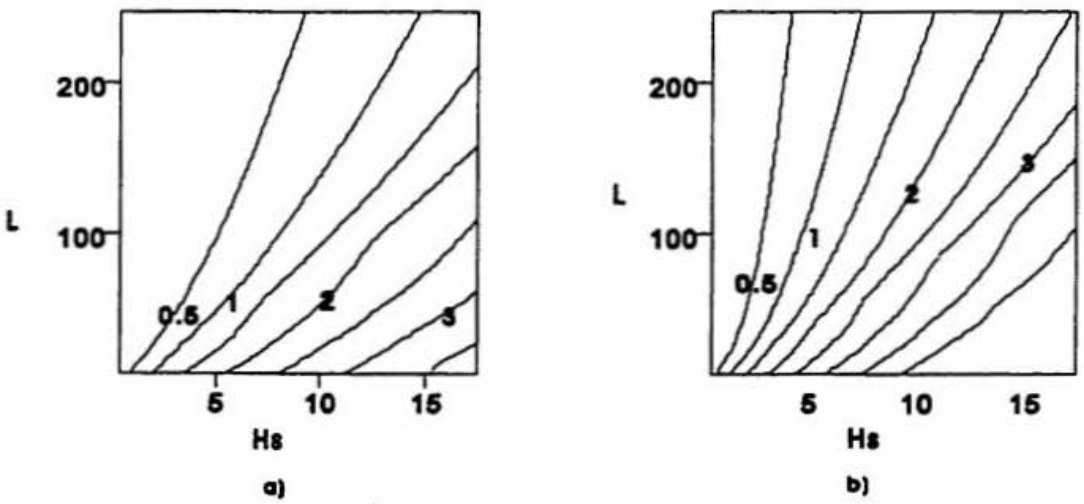

Figure 7.7 a) Significant surge velocity (m/s), and
b) Average impact velocity (m/s)

The resulting distribution of encounters by impact velocity V and iceberg waterline length is shown in Figure 7.8 for the cases a) with no ice management (detection and towing), and b) with ice management. Figure 7.9 shows the difference $\Delta\eta$ between the η_t for the cases without and with detection and management. The velocities shown are total iceberg velocities.

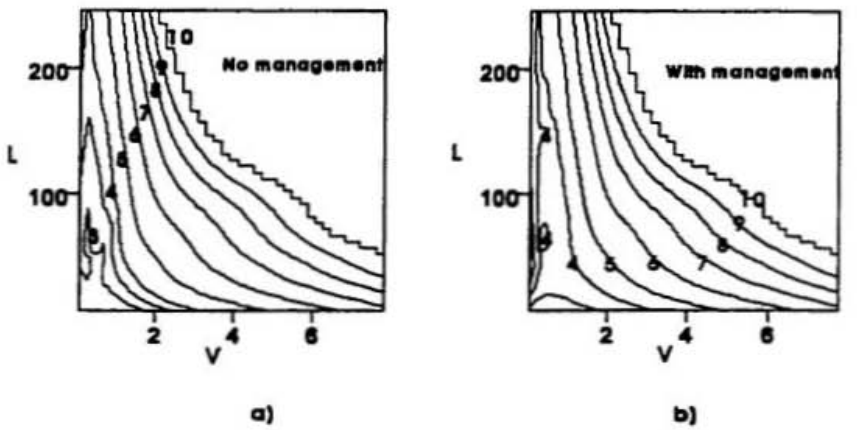

Figure 7.8 $-\log_{10}\eta_t$ for 1m/s V by 5 m L intervals

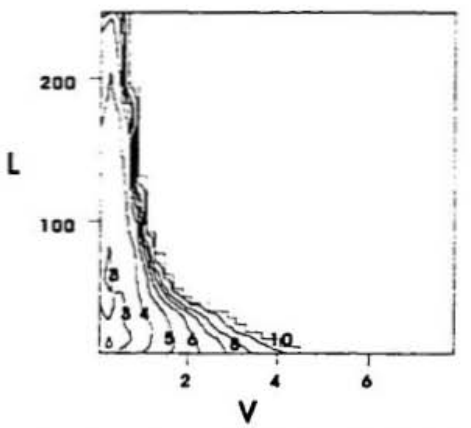

Figure 7.9 $-\log_{10}(\Delta\eta_t)$ for 1m/s V by 5 m L intervals

In the impact model, only the velocity component normal to the structure is considered. It is assumed that the icebergs hit with a uniform random offset and the normal velocity component is determined based on this offset.

Figure 7.10 shows the simulated maximum impact penetration and force as a function of V and L. The iceberg is modelled as a spherical with radius chosen so that the spherical iceberg has the same mass as an iceberg of length L with mass determined using equation 5.2. The GBS is treated as a rigid vertical wall. For the case in Figure 7.10, the nominal ice crushing pressure was taken as a constant 1 MPa.

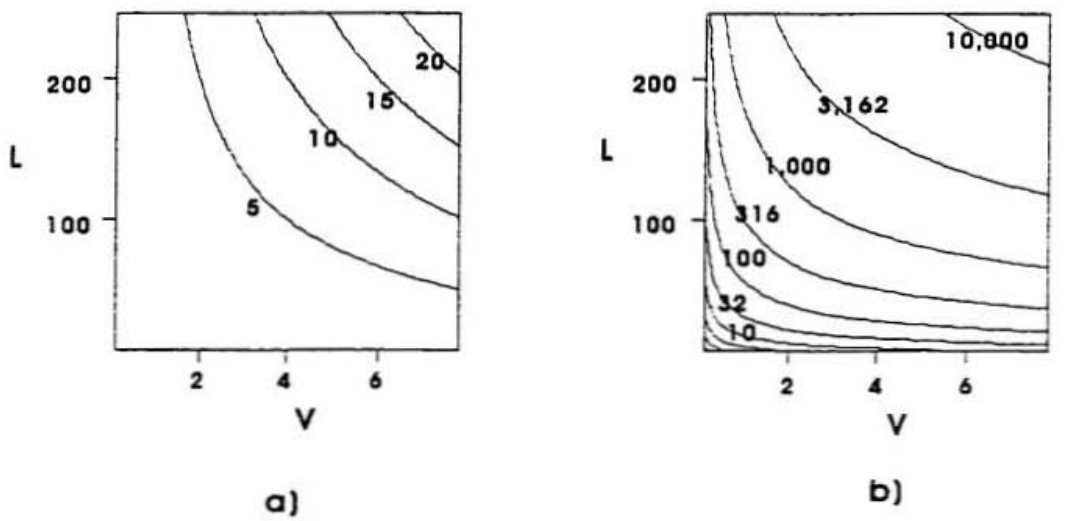

Figure 7.10 a) maximum impact penetration (m) as a function of V and L, and b) maximum impact force (MN) as a function of V and L.

As expected the force increases with both iceberg size and impact velocity. It should be noted that the extremely high forces in the upper right have negligible associated probabilities of occurrence as the velocities of large icebergs are limited.

In Figure 7.11, the iceberg sizes and (normal) impact velocities which are most likely to contribute to the design loads associated with probabilities of exceedance of 10^{-2} and 10^{-4} are shown. These plots were determined by tracking the combinations of input parameters that result in load values within a specified interval around the design load.

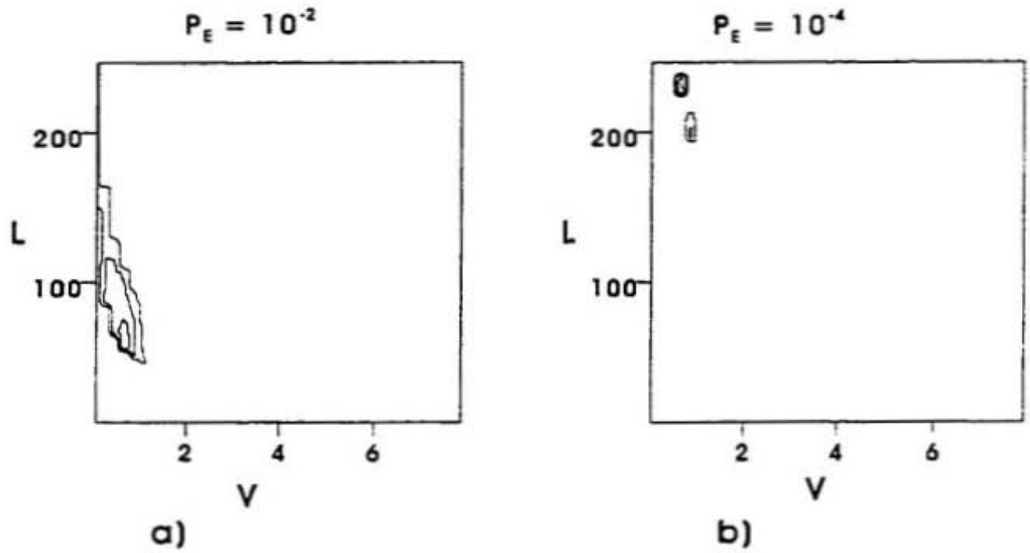

Figure 7.11 a) combinations of L and V contributing to 10^{-2} design load.
b) combinations of L and V contributing to 10^{-4} design load.

The outputs from a number of sensitivity analyses are shown in Table 7.1. The use of exceedance of 10^{-2} and 10^{-4} are indicated. It is seen that the 10^{-4} design loads tend to be dictated by the size of the largest icebergs considered. This indicates that the tail of the iceberg size distribution is very important and should be examined further. The depth of the sea bottom limits the iceberg sizes and should be considered. of a higher constant crushing pressure results in considerably higher loads. The use of the pressure area curve $P = 3\ A^{-0.4}$ decreases the loads significantly. The effect of the pressure area curve in reducing the load

is diminished for the more extreme impacts when a pressure area cut-off of 0.25 MPa is implemented and tend to the same load resulting when a constant pressure of 0.25 MPa is modelled. Using the base case model with the 1 MPa ice failure model, removing the ice management model resulted in a significant increase in design loads only at the higher probabilities of exceedance. Reducing the impact velocities by one quarter results in the 10^{-2} load being halved; for the 10^{-4} probabilities of exceedance, the load is reduced by one quarter.

Table 7.1 Design impact loads (MN) associated with specified probabilities of exceedance

	Model	Design probability of exceedance			
		10^{-2}	10^{-3}	10^{-4}	10^{-5}
1	1 MPa	171	630	1218	1744
2	4 MPa	344	1265	2455	3518
3	0.25 MPa	85	312	604	858
4	$3\ A^{-0.4}$ MPa	86	229	373	485
5	$3\ A^{-0.4}$ MPa with cut off at 0.25 MPa	86	306	599	856
6	1 MPa and no management	248	633	1218	1744
7	1 MPa and reduce velocities by 1/4	128	474	920	1312

To determine the effect of using random coefficients in the pressure area curve for ice failure, an importance sampling scheme was used to reduce the number of random samples required. Analyses were only conducted for the design load associated with a probability of exceedance of 10^{-4}. The distributions used for the coefficients C and D are described in Chapter 5. The sampling distributions used for choosing V, L, C, and D in the importance sampling scheme are given in Table 7.2.

Table 7.2 Parameters used for importance sampling distributions

Parameter	Sampling Distribution	Mean	Standard deviation	Lower cutoff	Upper cutoff
V	Gamma	0.8	0.6	*	*
L	Gamma	200	100	*	*
C	Gamma	3.6	1.65	0	9
D	Gamma **	0.5	1.5	-0.8	0

* determined by intervals set for overall numeric integration
** distribution generated for |D|

The importance sampling scheme was set up to run 10 simulations of 1000 runs each in order to indicate the rate of convergence regarding the design value. The model was run a second time with coefficients C and D kept constant at the mean values of 3 and -0.4, respectively. The purpose of the second run was to compare the results using importance sampling with earlier results based on direct integration. For this test run, the exact same sequence of random numbers was used for V and L as in the simulation with C and D random. The results of the simulations are given in Table 7.3.

The value of 384 MPa when using the constant coefficients is higher than the value of 373 MPa in Table 7.1 and is slightly more than one standard deviation different. This may be in part because the distribution is not Gaussian.

Table 7.3 Design loads (MN) for 10 consecutive simulations using both constant and random pressure area coefficients

Simulation	Simulation using constant coefficients	Simulation using random coefficients
1	385	1112
2	424	1263
3	403	1261
4	396	1408
5	392	1230
6	271	1153
7	344	431
8	404	796
9	408	1240
10	414	750
Mean	384	1064
Standard Deviation for Mean	7	17

To improve the analysis, the number of simulations could be increased or the choice of importance sampling distributions could be reassessed. The sampling distributions and distributions of values contributing to an interval around the design load are shown in Figure 7.12 for comparison. It is seen that the sampling distributions for L and D could be improved. The main result is that using the random distributions for C and D from the study by Carter et al. (1995) in place of the pressure-area curve $P(A) = 3A^{-0.4}$ results in significantly higher design values.

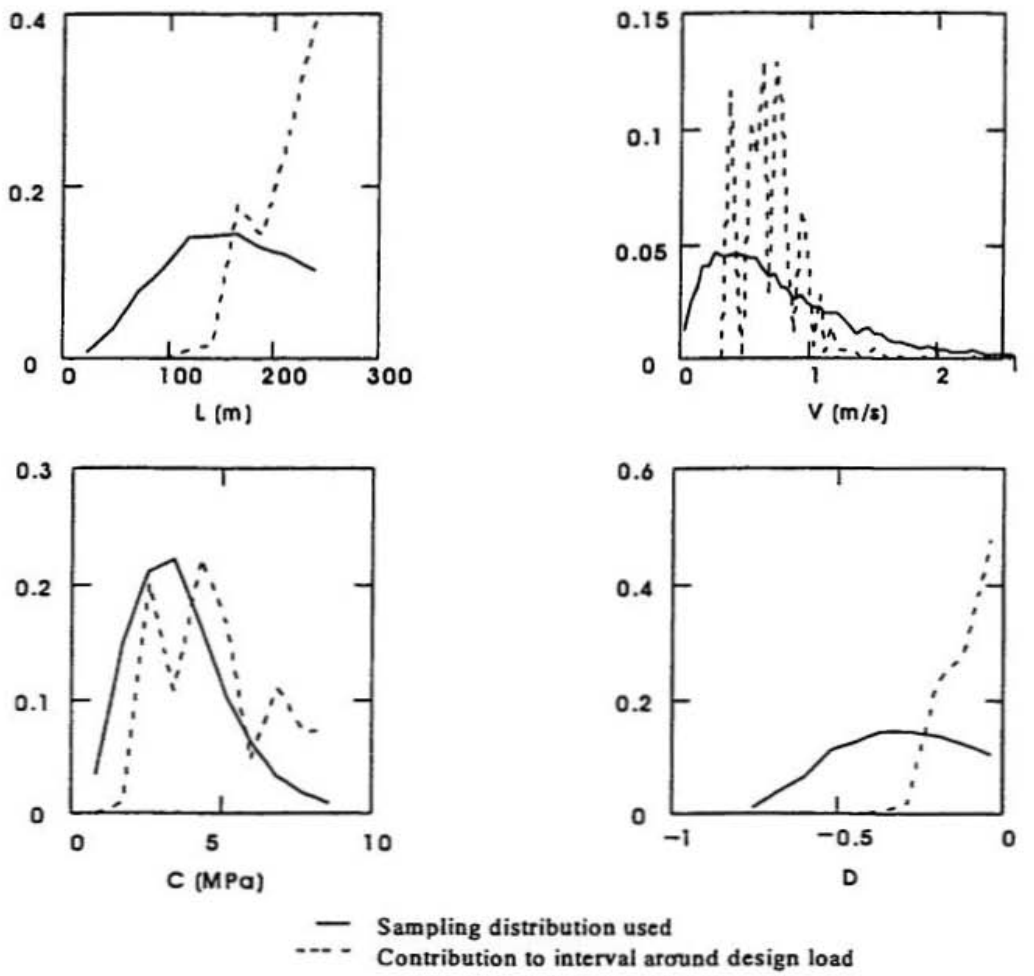

Figure 7.12 GBS - Sampling Distributions Used and Contribution to Interval Around the Design Load

7.2.5 Design loads for an FPSO

In considering the design loads on an FPSO, the following models regarding the detection and management system were considered:

1) no management,

2) the linear detection model (the smallest detectable iceberg in any sea state set at $L = 6\,H_s$) and the model for towing success described in Section 7.3,

3) the detection model including uncertainty and the model for towing success described in Section 7.3, and

4) Model 3, plus a 2% probability that the mooring disconnect system will not function given an approaching iceberg which cannot be towed.

The models were run for the case of impacts on the bow of an FPSO with a 35 m beam. The results of the different models on the 10^{-4} design value are shown in Table 7.4. It is seen that detection and management has a significant impact on the design loads. This difference would be even more pronounced if any of the other ice failure models was used. The addition of uncertainty in the detection model increased the design load by 13%. From the Model 4 results, it is seen that unreliability in the mooring disconnect system can significantly increase design loads. Also the use of random coefficients in the pressure area curve can significantly increase design loads. It is important to note that small changes in the pressure area coefficient can make a significant difference. For example, when for Model 2 the pressure area curve was changed to $3\,A^{-0.5}$, the design load dropped to 34 MN.

Table 7.4 Results of analyses of 10^{-4} design loads (in MN) for the bow of an FPSO

Operational model		Ice failure model		
		1 MPa	3 $A^{-0.4}$	Random coefficients
1	No detection and management	-	362	-
2	Linear detection model	-	47	-
3	Linear detection model with uncertainty	90	53	66±3*
4	Model 3 with 2% probability cannot disconnect mooring system	-	126	-

* see below

In Figure 7.13, the sizes of icebergs and velocities which are most likely to contribute to design loads with associated probabilities of exceedance of 10^{-2} and 10^{-4} are indicated. These are based on the Model 3 runs with P=3 A^{-4}, and may change considerably for other models

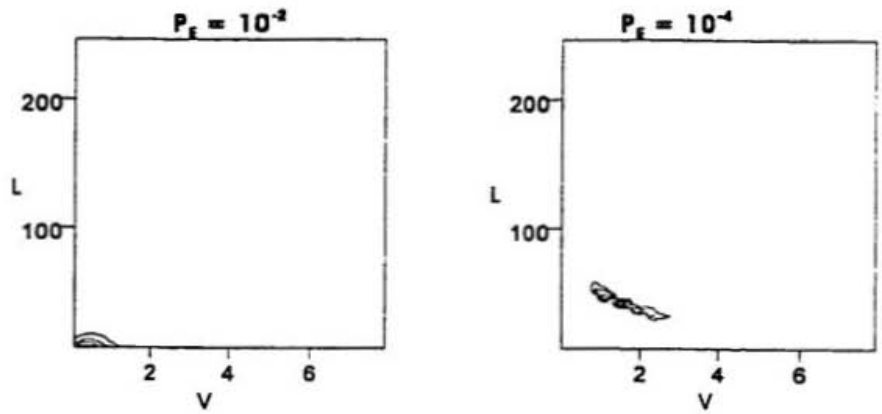

Figure 7.13 Areas of contribution to 10^{-2} and 10^{-4} design loads

The sensitivity of the design load to impact velocity was tested by reducing the impact velocities by 1/4 while running Model 3 in combination with the pressure area curve. The resulting design load dropped from 53 MN to 43 MN. While these differences are significant, the loads are most sensitive to the assumptions regarding the ice failure model.

For the FPSO, the sampling distributions used for choosing *V*, *L*, *C*, and *D* in the importance sampling scheme are given in Table 7.5.

Table 7.5 Parameters used for importance sampling distributions

Parameter	Sampling Distribution	Mean	Standard deviation	Lower cutoff	Upper cutoff
V	Gamma	2	3	*	*
L	Gamma	50	100	*	*
C	Gamma	3.6	1.65	0	9
D	Gamma **	0.5	1.5	-0.8	0

* determined by intervals set for overall numeric integration
** distribution generated for |D|

As for the GBS, the importance sampling scheme was set up to run 10 simulations of 1000 runs each in order to indicate the rate of convergence regarding the design value. The results of the simulations are given in Table 7.6.

The increase in design load with random coefficients for the pressure-area relationship of 53 MN to 66 MN is less severe than the increase from 384 MN to 1064 MN for the fixed system. This results because the final contact areas are larger for the large icebergs impacting the GBS, and the influence of the exponent D in the pressure-area relationship is more significant at large areas. It should be noted that as D increases to zero,

the final contact area reduces. While this reduces the increase in load as D increases, the effect is less important than the magnitude of the final contact area.

The sampling distributions and distributions of values contributing to an interval around the design load are shown in Figure 7.14 for comparison.

Table 7.6 Design loads (MN) for 10 consecutive simulations using both constant and random pressure area coefficients

Simulation	Simulation using constant coefficients	Simulation using random coefficients
1	58	53
2	53	66
3	59	69
4	48	67
5	49	72
6	49	65
7	55	62
8	46	65
9	57	76
10	52	70
Mean	53	66
Standard Deviation for Mean	2	3

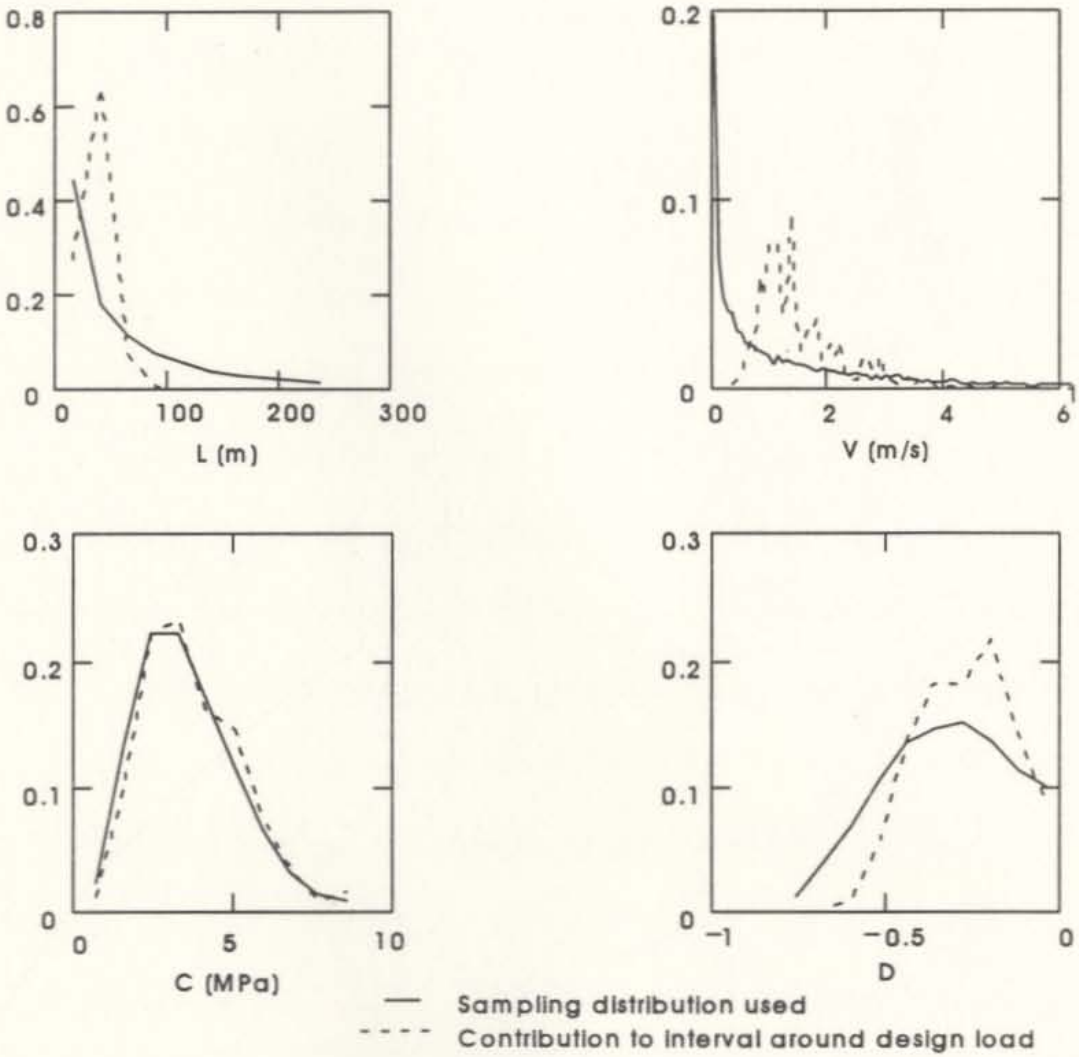

Figure 7.14 GBS - Sampling Distributions Used and Contribution to Interval Around the Design Load

7.3 Downtime due to iceberg incursion

A rough estimate of the amount of downtime due to iceberg incursions at a floating production site was obtained using the method below. Ice alert zones are typically defined in terms of the amount of time (sometimes denoted as "T-time") to shut down operations and disconnect the vessel mooring system. For each iceberg present, the amount of time that it

would take to reach the production vessel given its position, speed, and direction, as well as the prevailing and forecast weather conditions is estimated. If this time is less than the T-time, the operators will begin shutting down and disconnecting. Greg Lever (1995) suggested that normal disconnect procedures would require 8 hours and that 3 to 4 days would be required to reconnect. In addition, an emergency disconnect procedure could be implemented in a time of 1 hour but could require 6 to 7 months of work to reconnect.

To model the amount of downtime explicitly would require weather and current time series and a reasonably accurate iceberg trajectory forecast model. An alternative model is a Markov trajectory model of the type developed by Petro-Canada in the 1980's (Fuglem et al., 1984) . In this model, iceberg hourly speeds and directions are simulated based on the previous speed and direction and observed probabilities of changing states. The type of model implicitly includes the distributions and frequency of changes in the environmental conditions and hence the driving forces. In the Markov model developed, speed and direction were treated independently. In fact, there likely is some correlation between speed and direction as icebergs moving in a storm may be less likely to abruptly change direction. In calmer conditions tides and eddy currents will be more important. The assumption of independence of speed and direction could affect the estimated downtime.

An alternative approach for obtaining a quick estimate of potential downtime is applied here. Given a specified T time, the minimum distance an iceberg travelling at velocity v would have to travel to reach the production site is vT. Using the distribution of iceberg drift velocities by H_S and L developed previously, one can directly determine the minimum distance at which one would disconnect assuming that the conditions remained

constant and the iceberg headed straight towards the platform. This distribution is shown in Figure 7.15 .

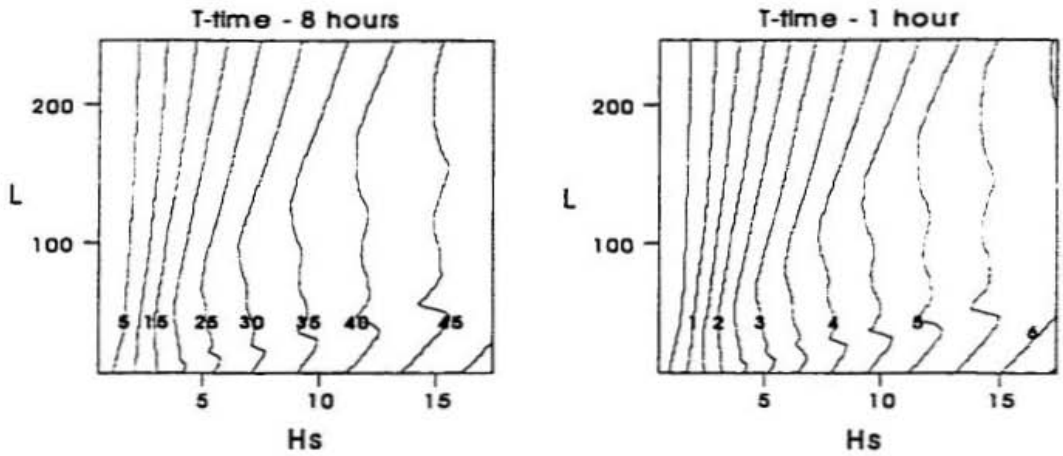

Figure 7.15 Minimum travel distances (km) given drift velocity

Note that except for the higher sea states with the 8 hour zone, most of these distances are withing the optimum detection range (around 30 km) from the production vessel. The number of times per year that icebergs enter a zone of equivalent radius is plotted in Figure 7.16 . The values on the contours are the negative logarithm base 10 of the expected number of entries per year. For example 3 represents 10^{-3} entries on average per year.

To estimate the amount of downtime due to normal disconnect events, it is assumed that a disconnect is invoked and downtime results whenever a detected iceberg entering the 8 hour zone cannot be towed. In the detection model, the range of detection is not explicitly considered as the optimal detection range is adequate in most cases. The proportion of events where towing is not possible is determined using the towing model. The resulting expected annual number of downtime events by L and H_S is shown in Figure 7.17 . The

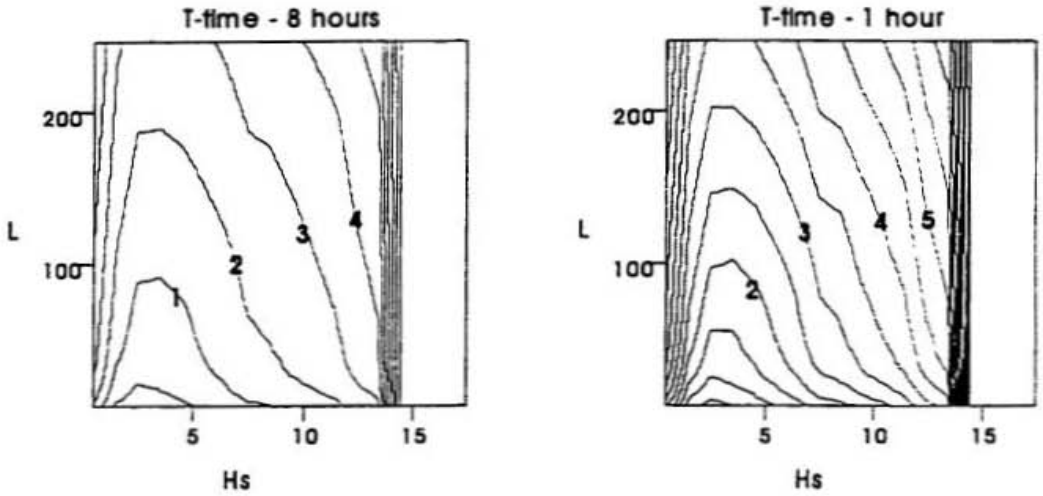

Figure 7.16 Number of icebergs (10^{-x}) per year entering zones of radii R_{min}.

expected amount of downtime in each case was assumed to be 4 days, including the amount of time that the iceberg is within the zone.

The number of emergency disconnects is estimated as follows. Even if an iceberg is initially undetected at 8 km, there is still a chance that it would be detected before reaching the 1 hour alert zone, for example by the standby vessel. For illustration purposes, it will be assumed that this occurs for 10% of the icebergs which cannot be towed (in fact, given the reduced detection time, there may be more icebergs which cannot be towed, this is not accounted for). An emergency disconnect is assumed to occur in each case that an iceberg reaches the 1 hour alert zone. In addition, if an iceberg is detected at 8 km but cannot be towed, there is a chance that there will be problems with the mooring disconnect system. A value in the range of 2% has been suggested (Berry, 1992). In such a case, an emergency disconnect might be invoked once the iceberg reaches the 1 hour alert zone. Finally, as the

operators may not disconnect for smaller icebergs, different limiting iceberg sizes may need to be considered. To illustrate, the amount of downtime for all icebergs and for icebergs of waterline length greater than 35 m will be considered.

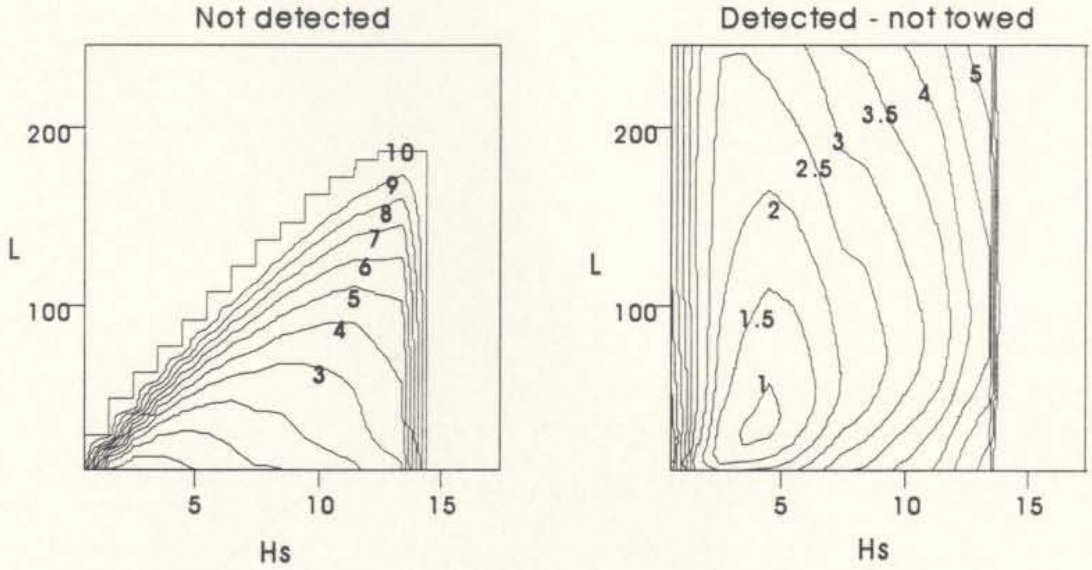

Figure 7.17 Number of icebergs (10^{-x}) per year entering 8 hour alert zone.

The expected annual numbers of downtime events for each case is shown in Table 7.7 and the resulting downtimes are shown in Table 7.8. These downtimes are rather high and the actual criteria used for determining when to disconnect should be reviewed with regard to downtime. In particular, the sizes of the alert zones may be too large as icebergs are unlikely to travel directly toward the platform. Also, the mooring may not actually be disconnected until the iceberg is much closer, the previous time used to prepare for disconnect. The operators may also decide not to disconnect for small icebergs. The cut-off size would be related to the ice strengthening chosen for the vessel. In this case there might be an economic trade-off between downtime and ice strengthening over and above the requirements for safety.

Table 7.7 Expected number of incursion events per year

Expected number of encounters per year	8 hour alert		2 hour alert	
	All bergs	> 35 m	All bergs	> 35 m
Total	39.9	11.6	9.8	1.5
Not detected	18.9	0.27	4.7	0.03
Detected, not towed	6	4.7	1.5	0.59
Detected and towed	14	6.6	3.5	0.85

Table 7.8 Downtime due to iceberg incursions (days)

	All icebergs	Icebergs > 35 m
Regular disconnect	24	18
Emergency disconnect (iceberg detected late)	43	0.6
Emergency disconnect (regular disconnect fails)	22	17
Total	88	36

A model that accounts for different degrees of shutdown depending on how close the iceberg approaches can be set down as follows (it has not been implemented here). Because the number of entries to an alert zone is proportion to the radius of the zone, for a given L and H_S the number of iceberg incursions for a given T-time will be proportional to T. If one determines the expected annual number of entries to the 1 hour zone η_1, the expected annual number of entries to a T hour zone is T times η_1. The modeller then needs to assign a function D(T) giving downtime as a function of T and integrate

$$\int_0^{T_{max}} \eta_T(T) \cdot D(T)\, dT \qquad (1)$$

to get the expected amount of downtime due to iceberg incursions.

7.4 Economic analysis of FPSO type systems for small fields

To illustrate how to incorporate costs and downtime related to icebergs, example runs were made for FPSO type systems for field sizes of 50, 100, and 200 million barrels. The analyses are conducted using the economic and downtime models described in Chapters 4, 5, and 6. The economics model was calibrated in large part against available data on the larger Terra Nova field; even though the subsea system differs. For the analyses here, the overall system used is a scaled down version of the system modelled in Chapter 4. The water depth is 95 metres and the subsea system consists of single wells tied to 6 well manifolds. The produced fluids from these manifolds are then routed to riser bases near the production vessel. To account for the differences in field size, the number of oil wells, the peak processing rate, and the areal extent of the reservoirs are reduced proportionately to the reduction in field size relative to the Terra Nova field.

Three analyses are conducted for each field as follows. In the first analysis, the systems are designed for the hypothetical case that no icebergs are present, This run is conducted to get a feel for the effect of icebergs on the overall economics. In the second analysis, denoted as "Option A", it is assumed that ice detection and management, vessel ice strengthening, a mooring quick release system, and protection of subsea equipment are

implemented. The associated capital and operating costs are included as well as the effect of additional downtime. The third analysis, denoted as "Option B", considers a system identical to that in Option A except that rather than protecting the subsea equipment, occasional damage with the consequent repair costs and downtime is accepted.

In the analyses, a base oil price of $20 US has been used. A sensitivity analyses of the economics with respect to oil price is included. A base discount rate of 0.12 is used in calculating the NPV for overall comparisons. In considering the effect of downtime with and without icebergs present, the average downtime unrelated to icebergs is taken as 37 days and the downtime due to shutting down due to iceberg incursions is taken as an additional 37 days. For option B, the additional downtime for repairs of subsea equipment when damaged by iceberg scours is included.

The important inputs and intermediate values in the analyses are presented in Tables 7.7 through 7.9. Some points to note are as follows. The sizes of the FPSO and shuttle tankers may be too small relative to those typically implemented and should be considered further. Also, the number of shuttle tankers is kept the same throughout the development. In actual cases, the number would be reduced once the peak processing rate dropped significantly. This would reduce operating costs and effectively return capital if the tankers were sold or used for another project. The cost for ice strengthening the FPSO was taken to be the same proportion as for a tanker. It would be more appropriate to relate the strengthening cost factor to the cost of the basic ship structure as the basic FPSO cost is different than that of shuttle tankers.

Figures 7.15 through 7.20 show the remaining reserves, daily production rates, and net cashflows as a function of time, and net present values as a function of discount rate for the three field sizes. Cash flows and net present value curves are given for the case of no icebergs and for Options A and B. Summaries of net present values and total cash flows are given in Table 7.10. It is of note that with the assumptions given, the case of using subsea protection appears considerably more expensive than accepting scour incidents and repairs. The probability of environmental damage due to an oil spill has not been accounted for and must be considered if Option A is chosen. Also, additional costs may be incurred for Option B to insure that the systems are fail safe regarding oil spills or blowouts. It is of note that development of the 50 million barrel field is not economical in all cases. The 100 million barrel field would be marginally economical if there were no icebergs. The 200 million barrel case is economical in all cases including Option A with downtime.

In Figure 7.21, the results of a sensitivity analysis for the price of oil are presented. It is seen that the economics are very sensitive to the price of oil. Even the 100 million barrel field, as modelled, would be economical with prices over 25$ US per barrel. The smaller fields would not be economic unless there was a considerable increase in the price of oil.

Table 7.9 Economic Analyses of FPSO Type Systems (1 of 3 pages)

Item	Unit	Reservoir size (MBbl)		
		50	100	200
General				
Initial reserves	MBbl	50.00	100.00	200.00
Peak processing capacity	bopd	14492.75	28985.51	57971.01
Width or reservoir	km	3.05	4.31	6.09
Length of reservoir	km	2.28	3.23	4.57
Wells				
No. prod. wells		3.00	6.00	12.00
Peak prod. rate per well	bopd	10000.00	10000.00	10000.00
Mean drilled dist. per well	km	5.83	5.83	5.83
Mean cost per well, drilled and completed	MCdn	35.47	35.47	35.47
Total cost of dev. drilling	MCdn	106.41	212.82	425.63
No. wells drilled per year		4.00	4.00	4.00
Subsea system - unprotected				
Cost per subsea tree	MCdn	3.60	3.60	3.60
Total cost subsea trees	MCdn	10.80	21.60	43.20
No. manifolds		1.00	1.00	2.00
Cost of manifold per well	MCdn	1.80	1.80	1.80
Total cost of manifolds, installed	MCdn	5.40	10.80	21.60
Cost of flowlines (per km per bopd)		0.09	0.09	0.09
Dist. from wells to manifold	km	0.50	0.50	0.50
Total distance of lines from wells to manifolds	km	1.50	3.00	6.00
Total cost of lines from wells to manifolds	MCdn	1.35	2.70	5.40
Mean distance from manifolds to riser bases	km	0.93	1.32	1.70
Total distance from manifolds to riser bases	km	0.93	1.32	3.40
Total cost of lines from manifolds to riser bases	MCdn	5.03	7.11	18.36
Cost per riser base	MCdn	1.80	1.80	1.80
Total cost of riser base	MCdn	1.80	1.80	3.60
Cost of risers per km per bopd	MCdn	0.18	0.18	0.18
Total cost of risers	MCdn	0.54	1.08	2.16

Table 7.10 Economic Analyses of FPSO Type Systems (2/3)

Item	Unit	Reservoir size (MBbl) 50	100	200
Total cost of unprotected subsea system assoc. with prod. wells	MCdn	24.92	45.09	94.32
Cost factor for control system		0.20	0.20	0.20
Cost factor for injection wells		0.50	0.50	0.50
Cost of unprotected subsea sys.	MCdn	44.86	81.17	169.77
Process, FPSO, and Tankers				
Cost of process equipment	MCdn	80.10	134.71	226.55
Mass of 6 days peak production	tonne	11594.20	23188.41	46376.81
Cost of FPSO	MCdn	50.19	84.42	141.97
Cost of turret	MCdn	44.35	48.70	57.39
No. of shuttle tankers		3.00	3.00	3.00
Ratio tanker deadweight to cargo deadweight		1.06	1.06	1.06
Shuttle tanker deadweight	tonne	12336.23	24672.46	49344.93
Cost per shuttle tanker	MCdn	42.22	60.21	85.85
Total Capex of shuttle tankers	MCdn	126.66	180.62	257.56
Other Capex	MCdn	96.77	162.75	273.71
Total Capex	MCdn	549.33	905.16	1552.58
No. years initial Capex spread over		2	2	2
Opex assuming no icebergs				
Annual Opex/ Initial Capex (excluding shuttle tankers)		0.09	0.09	0.09
Annual Opex other than shuttle tankers	MCdn	35.93	61.59	110.08
Annual Opex per shuttle tanker	MCdn	0.78	1.55	3.11
Total annual Opex for shuttle tankers	MCdn	2.33	4.66	9.33
Total annual operating costs	MCdn	38.26	66.25	119.4
Icebergs related costs				
Cost factor for ice strengthening FPSO		0.05	0.05	0.05
FPSO cost factor - addition iceberg related costs		0.00	0.00	0.00
Total ice related Capex for FPSO	MCdn	2.51	4.22	7.10
Cost factor for ice strengthening a shuttle tanker		0.05	0.05	0.05
Shuttle tanker cost factor - add. iceberg related costs		0.10	0.10	0.10

Table 7.11 Economic Analyses of FPSO Type Systems (3/3)

Item	Unit	Reservoir size (MBbl) 50	100	200
Total ice related Capex for shuttle tankers	MCdn	19.00	27.09	38.63
Annual costs for ice surveillance	MCdn	3.00	3.00	3.00
Annual cost for ice towing	MCdn	3.00	3.00	3.00
Total annual operating costs related to icebergs	MCdn	6	6	6
Option A - additional costs				
Cost per glory hole	MCdn	0.47	0.47	0.47
Cost of all glory holes	MCdn	2.34	3.74	7.48
Cost factor to bury pipelines		0.60	0.60	0.60
Cost to bury lines from wells to manifolds	MCdn	2.16	4.32	8.64
Costs to bury lines from manifolds to riser base	MCdn	8.05	11.38	29.37
Capex for protection of subsea equip. (Prod. wells)	MCdn	12.55	19.45	45.49
Capex for protection of subsea equip. (Complete sys.)	MCdn	22.59	35	81.89
Option B - additional costs				
Expected no. of hits per year per subsea item	MCdn	0.00	0.00	0.00
Cost to repair a subsea tree	MCdn	9.00	9.00	9.00
Cost to repair a manifold	MCdn	3.60	3.60	3.60
Cost to repair a riser base	MCdn	3.60	3.60	3.60
Total cost to repair trees	MCdn	0.00	0.00	0.00
Total cost to repair manifolds	MCdn	0.00	0.00	0.00
Total cost to repair riser bases	MCdn	0.00	0.00	0.00
Exp. avg. no. incidences with lines from wells to manifolds		0.00	0.00	0.00
Exp. ann. cost of repairs for above	MCdn	0.00	0.00	0.00
Exp. no. incidences with lines from manifolds to riser bases		0.00	0.00	0.00
Exp. ann. cost of repairs for above	MCdn	0.00	0.00	0.00
Total expected annual cost of repairs, (prod. wells)	MCdn	0.00	0.00	0.01
Total expected annual cost of repairs, (complete sys.)	MCdn	0.00	0.01	0.01
Expected annual downtime for repairs (prod. wells)	days	0.02	0.03	0.03
Expected annual downtime for repairs (complete sys.)	days	0.03	0.06	0.06

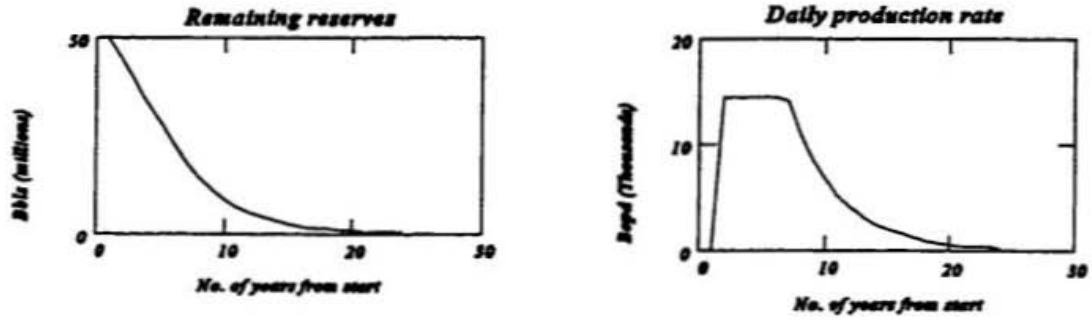

Figure 7.18 Remaining reserves and daily production rate for 50 million barrel field

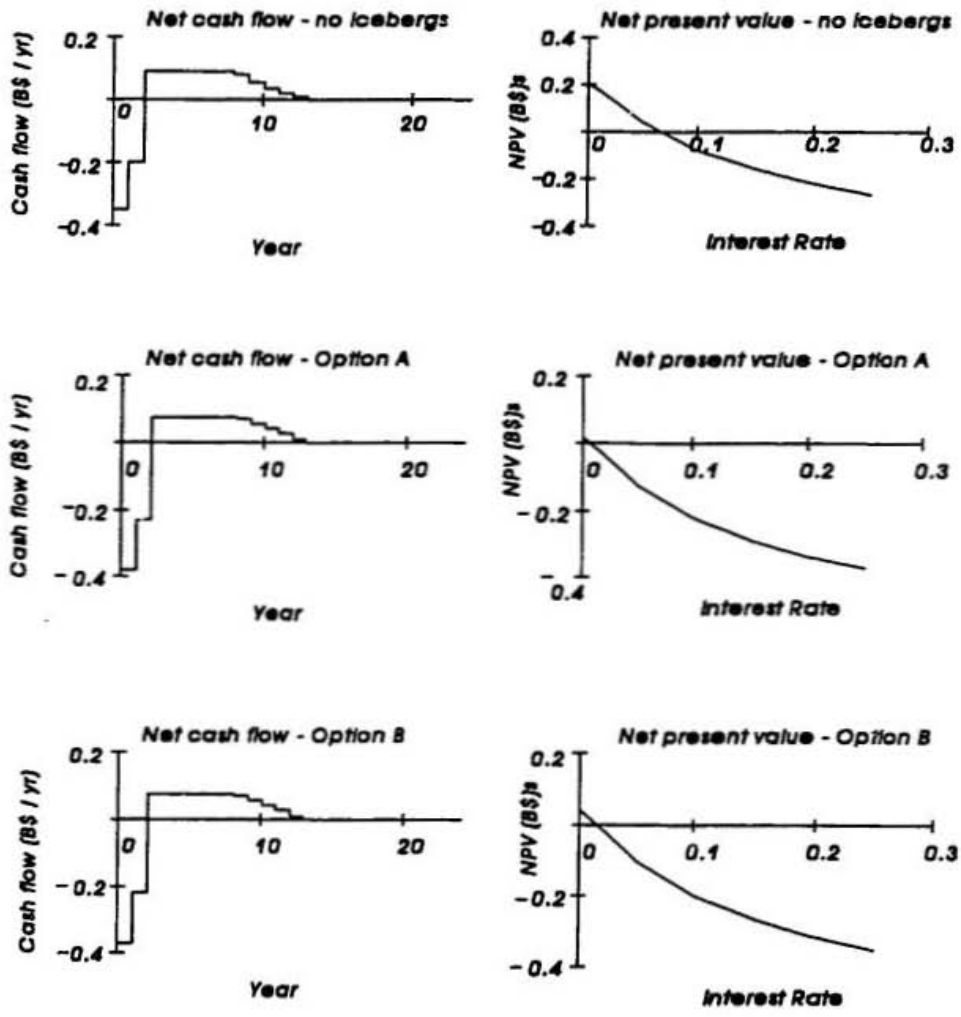

Figure 7.19 Cash flows and NPVs for 50 million barrel field

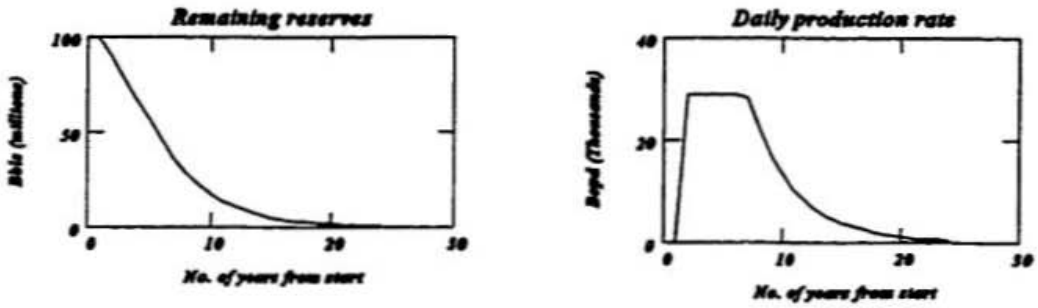

Figure 7.20 Remaining reserves and daily production rate for 100 million barrel field

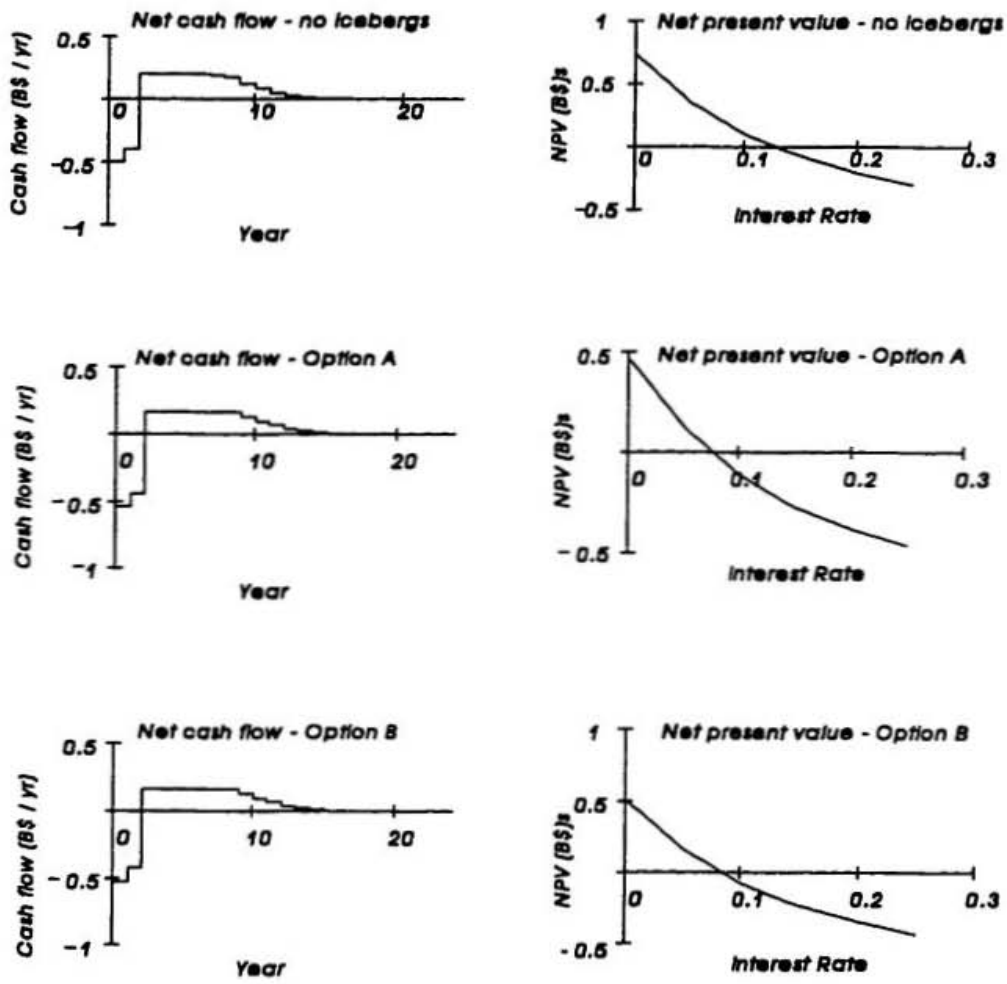

Figure 7.21 Cash flows and NPVs for 100 million barrel field

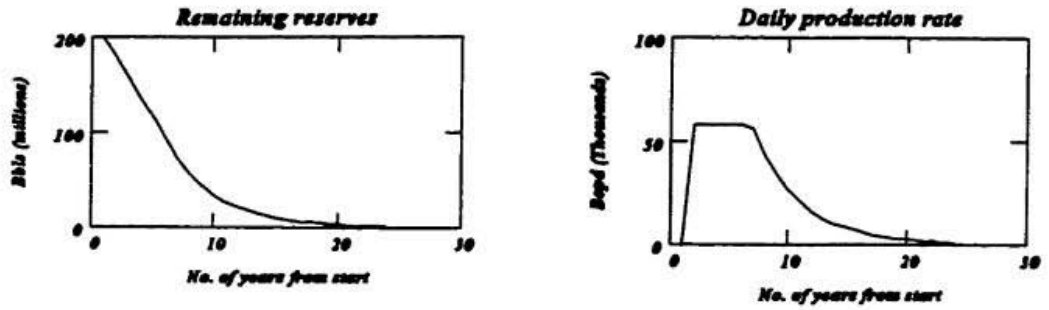

Figure 7.22 Remaining reserves and daily production rate for 200 million barrel field

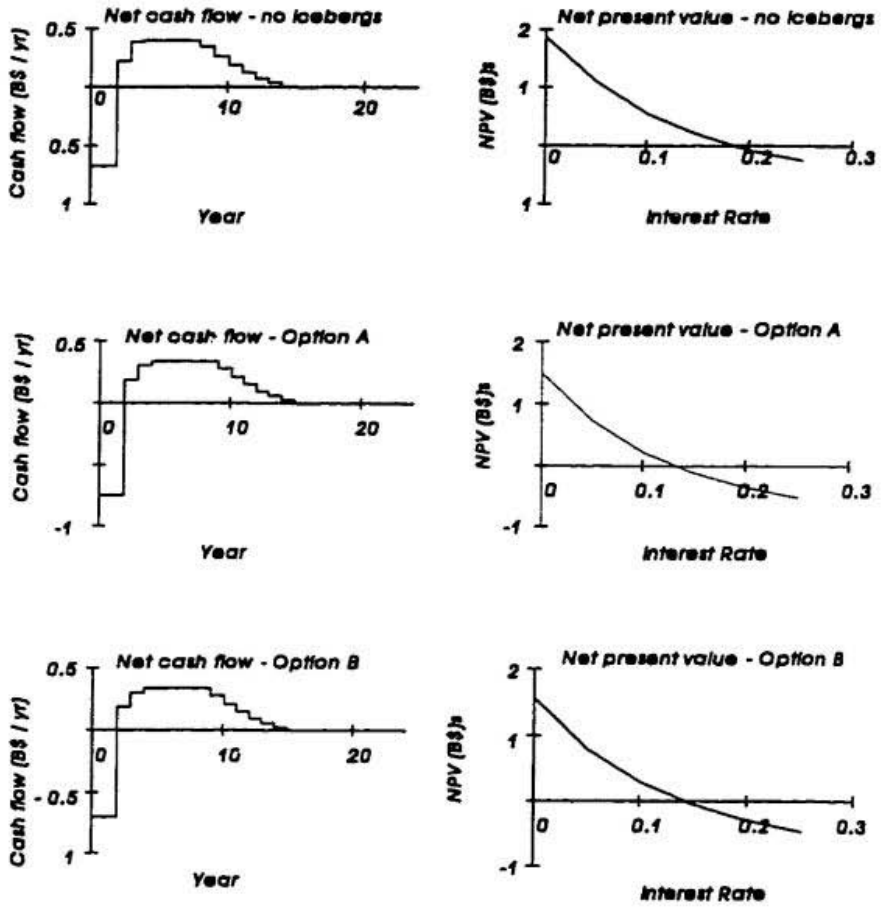

Figure 7.23 Cash flows and NPVs for 200 million barrel field

Table 7.12 Economic Analyses of FPSO Type Systems

50 million barrel field		No Icebergs	Option A	Option B
Net present values (no downtime)	MCdn	-76	-168	-147
Net present values (with downtime)	MCdn	-116	-254	-232
Total production (no downtime)	MBbl	45	43	43
Total production (with downtime)	MBbl	45	46	46
Years production (no downtime)		11	10	10
Years production (with downtime)		11	12	12
No. of days downtime per year	days	36.5	73	73.031
Sum Capex (no downtime)	MCdn	549	613	591
Sum Opex (no downtime)	MCdn	421	443	443
Sum Revenue (no downtime)	MCdn	1226	1184	1184
Sum Capex (with downtime)	MCdn	549	613	591
Sum Opex (with downtime)	MCdn	421	531	531
Sum Revenue (with downtime)	MCdn	1179	1163	1163
100 million barrel field				
Net present values (no downtime)	MCdn	96	-18	16
Net present values (with downtime)	MCdn	19	-183	-150
Total production (no downtime)	MBbl	89	89	89
Total production (with downtime)	MBbl	92	93	93
Years production (no downtime)		11	11	11
Years production (with downtime)		12	13	13
No. of days downtime per year	days	36.5	73	73.06
Sum Capex (no downtime)	MCdn	905	991	956
Sum Opex (no downtime)	MCdn	729	795	795
Sum Revenue (no downtime)	MCdn	2451	2451	2451
Sum Capex (with downtime)	MCdn	905	991	956
Sum Opex (with downtime)	MCdn	795	939	939
Sum Revenue (with downtime)	MCdn	2435	2402	2402
200 million barrel field				
Net present values (no downtime)	MCdn	548	375	452
Net present values (with downtime)	MCdn	397	55	132
Total production (no downtime)	MBbl	183	183	183
Total production (with downtime)	MBbl	187	187	187
Years production (no downtime)		12	12	12
Years production (with downtime)		13	13	13
No. of days downtime per year	days	36.5	73	73.06
Sum Capex (no downtime)	MCdn	1553	1700	1618
Sum Opex (no downtime)	MCdn	1433	1505	1505
Sum Revenue (no downtime)	MCdn	5030	5030	5030
Sum Capex (with downtime)	MCdn	1553	1700	1618
Sum Opex (with downtime)	MCdn	1552	1630	1630
Sum Revenue (with downtime)	MCdn	4992	4804	4803

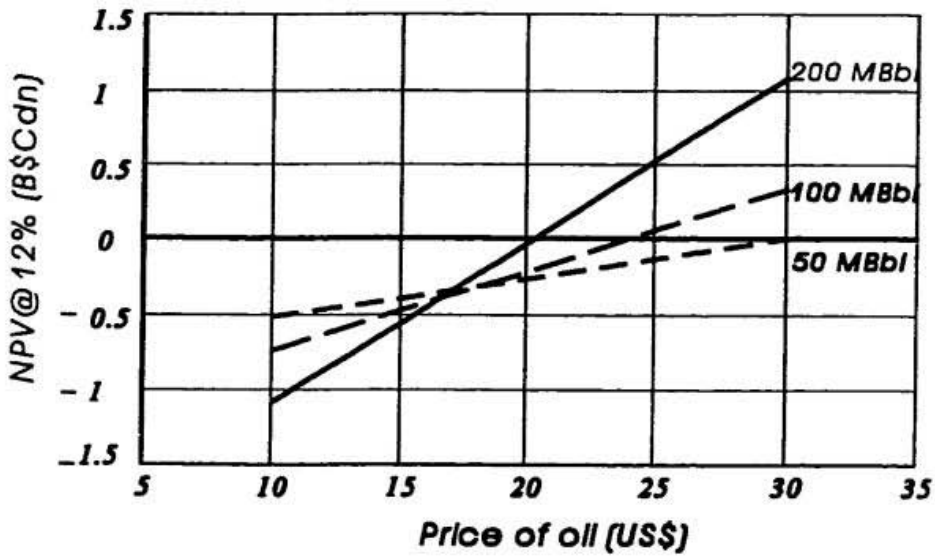

Figure 7.24 Sensitivity of NPVs to the price of oil

8 CONCLUSIONS

There is significant interest at present in exploration and development on the Grand Banks; it is expected that this will increase as infrastructure for the Hibernia and Terra Nova fields is developed. The presence of icebergs and high sea states on the Grand Banks presents a unique challenge to the oil industry and has not previously been dealt with. At present, this challenge is being addressed by using a massive GBS at Hibernia that will withstand impacts from on the Grand Banks icebergs and by using a floating system at Terra Nova that will move out of the path of icebergs which cannot be towed.

The presence of icebergs results in increased risks and development costs. In order to be able to improve future production system designs and operational procedures, it is important to continue to improve our understanding of how icebergs affect production system designs and operations, to reduce uncertainties in critical areas, and to make improvements. At present, it is felt by many that the cost of fixed structures could be reduced significantly. This is possible if wave loads can be reduced and the validity of the pressure-area relationship for ice failure can be demonstrated. In order to reduce design ice loads for floating systems, it is necessary to validate detection capabilities in storm conditions.

The problem of estimating design iceberg impact loads for reliability-based designs has been considered for two structures, a GBS and a FPSO. Only global impacts on the side of the GBS and the bow of the FPSO have been considered. In a full design analysis, the models would need to be extended. For the FPSO, the design impacts loads for the sides of the vessel would be required. For the GBS, impact loads on the column and deck would be required. In addition, local ice loads on critical panel sizes would be needed. Design iceberg

impact loads were determined based on a probability of exceedance of 10^{-4} per year. This corresponds to a risk levels of 10^{-5} per year, assuming an additional order of magnitude of safety is built into the structural design.

In determining the design loads, the models and input distributions should always be chosen using the best information available. Conservative assumptions should not be built in at each stage, but should be considered after sensitivity analysis have been run in order to determine the effect of different assumptions on the calculated design loads. The steps involved in determining the iceberg impact loads were as follows.

1. The areal density of icebergs in the vicinity of interest was determined for each month over a 30 year period from IIP charts.
2. The monthly distributions of sea state were combined, weighted by the average proportion of icebergs in each month.
3. A model for the drift velocity of icebergs in different sea states was developed to determine the number of icebergs passing near the structure and the drift velocities at impact.
4. An encounter model was developed to determine the expected number of impacts per year in the absence of detection and management.
5. Detection and management was modelled and the effectiveness in reducing impacts incorporated.
6. A probabilistic model for the combined drift and wave-induced velocities of icebergs was developed and applied incorporating previous analytical and experimental work by Jim Lever (Lever et al., 1988b).

7. In modelling the impact dynamics, the iceberg was treated as a sphere of equivalent mass and the structure was treated as a vertical rigid wall.

8. The failure strength of ice was modelled using a pressure-area relationship of the form $P = C\,a^D$ with random coefficient C and D. The distributions for the parameters were based on results of a calibration for icebreakers ramming into large multiyear flow (Appendix A).

9. The models were run within a probabilistic framework to determine the distributions of impact loads. Based on the estimated number of impacts per year, design loads corresponding to specified annual probabilities of exceedance were determined.

For the cylindrical GBS, it was shown that design loads are most likely to result in moderate sea conditions when icebergs which are too large to tow successfully run into the platform. When random coefficients were used for the pressure-area relationship, a 10^{-4} design load of 1064 MN was calculated. This is considerably higher than the value of 384 MN obtained when mean values were used for the pressure-area coefficients, but is less than the value 1218 MN based on a constant ice crushing strength of 1 MPa. It was found that the design loads were reasonably sensitive to the impact velocity and the number of impacts (see Table 7.1, the sensitivity to the number of impacts can be determined from the probabilities of exceedance, i.e. a 10 fold change in the number of impacts is equivalent to a 10 fold change in the probability of exceedance). The design load of 1064 MN is considered conservative because the use of a spherical shape for the iceberg results in first, direct impacts (no eccentricity) and second, the rapid development of large contact areas.

It should be noted that a fixed relationship between waterline length and iceberg mass was used; adding the uncertainty in this relationship would increase the design load.

For the FPSO, it is shown that the design loads are most likely to result from smaller icebergs in storm conditions when icebergs are difficult to detect and tow. When random coefficients were used for the pressure-area relationship, the resulting 10^{-4} design load was 66 MN. The result when mean values was used for the pressure-area coefficients was 53 MN. There is less of a difference than for the fixed structure because the final contact area is smaller. The effect of adding uncertainty in the detection probability was to increase the design load approximately 10%. The effect of adding a 2% probability that the vessel cannot disconnect was to more than double the design load to 126 MN. In conclusion, the design loads for the floating system are most sensitive to the assumptions on the efficiency of the detection and management system and the reliability of the mooring disconnect system. It should be noted that the range of uncertainty in the detection and management relationship was notional and was included to show the sensitivity of the design load to this parameter. The effect of impact velocity was found to be smaller for the FPSO than for the GBS.

An economic model was developed to determine revenues and cost as a function of time, and from those calculate the net present value. The revenues are determined based on the price of oil, the nominal amount of oil produced, and the amount of downtime. While the amount of downtime due to icebergs entering alert zones appears significant, scouring of subsea equipment appears to be so infrequent that the expected downtime is negligible. The model of capital costs has been set up to allow a user to specify costs in terms of either fixed values or parametric curves in which case variations in cost with size or number of

items can specified. Example calculations are presented for the economics of floating production systems in developing smaller fields. While many of the values used in the model are notional, the framework could be used with enhanced values to analyse a number of production options, including the use of minimal systems where the production system is only used for production during part of the year. In an overall comparison of systems, consideration is required of the costs of loss of life and environmental damage. These factors will be related to the total risk rather than the target risks for design loads.

In a probabilistic study, the manner in which model uncertainty and subjective assessments are incorporated is important. Different degrees of judgement are assessment of various data inputs and choice of models; this is an inherent part of modelling. Assessments based on outputs of models must be considered as conditional on the sets of assumptions used in the models (even when the models are used within a probabilistic framework). Sensitivity analyses should be conducted to determine which parameters and assumptions have the greatest effect on the results and whether significant variation is likely. If significant variation is possible and there is risk of loss of life and equipment and environmental damage, it is necessary to use more conservative designs or else obtain better information.

Based on the analyses carried out, it is seen that further research on ice failure mechanics and on detection, management, and disconnect reliability are important. To determine an appropriate rate of change in detection probabilities for the detection model, the variation in radar cross-sections of icebergs and the variation in sea clutter for a given H_s need to be examined along with other factors. It should be noted that better detection

methods have been developed than those used in the study; for example scan-to-scan integration techniques have been developed. While analytic studies can help to understand ice failure and iceberg detection problems, and identify what further information is required, ultimately field studies will be required. Other areas for inclusion or improvement include the following:

1. modelling of actual iceberg shapes to determine contact penetration-area relationships and impact eccentricities, especially for large structures;
2. better evaluation of towing success rate as a function of iceberg size (especially for large icebergs);
3. improved estimation of impact velocities; and
4. evaluation of effect of shape on wave-induced velocities.

REFERENCES

Abel, W. (1994) *Personal Communication*

Alfultis M. and Osmer S. (1988) *International Ice Patrol's Side-Looking Airborne Radar Experiment (SLAREX)*, 1988 International Ice Patrol Bulletin, No. 74, CG-188-43.

Anonymous (1994) *Exxon to appeal $5 billion Valdez spill judgement* Oil & Gas Journal. September 26, 1994, pg. 36-38.

Anonymous (1995) *Deepwater and Harsh-Market Rigs in Short Supply Worldwide*, Journal of Petroleum Technology, August 1995, pp 646-704.

ARLIS (1997). *Oil Spill Public Information Center - Web Site*, Alaska Resources Library and Information Services (ARLIS) Anchorage, Alaska
Internet Site: http://www.alaska.net/~ospic/

Arneberg, J.E., Guenther, K.T. (1993) *Trends for Future Development Planning in the Norweigan North Sea*, SPE - Offshore European Conference, Aberdeen, 7-10 Sept. 1993

Barnes, R. Paul (1996) *Personal Communication*, Canada-Newfoundland Offshore Petroleum Board.

Bayly, D.R., Williamsson, R. (1989) *Advances in Underwater Technology, Ocean Science and Offshore Engineering*, Volume 19: Diverless and Deep Water Technology, Society for Underwater Technology, Graham and Trotman, 1989.

Behrenbruch (1993) *Offshore Oilfield Development Planning*, Journal of Petroleum Technology, August, 1993.

Behrenbruch (1993) *Offshore Oilfield Development Planning*, Journal of Petroleum Technology, August, 1993.

Berry (1992) *Personal Communication*

Bishop, Gary P. (1989) *Assessment of Iceberg Management for the Grand Banks Area: Analysis of Detection and Deflection Techniques*, Prepared for Mobil Oil Properties, April, 1989.

Blen Kam, K.A., and Knapp, A.E. (1969) *Ice conditions on the Grand Banks. Ice Seminar, a conference sponsored by the petroleum society of CIM (The Canadian Institute of Mining and Metallurgy)*, Calgary, Alta., May 6-7, 1968. Special Vol. 10, 1969, pp 61-72.

Bruce, G.C. (1991) *Canada's Next Oil Producing Region*, NOIA Conference '91 Proceedings

Buck, James R. (1989) *Economic Risks Decisions in Engineering and Management*, Iowa State University Press.

Cammaert AB, Jordaan I.J., Fuglem M, Bruneau, S.E., Crocker, G, and Wishahy M. (1992) *Design Criteria for Ice Loads on Floating Production Systems - Final Report*, Contract report for Petro-Canada Resources, C-CORE Contract Number 92-C13.

Canada NewsWire (1996) *Royalty Regime Announced* June, 1996.

Canada NewsWire (1996) *Mobil Chevron and Murphy Select Canship Ugland to Manage Hibernia Shuttle Tanker - The Kometik.* September, 1996.

Canadian Standards Association (1992) *Code for the Design, Construction, and Installation of Fixed Offshore Structures*, CAN/CSA-S471-92, National Standard of Canada.

Carter, J., Daley, C., Fuglem, M., Jordaan, I., Keinonen, A., Revill, C., Butler, T., Muggeridge, K., and Zou, B. (1995) *Maximum Bow Force for Arctic Shipping Pollution Prevention Regulations - Phase II*, Report prepared for Transport Canada.

Cassimatis, P. (1988) *A Concise Introduction to Engineering Economics*, Unwin Hyman

Chipman W. (1992) *Oil and Gas Fields Offshore Newfoundland and Labrador - Development Potential and Scenarios.* NOIA Conference '92 Proceedings

Crocker, G. (1997). *Personal communication.*

Crocker, G. (1992). *Growler and Bergy Bit Populations on the Grand Banks.* C-CORE Internal Report, January 1992

Croasdale, K.R., and McDougall, J.R. (1994) *Research Planning Study for Canada's Frontier Oil and Gas - Second Edition.*, Work supported by the Federal Panel on Energy R&D, pg. 86.

CSA (1992) *General Requirement, Design Criteria, the Environment, and Loads*, CAN/CSA-S471-92, Part of Code for the Design Construction, and Installation of Fixed Offshore Structures, Canadian Standards Association, ©1992

Daley, C. (1994) *Development of Design Ramming Force for Arctic Vessels*, Canadian Coast Guard Report TP12150E.

Det norske Veritas (1977) *Rules for the Design, Construction and Inspection of Offshore Structures*, Appendix A, Environmental Conditions. Oslo, Norway.

Doble, P.A.C., Workman, D.M., Addy, P. (1994) *Gryphon A - Features and operational benefits*, Offshore Technology Conference, paper 7721.

Dome Petroleum Ltd. (1982) *Report on Full Scale Measurement of Ice Impact Loads and Response of the 'Canmar Kigoriak' - August and October 1981*. Prepared by Dome Petroleum Ltd.

de Finetti, Bruno (1972) *Probability, Induction and Statistics - The Art of Guessing*, John Wiley and Sons

Dominic, P.R. (1993) *Reservoir M*anagement in a Marginal North Sea Cluster Development, *SPE Offshore European Conference, Aberdeen, Scotland, 7-10 September, 1993*

D'Souza, R.B., Henderson, A.D., Barton, D.L., Hardin, D.J., Boyd, A., Solberg, I.C. (1993) *The Semisubmersible Floating Production System: Past, Present, and Future Technology*, SNAME, Transactions, Vol. 101, 1993, 437-484.

D'Souza, R.B., Delepine, Y.M., Cordy, A.R. (1994) *An Approach to the Design and Selection of a Cost-Effective Floating Production Storage and Offloading System*, Offshore Technology Conference, Houston, Texas, 2-5 May, 1994

Dunwoody, A. B. (1983) *The Design, Ice Island for Impact Against an Offshore Structure*, OTC 1983, paper 4550, pp. 325-330

Duthinh, D., Marsden, S. (1986) *Iceberg Impact Load on a Gravity Based Structure*, Cold Regions Eng., Proc. of the Fourth Int. Conf., ASCE. pp. 82-92.

Edwards, W.G. (1993) *Economic Development of Small Isolated Fields*, SPE - Offshore European Conf., Aberdeen, 7-10, 1993

El-Oun, Z.B., Corbally, J. (1994) *Process Engineering Design Aspects of Multiphase Flow Systems for the Exploitation of Marginal Fields*, 26'th Offshore Technology Conference, Houston, Texas, 2-5 may, 1994

El Tahan, M., Simms, A. (1989) *The Interaction of the Nekton 8000 FPV with Sea Ice and Bergy Bits, Phase I: Ice environmental data.* C-CORE Contract Report 88-C9.

Evening Telegram (1995) *Hibernia tankers won't be Canadian-made*, Provincial News Section, Mar. 25, 1995.

Exxon Valdez Oil Spill Restoration Office (1997). *Official Web Site.* Site supported by the Exxon Valdez Oil Spill Trustee Council, Anchorage, Alaska. Internet site: http://www.oilspill.state.ak.us/exxon.html

Falcimaigne, J.R. (1992) *Multiphase Flow: A Cost Efficient Solution for Marginal Field Developments*, European Petroleum Conference, Cannes, France, 16-18 Nov., 1992

Fenco Newfoundland Ltd. (1981a) *Iceberg Size and Physical-Mechanical Properties Review*, Volume A. Prepared for Mobil Oil Canada, Ltd.

Ferregut, C., Perchanok, M. and Daley, C.G. (1987) *Ship/ice collision probabilities in arctic shipping. Port and Ocean Engineering under Arctic Conditions*, Vol. 1, W.M. Sackinger and M.D. Jeffries (Eds.) University of Alaska, Fairbanks, pp. 631-643.

Frederking, R.M., Jordaan, I.J., and McCallum, J.S. (1990) *Field tests of ice indentation to medium scale, Hobson's Choice Ice Island*, 10th International IAHR Symposium on Ice, ESPOO, Finland, Vol. 2, pp. 931-944.

Fuglem M.K., Hotzel I.S., and Clark. (1984) *Iceberg collision probabilities by simulator*, Proceedings of the Specialty Conference on Computer Methods in offshore Engineering, Halifax, NS, pp. 475-487.

Fuglem, M.K., Duthinh, D., Lever, J. and Jordaan, I.J. (1991) *Probabilistic Determination of Iceberg Collision Design Loads for Floating Production Vessels.* Proceedings IUTAM-IAHR Symposium on Ice-Structure Interaction August 1989, Springer-Verlag, pp. 459-482.

Fuglem, M.K., Jordaan, I., Crocker, G. (1995) *Iceberg-Structure Interaction Probabilities for Design.* Submitted to the Canadian Journal of Civil Engineering.

Glen, I.F. and Blount, H. (1984) *Measurements of Ice Impact Pressures and Loads onboard CCGS Louis S. St. Laurent*, OMAE '84, Vol. 3, pp. 246-252.

Gruy, R.H., Etheridge, C.O., Krafft, M.J. (1994) *Why the Disconnectable Turret Makes Sense in Typhoon Corridors*, Offshore, May, 1994

Hansen, R.L., Rickey, W.P. (1994) *Evolution of Subsea Production Systems: A Worldwide Overview*, 26'th Annual Offshore Technology Conference, 2-5 May, 1994

Hasselmann, et al. (1973). *Measurements of Wind-Wave Growth and Swell Decay During the Joint North Sea Wave Project (JONSWAP)*, Deutsches Hydrograph. Institute.

Henery, D. and Inglis, R.B. (1995) *Prospects and Challenges for the FPSO*, Offshore Technology Conference, Paper 7695.

Hoffman, D., Ismaili, N.M., Nielsen, R. (1991) *The Design of Flexible Marine Risers in Deep and Shallow Water*, 23rd Annual Offshore Technology Conference, Houston Texas, May 6-9 1991

Hong, H.P. and Nessim, M.A. (1994) *Final Report - The Characterization and Analysis of Load and Load Effect Uncertainties for Fixed Offshore Structures and Their Code Implementation - Phase II*, C-FER report submitted to National Energy Board, SSC File # XSC93-00003-(400)

Hopkins, Thomas D. (1992) *Oil Spill Reduction and Costs of Ship Design Regulations* Contemporary Policy Issues, Vol. X, July, 1992.

Hotzel and Miller (1985) *Ice Management on the Grand Banks*, Proceedings of Oceans, San Diego, California.

HSE (1997a) United Kingdom Health and Safety Executive Press Release
Internet site: http://www.open.gov.uk/hse/e18396.htm

HSE (1997b) United Kingdom Health and Safety Executive Press Release
Internet site: http://www.open.gov.uk/hse/e36.htm

Hunt, E.C., Butman, B.S. (1995) *Marine Engineering Economics and Cost Analysis*, Cornell Maritime Press.

Inderberg, O. and Lunde, E.H. (1994) *Experiences With Respect to Cost-Effective Marginal Field Developments*, 26th Annual Offshore Technology Conference, Houston, Texas

Isaacson, M. (1988) *Influence of Wave Drift Forces on Ice Mass Motions*, OMAE 1988, Vol. II, pp. 125-130.

Isaacson, M., McTaggart, K. (1989) *An Iceberg Collision Reliability Model Incorporating Hydrodynamic Effects*, Proc. of the Eighths Int. Conf. on Offshore Mech. and Arctic Eng., Vol. 4, pp. 293-308.

Jewell, S., Marshall, D.,L., Collins, P. (1992), *The Ivanhoe/ Rob Roy Fields: Operation Innovation on a Major Subsea Development*, JPT - March 1992, page 262

Johnson, M.J. Ryan, (1991) *A radar performance prediction model for iceberg detection*, 11th International Conference on Port and Ocean Engineering under Arctic Conditions, St. John's, Nfld 1991.

Jordaan, I.J. (1997) *Personal communication.*

Jordaan, I.J., Xiao, J. and Zou, B. (1993) *Fracture and Damage of Ice: Towards Practical Implementation*, 1993, Ice Mechanics, AMES, Vol. 163, pp. 251-259.

Jordaan, I.J. (1987) *Probabilistic Analysis of Environmental Data for Design of Fixed and Mobile Arctic Offshore Structures*, Reliability and Risk Analysis in Civil Engineering, Proceedings of ICASP5, the Fifth International Conference on Applications of Statistics and Probability in Soil and Structural Engineering, Vancouver, B.C., May 25-29, Vol. 2, 1987, pp. 1130-1137.

Jordaan, I.J., and Maes, M.A. (1984) *Probability, exchangeability and extremes: With discussion if iceberg loading*. Dept. of Civil Engineering, University of Calgary, Calgary, Alberta, Paper presented at the Second Canadian Seminar on Systems Theory for the Civil Engineer, Calgary, 16-17 May 1984.

Jordaan, I.J. (1983) *Risk Analysis with Application to Fixed Structures in Ice*, Seminar-Workshop on Sea Ice Management, Memorial University of Newfoundland, St. John's, Newfoundland, November 1983.

Jordaan, I.J. and Maes, M.A. (1991) *Rationale for Load Specifications and Load Factors in the New CSA Code for Fixed Offshore Structures*, Canadian Journal of Civil Engineering, Vol. 18, No. 3, pp. 454-464.

Jordaan, I.J., Crocker, G., Fuglem, M., Xiao, J. (1992) *Hibernia Shuttle Tanker - Glacial Ice Interaction On the Grand Banks*, Report Submitted to Hibernia Management and Development Company, Ltd.

Jordaan, I.J., Fuglem, M., and Matskevitch, D. (1996) *Pressure-area Relationships and the Calculation of Global Ice Forces*, IAHR - 13th International Symposium on Ice, Beijing, China, August 27-30, 1996.

Kalos M., and Whitlock P. (1986) *Monte Carol Methods - Vol 1 -Basics*, John Wiley and Sons

Knott, David (1994) *Floating production systems hit stride in North Sea fields*, Oil and Gas Journal, May 23, 1994, pp 23-28.

Lamb, H. (1932) *Hydrodynamics*, 6th Edition , Cambridge/Dover.

Leaf, R.C., Pittard, F.J. (1994) *Offshore Horizontal Technology Increases Field Life and Monetary Savings*, 26'th Annual Offshore Technology Conference, Houston, Texas, 2-5 May, 1994

Leblond, P.H., Calisal, S.M. and Isaacson, M (1982) *Wave Spectra in Canadian Waters*, Canadian Contractor Report of Hydrography and Ocean Sciences, No. 6, Dept. of Fisheries and Oceans, Ottawa.

Le Tirant, P., Meunier, J. (1990) *Anchoring of Floating Structures*, Design Guides for Offshore Structures, Editions Technip, Paris (OEIC - B02307)

Lever, G. (1991) *Floating Production System Design Considerations for East Coast Canada,* World Petroleum Congress (13th: 1991: Buenos Aires, Argentina)

Lever, G. (1995) *Personal communication to Canadian Offshore Design for Ice Environments project team.*

Lever, G. (1994) *Subsea Options for East Coast Canada*, Introduction to Subsea Development Presentation at NOIA.

Lever, J.H., Attwood, D. and Sen, D. (1988a) *Factors affecting the prediction of wave induced iceberg motion*. Cold Regions Science and technology, 15, pp. 177-190.

Lever, J.H., Sen, D. and Attwood, D. (1988b) *The influence of shape on iceberg wave induced velocity statistics*. 7th International Conference on Offshore Mechanics and Arctic Engineering, Houston, TX, Vol. IV, pp. 125-132.

Lever, J.H., Colbourne, B and Mak, L. (1989) *A model study of the wave-driven impact of bergy bits with a semi-submersible platform*. Eighth International Conference on Offshore Mechanics and Arctic Engineering. Vol IV. pp. 393-403.

Lewis, E.V. (1989) *Principles of Naval Architecture*, Vol. 3, SNAME

Lindberg, K., Anderson, L. (1987) *Ice Impacts on Semi-Submersibles*, Sixth Int. Offshore Mech. and Arctic Eng. Sym., Vol. 4, pp. 313-320.

Lindley, D.V. (1982). *Scoring Rules and the Inevitability of Probability*. International Statistical Review. 50. pp. 1-26.

MacLaren Plansearch Ltd. (1991) *Wind and Wave Climate Atlas Vol 1 - The East Coast of Canada*, Prepared for the Transportation Development Centre.

Maclean's (1984). *A Preventable Tragedy*. August 27, 1984, p 45.

Madsen, H.O., Krenk, S., Lind, N.C. (1986) *Methods of Structural Safety*, Prentice Hall (TA656.M33)

Maes, M. and Jordaan, I. (1984) *Probabilistic Analysis of Iceberg Loads on Ice Structures*, Proceedings of the IAHR Ice Symposium, Hamburg

Maes, Alfons (1985) *Extremal Analysis of Environmental Loads on Engineering Structures*, Doctoral Thesis, University of Calgary

Mak, L.M., Lever, J.H., Hinchey, M.J., and Duthinh, D. (1990) *Wave-induced Bergy Bit Motion Near a Floating Oil Production Platform*, The Ninth International Conference on Offshore Mechanics and Arctic Engineering, Volume IV, pp. 205-215.

Markham, W.E. (1980) *Sea Atlas - Eastern Canadian Seaboard*, Environment Canada, Toronto.

Marko, J. (1993) *Personal Communication*

Matskevitch, D.G. (1996) *Eccentric Impact of an Ice Feature: Linearized Model.* Cold Regions Science and Technology, Volume 25, Issue 3, April 1997, page 159-171

Matskevitch, D.G. (1997) *Eccentric Impact of an Ice Feature: Non-linear Model.* Cold Regions Science and Technology, (in press, paper #270).

Matskevitch D.G. (1997) *Analytical Model of Iceberg Impact Accounting for 3D Effects.* Cold Regions Science and Technology, (submitted, paper # 274)

McGuire, L.V., Kearns, J. (1988) *The Operational Aspects and Reliability of Floating Production Systems*, 1988 Offshore Technology Conference

McKenna R., Marshall A., Jordaan I. (1988) *The Application of AES Environmental Data to Ice Interaction Modelling*, report Submitted to Canadian Climate Centre, Atmospheric Environment Service, Environment Canada.

McTaggart, Kevin Andrew (1989) *Hydrodynamics and Risk Analysis of Iceberg Impacts With Offshore Structures*, Ph.D. Thesis in Civil Eng., The University of British Columbia

Melchers, R.E. (1987) *Structural Reliability - Analysis and Prediction*, Ellis Horwood Ltd.

Miller, Ross M. (1990) *Computer-Aided Financial Analysis*, Addison-Wesley Publishing Company.

Mobil Oil Canada, Ltd. (1985) *Hibernia Development Project - Environmental Impact Statement - Volume IIIa Biophysical Assessment*

National Research Council (1991) *Tanker Spills*, National Academy Press, Washington, D.C.

Nessim, Maher A. 1983, *Decision-Making and Analysis of Errors in Structural Reliability*, Doctoral Thesis, Department of Civil Engineering, University of Calgary.

Nevel, D. (1986) *Iceberg Impact Forces*, IAHR Symposium, Iowa City, Iowa.

Ocean Engineering Research Centre, Memorial University of Newfoundland. (1995). *Canadian Offshore Design for Ice Environments, First Annual Report, Volume 1* , Report prepared for Department of Industry, Trade and Technology, Government of Newfoundland and Labrador.

Ocean Engineering Research Centre, Memorial University of Newfoundland, (1995) *Canadian Offshore Design for Ice Environments, First Annual Report, Volume 2*, Report prepared for Department of Industry, Trade and Technology, Government of Newfoundland and Labrador.

Ochi, M.K., Hubble, E.N. (1976). *Six-Parameter Wave Spectra*, Proceedings of the Fifteenth Coastal Engineering Conference, July 1976, pp. 301-328.

Melchers R. (1987) *Structural Reliability - Analysis and Prediction*, Halsted Press

NRC Committee on Tank Vessel Design (1991) *Tanker Spills - Prevention by Design*, US - National Research Council, Published by National Academy Press.

Petro-Canada (1996) *Development Application for the Terra Nova Development*, Prepared by Petro-Canada on behalf of the Terra Nova Partners.

Petrie, B. (1982) *Aspects of the Circulation on the Newfoundland Continental Shelf*, Bedford Institute of Oceanography, Dartmouth Nova Scotia, Canadian Technical Report of Hydrography and Ocean Sciences, #11, p.78

Pond, S. and Pickard, G. (1983) *Introductory Dynamical Oceanography*, 2nd ed., Pergamon Press., Great Britain.

Pritsker, A. and Pegden, C. (1979) *Introduction to Simulation and SLAM*, Systems Publishing Corporation

Press W., Teukolsky S., Vetterling W., Flanner B. (1992) *Numerical Recipes in C - The Art of Scientific Computing*, Second Edition, Cambridge University Press

Raiffa, H., Schlaiffer, R. (1961) *Applied Statistical Decision Theory*, M.I.T. Press

Reddy, D.V., Arockiasamy, M., Cheema, P.S., and Riggs, N.P. (1980) *Monte Carlo simulation of iceberg import probabilities*. Cold Regions Science and Technology, 1: 293-297.

Reddy, D.V., and Cheema, P.S. (1981) *Simulation of iceberg shapes and their impact probability*. Proceedings of the 6th international conference on Port and Ocean Engineering under Arctic Conditions (POAC), Quebec, Que., July 1987, pp. 1381-1392.

Reliability Consulting Programs (RCP) (1995) *Strurel - A Structural Reliability Analysis Program System - Theoretical Manual.*

Robert, Nicole and White, Leslie (1995) *Oil Spill Liability.* Internet document prepared in conjunction with course BA436: Insurance Planning and Alternatives for Business, Dr. Norma Nielson, College of Business, Oregon State University
Internet site: http://www.bus.orst.edu/faculty/nielson/industry/oil/OIL.HTM

Rossiter, J., Arsenault, L., Guy, E., Lapp, D., Welder, E., Mercer, B., Dempsey, J., and McLaren, E. (1985) *Assessment of Airborne Imaging Radars for the Detection of Icebergs*. ESRF, Report No. 16, 321 p.

Rubinstein R. (1981) *Simulation and the Monte Carlo Method*, John Wiley and Sons

Ryan, Joseph P. (1985) *Enhancement of the Radar Detectability of Icebergs* Environmental Studies Revolving Funds Report No. 022, Ottawa, 93 pp.

Ryan, J.M., Johnson, M. J. (1992) *Radar Performance Prediction for Target Detection at Sea*, Accepted to RADAR '92, Brighton, England, October 1992.

Sanderson, T.J.O. (1988) *Ice Mechanics - Risks to Offshore Structures*, Graham and Trotman Ltd. London U.K., 253p.

Sasanow, S. (1994) *Under-Estimating Platform Add-Ons to Take New Subsea Production*, Offshore, March 1994.

Schlager, Neil (Edittor) (1994) *When Technology Fails*, Section on Ocean Ranger oil-drilling rig sinking, pg 326-331.,

Seaconsult (1988) *Terra Nova Development Studies - 1988 - Physical Environmental Data for Production Systems at Terra Nova.* Proprietary study prepared for Petro-Canada Inc.

Sen, D.C. (1988) *Process Design for Offshore Oil and Gas Production in Cold Ocean Environment*, The Canadian Journal of Chemical Engineering, Volume 66, Oct. 1988

Smith, J.Q. (1988) *Decision Analysis - A Bayesian Approach*, Chapman and Hall.

Smith, S. and Donaldson, N. (1987) *Dynamic Modelling of Iceberg Drift Using Current Profiles*, Canadian Technical Report of Hydrography and Ocean Sciences, No. 91

Terra Nova Development Studies (1988) *Physical Environmental Data for Production System at Terra Nova*

Traub J. and Wozniakowski H. (1994) *Breaking Intractability*, Scientific America, January, 1994

UKOOA (1997). *Offshore Safety ... setting the record straight.* a internet document provided by the United Kingdom Offshore Operators Association, London, England. Internet site: http://www.ukooa.co.uk.safety/offshore.html

Woodworth, Bonnie (1984). *Settling the rig disaster*. Maclean's, January 9, 1984. pg 25.

Wishahy, M.A., (1988) *Time-Domain Numerical Simulation of the Motion of Small Floating Bodies Drifting in Waves*, A Ph.D. Thesis, Memorial University of Newfoundland, pp. 134.

APPENDIX A

SUMMARY OF RESULTS FROM THE STUDY

"MAXIMUM BOW FORCE"

A.1 Introduction

In this appendix, relevant information from the study "Maximum Bow Force Study for Arctic Shipping Pollution Prevention Regulations" (Carter et al., 1995) is presented. The information deals with the calibration of random coefficients for a pressure-area relationship for global ice-crushing failure. The relationship required for use in conjunction with an analytic ice ramming model to estimate maximum bow forces for vessels of different ice class and size. The calibration was based on global forces recorded during ramming trials by icebreakers. By using an ice failure model with random coefficients, it was possible to reasonably model the distributions of maximum loads observed in actual ramming trails.

The results are relevant to the problem of impacts with icebergs because the recorded ramming loads consist of the only available field data where the impact velocities and contact areas are close to those that would occur in a significant iceberg impact. In the F_{MAX} study, only rams with multiyear ridges were considered; this is important because multiyear ice is relatively free of brine and is therefore more like glacial ice. Furthermore, only rams where the ice failure mode was predominately crushing, as opposed to flexural failure, were considered.

In the remainder of Section A.1, a short background to the Maximum Bow Force study is given and the requirement for a random ice failure model is identified. In Section A.2, the development of a deterministic ramming model to simulate rams with specified vessel, floe, and ice strength parameters is presented. In particular, the requirement for special modifications to existing models to match observed ram load time traces is highlighted. Without these modifications, the following calibration process would have been

very difficult. In Section A.3, the procedure for calibrating the random ice failure model using observed data from ramming trials is presented. Parameters for specific vessels mentioned are listed in Table A.1.

The Arctic Shipping Pollution Prevention Regulations (ASPPR) were enacted in 1972 to ensure that vessels in the Arctic Ocean are designed and operated in a manner so as to minimize risks to the environment. As a result of additional experience gained in the design and operation of vessels for the region, a number of areas where the regulations could be improved became apparent and work on a revised set of regulations resulted in a set of proposals in 1989. These were the Proposed Revisions to the Arctic Shipping Pollution Prevention Regulations (*ASPPR Proposals*). The proposed revisions were reviewed and verified by Carter et al. (1992). In that study, the calculation of the maximum bow force experienced in rams with multiyear ice, referred to as "F_{max}", was raised. It was considered that further work should be carried out to refine the calculation method.

In the first phase of the Maximum Bow Force study, the general rationale and methods for determining F_{max} were decided upon by consensus of the study group. A decision was made to use a probabilistic approach which accounts for the number of collisions and the variations in the sizes and thickness of the ice features impacted, the initial impact velocities, and the strength of the ice. As well, attention would also be given to the different possible failure modes of the ice which occur depending on the thickness of the ice and the displacement, shape, and velocity of the vessel. The goal of Phase II of the study was to determine values of F_{max} such that any vessel designed for a given operational mandate and in accordance with the appropriate corresponding class would have a sufficiently low risk

of hull girder failure. The connection between F_{max} and the design of scantlings was also examined.

In all large scale ice-structure interactions which occur at rates high enough that there is crushing of ice, it is found that there is a scale effect such that the average pressure decreases with contact area. In addition, it is found that the ice failure forces vary significant through an interaction and vary significantly between interactions involving the same geometries and very similar ice. Typical load-time traces are shown in Figure A.3 based on Masterson et al. (1992). These traces were observed in medium scale ice tests in which a hydraulic ram was pushed into vertical ice faces cut into a tunnel in an iceberg. The curves shown the first part of the interaction when the ice was prone to spall. Even with similar geometries and reasonably consistent ice, it is seen that the curves vary significantly. In the case of ship rams it is observed that for apparently "identical" rams produce forces that vary considerably. It was also found during the course of the study that the distribution of rams could not be modelled a fixed pressure-area relationship for ice failure. It is to be expected that one would find event more variations in ramming events than in the Pond Inlet tests. These would include larger flaw structures as well as larger temperature variations.

The reason for the variation can be found in the nature of ice failure as pointed out by Jordaan in the F_{MAX} study.

> *The actual contact is characterized by a number of high pressure zones. Figure A.4 illustrates the formation of one of these zones, while Figure A.5 shows the plane of contact with a number of such zones. At various times during the interaction, pieces of ice will spall off, as illustrated in Figure A.4.*

Spalling is related to random flaws in the ice and will lead to a drop in load. The behaviour of an individual high pressure zone would contain some fluctuations in load, often with a relatively constant average load. The behaviour is related to complex crushing and extrusion processes in the ice, and the approximate constancy of the load is not to be interpreted as classical plastic behaviour, although the effect is the much the same, i.e. dissipation at constant load.

The basic idea of using a pressure-area curve is to follow the development of nominal contact area with time. The nominal contact area is the projection of the structural shape onto the original shape of the ice feature, as the penetration increases. The nominal area is used as it is very difficult to measure the actual contact area left after spalling events. The pressure used in the relationship is the average pressure over the nominal area as opposed to the actual contact area.

To capture the decrease in average pressure with nominal contact areas, a pressure-area curve of the form $p = ca^d$ was implement, where a is the nominal area and c and d are constants. By varying c and d, a variety of shapes can be obtained. For example, the values can be changed to approximately fit such pressure-area relations as shown in Figure A.1. To model the random variations in the ice failure process in addition to the area effect, it is appropriate to introduce randomness into the pressure-area relationship. This was been done by treating c and d as random (denoted thus as C and D), and by calibrating against measured data obtained in ramming trials.

A.2 Ice vessel interaction model

In this section, some of the more relevant aspects of the development of a deterministic ramming model for the study are reviewed. The basic interaction between an icebreaker and a large multiyear flow is illustrated in Figure A.4. To break up a large ice floe, the captain of an icebreaker may run the icebreaker at the floe. In a direct ram, the major displacements of the vessel and floe will be in the three degrees of freedom surge , heave, and pitch. In addition, flexure of the vessel and ice may play a roll in the impact dynamics. For thinner ice sheets, flexural failure of the ice may be important. For the calibration of the ice crushing failure model, only impacts with thick features where flexural failure was unlikely to occur were considered.

As the icebreaker impacts the floe, the front face of the icebreaker initially has a high normal velocity to the ice and the ice fails in crushing. This portion of the ram is known as the initial crushing phase. The reactive force on the bow of the icebreaker slows the vessel down and accelerates the bow upward. At some point, the velocity of the vessel at the bow will be approximately tangential to the bow plating. At this point the force on the ice is generated mainly by the weight of the vessel. This portion of the ram is known as the beaching phase. The maximum load during the beaching phase is determined in part by the distance the vessel rides up the ice.

The transition from initial crushing to beaching is generally not smooth because of the random failure processes in the ice and because the vessel may have enough pitch and heave momentum to lose contact with the ice. The transition also varies in nature considerably depending on the size of the vessel. This is illustrated in the recorded time

traces of vertical bow force for the Canmar Kigoriak and M.V. Arctic shown in Figures A.6 and A.7 respectively. With the smaller vessel (Kigoriak), there is a large initial crushing load. Because of the vessel is relatively short and has a small radius of gyration, the vessel tends to loose contact with the ice during hard rams. It is of note that on hard rams, the initial crushing load can be larger than the final beaching load. For the larger vessel (M.V.Arctic), there are fewer losses of contact and the beaching load is generally larger than the initial crushing load. This transition from dominance of initial crushing load to dominance of beaching load with vessel size is important in understanding the random nature of the ice failure and its effect on the maximum bow force.

In trying to model the rams numerically, it was found that when a pressure-area curve was used during the beaching phase, rapid fluctuations in force could occur as the vessel lost and regained contact. This problem could not be solved using an elastic layer; it was necessary to use a mechanism that absorbed impact energy during beaching. This aspect is discussed further.

The main objective in developing a deterministic, time-domain, impact model was to be able to generate time traces of loads that had the same characteristics as observed in real ramming events and to be able to match observed distributions of maximum impact loads by using a random ice failure model. The deterministic ramming model was based on a previous work by Daley and Riska (1990). In the course of the study, several additional modelling requirements for the study were identified and implemented.

In the initial model by Daley and Riska(1990), the motion of the icebreaker is modelled using three degrees of freedom, surge, heave, and pitch. The geometry of the

vessel bow and ice floe are simplified such that the contact interaction is as shown in Figure A.5. The interaction is modelled in the time domain approach using a Runge-Kutta numerical integration algorithm. At each time step, the new displacement and resulting ice force is determined. From this, the accelerations and displacements of the vessel are determined. The model is run until the forward motion of the vessel reached zero.

In the model, the vessel heave and pitch stiffness are converted to an equivalent vertical spring stiffness at the bow. The vessel mass and added mass are converted to equivalent vertical and horizontal masses at the bow. Both mass and stiffness are functions of several vessel parameters such as length, beam, draft, form coefficients and bow geometry. The ice is modelled as a rigid sheet of constant thickness. The ice force is modelled using a pressure-area relationship.

A number of modifications to the initial model were made as follows. Many icebreakers have an ice skeg (also known as an ice knife) on the lower bow which stops the vessel from riding too far up on the ice and losing roll stability. To accurately model the observed time traces and maximum loads it was necessary to model these skegs or the beaching loads became too large. The effect of the skeg was incorporated by making corrections to the forward projected area of the vessel. Additional areas are provided for each vessel in the form of a digitized curve giving the additional forward projected area. The additional horizontal force due to the ice skeg is determined from the pressure-area curve based on the area of the ice skeg only, i.e. it is assumed that the ice skeg will impact relatively intact ice below the vessel and will not be significantly affected by the overall confinement.

The volume of ice removed and the contact areas can be limited by the thickness of the ice, the draft of the vessel, or the width of the vessel. A check implemented for these conditions as the vessel rode up the ice and, if necessary, the equations for contact area were modified.

To be able to accurately model the sudden variations in load as the vessel lost and regained contact, it was found necessary to use an adaptive time stepping method. For this, the Runge-Kutta procedure "RKQS" specified in Press et al. (1992) was used. The time step is adjusted so that the total error is approximately within bounds specified by the user. The error associated with any given step is estimated from the difference between the output calculated using a single time step and the output calculated using two time steps of half the duration. The time step is reduced until the desired accuracy is achieved. The successful time increment is then used as the starting point for the subsequent step. If the initial time increment for any step results in an estimated accuracy significantly greater than the desired accuracy, the initial time increment to be used for the subsequent step is increased accordingly.

The first mode of flexural response of the vessel was added to determine its effect on the impact. For this, the routine "STIFF" (Press et al., 1992) was required instead of "RKQS". This procedure is appropriate when there are two or more first order differential equations involved with significantly different time scales (in this case the natural periods in pitch/heave and flexure are significantly different). An implicit differencing algorithm is used so that the solution does not become unstable if relatively long time steps are used for parameters which do not significantly affect the results. When running this program for large

numbers of simulations, it was found that very infrequently numerical instabilities would occur in the matrix inversion routine causing the simulation program to abort.

The most important change in the model relates to the problem of the appropriate ice failure model to use for loss of contact and beaching. In the original model, an linear elastic spring was used during the impact; for the cases previously considered, this spring resulted in a smoother curve and removed some numerical problems. When applied for the smaller vessels, it was found that the spring resulted in oscillating beaching forces with very high maximum loads. A significant problem was that with the spring, energy was not being dissipated.

On removal of the spring, it was found that the vessel repeatedly lost and regained contact. In addition, the loads increased with the increased nominal contact area as the vessel beached. Because the rate of penetration at the bow during beaching is close to zero and contact is at times lost and regained, a strict application of the pressure-area is not appropriate. When the vessel is crushing at a high penetration rate, it is damaging the ice through spalling and other mechanisms such as micro-fracturing. On removal of contact or change to much lower penetration rates, there effectively remains a softened layer of ice.

The following method was used to rectify the model. On recontact, the force is increased linearly from 90% of the beaching load (if it is less than the pressure-area load) up to the pressure-area load through a layer of damaged ice 0.2 m in thickness. Often contact would be lost again during this process, but the small "softening" effect was enough to remove the worst anomalies caused by instantaneous development up to the pressure-area curve.

The model was set up to run and plot the outputs of simulated rams for verification and sensitivity analyses. Figures A.8 through A.13 show simulated time traces of forces for the Canmar Kigoriak, M.V. Arctic, and NLD vessel for impact velocities of 2.5, 5.0, and 7.5 m/s and pressure-area relationships of $p=3a^{-0.4}$ [MPa] and $p=6a^{-0.4}$ [MPa]. It should be noted that, though loss of contact is predicted, the associated change in trajectory of the vessel is very small. As a result of the model for the damaged layer on recontact, the vessel rides up the ice face without the interaction pressure necessarily reaching the pressure-area curve before contact is lost once more.

For the Canmar Kigoriak rams, the model predicts a distinct initial impact as actually observed. This is especially notable for the higher ice strength case, where the initial impact force is greater than the maximum beaching force. For both the M.V. Arctic and the NLD vessel, there is a distinct initial impact phase for higher impact velocities and ice strengths. The addition of a damaged layer has a significant effect in lowering the beaching force, as expected. As the damage layer thickness is increased, the frequency of loss of contact is reduced and the final beaching load is reduced slightly.

A.3 Probabilistic calibration of pressure-area relationship

The selection of an appropriate set of random ice strength parameters was carried out by means of a calibration process in which actual trials were simulated. Rather than the deterministic formulation $p = ca^d$, c and d are treated as being random and denoted with capital letters. Consequently P is also random and is denoted by a capital letter:

$$P = Ca^{D} \ . \qquad (10.1)$$

The parameters C and D are modelled using lognormal and normal distributions, respectively. The purpose of the calibration is to select an appropriate mean and standard deviation for C and D so that the ramming model can simulate accurately the distribution of bow forces from the observed data.

The main calibration used data from three vessels, namely the Canmar Kigoriak, M.V. Arctic and Manhattan. For these three vessels, ramming data was taken from four voyages: the Spring and October 1983 Canmar Kigoriak trials, the 1984 M.V. Arctic trials and the 1969 Manhattan Northwest Passage voyage. Typically, the ramming data consisted of a record of impact velocity and bow force. Other data, such as impact duration, vessel surge and vessel rise, were included in certain data sets. A complete listing of items observed in each data set is given in Table A.2. During the 1969 Manhattan voyage, a surge value of 27.4 m was observed for the ram corresponding to the highest velocity. The results of the simulations were 32.7 m, 38.9 m and 38.9 m for cases 1, 4 and 10, respectively. The rams for the 1981 Canmar Kigoriak trials (Dome, 1981; VTT, 1981; and Offshore Research, 1981) were also used in the calibration but not included because it was found to be difficult to reconcile the different versions of the data records. The results were judged to be generally similar to the ones that have been included in this report.

Canadian Marine Drilling Ltd. (CANMAR) conducted tests in 1983 using the Canmar Kigoriak and her sister ship, the Robert Lemeur. The objectives of these tests were as follows (CANMAR, 1985):

- evaluating the global ice forces as a function of time,
- determining the effect of dynamic magnification due to natural frequencies of vessel,
- determining the effect of unsymmetric rams,
- measuring the hull rigid body and vibrational accelerations, and
- determining the global failure criteria of ice.

On June 14, the Canmar Kigoriak conducted 18 rams on first year ridges in landfast ice. On July 3-5, the Canmar Kigoriak conducted 182 rams on grounded first year ridges in open water. Between October 5-13, the Canmar Kigoriak performed 202 rams on multiyear features. Ramming velocities ranged from 3 to 15 knots. Six rams into multiyear features grounded in 28 m of water were conducted, the rest of the rams were with floes. The masses of the floes rammed ranged between 45 and 700 kilotonnes.

Full-scale trials using the M.V. Arctic were carried out in 1984, sponsored by Transport Canada. The stated objective in conducting the tests was to obtain the total bow force acting on the vessel as a function of indentation into a large multiyear ice feature (German and Milne Ltd. and VTT, 1985). When the tests were conducted, previous warm weather made it difficult to find thick floes that would fail in crushing and could withstand large numbers of repeated collisions at different velocities. In all, 142 rams involving nine floes were eventually conducted. In conducting the rams, floes were first rammed at a low

velocity, which was subsequently increased for repeat rams. Throughout the trials, the ramming velocities were limited to below 4 knots.

In October 1969, the Manhattan conducted a number of rams into an ice island in Barrow Strait. The displacement of the ice island was estimated at two to three times that of Manhattan. The thickness was given as approximately 45 m. The maximum ramming velocity was about 5 knots (MARAD, 1969).

A simulation model that can accurately predict the above observations would require a set of values for the mean and standard deviation of both C and D to cover a wide range of ice conditions. Table A.3 shows the different cases modelled. The distributions of C and D were sampled using Monte Carlo methods to model the Canmar Kigoriak and M.V. Arctic results, while a run, using the mean values of these distributions, was conducted to allow a comparison with the Manhattan results. This method was used as there are only five results from the Manhattan, all ramming the same ice island.

The results of the calibration are given by two plots for each run: a probability density function of vertical bow force and a log plot of bow force against probability of exceedance. Figures A.1 to A.12 contain both plots for the three best cases. To determine which case produced the best fit to the observed data, a criterion was established such that the highest 20% of the results were compared with measurements, so as to give a least squares assessment of the agreement. The observed and simulated data were sorted by bow force and the highest 20% of the forces were then selected. The goodness of fit, G, was evaluated as

$$G = \frac{\sqrt{\sum_{i=1}^{n} (y_{si} - y_{oi})^2}}{n} \qquad (10.2)$$

where y_{oi} is the ith observed vertical bow force, y_{si} is the ith simulated vertical bow force and n is the number of rams simulated. The results of this evaluation process can be found in Tables A.4 and A.5. The best fit was obtained from case 4 with a pressure-area relationship of

$$C: \mu = 3MPa \qquad \sigma = \pm 1.5MPa$$
$$D: \mu = -0.4 \qquad \sigma = \pm 0.2$$

where μ is the mean and σ is the standard deviation.

The mean values of C and D are quite close to the coefficients $C = 3.33$ and $D = -0.43$ achieved independently from a linear best fit to average pressure-area combined from a larger number of sources. The results are described in Appendix B of Carter et al. (1995), and the analysis included ice failure data from Hans Island, Molikpaq, Canmar Kigoriak, M.V.Arctic, and Pond Inlet. It is important to note that the curve consists of pressures and areas from different ice interaction events rather than the change in area and pressure during interaction events.

A number of comparisons were made for other parameters, such as impact duration, vessel surge and vessel rise. The rise of the vessels was estimated well in most cases whereas the surge was not estimated as well. The impact durations were often overestimated. However, a preset "window" of time was used so that if the durations actually

exceeded this value, only the "window" was recorded. This observation was relayed to the project team based on field experience. The simulation "clock" starts at the smallest load and includes a small period when no force would be perceived. In any event, the vessel slows down towards the end of the ram, with the force reaching a level plateau called the "beaching" force. The results are insensitive to the location of the end point. The recorded surge values were selected rams in which mainly crushing took place. On the other hand, the simulations were carried out for a full range of ice failure mechanisms.

Table A.3 summarizes the selection (cases 4, 10 and 1) that were used subsequently for the Maximum Bow Force final runs. Case number 4 had the highest evaluation and has been used as the base case in chapter 5. Case 10 had the second highest evaluation and therefore was included. This case also contained a higher standard deviation on the parameter C. This would test the effect on extreme loads of a larger standard deviation of ice strength. Case 1 has been included because it has a high standard deviation and also a large mean ice strength. This is expected to provide a more demanding simulation of initial impact force for all vessels. This is of particular importance for smaller vessels.

Table A.1 Vessel Parameters

Symbol	Description	Canmar Kigoriak	M.V. Arctic	Manhattan	NLD
L_{BP}	Length between perpendiculars [m]	79.3	196.6	286	260
B	Breadth [m]	17.25	22.86	44.81	44
T	Draft [m]	8.5	10.93	15.85	16
D	Displacement [kilotonnes]	6.615	38.94	150	140
P	Shaft power [MW]	12.2	10.86	-	20.5
δ_F	Bow mass factor	0.35	0.354	-	0.395
C_B	Block coefficient	0.537	0.74	0.73	0.72
C_{WP}	Waterplane coefficient	0.937	0.856	0.85	0.825
γ	Stem angle [degrees]	24	30	17	22
α	Bow opening angle [degrees]	61	33.5	30	53
α_2	2nd bow opening angle [degrees]	36	-	-	-
X_a	Distance used to define a spoon-shaped bow [m]	1.5	-	-	-

Table A.2 Items Recorded During Ramming Trials

VOYAGE	ITEMS RECORDED IN OBSERVED DATA
Canmar Kigoriak Spring 1983	Impact velocity, maximum bow force, vessel rise time
Canmar Kigoriak October 1983	Impact velocity, maximum bow force, vessel rise time
M.V. Arctic 1984	Impact velocity, maximum bow force, vessel surge, vessel rise
Manhattan 1969	Impact velocity, beaching force, vessel surge, vessel rise, impact duration

Table A.3 Ice Strength Parameters

CASE	*C* [MPa]		*D*	
	μ	σ	μ	σ
1	6	± 3	-0.4	± 0.2
2	0.5	± 0.25	-	-
3	1.5	± 0.75	-	-
4	3	± 1.5	-0.4	± 0.2
5	8	± 4	-0.7	± 0.35
6	2.5	± 2.5	-	-
7	6	± 6	-0.4	± 0.2
8	6	± 3	-0.4	± 0.4
9	4	± 2	-0.4	± 0.2
10	3	± 3	-0.4	± 0.2
11	3	± 1.5	-0.4	± 0.4

Table A.4 Evaluation of the Four Best Sets of Ice Strength Parameters

CASE	*C* [MPa]		*D*		EVALUATION, *G*
	μ	σ	μ	σ	
4	3	± 1.5	-0.4	± 0.2	0.071
10	3	± 3	-0.4	± 0.2	0.075
1	6	±3	-0.4	±0.2	0.113

Table A.5 Evaluation of Ice Strength Parameters for Canmar Kigoriak, M.V. Arctic and Manhattan

CASE	CANMAR KIGORIAK	M.V. ARCTIC	MANHATTAN	OVERALL EVALUATION
4	0.072	0.020	0.171	0.071
10	0.087	0.014	0.171	0.075
1	0.094	0.044	0.292	0.113

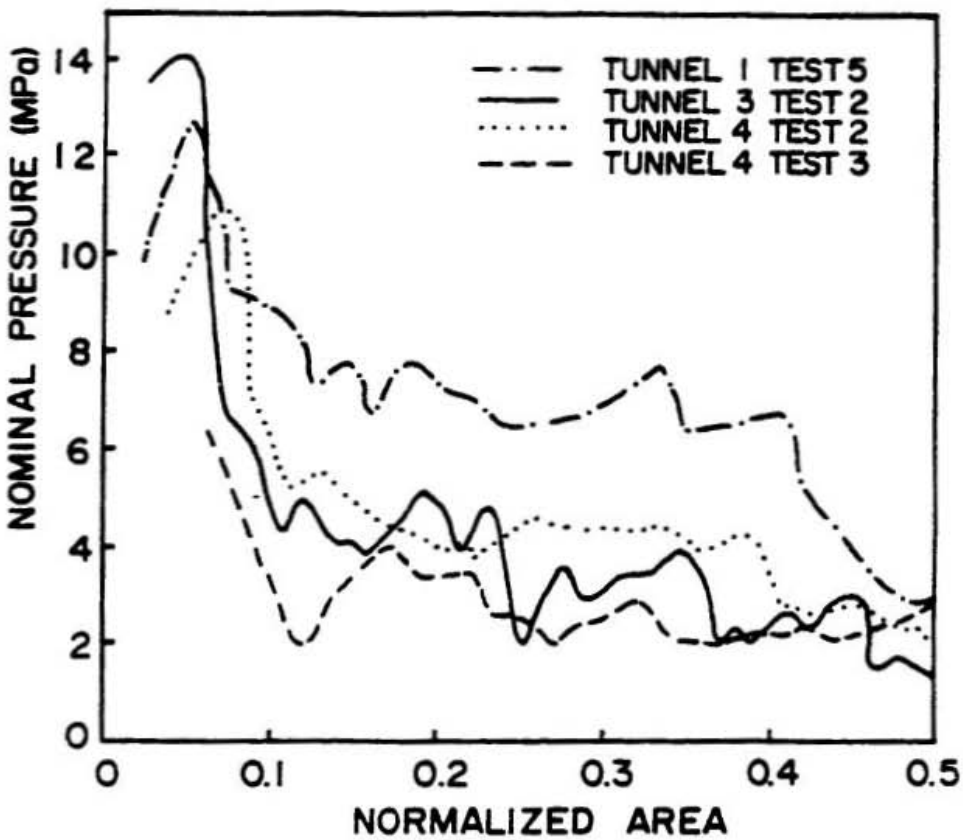

Figure A.1 Measured Pressure-Area Relationships (Master son et al., 1992).

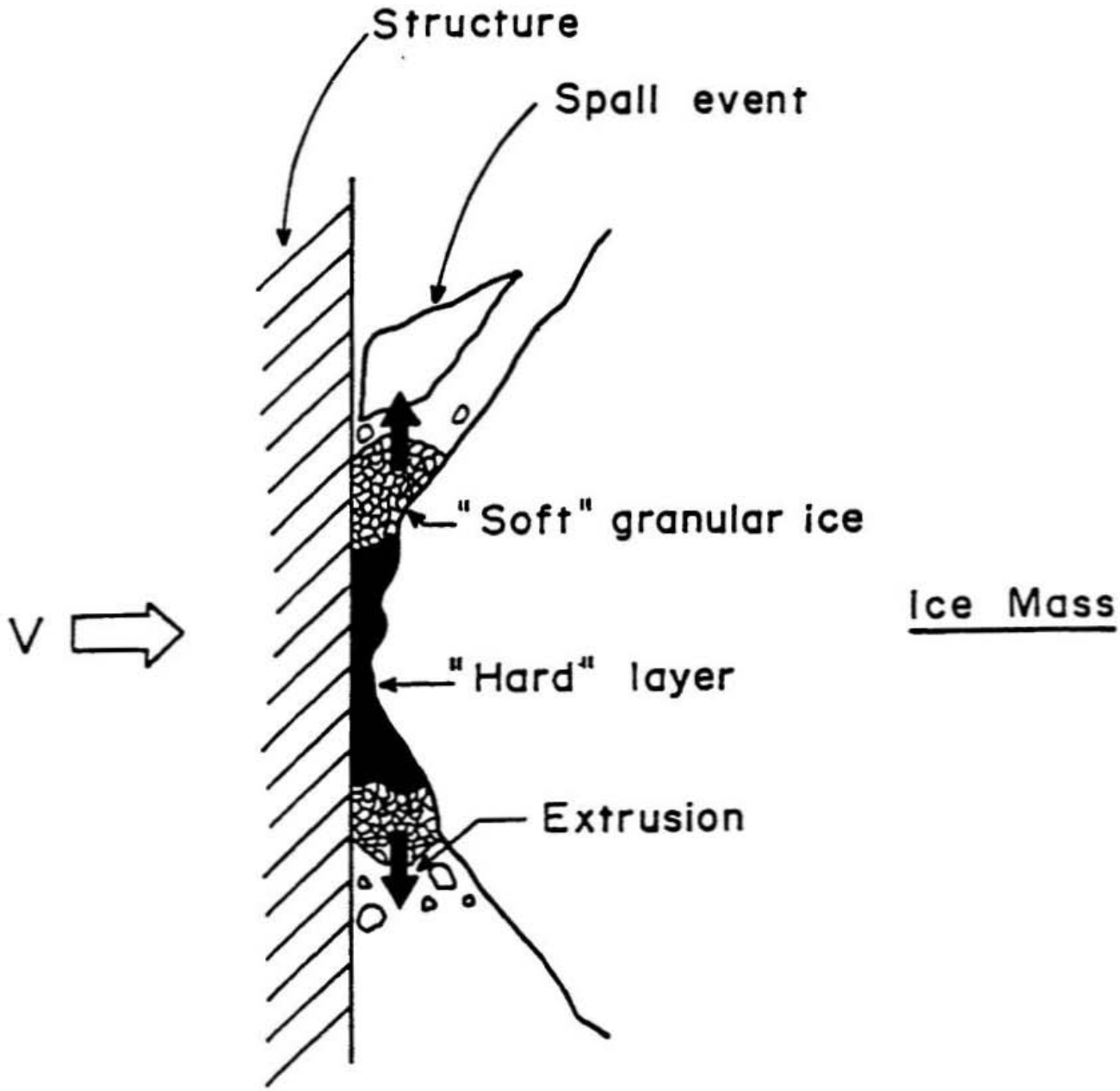

Figure A.2 Schematic of a High Pressure Zone.

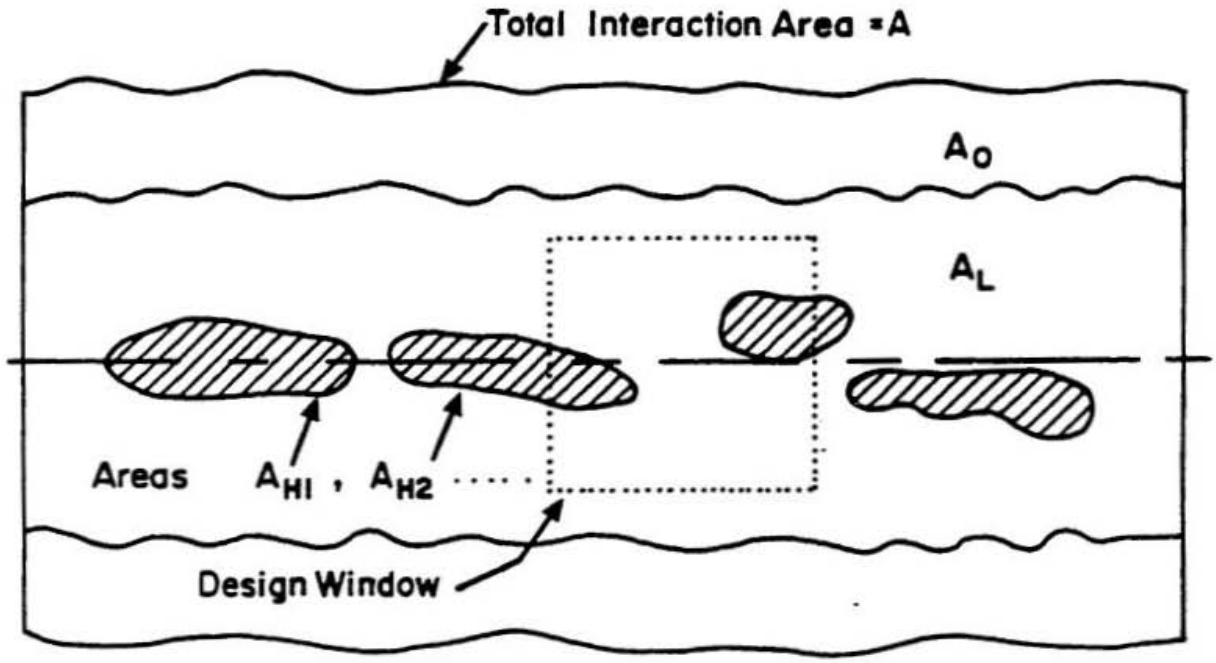

Figure A.3 Critical Zones of High Pressure A_{H1}, A_{H2}, ... and Design Window (Jordaan et al., 1993).

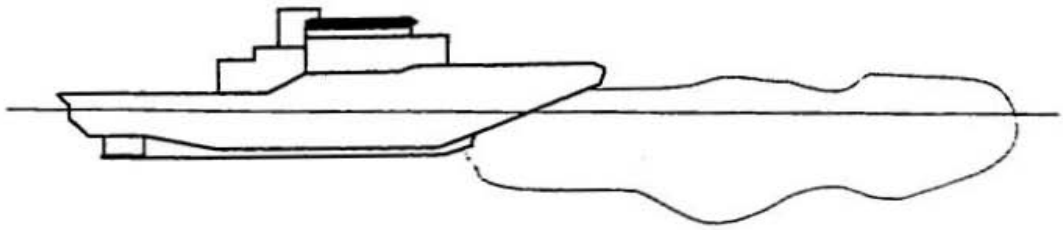

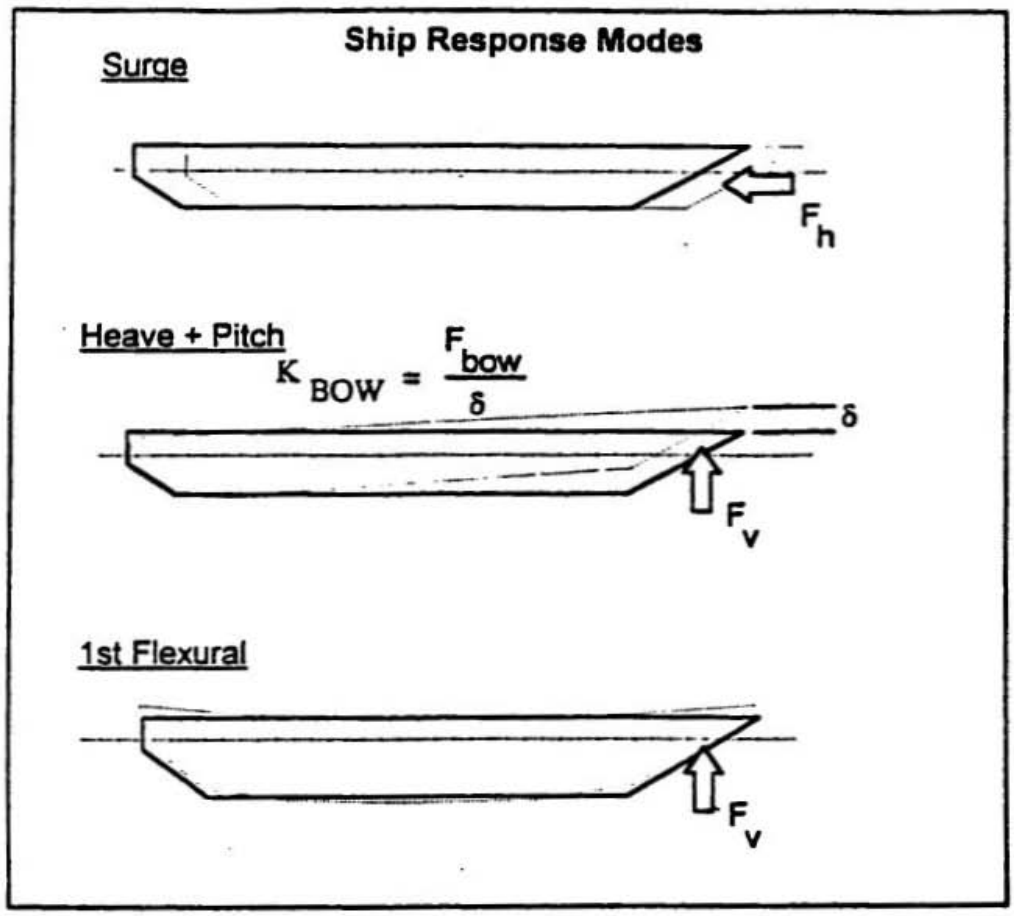

Figure A.4 **Description of the Ice-Vessel Interaction Model (Daley and Riska (1990).**

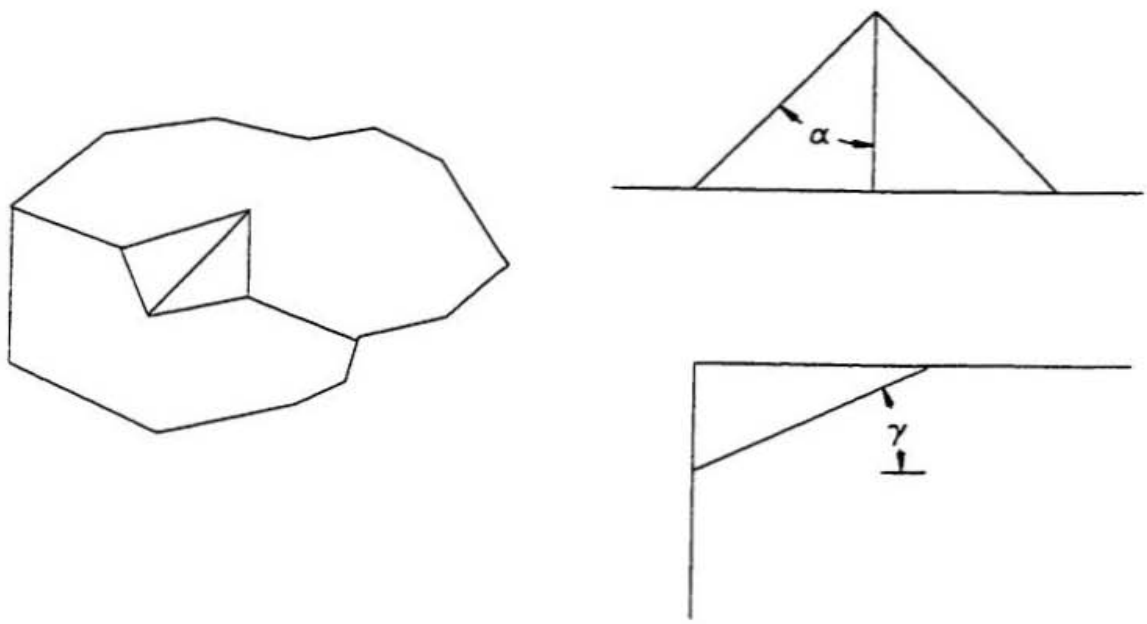

Figure A.5 Definition of Penetration Geometry for a Wedge-Shaped Bow.

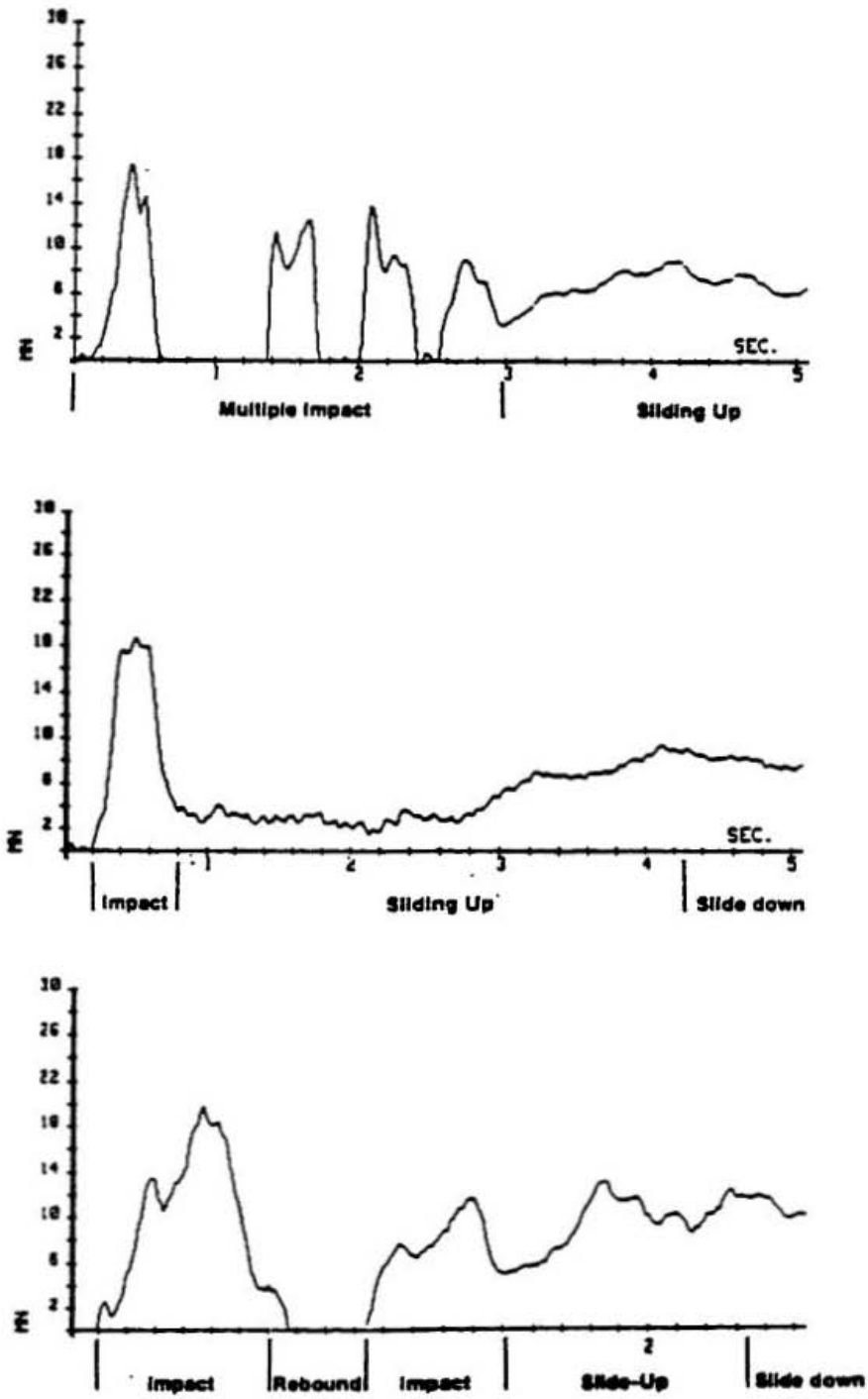

Figure A.6 **Example Time Traces of Vertical Bow Force from the Canmar Kigoriak October 1981 Trials.**

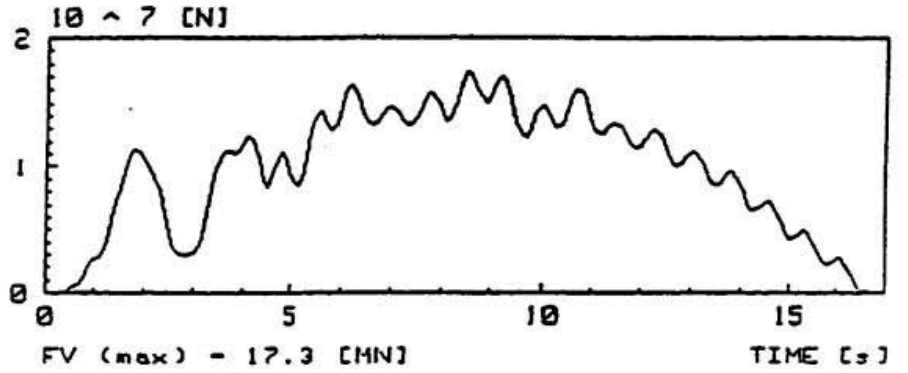

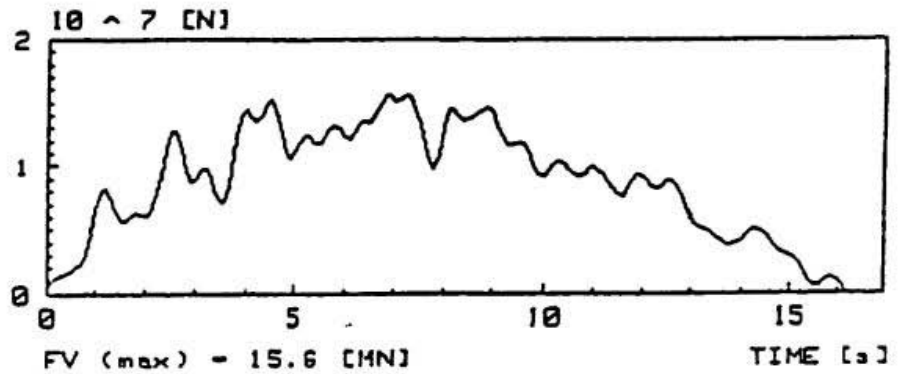

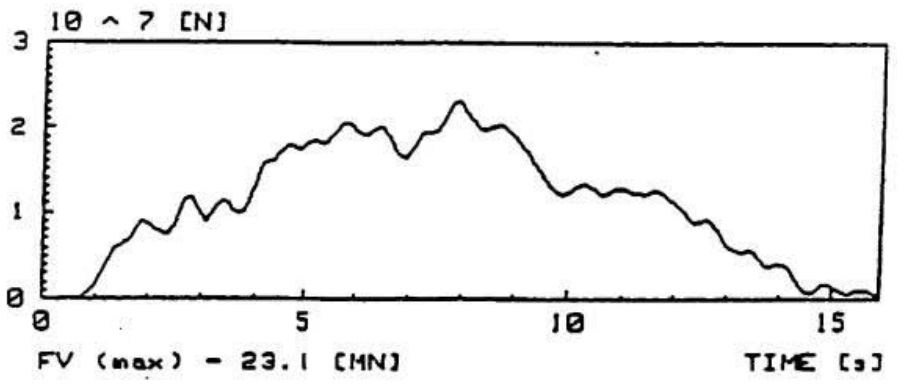

Figure A.7 **Example Time Traces of Vertical Bow Force from the M.V. Arctic 1984 Trials.**

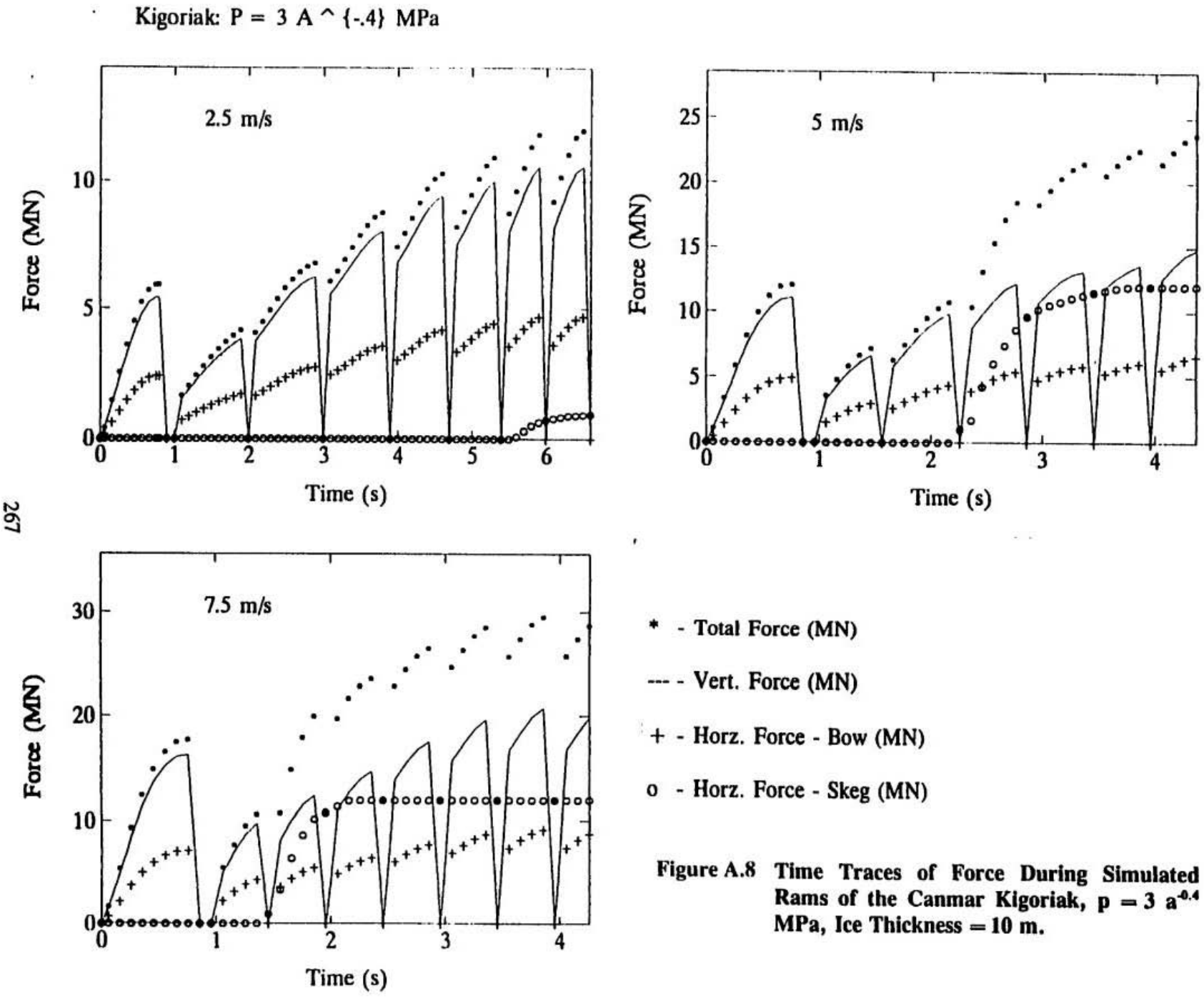

Figure A.8 **Time Traces of Force During Simulated Rams of the Canmar Kigoriak, $p = 3\ a^{-0.4}$ MPa, Ice Thickness = 10 m.**

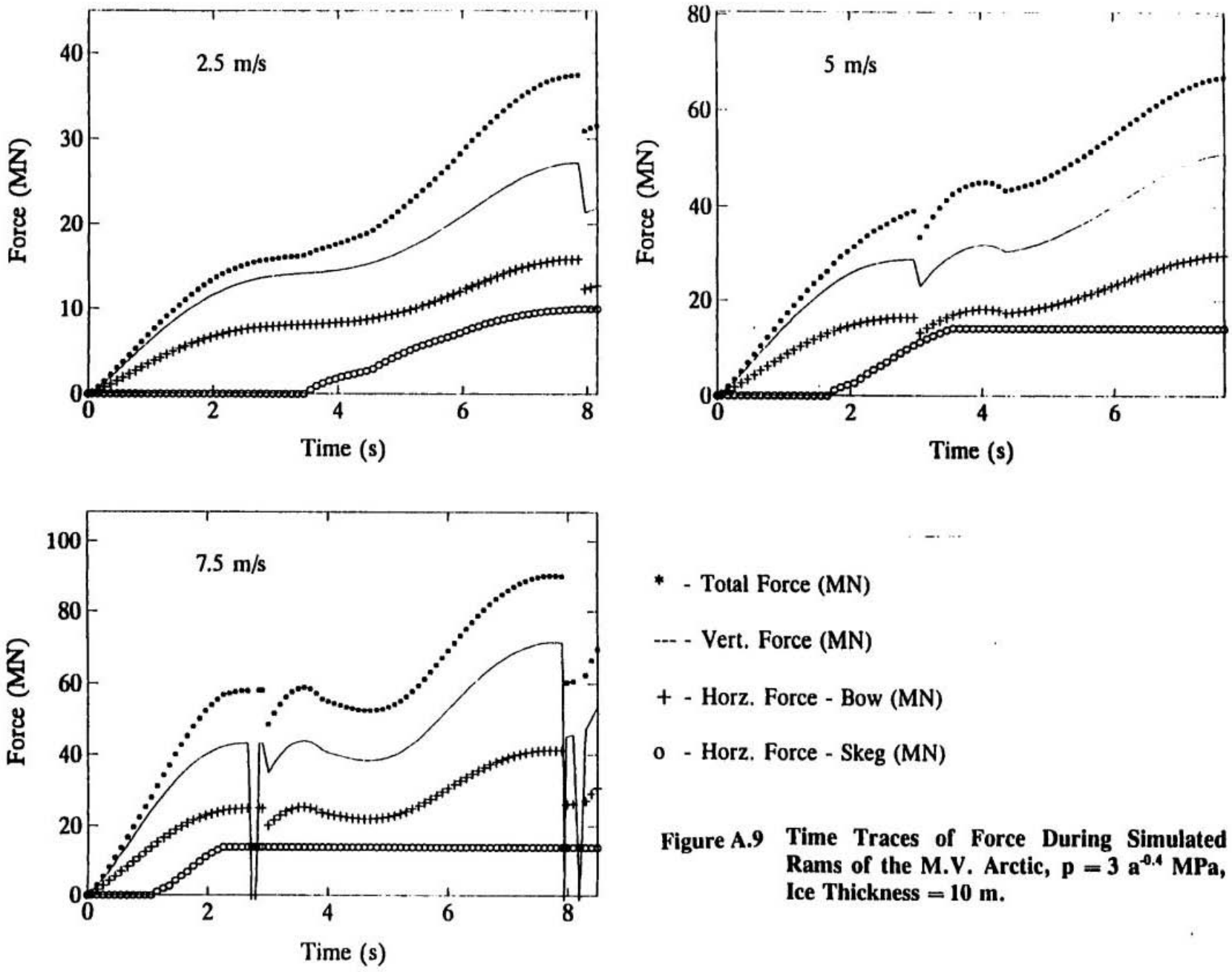

Figure A.9 **Time Traces of Force During Simulated Rams of the M.V. Arctic, $p = 3\ a^{-0.4}$ MPa, Ice Thickness = 10 m.**

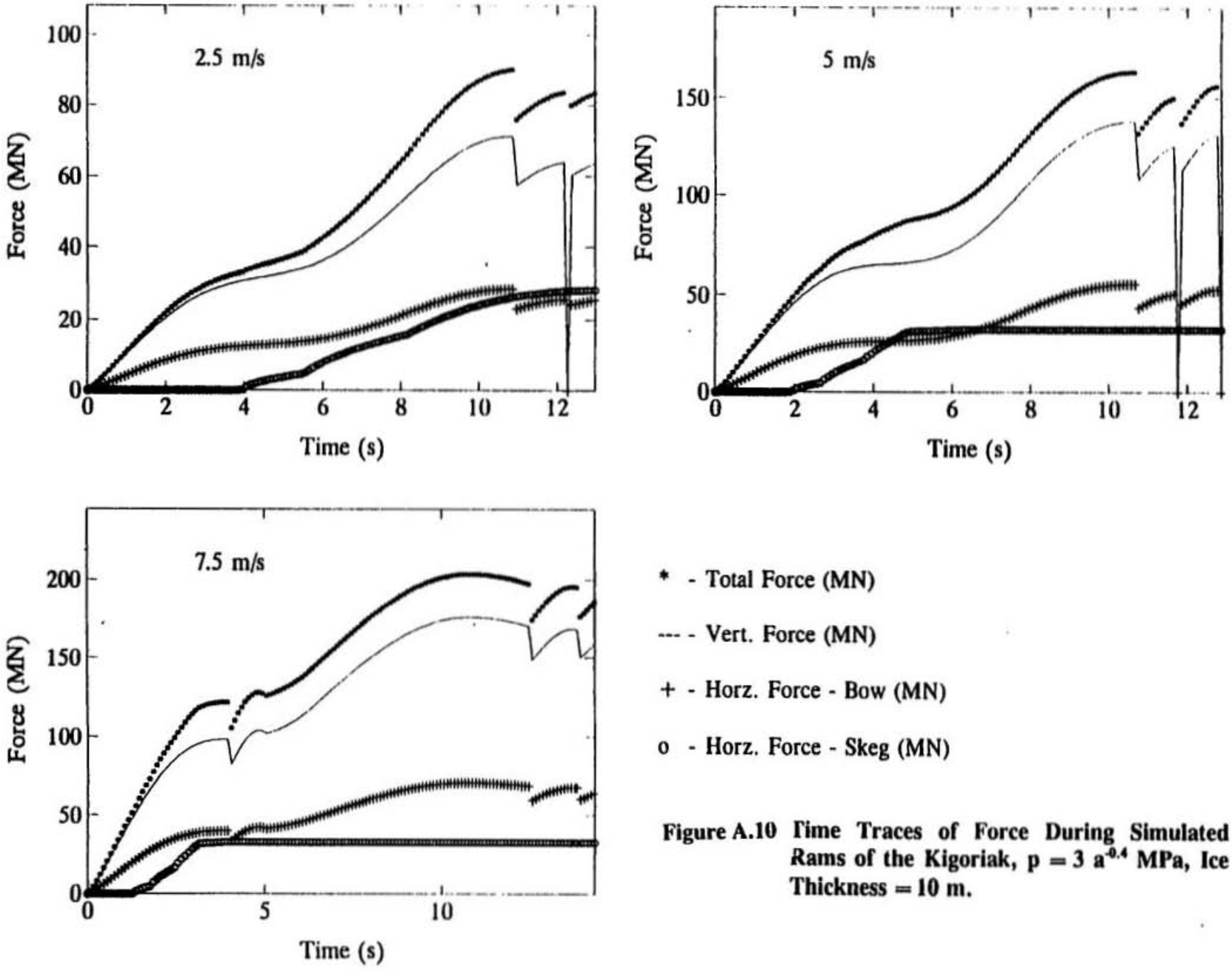

Figure A.10 Time Traces of Force During Simulated Rams of the Kigoriak, $p = 3\ a^{-0.4}$ MPa, Ice Thickness = 10 m.

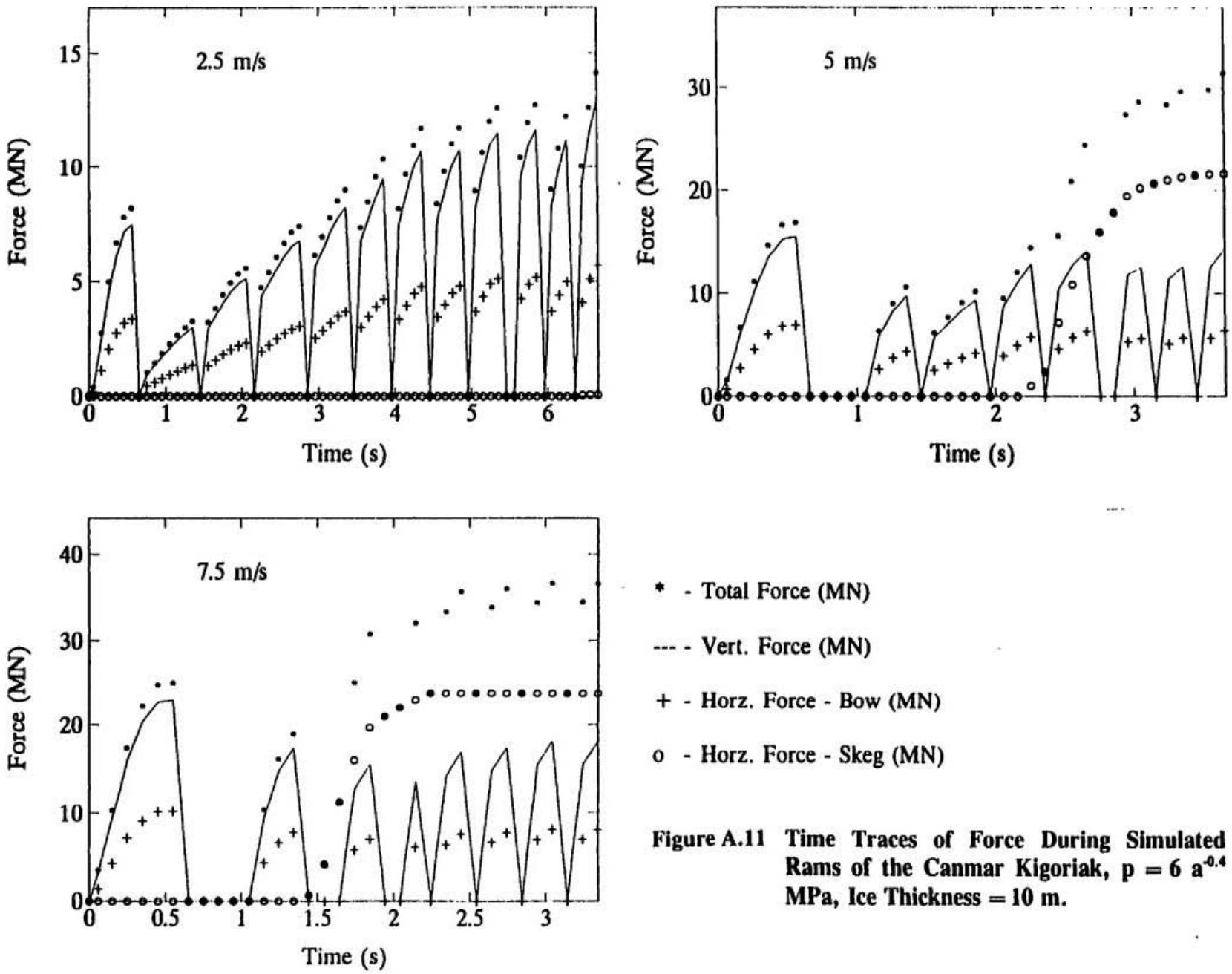

Figure A.11 Time Traces of Force During Simulated Rams of the Canmar Kigoriak, p = 6 $a^{-0.4}$ MPa, Ice Thickness = 10 m.

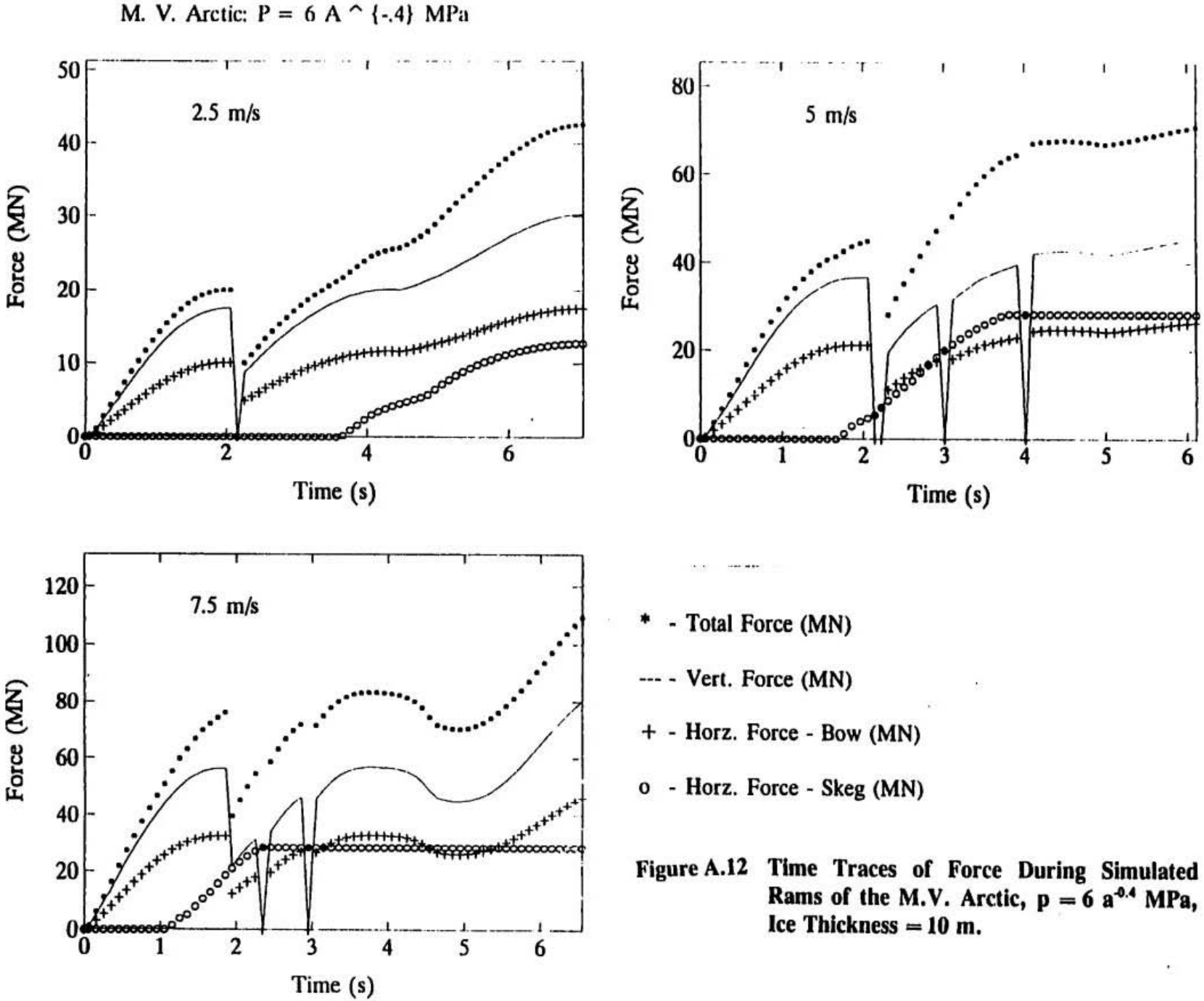

Figure A.12 Time Traces of Force During Simulated Rams of the M.V. Arctic, $p = 6\ a^{-0.4}$ MPa, Ice Thickness = 10 m.

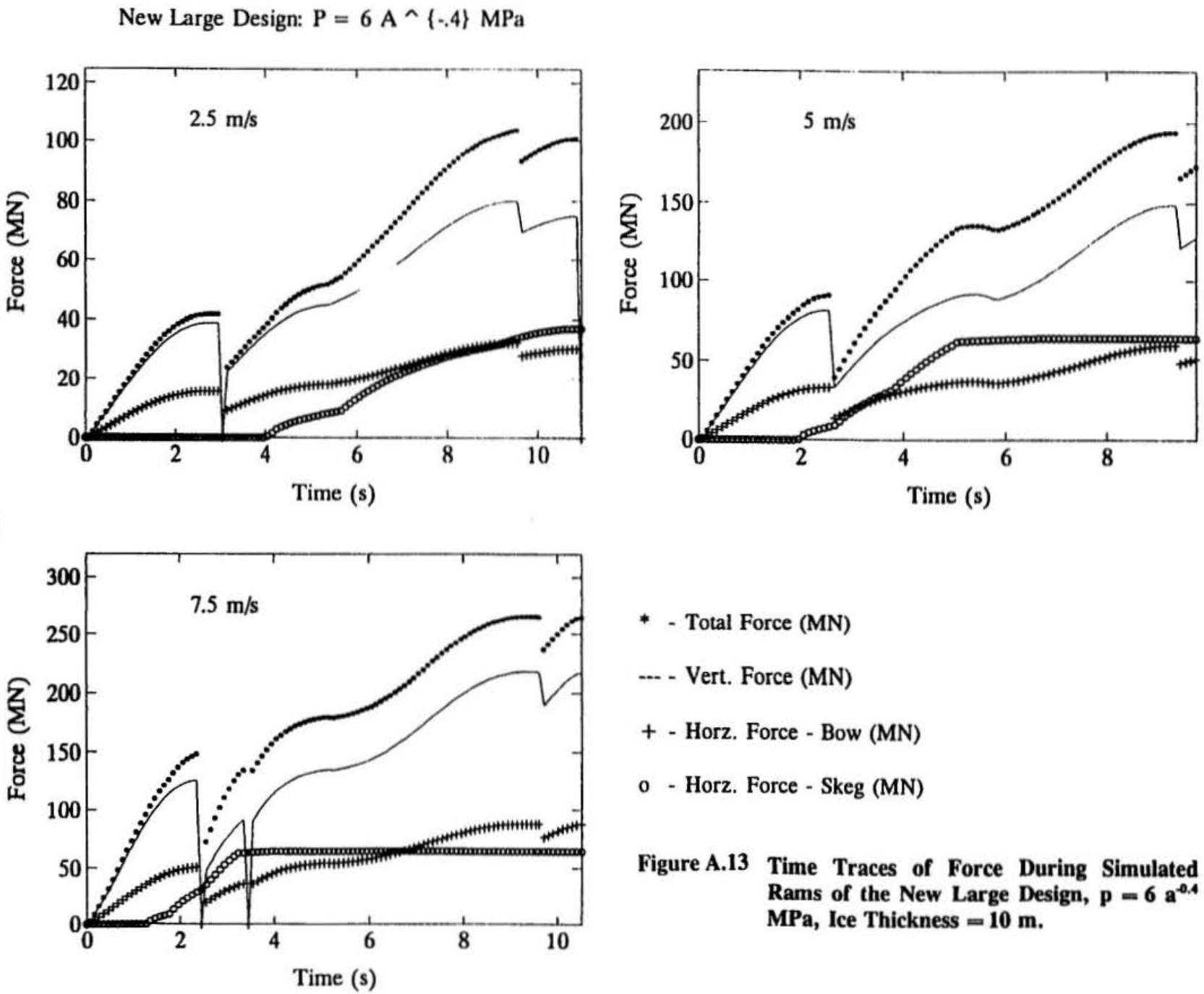

Figure A.13 **Time Traces of Force During Simulated Rams of the New Large Design, $p = 6\ a^{-0.4}$ MPa, Ice Thickness = 10 m.**

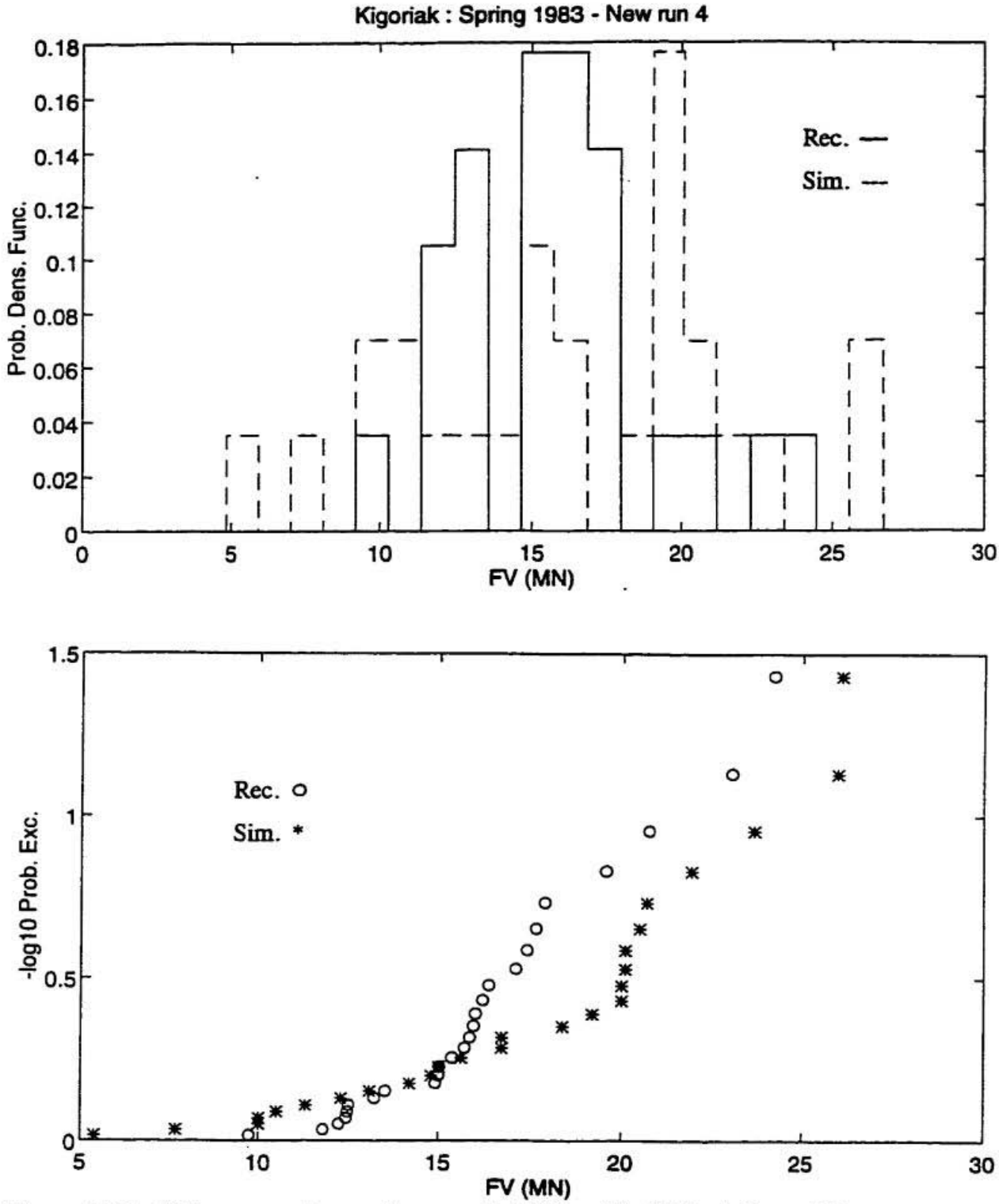

Figure A.14 **Histogram and exceedance probabilities of individual (Parent) Rams. Case 4: $p = 3a^{-0.4}$ MPa; $\sigma_C = 1.5$ MPa; $\sigma_D = 0.2$. Canmar Kigoriak Spring 1983.**

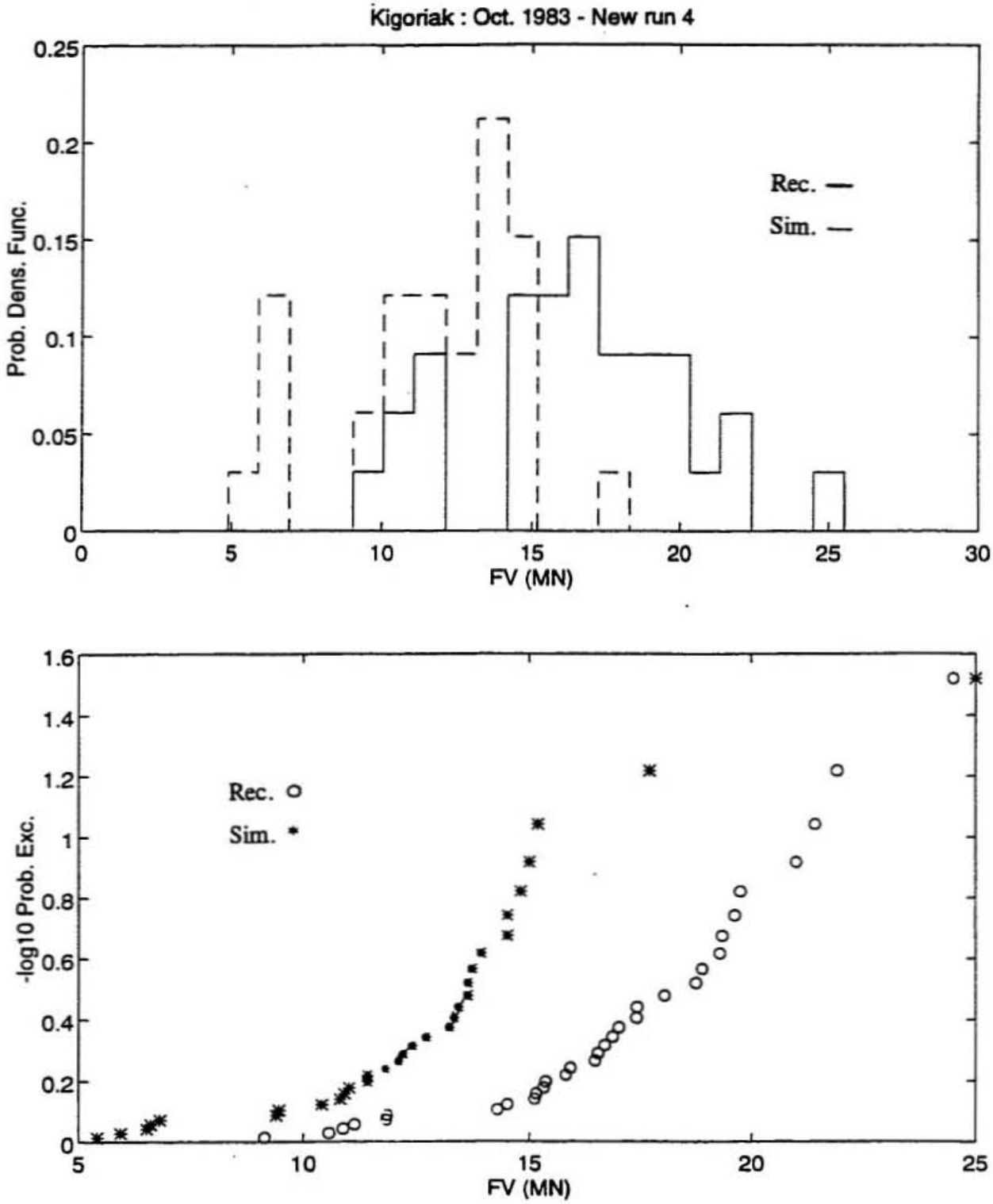

Figure A.15 **Histogram and Exceedance Probabilities of Individual (Parent) Rams. Case 4: $p = 3a^{-0.4}$ MPa; $\sigma_C = 1.5$ MPa; $\sigma_D = 0.2$. Canmar Kigoriak October 1983.**

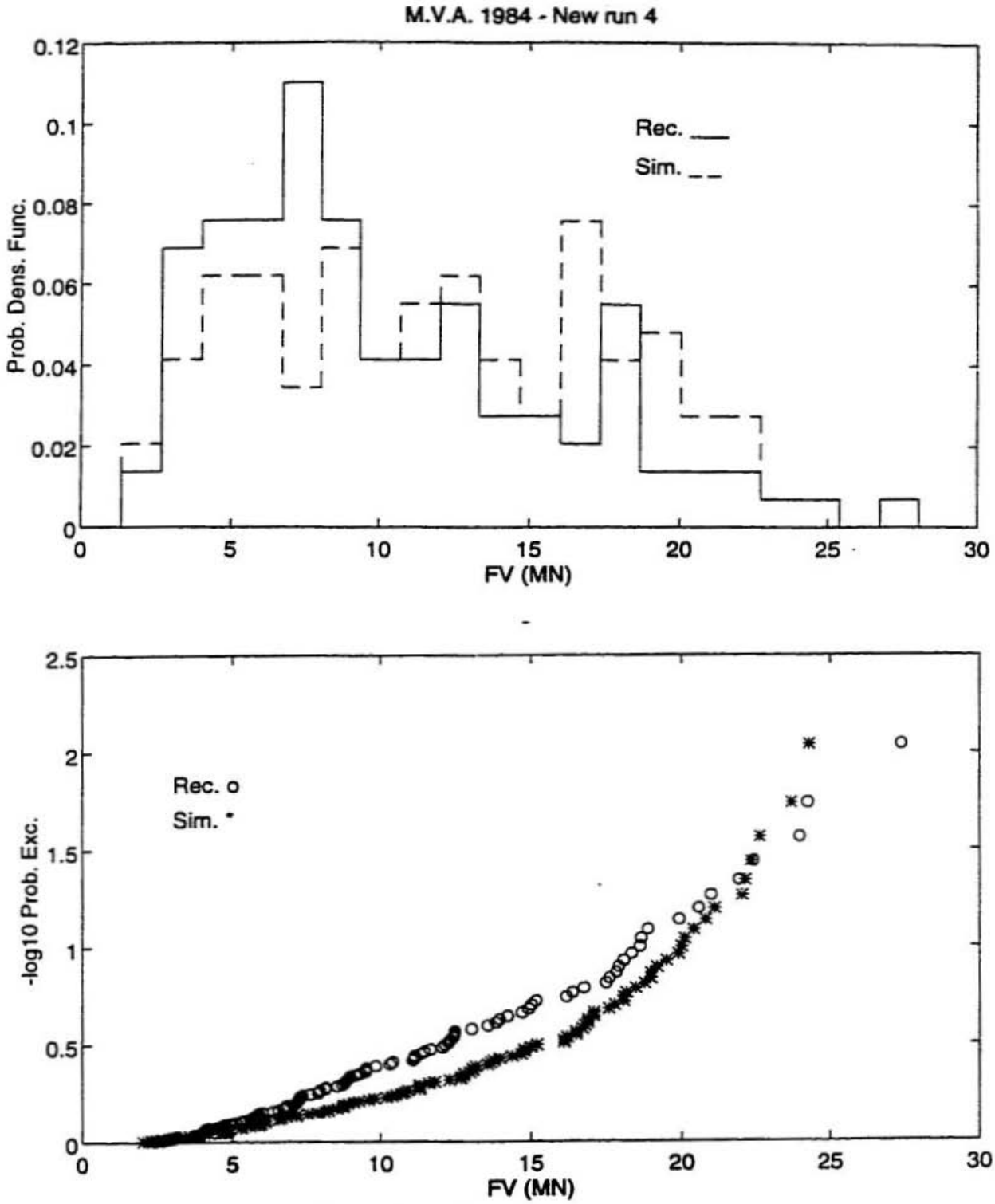

Figure A.16 **Histogram and Exceedance Probabilities of Individual (Parent) Rams. Case 4: $p = 3a^{-0.4}$ MPa; $\sigma_C = 1.5$ MPa; $\sigma_D = 0.2$. M.V. Arctic 1984.**

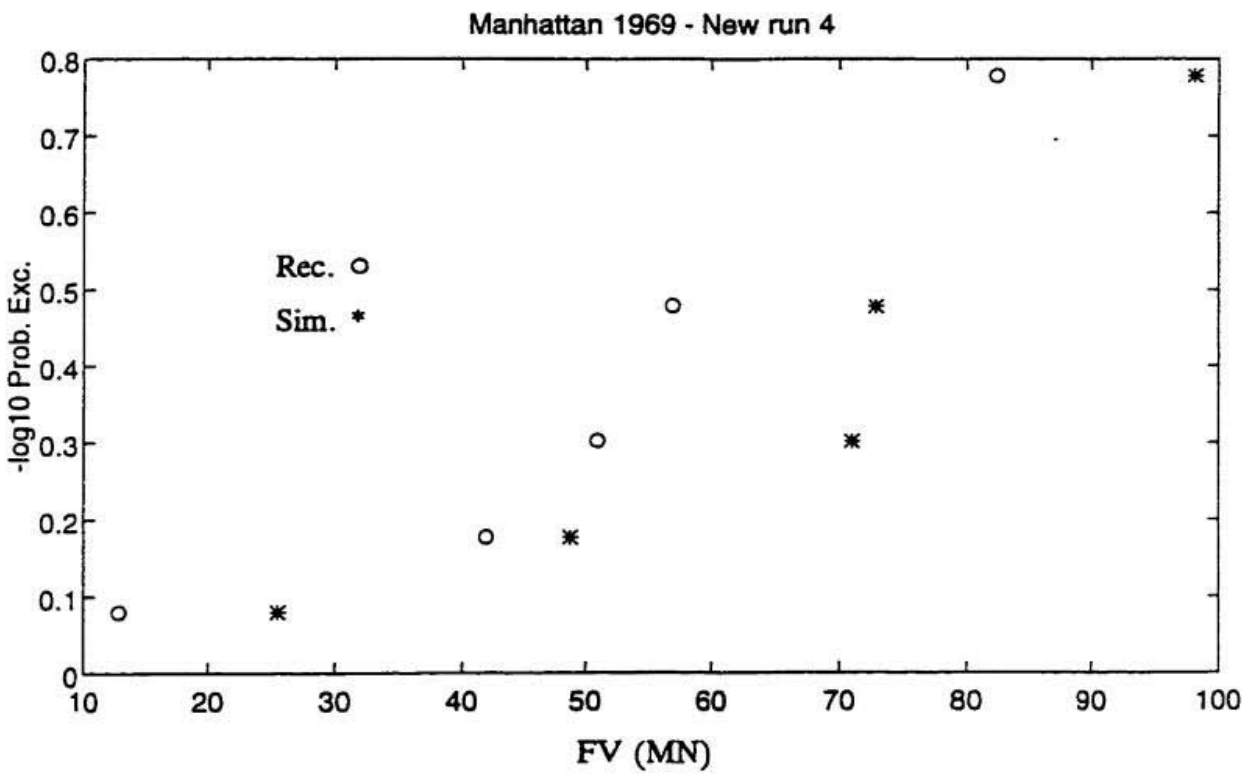

Figure A.17 **Histogram and Exceedance Probabilities of Individual (Parent) Rams. Case 4: $p = 3a^{-0.4}$ MPa; $\sigma_C = 1.5$ MPa; $\sigma_D = 0.2$. Manhattan Trials 1969.**

APPENDIX A - REFERENCES

Daley, C., 1994, "Development of Design Ramming Force for Arctic Vessels", *Canadian Coast Guard*, TP12150E.

Daley, C. and Riska, K., 1990, "Review of Ship-Ice Interaction Mechanics", *Report from Finnish-Canadian Joint Research Project No. 5 'Ship Interaction with Actual Ice Conditions', Interim Report on Task 1A*, M102, Helsinki University of Technology, Otaniemi.

Jordaan, I.J., Maes, M.A., Brown, P.W., and Hermans, I.P., 1993, "Probabilistic Analysis of Local Ice Pressures", *Journal of Offshore Mechanics and Arctic Engineering*, Vol. 115, pp. 83-89.

Masterson, D.M., Nevel, D.E., Johnson, R.C., Kenny, J.J. and Spencer, P.S., 1992, "The Medium Scale Iceberg Impact Test Program", IAHR Ice Symposium, Banff, Alberta, *Proceedings of the 11th. International Symposium on Ice*, Volume 2, pp. 930-966.

Michel, Bernard, 1978, "Ice Mechanics", *Les Presses de L'université Laval*.

Press, W.H., Tenkolsky, S.A., Vetterling, W.T. and Flannery, B.P., 1992, "Numerical Recipes in C: The Art of Scientific Computing", 2nd. Edition, *Cambridge University Press*.

Rawson, K.J. and Tupper, E.C., 1983, "Basic Ship Theory - Volume 1", *Longman Group Limited*, New York.

Riska, K., 1994, "The Determination of Bow Force of a Ship Ramming a Massive Ice Floe", prepared for *Canadian Coast Guard Northern*.

Canadian Marine Drilling Ltd. (CANMAR), 1985, "Kigoriak and Robert Lemeur 1983 Full Scale Impact Tests, Vol 1 & 2", TP6028E, *Final Report for Canadian Coast Guard Northern*.

Canadian Marine Drilling Ltd. (CANMAR), 1985, "Kigoriak and Robert Lemeur 1983 Ice Impact Tests, Refinement of Model Ship/Ice Interaction Energies", TP6813E, *Final Report for Canadian Coast Guard Northern*.

Carter, J., Daley, C., Fuglem, M., Jordaan, I., Keinonen, A., Revill, C., Butler, T., Muggeridge, K., and Zou, B., 1995, *Maximum Bow Force for Arctic Shipping Pollution Prevention Regulations - Phase II*, Report prepared for Transport Canada.

Dome Petroleum Ltd., 1982, "Final Report on Full-Scale Measurements of the Ice Impact Loads and Response of the Kigoriak August and October, 1981".

German and Milne Inc. and Technical Research Centre of Finland (VTT), Ship Laboratory, 1985, "M.V. Arctic - Tests Results and Analysis", TP6270E, *Final Report for Canadian Coast Guard Northern.*

Maritime Administration (MARAD) - U.S. Dept. of Commerce - Office of Commercial Development, 1969, "Report 209 - SS Manhattan Arctic Marine Project - Notes from the 1969 Manhattan Tests in the Northwest Passage".

Offshore Research Ltd., 1981, "Report on Analysis of Data Gathered During the "M.V. Canmar Kigoriak" Ice Impact Trials carried out in October 1981".

Technical Research Centre of Finland (VTT), 1982, "Measurement of Ice Pressures and Forces on the Canmar Kigoriak During Repeated Trials in 1981", research report number LAI-332/82, requested by Dome Petroleum Ltd. Canada.